n° d'ordre : 791

Modélisation des transferts ioniques dans les milieux poreux saturés: application à la pénétration des chlorures à travers les matériaux cimentaires

par

Anwar KHITAB

Présntée le 9 septembre 2005 devant la commision d'exemen
pour l'obtention du grade de docteur (spécialité : Génie Civil)

N° d'ordre : 791

THESIS FOR THE DEGREE OF PHILOSOPHY

THESE

Pour l'obtention du grade de

DOCTEUR de L'INSTITUT NATIONAL DES SCIENCE APPLIQUEES de Toulouse

Spécialité : Génie Civil

Présentée et soutenue publiquement

par

Anwar KHITAB

Modélisation des transferts ioniques dans les milieux poreux saturés: application à la pénétration des chlorures à travers les matériaux cimentaires

Jury

M. Lars-Olof Nilsson	**Rapporteur**
Mme S. LORENTE	**Examinatrice**
M. J.P. OLLIVIER	**Examinateur**
M. A.H. KHELIDJ	**Rapporteur**
M. J.M. TORRENTI	**Examinateur**
Mme G. ARLIGUIE	**Présidente du Jury**

Laboratoire Matériaux et Durabilité des Constructions, INSA-UPS

135, Avenue de Rangueil 31077 Toulouse cedex 4

Abstract

In this work, the problem of ionic species transport through concrete porous media has been documented. Chloride ions penetration in cementitious materials is one of the processes widely responsible for the degradation of concrete structures. Therefore there exists an immense need for its correct understanding and quantification. Different research groups worldwide have proposed different chloride ingress models. Here, a one-dimensional model based on a multi-species approach of the ionic transport is presented. It is the new version of a previous model MsDiff developed a few years ago in our group [TRU 00] that describes the diffusion of ionic species with the Nernst-Planck equation instead of Fick's laws. This newer version is named, the package version of MsDiff after it requires a package of five input data at any given age of concrete. With a multi-species approach, it is possible to take into account the interactions, which exist among different ionic species in pore solution of concrete. The numerical scheme of the model is based on finite difference method with Crank-Nickolson and Law-Wendroff techniques.

In order to run MsDiff, we do need an input data. Several experiments were performed accordingly to provide experimental feedback to MsDiff. Standard immersion tests were conducted to validate the outcomes of MsDiff. Special attention is given to the diffusion coefficients of the ions and the interactions between the ionic species and the solid phase.

In addition to MsDiff, some other existing models were also tried for the sake of comparison with the experimental chloride profiles.

Certain experimentation was conducted to watch the effect of exposure period, concrete age at exposure and concentration in the environmental solution.

In the end, the simulations were performed with MsDiff in order to calculate the chloride-induced corrosion initiation time using the experimental data already achieved while making use of different criteria adopted by different research groups in order to evaluate the corrosion initiation.

Key words: Chloride, penetration, concrete, multi-species, modeling, corrosion.

Résumé

Dans ce travail, le problème du transport d'espèce ionique à travers les milieux poreux saturés a été documenté. La pénétration d'ions chlore a travers les matériaux cimentaires est un des processus largement responsable de la dégradation des structures en béton armé. Ceci nécessite donc la compréhension et la quantification correctes de ce phénomène. Différents groupes de recherche ont proposé des modèles de pénétration des chlorures. Ici, un modèle unidimensionnel basé sur l'approche multi-espèce est présenté. C'est la nouvelle version d'un modèle précédent, MsDiff, développé il y a quelques années dans notre groupe [TRU 00] qui décrit la diffusion d'espèce ionique avec l'équation de Nernst-Planck au lieu des lois de Fick. La nouvelle version est appelée, la version 'package' de MsDiff car elle exige un ensemble de cinq données d'entrée à un certain âge du matériau. Avec l'approche multi-espèces, il est possible de prendre en compte les interactions qui existent entre les espèces ioniques différentes dans la solution interstitielle du béton. Le schéma numérique du modèle est basé sur la méthode des différences finies avec des techniques de Cranck-Nickolson et de Lax-Wendroff.

Afin de faire les simulations avec MsDiff, nous avons besoin des données d'entrée. Plusieurs essais ont été exécutés afin de les acquérire. Des essais standards d'immersion ont été effectués pour valider les résultats de MsDiff. Une attention particulière est donnée aux coefficients de diffusion des ions et aux interactions entre les chlorures et la phase solide du matériau. En plus de MsDiff, quelques autres modèles existants ont été également essayés pour la comparaison avec les profils expérimentaux de chlorure. Des expérimentations ont été faites pour observer l'influence de la période d'exposition, de l'âge du béton à l'exposition et de la concentration de la solution environnementale sur la pénétration des chlorures. Enfin, les simulations afin de calculer le temps d'initiation de la corrosion ont été effectuées avec MsDiff en utilisant les données expérimentales déjà obtenues tout en utilisant différents critères adoptés par différents groupes de recherche pour évaluer le temps d'initiation de corrosion.

Mots-clés : Chlore, pénétration, béton, multi-espèces, modélisation, corrosion

Acknowledgements

First of all I would like to present my gratitude to my supervisors **Prof. Jean-Pierre OLLIVIER** and **Dr. Sylvie LORENTE** for guiding me for a period of three years. Since the very first day of my PhD in 2002, Mr. OLLIVIER always gave me valuable advices which were so important for me and which helped me to accomplish this project with much ease and convenience. I am proud of working for three years under the supervision of a person whom I found so logical, honest and dedicated. I admire his understanding of the subject and am very grateful to him for imparting knowledge to me. I have been with Sylvie since 2001. She supervised the practical part of my DEA. I can never forget her utmost kindness she provided to me since the very first day of my internship in DEA. With my weakness in French language, it became possible to advance due to her. I admire her commitment and dedication to the research work. More important was her constant worry in the precision of the work and her availability whenever I was in need of her. When I started my DEA project with her, she used to talk in English but at the same time also encouraging me to improve my language skills in French. Whatever the French language level I have now, is largely due to her help. I certainly remember those first days when I used to commit French language blunders which never bothered her.

In Pakistan, chemistry is not taught to civil engineering students. My research work in LMDC necessitated a fair knowledge of chemistry. Fortunately I had the company of some good chemists in the laboratory who guided me at each step. I would like to thank a lot **Mme. Simon JULIEN** and **Melle. Maud SCHIETTEKATTE**. Their presence and assistance helped me to overcome my weaknesses in chemistry. My work was largely based in the chemical laboratory of the department. Here I learnt how to work in the form of a team while doing my own work and also at the same time caring for the other colleagues. I would also like to appreciate the assistance of my friends **Benjamin VINCENT**, **Jean-Claude DEGEILH** and **Frédéric REAU** from “Transfert de technologie” for helping me during my experimentation.

I have had the marvelous company of my friends **George WARDEH**, **Laurent RABREAU**, **Mehdi SBARTAI**, **Tanh Son NGUEYEN** and **Céline PERLOT**. They were my colleagues with whom I shared the same office during all the three years. We had a wonderful time while gossiping, chatting and laughing. There were the hard moments and our chatting lessened the hardness of that time. Dear friends many thanks to you. **Pascal BEGUE** joined us in the last year of my thesis. Yet her kindness and a tremendous sense of humor made her an important figure among us. Many thanks to **Maher EL BARRAK**, **Gilles KLYSZ**, **Alexandra BERTRON**, **Mahmoud ISMAIL** and **Marie**

COUTAND who were my neighbors in the department and with whom I enjoyed many moments of joy.

I would also like to mention the kindness and valuable help of the technicians of LMDC. **Mr. Bernard ATTARD** assisted me to fabricate concrete specimens, **Mr. Albert FENOUIL** skilled me to grind concrete specimens and overall **Mr. Jean RENERA** who was always available whenever I was in need of him either for my paperwork or computer related tasks. My good wishes are always with these valuable personalities of this laboratory. I want to present special my thanks to **Mme. Cébastine BERGEZ**, **Melle. Anne BOUCHE** and **Mr. Richard MATHE** for their kindness and assistance. I would also like to mention **Melle. Salima HACHEMI** for the administrative help she provided to me.

I can never forget the help of my life partner **Nuzhat** with whom I also share two sons. I feel sorry for all the hardships she had to bear while I was doing my PhD. I would like to mention that it was impossible for me to carry out this work if she had not encouraged me.

At the end it would be injustice not to mention some persons whose presence was essential to accomplish this job and these nice persons belong to **LORENTE** family. I owe to Henri and Sylvie who personally helped me at each difficult moment during this thesis.

I would also like to thank **Prof. Lars-Olof NILSSON** and **Prof. Abdel Hafid KHELIDJ** for accepting the role of rapporteurs for my thesis report and proposing modifications which improved the quality of this work. I would like also to offer many thanks to **Prof. Jean-Michel TORRENTI** for accepting to become the member of jury. I also like to present gratitude to **Prof. Ginnette ARLIGUIE** for being the president of the jury on the day of defense. **Mme. ARLIGUIE** was my teacher in DEA and also executive of the department. I thank her for all efforts to impart knowledge to me and valuable comments regarding thesis work.

I am thankful to the ministry of education government of France for providing me financial support from in the form of educational grant throughout this tenure.

Overall I salute all my colleagues, lecturers, professors and technicians for bearing me with all my weaknesses in French language for three years. In fact I enjoyed living three years in a community of an excellent research caliber.

TABLE OF CONTENTS

NOMENCLATURE

Latin letters

A	Concrete cross-sectional area,
C	Total chloride concentration per unit mass of concrete,
C_i	Initial total chloride concentration per unit mass of concrete,
C_{cr}	Chloride critical concentration for corrosion,
C_s	Surface total chloride concentration per unit mass of concrete,
C_t	Total chloride concentration per unit volume of concrete,
c	Free chloride concentration per unit volume of pore solution,
c_i	Free concentration of ion i in moles/m^3 of solution,
c_{in}	Initial chloride concentration of pore solution,
$c_{f,s}$	Free chloride concentration at concrete exposed surface,
c_b	Bound chloride concentration per unit volume of the material,
$c_{b,chem}$	Chemically bound chlorides concentration,
$c_{b,phy}$	Physically bound chlorides concentration,
$c_{m,b}$	Bound chloride concentration per unit mass of the material,
$c_{m,b}$	Bound chloride concentration in % mass of the material,
c_v	Free chloride concentration per unit volume concrete,
D	Chloride diffusion coefficient in water in m²/s,
D_a	Chloride apparent diffusion coefficient in water in m²/s,
D_e	Chloride effective diffusion coefficient in m²/s,
D_i	Effective diffusion coefficient of ion i in m²/s,
D_{NPS}	Chloride diffusion coefficient measured with LMDC test in m²/s,
D_{RCM}	Rapid chloride migration coefficient in m²/s (NT Build 492),
D_{ss}	Chloride steady state migration coefficient (ClinConc model),
D_w	Water diffusion coefficient in m²/s,
E_a	Activation energy for diffusion in Joule/mol
E_b	Activation energy for chloride binding in Joule/mol
F	Faraday constant (96480 J/(V.mol)),
I	Current in amperes,
J	Chloride flux in water in moles/(m².s),
J_i	Flux of ion i in moles/(m².s),

J_e Chloride effective Chloride flux in moles/(m².s),

j Current density in Ampere/m²,

k Ratio of effective diffusion coefficient of ion *i* and that of chloride ion in water,

L Concrete thickness,

N Number of nodes in MsDiff modeling,

n Number of ionic species in medium,

p Material porosity in %age,

R Ideal gas constant (8.314 J/(mol.K)),

T Absolute temperature in K,

t Time dimension (s),

t Concrete age in days,

t_{ex} Concrete age at exposure to saline environment,

u_i Electrical mobility,

V Volume in m^3,

v Liquid velocity in concrete pores

W_{gel} Gel content in concrete (kg/m^3 of concrete),

WC Water to Cement ratio,

w Pore solution water content,

X Tolerance,

x displacement ,

x_p Penetration depth from exposed surface,

z_i Charge number of ion *i*,

Greek letters

α Empirical coefficient for chloride binding isotherm,

β Empirical coefficient for chloride binding isotherm,

γ Ionic mobility coefficient,

ε_0 Coefficient of dielectricity or permittivity of vacuum (8.854E-12 C/V),

$\widetilde{\varepsilon}$ Relative coefficient of dielectricity (for water at 25°C, $\widetilde{\varepsilon}$ = 78.54),

ρ Concrete density in kg/m^3,

ρ_w Water density in kg/m^3,

ψ Electrical potential,

σ	Time dependency factor for diffusion coefficient,
τ	Material tortuosity,
γ	Chemical activity coefficient,
ξ	Dielectric permittivity of medium,
θ	Degree of hydration in %age,
Δt	Time step in modeling,
Δx	Incremental distance in modeling,

Indexes

Cl	Chloride,
FA	Fly ash,
i	Ion,
in	Intrinsic,
K	Potassium,
Na	Sodium,
OH	Hydroxide,
PC	Portland cement,
r	Reference,
SF	Silica Fumes,
SG	Slag

LIST OF FIGURES

LIST OF TABLES

OBJECTIVES AND OUTLINES OF THESIS

Objectives and outlines of thesis

The objective of this thesis work is to develop a numerical model, which predicts the chloride penetration in cementitious materials. The work was carried out in Laboratoire Matériaux et Durabilité des Constructions of Toulouse. The basic intention was to renovate the already existing MsDiff model, developed in 2000 by O.TRUC [TRU 00], into a more user-friendly, more comprehensive and more inclusive one. In this regard, it was considered to re-evaluate the physical and numerical structure of the present model, improve its competency and performance and to provide experimental feedback for the validation of its new version.

The present work consists of three main parts, constituting ten chapters. Essential conclusions are provided at the end of each chapter.

The first part is dedicated to a bibliographic review. This part consists of three chapters. The first chapter deals with of ionic diffusion. Emphasis is also given to multi-species theory, which provides the bases for model MsDiff. The second chapter comprises of the existing chloride penetration models. Arguments in favor of further work are given at the end of this chapter. The third chapter includes the description of MsDiff model i.e. its fundamentals, the governing equations, the input data required to run this model and the model outcomes. Reasons in favor of MsDiff as our target model are also pointed out in this chapter. In addition, the numerical scheme of MsDiff is also discussed.

The second part, comprising of chapters 4 and 5 is devoted to the methodology and experimental work. An extensive experimental program was inevitable to achieve two goals: primarily to attain input data for MsDiff and secondarily to validate MsDiff outcomes with the experimental results. In this part, chapter 4 describes the standard test methods thought to be helpful to achieve our targets. In this chapter, the choice for particular tests carried out is also justified. Chapter 5 includes the experimental program and the description of concrete material chosen for the task.

The third part of this thesis report consists of chapter 6, 7 and 8. This important part is mainly meant to judge models outputs against experimental results. The experimental results and numerical outcomes with MsDiff are compared in chapter 6. The importance of concrete age at exposure to saline environment is also emphasized in this chapter. The experimental results are also compared with the simulations made with chloride ingress models other than MsDiff in chapter 7.

The chloride penetration might provoke corrosion of the steel bars embedded in reinforced concrete structures, which are exposed to marine environment or de-icing salts. The chloride

ingress study is basically conducted to evaluate the chloride-induced corrosion initiation time. Chloride profiles serve to determine how deeper the chlorides have penetrated into a structure. And in this way the chloride content at the steel reinforcement provides information whether its value has not crossed a certain threshold value, which leads to the initiation of steel corrosion. Chapter 8 deals with the utilization of model MsDiff as a tool to determine the chloride-induced corrosion initiation time.

At the end, a general conclusion about the work and perspectives are presented in chapter 9 separately, followed by the references.

IONIC DIFFUSION

CHAPTER 1

IONIC DIFFUSION

1.1 Introduction

Diffusion accounts for the fact that an open bottle of perfume can quickly be smelled across the room. It is regarded as a process whereby particles of liquids, gases and solids intermingle as the result of their spontaneous movement caused by thermal agitation and in dissolved substances move from a region of higher to lower concentration.

Diffusion or movement of a chemical species (ions, molecules) from an area of higher concentration to an area of lower concentration is an important phenomenon in many diverse fields (from protein channels [NAD 03] to cementitious [TRU 00]).

Many results of systematic analysis of concrete deterioration in marine environment reveal that almost all are concerned to ionic diffusion [BER 88]. Among these, chloride diffusion and sulfate attack are two main deteriorating factors. De-icing salt (sodium chloride) is applied to remove snow and ice from highways and bridges. The elements most at risks are the bridge decks which are protected by a water proof membrane, chloride ions can penetrate into the concrete through retaining walls, parapets, bridge columns, through faulty joints etc.

Steel embedded in concrete is normally protected against corrosion by the high alkalinity existing in the porous solution of the cement paste. The pH of concrete is determined by equilibrium between the hydrates and the pore solution. One of the by-products of the hydration reactions is calcium hydroxide, which provides the alkalinity. The presence of a high pH is responsible for the presence of a passive iron oxide film on the surface of embedded reinforcing steel. But this corrosion protection is at high risk in the presence of chlorides. The chloride ions present within the pore structure of the concrete interfere with the passive protective film formed on reinforcing steel.

Chloride induced corrosion results in localized breakdown of the passive film. The result is rapid corrosion of the metal at the anode leading to the formation of a 'pit' in the bar surface and significant loss in cross sectional area. This is known as 'pitting corrosion'. Occasionally a bar may be completely eaten through. After this initiation (local breakdown of the film) an anode forms where the film has broken, while the unbroken film (or protective layer) acts as a cathode. This will accelerate localized attack and pits will develop at the anodic spots. The electrolyte inside the growing pit may become very aggressive (acidification) which will

further accelerate corrosion. Thus on one hand, it results in steel bar cross-section reduction leading to lesser bar strengths. On the other hand, the corrosion products formed on steel as a result of chloride ions have much greater volume than the metal consumed in the corrosion reaction. The increase in volume around the steel bars exerts great disruptive tensile stress on the surrounding concrete. If the resultant tensile stress is greater than the concrete tensile strength, concrete cracks, leading to more changes by allowing water and chlorides direct access to the steel bars. As the corrosion proceeds, these cracks widen leading to the complete spalling of concrete.

Chloride induced reinforcement corrosion may occur even in apparently benign conditions where the concrete quality appears to be satisfactory. Even if there is poor oxygen supply reinforcement corrosion may still take place. It is for this reason therefore that failure of reinforcement may occur without any visual sign of cracking.

The present study is focused in the mechanism of chloride penetration by diffusion in cementitious materials.

1.2 Fick's law

The typical approach to characterize diffusive transport of ions in porous materials begins with Fick's law of diffusion. Whenever a concentration gradient of a species $\partial c/\partial x$ exists in a finite volume of a substance, the species will have the natural tendency to move in order to distribute itself more evenly within the substance and decrease the gradient. Given enough time, this flow of species will eventually result in homogeneity within the substance, causing the net flow of species to stop. The mathematics of this transport mechanism was formalized in 1855 by Adolf Fick, who, while working with salts postulated that the flux of material across a given plane is proportional to the concentration gradient across that plane:

$$J = -D\frac{\partial c}{\partial x} \qquad \textbf{[1.1]}$$

Here J (mol/m².s) is the diffusion flux, D (m^2/s) the constant of proportionality referred to as the diffusion coefficient of species, c (mol/m^3) the concentration and x (m) the position. The negative sign indicates that the diffusing mass flows in the direction of decreasing concentration.

It should be kept in mind that the above equation is valid for the diffusion of molecules in an ideal solution.

For a porous medium, things should be a little bit different as in addition to porous solution, the diffusion is also subjected to the complex geometry of porous structure i.e. its constrictivity, tortuosity etc. [OLL 02].

The diffusion coefficient of a species in a saturated porous medium depends upon the geometry of the porous structure and the diffusion coefficient of that species in an ideal solution. Hence the Fick's first law of diffusion for a saturated porous medium can be written as follows:

$$J_e = -D_e \frac{\partial c}{\partial x} \qquad \textbf{[1.2]}$$

Where J_e is the effective flux and D_e is the effective diffusion coefficient, which takes into account the complexity of porous structure. The value of D_e is found to be 1000 times lesser than that of D as observed from experiments.

1.3 Nernst-Planck system of equations

The Nernst-Planck equation is commonly used in various fields and while its complete derivation for each field including for saturated porous media can be found out elsewhere, we just intend to present its brief introduction for the present study.

For an ionic species i, present in infinitely diluted solution, Fick's first law of diffusion is described as:

$$J_i = -D_i \frac{\partial c_i}{\partial x} \qquad \textbf{[1.3]}$$

Since the ions are charged particles, therefore their movement in an electrolyte is governed by not only the concentration gradient but also a local electrical gradient due to other ions in their vicinity, known as membrane potential [REV 99] and the ionic flux due to this electrical gradient is given by:

$$J_i = -u_i c_i \frac{\partial \psi}{\partial x} \qquad \textbf{[1.4]}$$

where u_i is the ionic mobility and ψ is the local electrical potential. The combined flux will be a sum given by equations **[1.3]** and **[1.4]**.

$$J_i = -D_i \frac{\partial c_i}{\partial x} - u_i c_i \frac{\partial \psi}{\partial x} \qquad \textbf{[1.5]}$$

The ionic mobility and diffusion coefficient in dilute solutions are related by the Nernst-Einstein equation:

$$u_i = \frac{D_i z_i F}{RT} \quad \textbf{[1.6]}$$

Putting the value of ionic mobility from **[1.6]** into **[1.5]**:

$$J_i = -D_i \frac{\partial c_i}{\partial x} - \frac{z_i F}{RT} c_i D_i \frac{\partial \psi}{\partial x} \quad \textbf{[1.7]}$$

Where z_i is the charge number, R is the ideal gas constant, F is the Faraday's constant and T is the absolute temperature. The above equation **[1.7]** is known as the Nernst-Planck equation, used for the diffusion of charged particles in an infinitely diluted electrolyte.

For the case of a saturated porous medium, the equation **[1.7]** is transformed into equation **[1.8]**.

$$J_{e,i} = -D_{e,i} \frac{\partial c_i}{\partial x} - \frac{z_i F}{RT} c_i D_{e,i} \frac{\partial \psi}{\partial x} \quad \textbf{[1.8]}$$

Where $J_{e,i}$ is the effective flux and $D_{e,i}$ is the effective diffusion coefficient of ion i. Note that the effective values of these parameters are meant to take into account the porous structure to which an ion is subjected while traveling through porous solution.

1.4 Free and bound chlorides

Chloride ions exist in two forms in concrete, i.e. free chloride ions mainly found in the capillary pore solution and chloride ions bound to the concrete solid surface due to interactions with the cement hydration products and the term 'total chlorides' in literature means the sum of free and bound chlorides.

$$C_t = c_v + c_b \quad \textbf{[1.9]}$$

In equation **[1.9]**, C_t, c_v and c_b are the total, free and bound chloride concentrations respectively. In case of seawater or de-icing salts, where chlorides penetrate the surface of the concrete, the ratio free to combined chloride may be 50:50 [ARY 90].

Although the free chloride is generally believed to be responsible for the initiation of corrosion [HOP 85], the threshold value needed to initiate corrosion is mostly provided in terms of total chlorides and occasionally in terms of free chlorides. According to Mohammed et al. [MOH 03], this may be due to the difficulties in evaluating free chloride contents in concrete. Nevertheless, chloride binding is an extremely important phenomenon as the capacity of a material to bind chlorides will dictate how much free content is available to cause damage.

There are four major compounds in Portland cement, C_3A, C_4AF, C_3S and C_2S. Among these four phases, aluminate (C_3A) and aluminoferrite (C_4AF) phases in cement have been found to be responsible for the chemical binding of chlorides [SUM 04]. The increase of sulfate content tends to reduce chloride binding as the sulfates have a greater tendency to bind with C_3A than chlorides. Thus C_3A, C_4AF and sulfates are the principal parameters to affect chemical chloride binding. It should be kept in mind that only that part of C_3A and C_4AF contributes to chemical binding, which reacts only during exposure period to form Friedel salt and calcium chloroferrite. On the other hand, physical binding depends upon the content of hydrated products like C-S-H [JUS 98] i.e. calcium-silicate-hydrate, a product of hydration reaction of two calcium silicates (C_3S and C_2S). Thus in brief, the total bound chlorides are the sum of those bound chemically and those bound physically.

$$c_b = c_{b,\,chem} + c_{b,\,phy} \qquad \textbf{[1.10]}$$

Where $c_{b,chem}$ is the chemically bound chloride concentration, $c_{b,phy}$ is the physically bound one and c_b on left hand side of equation **[1.10]** implies their respective sum.

1.5 Mass balance equation

Consider an infinitesimal volume of an infinitely diluted solution (with no pressure gradient) of thickness dx and cross-sectional area A, as shown in **Figure 1.1**. Let J_1 be the influx of species into the volume and J_2 the flux, coming out of the volume over a time increment of ∂t. The difference between the two fluxes must contribute to the change in concentration ∂c in this volume. Thus mathematically we can write equation **[1.11]**, considering flux as a continuous function of distance x:

$$(J_1 - J_2)A\partial t = Adx\partial c \qquad \textbf{[1.11]}$$

Since the flux is a continuous function of x, we can additionally describe from **Figure 1.1.**

$$(J_1 - J_2) = -\frac{\partial J}{\partial x}dx \qquad \textbf{[1.12]}$$

Now inserting the net flux value from equation **[1.12]** into **[1.11]** and re-arranging, the mass conservation equation for an infinitesimal volume of solution can be written as:

$$\frac{\partial c}{\partial t} = -\frac{\partial J}{\partial x} \qquad \textbf{[1.13]}$$

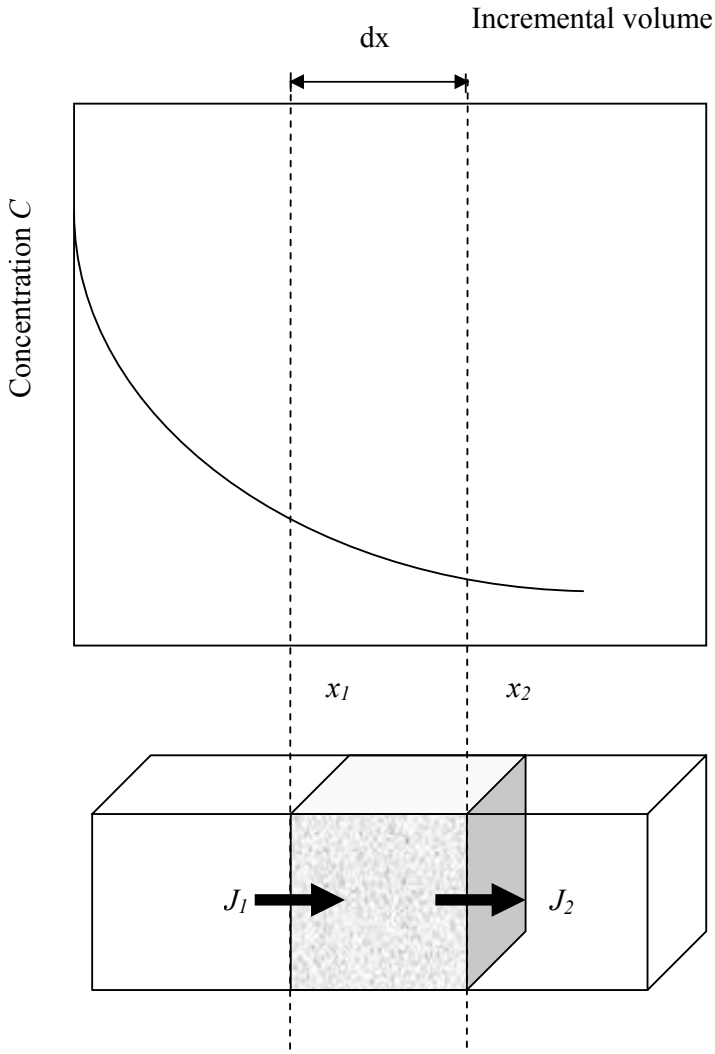

Figure 1.1 Graphical presentation: Conservation of mass

The equation of flux J (for ions) by Nernst-Planck equation for the case of an ideal solution is given by equation **[1.7]**. Inserting the value of flux from **[1.7]** into **[1.13]** (assuming a constant diffusion coefficient), we obtain equation **[1.14]**.

$$\frac{\partial c_i}{\partial t} = D_i \frac{\partial}{\partial x}\left(\frac{\partial c_i}{\partial x} + \frac{z_i F}{RT} c_i \frac{\partial \psi}{\partial x} \right) \qquad \textbf{[1.14]}$$

If we change the infinitesimal solution volume by that of a reactive saturated porous medium, the situation would be a little bit different. Consider that C_t are the total chlorides in mol/m^3 of the infinitesimal volume of the material, entering the medium. The equation **[1.14]** previously

written for an infinitely diluted solution will acquire the following form for a reactive porous medium:

$$\frac{\partial C_t}{\partial t} = D_{e,i}\frac{\partial}{\partial x}\left(\frac{\partial c_i}{\partial x} + \frac{z_i F}{RT}c_i\frac{\partial \psi}{\partial x}\right) \quad \textbf{[1.15]}$$

Being a reactive medium, the solid surface of the material all along the circumference of pores will react with the ionic species moving in pores. Therefore, certain species will be bound to the solid surface. Let $c_{m,b}$ represent the bound species in mol/kg of solid surface and c_i the free ones in moles/m^3 of the pore solution. Mathematically we can write as:

$$C_t = pc_i + (1-p)\rho c_{m,b} \quad \textbf{[1.16]}$$

Where p is material porosity and ρ is the material dry density in kg/m^3 of solid.

Considering the interactions with the solid phase as concentration dependent and inserting the value of C_t from equation **[1.16]** into **[1.15]**, we obtain equations **[1.17]** and **[1.18]**. These two equations (**[1.17]** and **[1.18]**) describe the un-steady state ionic transport in pore solution (using Nernst-Planck equation):

$$\frac{\partial c_i}{\partial t} = \frac{D_{e,i}}{p + (1-p)\rho \partial c_{m,b,i} / \partial c_i}\frac{\partial}{\partial x}\left(\frac{\partial c_i}{\partial x} + z_i\frac{F}{RT}c_i\frac{\partial \psi}{\partial x}\right) \quad \textbf{[1.17]}$$

Or

$$\frac{\partial c_i}{\partial t} = D_{app,i}\frac{\partial}{\partial x}\left(\frac{\partial c_i}{\partial x} + z_i\frac{F}{RT}c_i\frac{\partial \psi}{\partial x}\right) \quad \textbf{[1.18]}$$

If the ions are no more considered as the charge carrying particles, we can neglect the second term on right hand side of equation **[1.17]** or **[1.18]** i.e.

$$\frac{\partial c}{\partial t} = \frac{D_e}{p + (1-p)\partial c_{m,b} / \partial c}\frac{\partial^2 c}{\partial x^2} = D_{app}\frac{\partial^2 c}{\partial x^2} \quad \textbf{[1.19]}$$

If it is further assumed that no interactions occur between the species and the material solid surface, we have:

$$\frac{\partial c}{\partial t} = \frac{D_e}{p}\frac{\partial^2 c}{\partial x^2} = D_{app}\frac{\partial^2 c}{\partial x^2} \quad \textbf{[1.20]}$$

Equation **[1.19]** and **[1.20]** represent the Fick's second law of diffusion.

1.6 Semi-infinite source diffusion

In the case of a semi-infinite medium, an analytical solution to Fick's second law of diffusion exists which requires a constant surface concentration, while the boundary conditions are given by the following equations:

$$c(x,0) = c_{in} \quad \textbf{[1.21]}$$

$$c(0,t) = c_{f,s} \quad \textbf{[1.22]}$$

$$c(\infty,t) = c_{in} \quad \textbf{[1.23]}$$

where c_{in} and $c_{f,s}$ are the initial and surface free chloride concentrations. The analytical solution to Fick's second law (equations **[1.19]** and **[1.20]**) under conditions **[1.21]** to **[1.23]** and a D_{app} independent of (x,t) is given by [CRA 75]:

$$c(x,t) = c_{in} + (c_{f,s} - c_{in})\,erfc\left(\frac{x}{2\sqrt{D_{app}.t}}\right) \quad \textbf{[1.24]}$$

As discussed in the previous section (free and bound chlorides), the usual practice to analyze chloride diffusion by Fick's second law of diffusion is to take into account the total chloride content and not the free ones. Consider equation **[1.15]**. If ionic species are no more considered as the charge carriers, the equation **[1.15]** can be written as:

$$\frac{\partial C_t}{\partial t} = D_e \frac{\partial^2 c}{\partial x^2} \quad \textbf{[1.25]}$$

For the case of a saturated porous medium assuming no interactions with the solid surface, we have from equation **[1.16]**:

$$c = \frac{C_t}{p} \quad \textbf{[1.26]}$$

Putting the value of c from **[1.26]** into **[1.25]**, we have:

$$\frac{\partial C_t}{\partial t} = \frac{D_e}{p}\frac{\partial^2 C_t}{\partial x^2} = D_a \frac{\partial^2 C_t}{\partial x^2} \quad \textbf{[1.27]}$$

Considering that bound species follow a linear behavior with respect to the free ones, we can have:

$$c_{m,b} = Kc \quad \textbf{[1.28]}$$

$$c = \frac{C_t}{p + (1-p)\rho K} \quad \textbf{[1.29]}$$

With the transformations as offered by equation **[1.29]**, we can convert equation **[1.25]** into equation **[1.30]** as follows:

$$\frac{\partial C_t}{\partial t} = \frac{D_e}{p + (1-p)\rho K}\frac{\partial^2 C_t}{\partial x^2} = D_a \frac{\partial^2 C_t}{\partial x^2} \quad \textbf{[1.30]}$$

If we choose to present values in mol/kg of material instead of per m^3 of material (as is the practice in most chloride ingress models, which will be discussed in chapter 2), we have:

$$C_t = \rho(1-p)C \quad \textbf{[1.31]}$$

where C is the total species concentration in mol/kg of material. With the above equations the Fick's second law for the case of total chlorides can be re-arranged as following:

$$\frac{\partial C}{\partial t} = D_a \frac{\partial^2 C}{\partial x^2} \quad \textbf{[1.32]}$$

With the initial and boundary conditions, described by equations **[1.21]** to **[1.23]** for the case of total chlorides per unit mass of the material, the analytical solution to equation **[1.32]** can be written as:

$$C = C_i + (C_s - C_i)erfc\left(\frac{x}{2\sqrt{D_a t}}\right) \quad \textbf{[1.33]}$$

In the above equation, C_i and C_s are the initial and the surface total chlorides per unit mass of the material. This is the above equation **[1.33]**, widely used to determine the chloride profiles. The chloride ingress modeling based on equation **[1.33]** will be discussed in detail in Chapter 2. It should be kept in mind that the above equation is based on the assumption of a constant surface concentration and a constant apparent diffusion coefficient.

1.7 Multi-species theory

For quite a long time, the chloride diffusion has been expressed by Fick's laws in civil engineering research because of simplicity while using analytical solution given by equation **[1.33]**, lack of high-speed computers and perhaps due to lack of knowledge. While these laws might be valid for diffusion of molecules, the interpretation of ionic diffusion on the basis of these laws leads to incorrect observations. It was thereafter thought that the ions being charged particles must influence the movement of each other. This argument led to the multi-species description of chloride transport [TRU 00 LI 00 MAR 01].

Let us consider an ion. Its flux in an electrolyte (infinitely diluted, where unit activity prevails) is given by the Nernst-Planck equation. Recall equation **[1.8]**.

The movement of the ionic species in opposite directions induces an electrical potential between them. This electrical potential is called the liquid-junction potential [REV 99]. This phenomenon tends to accelerate the slower ions while decelerating the fast-moving ones. The current law states that:

$$F\sum_i z_i J_i = 0 \qquad \textbf{[1.34]}$$

This equation also applies to electrically enhanced ionic transport, which is the basis of migration tests.

Combining equations **[1.8]** and **[1.34]**, we have:

$$\frac{\partial \psi}{\partial x} = -\frac{RT}{F}\frac{\sum_i z_i D_i \frac{\partial c_i}{\partial x}}{\sum_i z_i{}^2 D_i c_i} \qquad \textbf{[1.35]}$$

Equation **[1.35]** comes in combination with the continuity equation. This system of equations does not have an analytical solution. The numerical method chosen in this thesis is presented in chapter 3.

1.8 How to predict corrosion initiation time with chloride penetration

In the introduction of this chapter, the consequences of the chloride ion penetration on cementitious material have been described. Whenever a cementitious material like concrete is in contact with a salt solution like marine environment, the chlorides penetrate into it. This penetration increases with the exposure time. The chloride profiles are shown in **Figure 1.2**. These chloride profiles are the ones achieved at the end of the time (t1, t2, t3 and t4), during which an imaginary structure was in contact with an exposure saline solution. It should be kept in mind that this figure is just for demonstration purposes and all the values are non-dimensional. The criterion for corrosion initiation, which is adopted during the present study is different and will be demonstrated in chapter 9 of this work.

In this figure, t1< t2 < t3 < t4.

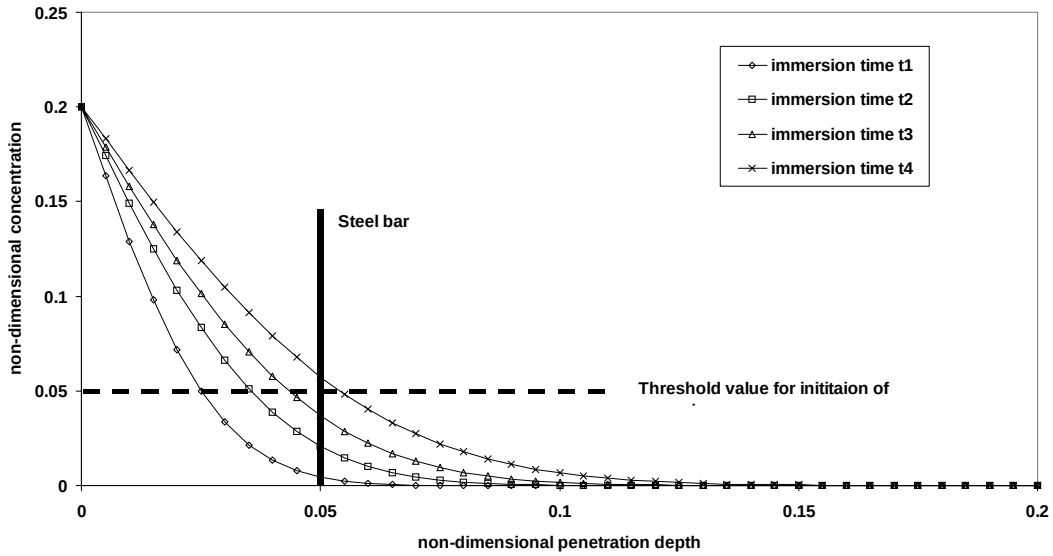

Figure 1.2 Chloride profiles in reinforced concrete

In the above figure, the concentration at steel bar increases with increase in immersion period till a time is reached, where the concentration exceeds a certain threshold value (0.05 for example), which causes the initiation of corrosion of steel bar. In **Figure 1.2**, this time is reached between the immersion times, t3 and t4. Thus using this technique, the life of a concrete structure, which is exposed to marine environment, vis-à-vis chloride induced reinforcement corrosion can be calculated. Another demonstration of this technique is to present the chloride concentration directly at the steel bar instead of as a function of penetration depth from the exposed surface. If the chloride concentrations at steel bars are determined at various immersion periods, we obtain what is shown in **Figure 1.3**. In this figure, it can be observed that the chloride concentration at steel bar exceeds the threshold value of 0.05 at a time of immersion, slightly less than 0.3. Hence this time corresponds to corrosion initiation period.

As mentioned above, this demonstration just gives an idea of calculation of corrosion initiation time. There are different criteria, adopted by different research groups, but all are based upon a threshold value for the corrosion initiation. These ideas will be discussed in detail in chapter 9.

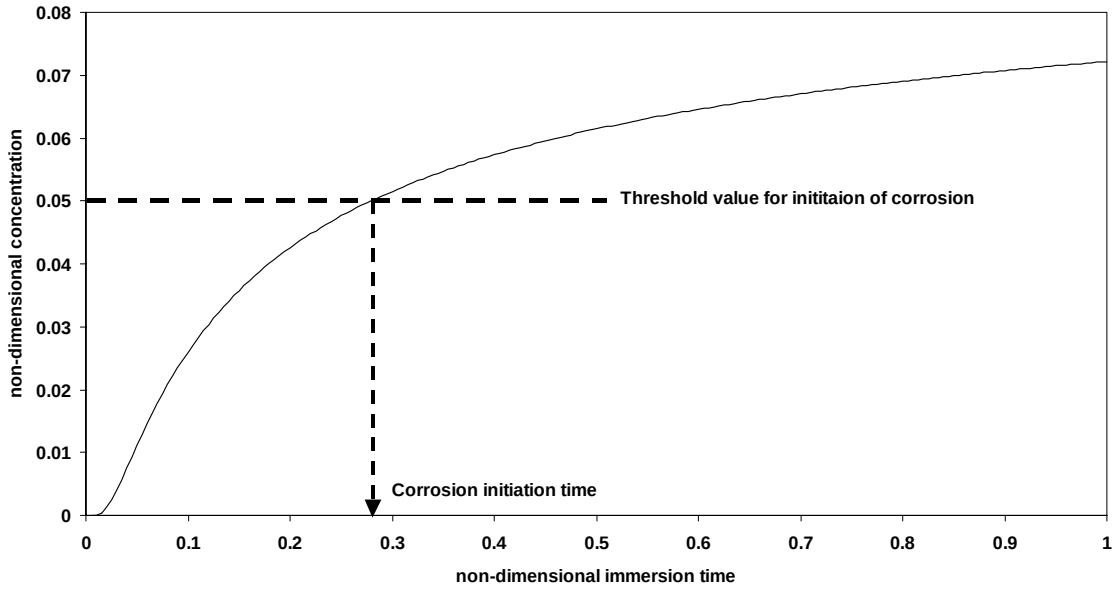

Figure 1.3 Prediction of corrosion with chloride penetration into concrete

1.9 Conclusions

In this chapter, the importance of chloride diffusion with respect to cementitious materials has been discussed. Firstly, the chloride ion diffusion was treated with Fick's laws. Since these ions are charged particles, Fick's laws are incapable for providing a complete vision of diffusion. This drawback of Fick's laws led to the utilization of more correct technique that is Nernst-Planck equation. With the help of this equation, the chloride ions are treated as charged particles. Then chloride ions are not the only species in the system. They are accompanied by other ions, which have an effective influence on its movement. The Multi-species description of diffusion addresses the influence of other ions on chloride transport. When these ions move in concrete porous media, their movement is also affected by the solid phase. There are interactions, both physical and chemical and these interactions have tremendous influence on chloride movement. At the end, the purpose of the chloride penetration studies is discussed i.e. the chloride-induced corrosion and the usual technique, adopted to determine the corrosion initiation time. In the next chapter, a brief introduction of few of the most important existing chloride diffusion models is described.

References

[BER 88] N. S. Berke, D. W. Peifer, Y. G. Weil, Protection against chloride induced corrosion, Concrete International, Vol. 10, pp. 45-55, 1988.

[BOG 50] R. H. Bogue, Calculation of phase composition: The chemistry of Portland cement, Edwards Brothers, Inc., Ed., Ann Arbor, MI, second printing, pp. 184-203, 1950.

[HOP 85] B. B. Hope, J. A. Page, J. S. Poland, The determination of the chloride content of concrete, Cement Concrete Research, Vol. 15(5), pp. 863-870, 1985.

[JUS 98] H. Justnes, A review of chloride binding in cementitious systems, SINTEF Civil and environmental Engineering, Cement and Concrete, N-7034 Trondheim, Norway.

[MOH 03] T. U. Mohammed, H. Hamada, Relationship between free chloride and total chloride contents in concrete, Cement and Concrete Research, Vol. 33, pp. 1487-1490, 2003.

[NAD 03] B. Nadler, Z. Schuss, A. Singer, R.S. Eisenberg, Ionic Diffusion Through Protein Channels: From molecular description to continuum equations, Technical Proceedings of the 2003, Nanotechnology Conference and Trade Show, Vol. 3, 2003.

[NIA 89] Q. Niang, T. J. Sejnowiski, An electro-diffusion model for computing membrane potentials and ionic concentrations in branching dendrites, spines and axons, Biol. Cybern, Vol. 62, pp. 1-15, 1989.

[OLL 02] J.P. Ollivier, M. Carcassès, J. P. Bigas, O. Truc, Diffusion des ions dans le béton saturés, Revue française de Génie Civil, Vol. 5, pp. 227-250, 2002.

[SNY 01] K. A. Snyder, J. Marchand, Effect of speciation on the apparant diffusion coefficient in non reactive porous systems, Cement and Concrete Research, Vol. 31, pp. 1837-1845, 2001.

[SUM 04] T. Sumranwanich and S. Tantermsirikul, A model for predicting time-dependent chloride binding capacity of cement-fly ash cementitious system, Materials and Structures, Vol. 37, pp. 387-396, 2004.

[TRU 00] O. Truc, Prediction of Chloride Penetration into Saturated Concrete – Multi-species approach, Chalmers Univ. of Tech., Göteborg, Sweden, INSA, Toulouse, France, 2000.

CHLORIDE INGRESS MODELS

CHAPTER 2 : CHLORIDE INGRESS MODELS 32

CHAPTER 2

CHLORIDE INGRESS MODELS

2.1 Introduction

The history of chloride ingress modeling starts with Collepardi [COL 70] in the early seventies. He is the first person to present a mathematical model for chloride ingress in concrete. Having known the hazardous consequences of chloride attack on reinforced concrete structures, an immense need for its correct understanding and quantification was considered necessary. Since then several models have been presented by researchers and engineers worldwide. Some models are based on a general solution to Fick's laws (classical approach) while the others are based on the Nernst-Planck equation (the two approaches have been discussed in the previous chapter). In the following, a brief description of some of the most important models present today is given.

2.2 Models based on Fick's laws of diffusion

These models account only for the chloride penetration through the cementitious materials. The influence of other ions on the chloride transport is neglected, except ClinConc and LEO, where hydroxyl ion effect on chloride penetration is taken into account.

2.2.1 Erfc D=constant Model

Collepardi et al [COL 70] were the first to propose a solution to the Fick's second law of diffusion with the condition that both concrete surface concentration and apparent diffusion coefficient are constant. This is a model, which uses the analytical solution of Fick's second law of diffusion to calculate chloride profile in a saturated porous medium. This is a uni-dimensional model that considers the apparent chloride diffusion coefficient as a constant parameter.

$$C = C_i + (C_s - C_i)\,erfc\left(\frac{x}{\sqrt{4D_a\left(t - t_{ex}\right)}}\right) \qquad \textbf{[2.1]}$$

where C is the total chloride concentration as a function of depth x (from exposed surface) and time of exposure, C_i is the initial total chloride concentration, C_s is the surface total chloride concentration, t is the material age, t_{ex} is the material age at exposure (thus (t-t_{ex}) is

the exposure period, a structure is in contact with a saline environment) and D_a is the apparent chloride diffusion coefficient.

Input data

1. Surface chloride concentration,
2. Apparent chloride diffusion coefficient measured from one chloride profile by curve fitting [Appendix 4],
3. Exposure time.

Output data

Total chloride profiles as a function of time and distance from the exposed surface.

This is a very simple model and a very limited data is required to execute it. The model takes constant diffusion coefficient while actually the apparent diffusion coefficient decreases with time, which results in overestimated chloride penetrations. Moreover the assumption for constant apparent diffusion coefficient and surface concentration might be valid for very old structures (where these two parameters may change slightly over time), but for newly built structure, the assumption is far from reality**.**

2.2.2 False ERFC Model

This model is the contribution of Prof. L. O. Nilsson et al. [NIL 01] of the University of Chalmers in Sweden. The model describes chloride ingress through a porous saturated medium when both the apparent diffusion coefficient and the chloride concentration at the concrete surface are time dependent. This is an empirical model based on the Fick's second law of diffusion for a semi-finite medium.

$$C = C_s erfc\left[\frac{x}{2\sqrt{D_a(t)(t-t_{ex})}}\right] \qquad \textbf{[2.2]}$$

The model acquires the following relationships for the two parameters, $D_a(t)$ and C_s.

$$D_a(t) = D_{a,r}\left[\frac{t_r}{t}\right]^{\sigma} \qquad \textbf{[2.3]}$$

$$C_s = A\ln(t-t_{ex}) + B \qquad \textbf{[2.4]}$$

In order to have the relations C_s and $D_a(t)$, at least two experimental chloride profiles for the same material and with the same environmental conditions taken at two different times should be available. From these profiles, the apparent diffusion coefficient and the surface chloride concentration can be determined by curve fitting of the experimental data. The above relations, **[2.3]** and **[2.4]** can be deduced by plotting C_s and D_a as function of time on semi-log paper.

Input data

1. Surface chloride concentration at two (at least) reference times,
2. Apparent diffusion coefficient at two (at least) reference times,
3. Exposure time.

Output data

Chloride profiles as function of time and depth.

This is a simple model which requires nothing but at least two experimental profiles in order to determine the apparent diffusion coefficient and surface chloride concentration. The output chloride profiles depend upon the number of points used in the regression analysis.

2.2.3 DuraCrete Model

This model, formulated by Mejlbro [MEJ 96] is based on the solution to the Fick's second law of diffusion. The model is given by equation **[2.5]**:

$$C(x,t) = C_s\left[1 - erf\left(\frac{x}{\sqrt{4k_c k_e k_t D_{RCM,r}\left(\frac{t_r}{t}\right)^{\sigma} t}}\right)\right] \qquad \textbf{[2.5]}$$

Where k_c is the parameter which takes into account the effect of curing conditions, k_e considers the influence of environment (degree of saturation) on the diffusion coefficient, k_t is a factor which counts for the deviation of the chloride diffusion coefficient measured under accelerated conditions and a diffusion coefficient measured under natural conditions, $D_{RCM,r}$ is the rapid chloride migration test measured NT Build 492 [NT 99] at an age t_r of the material and σ represents the age dependency of the apparent chloride diffusion coefficient.

2.2.4 Modifications in Duracrete by Gehlen

The applied Duracrete model as described previously was later on sophisticated by Gehlen [GEH 00] by accounting for a convection zone just in the vicinity of the exposed surface in

which the chloride profile deviates from the behavior as presented by the Fick's second law of diffusion. The modified form of the analytical solution to Fick's second law of diffusion is described as follows.

$$C(x,t) = (C_{s,\Delta x} - C_i)\left[1 - erf\left(\frac{x - \Delta x}{\sqrt{4k_{RH}k_t k_T D_{RCM,r}\left(\frac{t_r}{t}\right)^{\sigma} t}}\right)\right] + C_i \qquad \textbf{[2.6]}$$

In the above equation, $C_{s,\Delta x}$ is the surface chloride concentration in a depth Δx termed as the depth of convection zone, C_i is the initial chloride concentration, k_{RH} is the relative humidity factor, k_T is the temperature parameter given by the equation **[2.7]** while $D_{RCM,r}$ is the chloride coefficient measured in saturated concrete under an electrical field at a reference time t_r and a reference temperature T_r.

Note that in equation **[2.6]**, the author of the model has proposed a value of Δx equal to 4 [GEH 00].

The model calculates the temperature parameter using the Arrhenius relation, as follows.

$$k_T = \exp\left[b_T\left(\frac{1}{T_r} - \frac{1}{T}\right)\right] \qquad \textbf{[2.7]}$$

Where b_T is the regression parameter, whose value is 4800 K.

Input data

1. Chloride diffusion coefficient $D_{RCM,r}$,
2. Relative humidity factor k_{RH} (k_{RH} =1 for submerged zone),
3. Initial chloride concentration,
4. Temperature factor k_T,
5. Test method factor k_t and age factor σ,

Output

Chloride profiles as function of time and distance from the surface.

This is a simple model and easy to use. If the experimental data corresponding to the transport properties is available, the output can be achieved with no difficulty, otherwise it involves the determination of diffusion coefficient and an estimated surface chloride concentration at the required time. The chloride diffusion coefficient has been related to the migration coefficient by empirical parameters.

2.2.5 ClinConc model

ClinConc or **Cl in Conc**rete was developed by Tang and Nilsson in 1994 [TAN 96]. This is a physical model based on finite difference technique as numerical approach. This model while simulating the chloride ingress in the pore solution utilizes the Fick's law of diffusion.

$$\frac{\partial c_i}{\partial t} = D_{app} \frac{\partial^2 c_i}{\partial x^2} \quad \textbf{[2.8]}$$

Where D_{app} is the apparent diffusion coefficient of ion i (chloride and hydroxyl here), c_i is the ionic concentration and x represents the space dimension. For total chloride distribution, the model implies the mass balance equation with non-linear chloride binding. The chloride binding is described by Freundlich isotherm. The model assumes a minimum chloride binding in summer and a maximum in winter. In summer, the higher temperature decreases the chloride binding capacity and increases chloride diffusivity while in winter, the lower temperature increases the chloride binding capacity and thus decreases the chloride diffusivity. In this model the exposure time is described as a sinusoidal function whereas the effect of temperature on diffusion and chloride binding is expressed by the Arrhenius equation.

$$D_{app,Cl} = D_{in,Cl} f(x) g(t) e^{\frac{E_a}{R}\left[\frac{1}{T_a} - \frac{1}{T}\right]} \quad \textbf{[2.9]}$$

Where $D_{app,Cl}$ is the chloride apparent diffusion coefficient at a depth x from the exposed surface at an age t of concrete, $D_{in,Cl}$ is the intrinsic chloride diffusion coefficient (the value can be determined using equation **[2.14]**), $f(x)$ accounts for depth from the exposed surface, $g(t)$ is the concrete age function, E_a is the activation energy for diffusion (E_a=40000 J/mol), R is the universal gas constant (8.314 J/(mol. K)), T_a is the average seawater temperature (degrees Kelvin) and T is the temperature (degrees Kelvin) at which $D_{app,Cl}$ is to be calculated. The seasonal variations in seawater temperature have been presented by a sine function whereas an average annual seawater chloride concentration (for submerged zone only) has been proposed.

The chloride binding is temperature and pH dependent in the model. The pH and temperature effects have been taken into account by the following equations.

$$f_{OH} = \frac{(B_{Cl})_{OH}}{(B_{Cl})_{OH,in}} = e^{0.59\left[1-\frac{[OH]}{[OH]_{ii}}\right]} \quad \textbf{[2.10]}$$

$$f_b(T) = \frac{c_b}{c_{b,r}} = e^{\frac{E_b}{R}\left[\frac{1}{T}-\frac{1}{T_r}\right]} \quad \textbf{[2.11]}$$

Where f_{OH} and $f_b(T)$ are the hydroxide content and temperature dependent coefficients for chloride binding, $(B_{Cl})_{OH,ini}$ and $c_{b,r}$ are the bound chlorides as determined by the equilibrium method in laboratory, $(B_{Cl})_{OH}$ and c_b are the corrected bound chlorides and E_b is the activation energy for chloride binding (42000 J/mol). The initial hydroxide concentration is calculated on the basis of the alkali content and pore content in concrete. The bound chlorides are given by equation **[2.13]**.

$$c_{m,b,Cl} = f_{OH} f_b(T) Q_{gel} \alpha c_{i,Cl}{}^{\beta} \quad \textbf{[2.12]}$$

where Q_{gel} is the hydrate gel in kg of gel/m^3 of concrete and α and β are the coefficients of Freundlich binding isotherm. The hydroxide diffusion coefficient is estimated by the following equation.

$$D_{app}(OH) = \frac{D_{in,Cl}}{1+K_{b,OH}}\left(\frac{D_{OH}}{D_{Cl}}\right)_{\text{infinitely diluted solution}} \quad \textbf{[2.13]}$$

where $K_{b,OH}$ is the hydroxide binding coefficient (assuming a value of 20 for calculation) and $D_{in,Cl}$ is the intrinsic chloride diffusion coefficient given by the following equation. The hydroxyl ion concentrations can be determined by using equation **[2.13]** in combination with equation **[2.8]**.

$$D_{in,Cl} = \frac{D_{ss}}{p} \quad \textbf{[2.14]}$$

where D_{ss} is the chloride diffusion coefficient determined by the steady state migration test [TAN 96] and p is the porosity of the material.

Input data

1. Concrete composition (cement type, cement content, w/c ratio, aggregate content) and age at the time of immersion,
2. Environmental conditions (chloride concentration, temperature),
3. Chloride diffusion coefficient as determined by the CTH method [TAN 96],
4. Chloride binding parameters as determined by the equilibrium method.

Output data

1. Free chloride concentration profiles,
2. Total chloride concentration profiles,
3. Free hydroxide concentration profiles.

The model does not take into account the influence of other species present in the porous cementitius medium. The effect of hydroxyl ions on chloride binding is accounted for by a parameter as defined by the equation **[2.10]**.

2.2.6 SELMER Model

The model was developed by SELMER Skanska [EUR 99]. This is an empirical model derived from curve fitting to experimental observations. The model is based on Fick's second law of diffusion for a semi-infinite medium with constant exposure.

$$C = C_i + (C_s - C_i)erfc\left(\frac{x}{\sqrt{4D_a(t - t_{ec})}}\right) \quad \textbf{[2.15]}$$

The model adopts apparent diffusion coefficient as a time dependent parameter as described in the following equation.

$$D_a(t) = D_{a,r}\left(\frac{t_r}{t}\right)^{\sigma} \quad \textbf{[2.16]}$$

In the above equation, the parameter σ shows the time dependency of apparent coefficient of diffusion.

$$\sigma = \delta + \lambda \quad \textbf{[2.17]}$$

where δ represents the effect of continued hydration of the cement and λ represents the beneficial effect of ion exchange which takes place between the aggressive environment and the concrete surface layer and which tends to block the chloride ingress into the material. The values of λ vary from 0.32 to 0.96 while those for δ are in the range of 0.1 to 0.2.

Input data

1. Surface chloride concentration (environmental load),
2. Initial chloride concentration,
3. Apparent diffusion coefficient at a reference time determined from exposure data (acid soluble chloride profiles),
4. Curing and exposure time.

Output data

Chloride profiles as a function of time and distance from the surface.

As stated earlier, this model uses the analytical solution to Fick's second law as a convenient tool for curve fitting and hence it is not clear whether chloride transport is due to diffusion or a combination of different processes. The high values for the exponent σ can considerably overestimate the chloride ingress.

2.2.7 Hetek Model

This is an empirical model based on 114 chloride profiles obtained over five years and a few laboratory studies [HET 96]. The model describes chloride ingress into concrete when the surface chloride concentration and the diffusion coefficient are time dependent. The model is the general solution to Fick's second law of diffusion. The specimens used were 1000x700x100 mm concrete slabs. The specimens were exposed to 14 ± 4 g/l (an average marine environment between North Sea and Baltic Sea).

The apparent diffusion coefficient and the surface chloride concentration are time-dependant according to following relations:

$$D_a(t) = D_{aex}\left(\frac{t_{ex}}{t}\right)^{\sigma}, \text{ where } 0 \le \alpha \le 1 \qquad \textbf{[2.18]}$$

$$C_{sa} = C_i + S\left[\left(t - t_{ex}\right)D_{aex}\left[\frac{t_{ex}}{t}\right]^{\sigma}\right]^{q}, \text{ where } 0 \le P \le 1 \qquad \textbf{[2.19]}$$

The incorporation of the time-dependent diffusion coefficient and surface concentration as mentioned by the equations **[2.18]** and **[2.19]** in the solution of Fick's 2nd law is the Mejlbro-Poulsen model.

A 'complete solution' of the Fick's second law is proposed:

$$C(x,t) = C_i + (C_{sa} - C_i)\Psi_q(z) \quad \textbf{[2.20]}$$

$$z = \frac{0.5x}{(t - t_{ex})D_a(t)} \quad \textbf{[2.21]}$$

The function Ψ_q is defined as:

$$\Psi_q(z) = \sum_{n=0}^{+\infty} \frac{q^{(n)}(2z)^{2n}}{(2n)!} - \frac{\Gamma(q+1)}{\Gamma(q+0.5)} \sum_{n=0}^{+\infty} \frac{(q-0.5)^{(n)}(2z)^{2n+1}}{(2n+1)!} \quad \textbf{[2.22]}$$

The function Γ(y) is given:

$$\Gamma(y) = \int_0^{+\infty} u^{y-1} \exp(-u)du \quad \textbf{[2.23]}$$

for y > 0. The notation used should be noted as:

$$q^{(0)} = 1; q^{(1)} = q; q^{(2)} = q(q-1)...q^{(n)} = q(q-1).....(q-n+1) \quad \textbf{[2.24]}$$

where $q^{(n)}$ has $n > 1$ factors.

If the chloride surface concentration is considered to be constant i.e. $q = 0$, the chloride profile is described by the well known error-function solution:

$$C(x,t) = C_{sa} - (C_{sa} - C_i)erf\left[\frac{0.5x}{\sqrt{(t - t_{ex})D_a(t)}}\right] \quad \textbf{[2.25]}$$

In the case when the diffusion coefficient is considered to be constant, $D_a(t)$ is replaced by D_a. The chloride profiles are governed by four parameters S_p, q, D_{aex} and σ. For convenience, the diffusion coefficients (D_1 and D_{100}) and surface chloride concentrations (C_1 and C_{100}) at time $t_1 = 1$ year and $t_{100} = 100$ years are determined from where the above four parameters can be calculated. The estimation of these parameters can be performed through the data from natural exposure. Once D_1, D_{100}, C_1, C_{100} are determined, the required parameters can be calculated as follows:

$$\vartheta = \frac{1}{2}\log_{10}\left[\frac{1}{t_{ex}}\right] \quad \textbf{[2.26]}$$

$$\sigma = \frac{1}{2}\log_{10}\left[\frac{D_1}{D_{100}}\right] \quad \textbf{[2.27]}$$

$$D_{aex} = D_1\left[\frac{D_1}{D_{100}}\right]^{\vartheta} \quad \textbf{[2.28]}$$

$$q = \frac{\log_{10}\left(\frac{C_{100}}{C_1}\right)}{\log_{10}\left(\frac{100 - t_{ex}}{1 - t_{ex}}\frac{D_{100}}{D_1}\right)} \quad \textbf{[2.29]}$$

$$S_p = C_1\left(\left(\frac{D_1}{D_{100}}\right)^{\vartheta}\frac{t_{ex}}{1 - t_{ex}}\right)^{q} \quad \textbf{[2.30]}$$

In order to obtain empirical coefficients, several experiments were performed on plain concrete. It was assumed that the correlation exists valid for concretes with puzzolanas.

$$C_1 = A_H eqv(WC)_b k_{Cl,env}\ [\%\ \text{mass binder}] \quad \textbf{[2.31]}$$

$$C_{100} = C_1 k_{C_{100},env}\ [\%\ \text{mass binder}] \quad \textbf{[2.32]}$$

$$D_1 = B_H \exp\left[-\sqrt{\frac{10}{eqv(WC)_D}}\right] k_{D_{1,env}}\ [\text{mm}^2/\text{yr}] \quad \textbf{[2.33]}$$

$$\alpha = (Ueqv(WC)_D + V)k_{\alpha,env} \quad \textbf{[2.34]}$$

$$D_{100} = D_1\left(\frac{1}{100}\right)^{\sigma} \quad \textbf{[2.35]}$$

A total of 978 chloride measurements in three local marine environments, three exposure times over five years and 13 types of concrete optimized the 20 parameters in the model.

Input data

1. Composition of concrete (water to cement ratio, binder content),
2. Initial chloride concentration,
3. Age of concrete when exposed to saline environment,
4. Exposure time,

Output data

Total chloride profiles

2.2.8 JSCE Model

This model was developed in revised JSCE (Japanese Society of Civil Engineers) specifications in 1999. The prediction of chloride ingress in concrete is based on the analytical solution to Fick's second law as follows,

$$C(x,t) = \gamma_{Cl} C_s \left[1 - erf \left[\frac{x}{2\sqrt{D_d (t - t_{ex})}} \right] \right] + C_i \qquad \textbf{[2.36]}$$

Where $C(x,t)$ is the design chloride content at depth x and time t, γ_{Cl} is a safety factor for taking into account the uncertainty of C_s and generally taken as 1.3, D_d is the design value of apparent chloride diffusion coefficient of concrete, C_s is the surface chloride content of concrete which is a function of distance from the coastline and C_i is the initial chloride constant.

According to JSCE specifications, the apparent chloride diffusion coefficient is derived from experimental chloride profiles in real structures and concrete specimens. In the absence of experimental data, the apparent chloride diffusion coefficient in OPC is generally assumed to be $2.02.10^{-12}$ and $0.92.10^{-12}$ m²/s in the submerged and the atmospheric zones respectively. The initial chloride content is assumed to be zero in the prediction. The surface chloride content per unit volume of concrete is 15.2 kg. The threshold chloride content for corrosion initiation is 2.5 kg/m^3 of concrete. The equation to determine D_p (cm²/s) is given as follows:

For concrete using OPC, $\log_{10} D_P = 4.5(WC)^2 + 0.145(WC) - 8.47$ **[2.37]-a**

For concrete using GGBS, $\log_{10} D_P = 19.5(WC)^2 - 18.3(WC) - 5.74$ **[2.37]-b**

These equations were derived from regression analysis between apparent diffusion coefficient and *WC*.

From D_p, a characteristic value of the apparent chloride diffusion coefficient D_k is calculated by using the following relation.

$$D_k = \gamma_P D_P \quad \textbf{[2.38]}$$

where γ_P is a safety factor, which takes into account the errors for predicted coefficient.

The design value of the apparent chloride diffusion coefficient to be used in equation **[2.36]** is calculated as follows,

$$D_d = \gamma_c D_k \quad \textbf{[2.39]}$$

γ_c is the material factor for concrete. Generally $\gamma_c = 1.0$

Input data

1. Material properties (*w/c* ratio, C_i),
2. Environmental load (C_s),
3. Apparent diffusion coefficient (in case of user data)

Output data

1. Total chloride profiles

For the apparent diffusion coefficient, no accelerated method has been specified. Rather it is obtained from results of chloride profiles in real structures and concrete specimens. According to the model, the effect of the age of concrete on apparent diffusion coefficient is not taken into account. Many uncertainties in the model are compensated by many safety factors.

2.2.9 Life-365 Model

This program was written by E. Bentz and M. Thomas in the University of Toronto [BEN 00]. The governing equation of the model is the Fick's second law of diffusion.

$$\frac{dC}{dt} = D_a \frac{d^2C}{dx^2} \quad \textbf{[2.40]}$$

The chloride apparent diffusion coefficient D_a is a function of both time and temperature and Life-365 uses the following relationship to account for time-dependent changes in diffusion.

$$D_a(t) = D_{a,r}\left(\frac{t_r}{t}\right)^{\sigma} \quad \textbf{[2.41]}$$

Where $D_a(t)$ is the apparent diffusion coefficient at time t, $D_{a,r}$ is the diffusion coefficient at some reference time t_r (28 days in Life-365) and σ is a constant (depending on mix proportions).

Life-365 selects values of D_r and σ based on the mix design details (i.e. water-cementitious material ratio and the type and proportion of cementitious materials). The user himself can also enter the value of the apparent diffusion coefficient. In order to prevent the diffusion coefficient decreasing with time indefinitely, the relationship shown in **[2.41]** is only valid up to 30 years. Beyond this time, the value at 30 years (D_{30y}) calculated from **[2.41]** is assumed to be constant throughout the rest of the analysis period.

Life-365 uses the following relationship to account for temperature-dependent changes in diffusion.

$$D_a(T) = D_{a,r} \exp\left[\frac{E_a}{R}\left(\frac{1}{T_r} - \frac{1}{T}\right)\right] \qquad \textbf{[2.42]}$$

Where $D_a(T)$ is the diffusion coefficient at temperature T, $D_{a,r}$ is the diffusion coefficient at some reference temperature T_r. E_a is the activation energy of the diffusion process (35000 J/mol), R is the gas constant and T is the absolute temperature.

In the model t_r refers to 28 days and T_r refers to 293K (20°C). The temperature T of the concrete varies with time according to the geographic location selected by the user. If the required location cannot be found in the model database, the user can input the necessary temperature data.

The chloride exposure conditions (e.g. rate of chloride build up at the surface and maximum chloride content) are selected by the model based on the type of structure (e.g. bridge deck, parking structure), the type of exposure (e.g. marine or deicing salts) and the geographic location. Alternatively, the user can also provide input data for these parameters.

The solution is carried out using a finite difference implementation of Fick's second law (equation **[2.40]**) where the value of D_a is modified at every time step using equations **[2.41]** and **[2.42]**.

For a base case (plain Portland cement with no special corrosion protection applied), the model assumes the following values:

$$D_{28} = 10^{-12.06+2.40(WC)} \text{ m}^2/\text{s} \qquad \textbf{[2.43]}$$

$$\sigma = 0.2 \quad \textbf{[2.44]}$$

$$C_{cr} = 0.05\,(\%\ \text{mass of concrete}) \quad \textbf{[2.45]}$$

where C_{cr} is the critical value of chloride concentration for corrosion initiation. The above relations are based on a database of the diffusion tests carried out in the University of Toronto. Life-365 applies a reduction factor to the value of D_{PC} calculated for Portland cement, based on the quantity of silica fume (*% SF*) in the concrete **[2.46]**. The relation is valid only up to 15% silica fume. The effect of silica fume on C_{cr} or σ is neglected in the model.

$$D_{SF} = D_{PC} \exp(-0.165SF) \quad \textbf{[2.46]}$$

The model modifies the value of σ depending upon the amounts of fly ash (%FA) or slag (%SG) according to the equation **[2.47]**. The relationship is valid up to replacement levels of 50% fly ash or 70% slag.

$$\sigma = 0.2 + 0.4\left[\frac{FA}{50} + \frac{SG}{70}\right] \quad \textbf{[2.47]}$$

Input data

1. Concrete mix composition,
2. Geographic location,
3. Type of structure (one dimensional or two dimensional),
4. Exposure conditions,
5. Depth of concrete cover to steel bars.

Output data

1. Chloride Profiles
2. The time to corrosion.

2.2.10 LEO Model

LEO model is an empirical model developed by EDF in France in 1998 [PET 00]. The model envisages chloride penetration in a saturated porous medium. Generally chloride ingress models provide information about the initiation of reinforcement corrosion but this model also addresses the structure evolution after corrosion initiation. It is based on the analytical solution of Fick's second law of diffusion for a semi finite medium as follows,

$$C(x,t) = C_i + (C_s - C_i)\left(1 - erf\left(\frac{x}{2\sqrt{k\eta D_a t}}\right)\right) \quad \textbf{[2.48]}$$

While the other terms in the above relation have been defined in all the above models, based on Fick's law, we find two additional parameters k and η. The parameter k is a correction factor for the ionic flux interaction between chloride and hydroxyl ions, while the parameter η takes into account the interactions ion-solid matrix. The following relation for α is proposed.

$$k = 1 + \frac{1}{4[Cl]} \quad \textbf{[2.49]}$$

Where [Cl] represents the environment chloride concentration in moles per liter.

The parameter η is calculated as follows:

$$\eta = \frac{1}{1 + 0.5\dfrac{W_{gel}}{w}} \quad \textbf{[2.50]}$$

Where W_{gel} is the gel content in concrete (kg/m^3 of concrete) and w is the water content in concrete pores (kg/m^3 of concrete).

It is important to note that the model makes use of a diffusion coefficient determined at laboratory temperature (20°C). For temperatures other than 20°C, the Arrhenius equation is used.

$$D_a(T) = D_{a,20°C} \exp^{E_a\left(\frac{1}{293} - \frac{1}{T}\right)} \quad \textbf{[2.51]}$$

where E_a is the activation energy for diffusion (~ 40000 J/mol).

Input data

1. Material composition,
2. Material properties (chloride apparent diffusion coefficient, initial chloride concentration, porosity),
3. Structure configuration (cover depth),
4. Isotherm of interaction (linear) for chloride binding phenomenon,
5. Exposure conditions (temperature, surface chloride concentration).

Output data

Free chloride profiles

This model gives chloride profiles using the mass equilibrium equation. The apparent diffusion coefficient is deduced either by migration test or immersion test. This is a one-dimensional model that does not take into account the effect of other ionic species present in the medium except hydroxyl ions.

2.2.11 LERM

This model was developed in Laboratoire d'Études et de Recherches sur les Matériaux (LERM) in France [HOU 00]. This is a physical model, which solves Fick's second law of diffusion by a finite element method (Newton-Raphson technique). The chloride ingress for a saturated porous medium is predicted. The model takes into account:

- the chloride-solid phase interactions through a binding isotherm
- the transport properties as a function of time and space,
- the evolution of boundary conditions.

The displacement of each ion present in the system is described by the partial derivative equation.

$$J_i = D(c)\frac{\partial c_i}{\partial x} + V(c)c_i \qquad \textbf{[2.52]}$$

$$\frac{\partial c_i}{\partial t} = \frac{\partial J_i}{\partial x} + F \qquad \textbf{[2.53]}$$

By inserting the value of the flux from equation **[2.52]** into **[2.53]**, we get,

$$\frac{\partial c_i}{\partial t} - \frac{\partial}{\partial x}\left(D_i \frac{\partial c_i}{\partial x}\right) - \frac{\partial (Vc_i)}{\partial x} = F(c_i) \qquad \textbf{[2.54]}$$

where c_i is the concentration of the ion, V is the resultant velocity of the ion in m/s (adsorption velocity, velocity under the effect of an electric field, pressure gradient), D_i represents the apparent diffusion coefficient of the ion in m²/s, F is a function which represents the interaction of ion with the solid phase whereas J_i is the flux of the ion.

The variation of the apparent diffusion with the time is given by,

$$D_a(t) = D_{a,r}\left(\frac{t_r}{t}\right)^{\sigma} \qquad \textbf{[2.55]}$$

The diffusion coefficient is determined by either diffusion or migration techniques. This models accounts for the evolution of the physical properties of the porous media and also the environmental parameters.

The output of the model are ionic profiles.

Equation **[2.54]** may be solved for several ionic species. Yet, the continuity equation written for a given ion is completely independent of the continuity equation for another species. There is no ion-to-ion dependency.

2.2.12 Conclusions

Most models based on the analytical solution to Fick's second law are more or less identical. The difference exists in making assumptions on the variations of the apparent chloride diffusion coefficient and surface chloride content. These differences in assumptions have come from the data used for the development of each model. Some of the models mentioned above suggest using a rapid diffusion method in order to determine the chloride diffusion coefficient. The co-relation between the natural diffusion coefficient and the accelerated diffusion coefficient is presented by an empirical coefficient. Look at equations **[2.2]** and **[2.3]**. The value of 'σ' is obtained from $D_a(t)$ and $D_a(t)$ is obtained by applying a curve fit using equation **[2.1]** by which the assumption is made that $D_a(t)$ does not change over time (during immersion) while actually $D(t)$ changes over time. A more correct way to determine 'σ' is proposed by Visser et al. [VIS 02]. The solution to Fick's second law of diffusion can now be derived as follows, taking $D_a(t)$ as time dependent.

$$C(x,t) = C_i + (C_s - C_i)\,erfc\left(\frac{x}{\sqrt{4\frac{D_r}{1-\sigma}\left(\frac{t}{t_r}\right)^{\sigma} t}}\right) \qquad \textbf{[2.56]}$$

But to use the above equation for curve fitting needs a value of 'σ', for which it is necessary to have multiple measured profiles from the same structure taken at different exposure times.

There might be another possibility to better use the above relation, as quoted by Stanish et al. [STA 03] by taking an average value of apparent diffusion coefficient (over the whole exposure period) in equation **[2.2]**. The following relation was suggested.

$$D_{average} = \begin{cases} D_r t_r{}^{\sigma} \dfrac{t_2{}^{1-\sigma} - t_1{}^{1-\sigma}}{(1-\sigma)(t_2 - t_1)} & \sigma \neq 0,1 \\ D_r t_r{}^{\sigma} \dfrac{\ln\left(\frac{t_2}{t_1}\right)}{(t_2 - t_1)} & \sigma = 1 \end{cases} \quad \textbf{[2.57]}$$

With the time $t_{average}$ is given by the following relation.

$$t_{average} = \begin{cases} \left(\dfrac{(1-\sigma)((t_2 - t_1)}{t_2{}^{1-\sigma} - t_1{}^{1-\sigma}} \right)^{1/\sigma} & \sigma \neq 0,1 \\ \dfrac{t_2 - t_1}{\ln\left(\frac{t_2}{t_1}\right)} & \sigma = 1 \end{cases} \quad \textbf{[2.58]}$$

2.3 Models based on the Nernst-Planck equation

2.3.1 Model presented by Li and Page

This is a two dimensional model presented by L.Y. Li of Aston university, Birmingham and C.L. Page of University of Leeds in UK [LI 00]. The model was actually meant for electrochemical extraction of chlorides from cementitious materials. However, the model can also be used to study ionic penetration in a material both with and without an applied electrical field. This model takes into account the influence of a number of factors on the transport behavior of the ions like porosity, tortuosity, the interactions between the pore liquid phase and cement solid phase along with the electrostatic coupling between the ions. The model presents a non-linear diffusion-convection equation which is solved numerically by Galerkin finite element technique using an explicit approach.

The transport of the ions is described by the mass balance equation, ionic flow and current conservation. By conserving the current, the mass balance and ionic flow equations for each ion present in the porous system can be written in the following form.

$$\frac{\partial c_i}{\partial t} = -\nabla(D_i \nabla c_i) + \nabla\left[z_i D_i (\frac{F}{RT} \nabla \psi) c_i \right] \quad \textbf{[2.59]}$$

$$\frac{F}{RT} \nabla \psi = -\frac{(I/F) + \sum z_i D_i \nabla c_i}{\sum z_i{}^2 D_i c_i} \quad \textbf{[2.60]}$$

where c_i represents the concentration of ionic species in the pores, D_i is the diffusion coefficient, z_i is the charge number, F is the Faraday constant, R is the general gas constant, T is the absolute temperature, ψ is the electrostatic potential, I is the current density and t is the time.

The above equations applicable to an ideal dilute solution were modified for a porous medium by taking into account the factors like porosity and tortuosity.

$$(\tau^2)\frac{\partial(c_i + c_b)}{\partial t} = -\nabla(D_i \nabla c_i) + \nabla\left[z_i D_i (\frac{F}{RT}\nabla\psi) c_i \right] \quad \textbf{[2.61]}$$

$$\frac{F}{RT}\nabla\psi = -\frac{(\tau I/p^{\frac{2}{3}}F) + \sum z_i D_i \nabla c_i}{\sum z_i^2 D_i c_i} \quad \textbf{[2.62]}$$

Where c_b represents the bound ion concentration, τ is the tortuosity of the pore structure (τ =1.5 to 3 for concrete) and p is the porosity of the medium. The above equations **[2.61]** and **[2.62]** are nonlinear convection-diffusion equations with variable coefficients from where the concentration profiles and the electrostatic potential for each ionic species can be determined for a given current density with known boundary and initial conditions.

The relation between the free and the bound chlorides is approximated by the Langmuir isotherm.

$$c_b = \frac{\chi_1 c}{w(1 + \chi_2 c)} \quad \textbf{[2.63]}$$

Where c_b and c are the bound and free chloride concentrations, w is the water content in which diffusion takes place, x_1 and x_2 are coefficients which can be determined experimentally. The model accounts for chloride binding. The binding of one chloride ion corresponds to the release of one hydroxyl ion.

Input data

1. The tortuosity of the porous structure,
2. The porosity of the material,
3. The diffusion coefficients of the ions present in the system,
4. The coefficients of binding isotherm,
5. Current density,

6. Initial and boundary conditions,
7. Test duration.

Output data:

1. Concentration profiles of the ions,
2. Potential gradients

While this 2-dimensional model has several advantages e.g. all the ions present in the medium are taken into consideration instead of considering only chloride, the influence of the ions on the transport phenomenon is accounted for, it has certain limitations: the intrinsic diffusion coefficients are difficult to determine, measurement of tortuosity is itself a difficult task.

2.3.2 STADIUM

This model was developed by SIMCO Technologies Inc., in collaboration with the Laval University Canada [MAR 01]. The model presents ionic diffusion, moisture transport, chemical reactions and chemical damage in an unsaturated cement system. The model yields the transport of all the ions present in the system. The ionic diffusion is presented by the extended Nernst-Planck system of equations while the electrical coupling between different ionic fluxes is taken into account by the Poisson equation. The effects of the chemical alterations are described in terms of porosity changes. The influence of the chemical reactions on the transport phenomenon is taken into consideration. The model accounts for eight different ionic species (OH^-, Na^+, K^+, SO_4^{-2}, Ca^{+2}, $Al(OH)_4^-$, Mg^{+2} and Cl^-) and nine solid phases (CH, C-H-S, ettringite, hydrogarnet, gypsum, Friedel's salt, brucite, mirabilite and halite).

In this model, the transport of the ions in the liquid phase is described by the continuity equation with an advective term as follows:

$$\frac{\partial c_i}{\partial t} = \frac{\partial}{\partial x}\left[D\frac{\partial c_i}{\partial x} + \frac{D_i z_i F}{RT} c_i \frac{\partial \psi}{\partial x} + D_i c_i \frac{\partial \ln \gamma}{\partial x} - c_i v \right] \quad \textbf{[2.64]}$$

Where c_i is the concentration of the species in liquid phase, D_i is the diffusion coefficient, z_i is the valence number, F is the Faraday constant, R is the ideal gas constant, T is the liquid temperature, ψ is the diffusion potential, γ is the chemical activity coefficient and v is the fluid velocity. The diffusion coefficient D_i is given as follows.

$$D_i = \tau\, D_{i,\,free\ water} \quad \textbf{[2.65]}$$

Where τ is the tortuosity of the porous structure and $D_{i,free\ water}$ is the ionic diffusion coefficient in bulk solution.

The chemical activity coefficient is calculated using the Davies equation as follows.

$$\ln\gamma = -\frac{A_T z^2\sqrt{I_s}}{1+aB_T\sqrt{I_s}} + \frac{(0.2-4.17e-5I_s)A_T z^2 I_s}{\sqrt{1000}} \quad \textbf{[2.66]}$$

Where I_s is the ionic strength of the solution, A_T and B_T are temperature dependent parameters. The diffusion potential ψ is calculated by using the Poisson equation,

$$\frac{\partial^2\psi}{\partial x^2} + \frac{F}{\xi}\sum^{n} z_i c_i = 0 \quad \textbf{[2.67]}$$

Where n is the total number of ionic species and ξ is the dielectric permittivity of the medium. The fluid velocity is described by a diffusion equation:

$$v = -D_{free\ water}\frac{\partial w}{\partial x} \quad \textbf{[2.68]}$$

Here $D_{,free\ water}$ is the water diffusion coefficient and w is the water content. The mass conservation of the liquid phase was also taken into account.

The spatial discretization of the coupled system is performed using the standard Galerkin procedure. The non-linear set of equations is solved using Newton-Raphson algorithm.

Input data

1. Initial composition of the material,
2. The characteristics of the material (compressive strength, density etc.),
3. The exposure conditions (ionic concentration, relative humidity, temperature etc.),
4. The initial composition of the pore solution,
5. The boundary conditions,
6. The porosity, and tortuosity
7. Ionic and moisture properties of the material

Output data

4 Concentration profiles of different species,

5 Prediction of the degradation of hydrated cement system exposed to an aggressive environment,

6 Prediction of spatial distribution of the solid phases after a certain exposure period.

The model has several advantages over some other models in the sense that it takes a lot of factors into consideration, which affect the transport of different ions. But at the same time one has to determine a large number of items so as to better use it.

2.3.3 Johannesson model

This is a theoretical model, developed by B. F. Johannesson of Lund institute of Technology Sweden in 2003 [JOH 03]. The governing equation of this model is given by the following equation:

$$\frac{\partial c_i}{\partial t} = \nabla\left(\widetilde{D}_i\left(\rho_w\right)\nabla\left(c_i\right)\right) + \nabla\left(\widetilde{A}_i\left(\rho_w\right) z_i c_i \nabla\left(\psi\right)\right) + \frac{D_w\left(\rho_w\right)}{\rho_w}\nabla\left(\rho_w\right)\nabla\left(c_i\right) + c_i \nabla\left(\frac{D_w\left(\rho_w\right)}{\rho_w}\nabla\left(\rho_w\right)\right) + f_i\left(n_{i=1,.....R}, \rho^c_{h=1,.....J}\right) \quad \textbf{[2.69]}$$

where the first term on right-hand side describes the diffusion of ions due to concentration gradient, the second term represents the diffusion of ions caused by the locally induced electrical potential gradient in pore solution, the third term is change of concentration of ion *i* due to convective flows caused by a motion of the pore solution phase, the fourth term models the effect on the ion concentration due to a change in the mass concentration of pore water in the concrete while the final term gives the loss or gain of ions due to mass exchange between ions in pore solution and concrete hydration products.

The mass density flow of water phase is given by

$$\frac{\partial \rho_w}{\partial t} = \nabla\left(D_w(\rho)\nabla\left(\rho_w\right)\right) \quad \textbf{[2.70]}$$

The governing equation for the electrical potential ψ is given by

$$-\nabla(\widetilde{\varepsilon}\varepsilon_0\nabla(\psi) = F\sum_{i=1}^{N} c_i\, z_i \quad \textbf{[2.71]}$$

where ε_0 is the coefficient of dielectricity or permittivity of vacuum (8.854E-12 C/V), $\widetilde{\varepsilon}$ is the relative coefficient of dielectricity (for water at 25°C, $\widetilde{\varepsilon}$ = 78.54), F is the Faraday's constant, c_i is the ionic concentration in pore solution and z_i is the ion charge number.

Parameters $D_i\ (\rho_w)$ and $A_i\ (\rho_w)$ are the ionic diffusion coefficient and ion mobility of i-th ion in pore solution respectively. The two parameters are related to bulk values (found in literature) by tortuosity $\tau\ (\rho_w)$.

$$\widetilde{D}_i = \tau(\rho_w) D_i \quad \textbf{[2.72]}$$

$$\widetilde{A}_i = \tau(\rho_w) A_i \quad \textbf{[2.73]}$$

The tortuosity factors in the range of 0.006-0.009 in saturated conditions for water to binder ratios of 0.35-0.55 have been given [JOH 03]. Note that the parameters capped with ~ correspond to the bulk values found in literature. Further also note that the author of this model uses an inverse definition for tortuosity (of that previously defined in equation **[2.65]**) hence the values of tortuosity are lesser than 1.

The mass balance principle for the local mass exchanges between pore solution phase and solid phase has been considered. Examples quoted are binding of chlorides and leaching of hydroxide [JOH 03].

$$\sum_{i=1}^{N} f_i\left(n_{i=1,\ldots..N}, \rho^c_{h=1,\ldots..J}\right) = \sum_{b=1}^{J} f_h\left(n_{i=1,\ldots..N}, \rho^c_{h=1,\ldots..J}\right) \quad \textbf{[2.74]}$$

Note that in equations **[2.69]** to **[2.74]**, the superscript *c* corresponds to concrete solid phase, while all the other parameters correspond to pore solution. In equation **[2.74]**, *i* represents the ions (leached) in the pore solution, *b* the ions (bound) in the hydration products, *N* the total number of species (leached) in pore solution, *J* the total number of species (bound) in hydration products, the symbol *h* corresponds to hydration products and *f* is the mass exchange function.

Input data

1. Material properties like tortuosity and ionic composition,
2. Ionic transport properties like diffusion coefficients,
3. Initial and boundary conditions

Output data

1. Free ionic profiles

This model can be used both for ionic penetration and leaching. This is a versatile model, which takes into account (i) ionic diffusion caused by concentration gradient, (ii) diffusion caused by the gradient of electrical potential, (iii) mass exchange between ions in pore solution and hydration products in concrete, (iv) convective flows caused by the motion of

pore solution phase and finally (v) the effect on the ion concentration due to change in the concentration of pore water in concrete.

2.3.4 Model presented by Stanish, Hooten and Thomas

This model was presented in 2004 [STA 04]. The silent feature of this model is to propose modifications to the traveling ions due to the porous structure.

When an electrical field is applied across a material specimen, the movement that causes the ions to move is the combination of diffusion and external electrical field. While the Fick's first law states diffusion, the migration is governed by the Nernst-Planck equation and the combined ionic flux moving can be described by the following equation:

$$J = -D\left(\frac{\partial c_i}{\partial x}\right) + \left(\frac{zFD_i}{RT}\right)c_i\frac{E}{L} \qquad \textbf{[2.75]}$$

All the terms, described above have been defined in the previous pages. Solving the above equation for the non-steady state, constant surface concentration, infinite thickness boundary conditions results in the following numerical solution:

$$c(x,t) = \frac{c_{f,s}}{2}\left(e^{ax}erfc\left(\frac{x+aDt}{2\sqrt{Dt}}\right) + erfc\left(\frac{x-aDt}{2\sqrt{Dt}}\right)\right) \qquad \textbf{[2.76]}$$

where $c_{f,s}$ is the exposure solution concentration. All the other terms of the above equation have been already described, the parameter a is given by the following equation:

$$a = \frac{zFE}{RTL} \qquad \textbf{[2.77]}$$

This model considers the overall ionic penetrability to be the product of two components: the particles movement in a solution and the resistance faced due to porous structure, i.e.,

$$P = P_s P_p \qquad \textbf{[2.78]}$$

where P_s is the penetrability of the particles traveling through the solution and P_p is the modification to the penetrability caused by the porous structure. In case of a pure diffusion process, $P_s = D$, while in case of a migration process, $P_s = D\frac{zF}{RT}$.

It was considered that any ion traveling through the concrete will have to pass through many pore bodies (of different shapes and orientations) and the average modification to

penetrability will be a product of the individual modifications of the separate pore bodies. Using the central limit theorem, which states that the product of a large number of independent factors will tend to the lognormal distribution, the resistance due to the pore structure is thought to be of the following form:

$$P_p(y) = \frac{1}{2\pi\left(ln(\zeta)\right)^2 ln(y)} exp\left(-\frac{1}{2}\left(\frac{ln(y) - ln(\lambda)}{ln(\zeta)}\right)\right)^2 \quad \textbf{[2.79]}$$

where λ and ζ are constants, namely the mean and standard deviation of the natural logarithm of the distribution of the modification to the ion penetrability provided by the pore structure, y represents the modification to the penetrability and the function P_p is the proportion of ions that experiences this modification. The function $P_p(y)$ is zero for all negative values of y. In order to conserve mass, the sum of $P_p(y)$ for all values of y is equal to one.

$$\int_{-\infty}^{\infty} P_p(y)dy = 1 \quad \textbf{[2.80]}$$

The concentration of ions at any depth at a given time is a function of the number of ions that have a sufficient velocity to travel that distance or farther. This depth is a function of the distance, the ions should travel in free solution, namely x, while the minimum modification factor that can be experienced by the ions and still reach that point is given by y in the following equation.

$$y = \frac{x}{\left(\frac{zFEDt}{RTL}\right)} \quad \textbf{[2.81]}$$

All the terms of above equation are already described. The coefficient D corresponds to that found in the infinitely diluted solution (values can be found in literature). Now the portions of ions with a modification factor greater than this can be described by:

$$F(y,\lambda,\zeta) = \int_{y}^{\infty} P_p(y)dy \quad \textbf{[2.82]}$$

$$F(y,\lambda,\zeta) = 1 - \int_{0}^{y}\left(\frac{1}{\sqrt{2\pi(ln(\zeta))^2 ln(u)}} exp\left(-\frac{1}{2}\left(\frac{ln(u) - ln(\lambda)}{ln(\zeta)}\right)^2\right)\right)du \quad \textbf{[2.83]}$$

Thus for a constant surface chloride concentration, the model describes the chloride concentration profile as follows:

$$c = c_{f,s}\left(1 - F\left(y, \lambda, \zeta\right)\right) + c_{in} \quad \textbf{[2.84]}$$

The surface concentration $c_{f,s}$ is the product of the solution concentration and the matrix porosity (thus it should be a free ionic concentration and not a total one).

Input data

1. Material properties like porosity and initial ionic composition,

Output data

1. Free ionic concentration profiles.

The model calculates chloride profiles, assuming constant exposure solution. In actual marine environments, this concentration obeys a seasonal variation, as is accounted for by ClinConc model. The distance, an ion travels in pore solution is considered to be a normalized function of the distance, that ion should travel while in a free solution. Model takes into account, the ionic diffusion coefficients, as found in infinitely diluted solution.

2.3.5 Conclusions

The chloride ingress models, based on Fick's laws of diffusion mainly serve to determine the total chloride content. In this regard, usually a threshold value for total chloride is provided, which if exceeded by the total chloride content at steel reinforcement should lead to the initiation of corrosion of rebar. It is a well-known fact that basically this is the chloride concentration in pore solution, which is responsible for the initiation of corrosion at steel surface. Therefore models describing the ingress of chlorides in the pore solution accounting for the influence of the membrane potential have been recently proposed. The diffusion coefficients of ions, other than chloride, have been extracted from values, found in the infinitely diluted solutions. These models, although sophisticated, need a lot of parameters to run the job.

References

[BEN 00] http://www.silicafume.org/specifiers-lifecycle.html.

[BRI 98] Brite-Euram project BE95-1347 'DuraCrete', 1998.

[COL 70] M. Collepardi, A. Marcialis, R. Turriziani, The kinetics of chloride ions penetration in concrete, *Il Cemento*, Vol. 67, pp. 157-164, 1970.

[EUR 99] EuroLightCon document BE96-3942/R3, 1999.

[GEH 00] C. Gehlen, Probabilistische Lebensdauerbemessung von Stahlbetonbauwerken-Zuverla¨ssigkeitsbetrachtungen zur wirksamen Vermeidung von Bewehrungskorrosion, Deutscher Ausschuss fur Stahlbeton, Heft 510, Beuth Verlag, Berlin, 2000.

[HET 96] HETEK Chloride penetration into concrete, State of the Art, Report No. 53, 1996.

[LI 00] L.Y. Li, C.L. Page, Finite element modeling of chloride removal from concrete by an electrochemical method, Corrosion Science, Vol. 42, pp. 2145-2165, 2000.

[MAR 01] J. Marchand, Modeling the behavior of unsaturated cement systems exposed to aggressive chemical environments, Materials and Structures, Vol. 34, pp. 195-200, 2001.

[MAR 02] J. Marchand, E. Samson, Y. Maltais, R.J. Lee, S. Sahu, Predicting the performance of concrete structures exposed to chemically aggressive environment-field validation, Materials and Structures, Vol. 35, pp. 623-631, 2002.

[MEJ 96] L. Mejlbro, The complete solution of Fick's second law of diffusion with time-dependent diffusion coefficient and surface concentration, Durability of concrete in saline environment, Cementa AB, Dandcryd Sweden, pp. 127-158, 1996.

[NIL 01] Nilsson, L., Prediction models for chloride ingress and corrosion initiation in concrete structures, Nordic Mini Seminar & fib TG 5.5 meeting, Göteborg, 2001.

[NT 99] NT Build 492, Chloride diffusivity in hardened concrete, NORDTEST, 1999.

[PET 00] I. Petre-Lazar, Evaluation du comportement en service des ouvrages en béton armé soumis à la corrosion des aciers, EDF, PHD thesis, France, 2000.

[STA 03] K. Stanish, M. Thomas, The use of bulk diffusion tests to establish time-dependent concrete chloride diffusion coefficients, Cement and Concrete Research, Vol. 33, pp. 55-62, 2003.

[TAN 96] L. Tang, Chloride transport in concrete – Measurement and predictions, Chalmers Univ. of Technology, Publication P-96:6, 1996.

[TRU 00] O. Truc, Prediction of Chloride Penetration into Saturated Concrete – Multi-species approach, Chalmers Univ. of Tech., Göteborg, Sweden, INSA, Toulouse, France, 2000.

[VIS 02] J.H.M. Visser, G.C.M. Gaal, and M.R. de Rooij, Time dependency of chloride diffusion coefficients in concrete, RILEM TMC Workshop, Madrid, 2002.

[WAN 01] Wang, Y., Li, L.Y., Page, C.L., A two dimensional model of electrochemical chloride removal from concrete, *Computational Materials Science*, Vol. 20, pp. 196-212, 2001.

MSDIFF PACKAGE VERSION

CHAPTER 3

MSDIFF-PACKAGE VERSION

3.1 Introduction

The objective of this chapter is to document a method of prediction based on a numerical model. As in other numerical codes, input data are necessary. The special focus here is to be able to derive the input data needed from a single sample of material, whatever its age. The analysis of a single sample would provide a 'package' of input data at a given age, while the model can be used to determine the chloride content in the material after any time of immersion into a containing chloride solution. The input data package consists of 5 parameters, namely density, porosity, pore solution composition, effective chloride diffusion coefficient and chloride binding isotherm. In addition the specified boundary conditions (ionic composition of the exposure solution) are required. The material porosity could either be put as user data or left to the mercy of the model to calculate. Note that in this approach we do not avoid the difficulties inherent in the determination of the five input data. But because measurements are difficult, it is proposed to make them only once, at a given age of the material. That is the reason why, for the sake of prediction, the model is required to account for the time dependence of the variables. It is also required to show when and in which case the time dependency feature is necessary.

At the end of this chapter, the numerical scheme of MsDiff is described in brief.

3.2 Model

The model MsDiff is based on a multi-species approach of the ionic transport. It accounts for the electrical interactions between the main ionic species present in the pore system. The flux of species is not expressed by the Fick's first law of diffusion **[1.1]** rather it is presented by the Nernst-Planck equation **[1.8]**. The model is one-dimensional and written for a saturated porous medium. It is additionally assumed that no pressure gradient exists, this justifying the fact that convection terms do not appear in the equations. The model does not account for water uptake due to self-dessication of the concrete. Surface layer formation and pore blocking (due to chemical reactions with magnesium and potassium in seawater), which influence chloride penetration from marine environment, are not accounted for in the model.

For the sake of convenience, we recall here the main equations (earlier described in chapter 1) structuring MsDiff. The ionic flux through a saturated porous medium is given by the Nernst-Planck equation.

$$J_{e,i} = -D_{e,i}\frac{\partial c_i}{\partial x} - \frac{z_i F}{RT} c_i D_{e,i}\frac{\partial \psi}{\partial x} \quad \textbf{[3.1]}$$

It is introduced in continuity equation **[3.2]**, leading to **[3.3]**.

$$\frac{\partial C_t}{\partial t} = -\frac{\partial J_{e,i}}{\partial x} \quad \textbf{[3.2]}$$

$$p\frac{\partial c_i}{\partial t} + (1-p)\rho\frac{\partial c_{m,b}}{\partial t} = D_{e,i}\frac{\partial}{\partial x}\left(\frac{\partial c_i}{\partial x} + z_i\frac{F}{RT}c_i\frac{\partial \psi}{\partial x}\right) \quad \textbf{[3.3]}$$

It is assumed that the interactions with the solid phase are concentration dependent, hence we can conclude equation **[3.4]**.

$$\frac{\partial c_{m,b}}{\partial t} = \frac{\partial c_{m,b}}{\partial c_i}\frac{\partial c_i}{\partial t} \quad \textbf{[3.4]}$$

Inserting equation **[3.4]** in **[3.3]** and re-arranging, we have:

$$\frac{\partial c_i}{\partial t} = D_i\left(p + (1-p)\rho\frac{\partial c_{m,b}}{\partial c_i}\right)^{-1}\frac{\partial}{\partial x}\left(\frac{\partial c_i}{\partial x} + z_i\frac{F}{RT}c_i\frac{\partial \psi}{\partial x}\right) \quad \textbf{[3.5]}$$

Note that in the current model, the interactions of the cations (Na^+, K^+) with the solid phase are believed to be negligible in comparison with chloride binding [WAN 01]. The binding of one chloride ion is assumed to be balanced by the release of one hydroxyl ion. The ionic diffusion is fully described by the electroneutrality condition **[3.6]** and the current law equation **[3.7]**.

$$\sum_i z_i c_i = 0 \quad \textbf{[3.6]}$$

$$F\sum_i z_i J_{e,i} = 0 \quad \textbf{[3.7]}$$

The electrical field can be calculated from equations **[3.1]** and **[3.7]**.

$$\frac{\partial \psi}{\partial x} = -\frac{RT}{F}\frac{\sum_i z_i D_i \frac{\partial c_i}{\partial x}}{\sum_i z_i{}^2 D_i c_i} \quad \textbf{[3.8]}$$

This model holds for constant boundary concentrations and for four different ionic species: Na^+, K^+, Cl^- and OH^-. It was written in such a way that any other species could be added simply by specifying the total number of ionic species, provided that the characteristics of the species are known. **Table 3.1** gives the diffusion coefficients for the 4 ions in an infinitely diluted solution.

Table 3.1 Ionic diffusion coefficients in infinitely diluted solution

Ionic species	Na^+	K^+	Cl^-	OH^-
Diffusion coefficient (1E12 m²/s)	1.33	1.96	2.03	5.30

Here it is assumed that the ratio between the diffusion coefficients of a species and the chloride diffusivity is the one found in an infinitely diluted solution.

$$\left.\frac{D_{e,i}}{D_{e,Cl}}\right|_{\text{material}} = \left.\frac{D_i}{D_{Cl}}\right|_{\text{infinitely diluted solution}} \qquad \textbf{[3.9]}$$

Where D_i represents the diffusion coefficient for Na^+, K^+ and OH^- and D_{Cl} for Cl^-.

The concrete properties are often measured 28 days after casting the material. Still it is possible that the concrete at this age is not mature enough to use these properties at a higher concrete age. In the model, following expressions [TAN 96] have been added to account for the evolution of effective diffusion coefficient with concrete age.

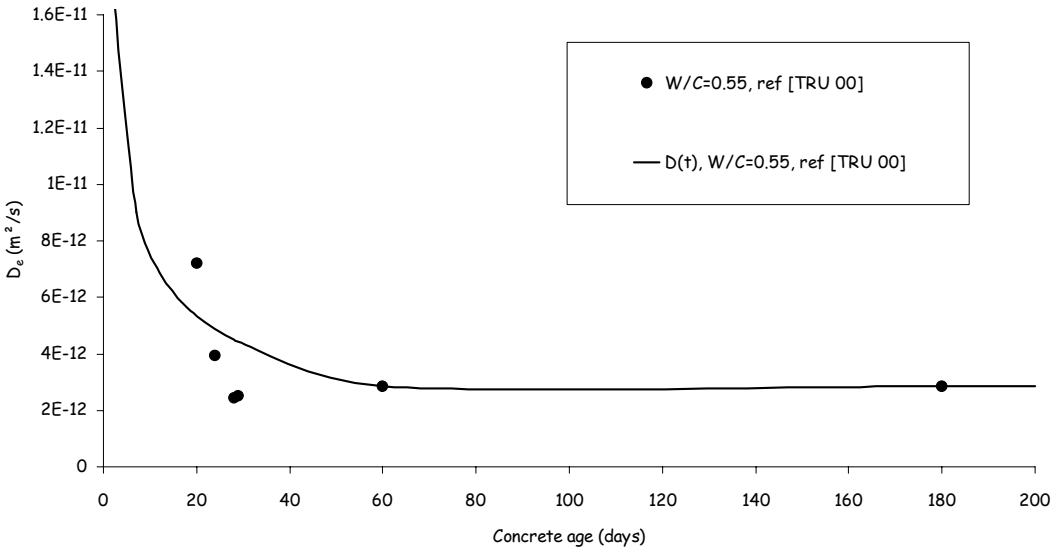

Figure 3.1 Evolution of D_e with concrete age [TRU 00]

$$D(t) = D_{cons\tan t}\left(\frac{t_{cons\tan t}}{t}\right)^{\sigma}, \text{if } t < t_{cons\tan t} \quad \textbf{[3.10]}$$

$$D(t) = D_{cons\tan t}, \text{if } t \geq t_{cons\tan t} \quad \textbf{[3.11]}$$

The equations state that after a certain material age, the diffusion coefficient becomes constant. According to Truc's experimental results, the effective diffusion coefficient of chloride reaches a constant value at the age of 70 days for the cement CEM I [TRU 00]. Hence $t_{constant}$ = 70 days has been implied in the model. Note that the cement CEM I was used during this work.

3.3 Chemical activity in concentrated electrolyte solutions

The model does not account for the chemical activity of the electrolytic solutions. A more complete version of the model consists in replacing **[3.1]** with:

$$J_{e,i} = -D_{e,i}\frac{\partial c_i}{\partial x} - \frac{z_i F}{RT}c_i D_{e,i}\frac{\partial \psi}{\partial x} - c_i\frac{\partial(\ln\gamma_i)}{\partial x} \quad \textbf{[3.12]}$$

where γ is the chemical activity coefficient This coefficient equates 1 in an infinitely diluted or ideal solution. The assumption of an ideal solution fails when the electrolyte solution exhibits a high ionic strength, which is typically the case with the pore solution of cementitious materials.

During the past few years, this issue has caught the attention of several research groups worldwide. For example, Truc et al. used a model based on Pitzer equations [PIT 79] and calculated the fluxes of ionic species and the potential created across a cement-based material by the ionic species in solution. Their results showed very little difference when compared with calculations based on assuming an ideal solution. Tang [TAN 99] reached the same conclusion. Samson et al. [SAM 99] proposed a modified version of the Davies law, allowing the calculations of the chemical activity coefficient γ for an electrolyte with high ionic strength. The modified version of the Davies law follows (with very good accuracy) the experimental data on the chemical activity coefficient of a sodium hydroxide solution. However, the numerical results presented by Samson et al. [SAM 99] on the concentration profiles of several ionic species through a membrane exhibit very little discrepancy when compared with or without the chemical activity term. A slight difference is observed when comparing the corresponding calculations for the membrane potential. Li and Page [LI 98] published some numerical results by using their own expression for the chemical activity

coefficient, which was based on empirical coefficients. Their results referred to diffusion under an electrical field.

It is important to emphasize that the results reviewed above were obtained by different research groups, which used markedly different approaches. Based on this literature review, it was concluded that accounting for the activity term in the model would not increase the accuracy of the results. Therefore in the present model the ionic concentration is maintained equal to the ionic activity.

3.4 Binding isotherm

As the equation **[3.3]** describes, our model requires a binding isotherm. It is an important tool as the bound ions do not contribute to the ionic transport. While the experimental binding isotherms will be discussed later, the present paragraph serves to describe the binding isotherm equation included in the model. For low concentrations (lesser than 500 mol/m^3-solution), it is assumed that the binding of chloride is a monolayer adsorption, described with a good accuracy by a Langmuir type equation. Conversely, this trend is not followed at higher concentrations. Instead of reaching a plateau, as predicted by the Langmuir isotherm, the bound amount of chloride continues to increase. According to Byfors [BYF 90], the chemical chloride ability to bind would be enhanced for the higher concentrations leading to a multi-layer adsorption. A Freundlich-like equation is often proposed when the free chloride concentrations are higher than 500 mol/m^3. However the results given by Freundlich equation exhibit an important discrepancy with the experimental data for lower chloride concentrations. In this model, a Langmuir binding isotherm equation is proposed, corrected by a power law equation for the higher chloride concentrations:

$$c_{m,b} = \frac{\alpha_1 \beta_1 c}{(1+\beta_1 c)} + \alpha_2 c^{\beta_2} \qquad \textbf{[3.13]}$$

Where α_1, β_1, α_2 and β_2 are the coefficients (obtained by curve fitting to experimental data), $c_{m,b}$ is the bound amount of chlorides in mol/kg of concrete and c represents the free chloride concentration in mol/m^3 of solution.

3.5 Material properties

The water porosity and density can be measured by well-known classical methods. These methods will be discussed in the next chapter ‘Experimental methods‘. The composition of the pore solution can be measured by pore solution extraction by squeezing from a concrete specimen. This method is also described in the next chapter.

Besides that, a new program for the calculation of porosity has been added in the model. This program uses degree of hydration calculated from Avrami's equation [TEN 00] and the porosity from POWERS model [POW 47] for cement paste (CEM I). In the following paragraphs, the step-wise program for porosity calculation is described.

3.5.1 Parameters required for porosity calculation

- Water density ρ_ω (kg/m^3),
- Cement density ρ_c (kg/m^3),
- Concrete air quantity A_c (m^3/m^3),
- Concrete cement content C (kg/m^3 of concrete),
- Concrete water content W (kg/m^3 of concrete),
- Cement Bogue's phase composition (C_3S, C_2S, C_3A, C_4AF) [BOG 50].

3.5.2 Initial porosity (POWERS model)

Initial porosity of cement paste is the ratio of volume of water to volume of water plus cement.

$$p_0(\%age) = \frac{W/C}{(W/C + 0.32)} \qquad \textbf{[3.14]}$$

Where W/C represents the water to cement ratio.

3.5.3 Degree of hydration for each cement phase (AVRAMI model)

The degree of hydration is defined as the ratio of hydrated mass of cement to initial mass of cement. The degree of hydration is calculated from the following equation.

$$\theta_i = 1 - \exp\left(-a_i (t - b_i)^{c_i}\right) \qquad \textbf{[3.15]}$$

Where θ is the degree of hydration for phase i (C_3S, C_2S, C_3A and C_4AF), t is the material's age (days) and a_i, b_i and c_i are the coefficients whose values are given in **Table 3.2**. It should be noted that the constants a_i, b_i and c_i have been determined for a specific Portland cement [TAY 87] and are used as an approximation for other Portland cements (CEM I). The combined degree of hydration for cement is assumed to be the weighted average of those of its four phases.

$$\theta_c = \theta_1 C_3S + \theta_2 C_2S + \theta_3 C_3A + \theta_4 C_4AF \qquad \textbf{[3.16]}$$

Where the subscripts *1*, *2*, *3* and *4* correspond respectively to C_3S, C_2S, C_3A and C_4AF. Avrami equations are generally implied to describe nucleation and growth reactions and are

not concerned to more complex reactions occuring in Portland cements however they can be used as a simple model to approximate the hydration of pastes older than 1 day [TEN 00].

3.5.4 Cement paste porosity

In the following, is given the relation to calculate the cement paste porosity in percentage with p_0 calculated from equation **[3.14]** and θ_c from equation **[3.16]**.

$$p_P(\%age) = (p_0 - 0.53\theta_c(100 - p_0)) \quad \textbf{[3.17]}$$

3.5.5 Concrete porosity

Once the cement paste porosity is known, the concrete porosity can be determined by multiplying it with the corresponding volumes of cement, water and air per cubic meter of concrete.

$$p(\%age) = p_P\left(\frac{C}{\rho_c} + \frac{W}{\rho_w} + A_c\right) \quad \textbf{[3.18]}$$

Table 3.2 Constants for Avrami's equation

Compound i	a	b	c
C_3S	0.25	0.90	0.70
C_2S	0.46	0.90	0.12
C_3A	0.28	0.90	0.77
C_4AF	0.26	0.90	0.55

It is worthy to note that the AVRAMI-POWERS model was adopted for its excellent comparison with the experimental data, obtained during this work.

3.6 Outcomes of the model

First of all, the model calculates the electrical potentials, using equation **[3.8]**. Once, electrical potential has been calculated, the continuity equation is solved for each species to determine the ionic concentrations **[3.3]**. Note that the ionic concentrations are the main result. At the end, the ionic fluxes are calculated by equation **[3.1]**. In addition to that, evolution of degree of hydration, material porosity and effective diffusion coefficient with materials age are also performed.

3.7 Numerical scheme of MsDiff

Let us recall the system of equations, as adopted by MsDiff. The electrical potentials are calculated using equation **[3.8]**. For the purpose of convenience to readers, the equation is re-quoted as **[3.19]**.

$$\frac{\partial \psi}{\partial x} = -\frac{RT}{F}\frac{\sum_i z_i D_{e,i}\frac{\partial c_i}{\partial x}}{\sum_i z_i{}^2 D_{e,i} c_i} \qquad \textbf{[3.19]}$$

While the free ionic concentrations are calculated by equation **[3.3]**, re-quoted here as **[3.20]**:

$$\frac{\partial c_i}{\partial t} = D_{e,i}\left(p + (1-p)\rho\frac{\partial c_{m,b}}{\partial c_i}\right)^{-1}\frac{\partial}{\partial x}\left(\frac{\partial c_i}{\partial x} + z_i\frac{F}{RT}c_i\frac{\partial \psi}{\partial x}\right) \qquad \textbf{[3.20]}$$

Or

$$\frac{\partial c_i}{\partial t} = D_{app}\frac{\partial}{\partial x}\left(\frac{\partial c_i}{\partial x} + z_i\frac{F}{RT}c_i\frac{\partial \psi}{\partial x}\right) \qquad \textbf{[3.21]}$$

Look at the above equations. These equations contain certain parameters, which have very different orders of magnitude. For example on one hand the diffusion coefficients are in the range of 10^{-12} m²/s and on the other hand, the concentrations are in the range of thousands of mol/m^3. In order to have stable computations, first of all the system of equations (**[3.19]** and **[3.21]**) was written in a non-dimensional way by setting the following conversions. Consider the case of a material of thickness L (m).

$$\tilde{x} = \frac{x}{L} \qquad \textbf{[3.22]}$$

$$\tilde{c} = \frac{c}{c_{\max}} \qquad \textbf{[3.23]}$$

$$\tilde{D} = \frac{D}{D_{\max}} \qquad \textbf{[3.24]}$$

$$\tilde{t} = \frac{t}{\Delta t} \qquad \textbf{[3.25]}$$

$$\tilde{\psi} = \frac{\psi}{\Delta \psi} \qquad \textbf{[3.26]}$$

Note that in the above equations, the parameters Δt and $\Delta\psi$ are presented in relations **[3.27]** and **[3.28]** respectively.

$$\Delta t = \frac{L^2}{D_{\max}} \qquad \textbf{[3.27]}$$

$$\Delta\psi = \frac{RT}{F} \qquad \textbf{[3.28]}$$

With the conversions expressed in equations **[3.22]** to **[3.28]**, we can transform the system of equations **[3.19]** and **[3.21]** into **[3.29]** and **[3.30]**. Note that in these equations, D_{max} is the maximum of all the ionic effective diffusion coefficients (m²/s) and c_{max} is the maximum concentration among all the ionic concentrations in pore solution, upstream or downstream.

$$\frac{\partial\widetilde{\psi}}{\partial\widetilde{x}} = -\frac{\sum_i z_i \widetilde{D}_i \frac{\partial\widetilde{c}_i}{\partial\widetilde{x}}}{\sum_i z_i{}^2 \widetilde{D}_i \widetilde{c}_i} \qquad \textbf{[3.29]}$$

$$\frac{\partial\widetilde{c}_i}{\partial\widetilde{t}} = \widetilde{D}_{app} \frac{\partial}{\partial\widetilde{x}}\left(\frac{\partial\widetilde{c}_i}{\partial\widetilde{x}} + z_i\widetilde{c}_i \frac{\partial\widetilde{\psi}}{\partial\widetilde{x}}\right) \qquad \textbf{[3.30]}$$

In equations **[3.29]** and **[3.30]**, the parameters capped with the sign ~ are those that have been adimensionalized. By assuming electroneutrality, the Poisson equation is equal to zero and the equation **[3.30]** can be replaced by equation **[3.31]**.

$$\frac{\partial\widetilde{c}_i}{\partial\widetilde{t}} = \widetilde{D}_{app}\left(\frac{\partial^2\widetilde{c}_i}{\partial\widetilde{x}^2} + z_i \frac{\partial\widetilde{c}_i}{\partial\widetilde{x}} \frac{\partial\widetilde{\psi}}{\partial\widetilde{x}}\right) \qquad \textbf{[3.31]}$$

Finite difference technique was chosen to solve the system of above equations. The equation **[3.29]** was discretized with a fully explicit centered scheme. The diffusive part of equation **[3.31]** was solved with a second order Cranck-Nickolson scheme, while for the convective part, an upwind Lax-Wendroff scheme was chosen. Consequently the concentration profiles were obtained with second order schemes, which provided both stability and accuracy in results. These numerical schemes can be found out in any of the technical books, written on numerical codes.

The whole code was implemented on a free environment Scilab, available on http://scilabsoft.inria.fr. The numerical code is divided into four function and one executable files. The four function files are named as ‘data’, ‘DDP’, ‘electro’ and ‘flux’, while the executable file is called as ‘MsDiff’. As the names reveal, the file ‘data’ is meant to insert input data, ‘DDP’ calculates the membrane potential, ‘Electro’ cares for electroneutrality and ‘flux’ determines the ionic fluxes. To recall, the model produces ionic concentrations, total chloride profiles, electrical potential and ionic flux. The results can be stored in any program like Microsoft excel.

3.8 Conclusions

In this chapter, the physical structure of the model MsDiff is outlined. The model solves the continuity/current law equations and accounts for the chloride interactions with the solid phase. In addition to boundary conditions, it requires a set of five experimental characteristics (if porosity is a user data) available from a single sample of material, namely density, porosity, pore solution composition, effective chloride diffusion coefficient and chloride binding isotherm. The input data does not evolve with time except the ionic diffusivities (if porosity is a user data), which are time dependent. At the end, the numerical scheme of the code MsDiff is briefly given.

References

[BIF 90] K. Bifors, Chloride-initiated reinforcement corrosion, chloride binding, CBI report 1:90, 1990.

[BOG 50] R. H. Bogue, Calculation of phase composition: The chemistry of Portland cement, Edwards Brothers, Inc., Ed., Ann Arbor, MI, second printing, pp. 184-203, 1950.

[PIT 79] K.S. Pitzer, Activity coefficients in electrolyte solutions, in R.M. Pytkowitz ed., Theory: on interaction approach. CRC Press, Boca Raton, Florida, pp. 157-208, 1979.

[POW 47] T.C. Powers, T.L. Brownyard, Studies of the physical properties of hardened Portland cement paste, Vol. 18, pp. 669-712, Michigan, USA, 1947.

[SAM 99] E. Samson, G. Marchand, J. Beaudoin, Modeling chemical activity effects in strong ionic solutions, Computational Material Sciences, Vol. 15, pp. 285-294, 1999.

[TAN 96] L. Tang, Chloride transport in concrete – Measurement and predictions, Chalmers Univ. of Technology, Publication P-96:6, 1996.

[TAY 87] H. F. W. Taylor, A method for predicting alkali ion concentration in cement pore solution, Adv Cem Res, Vol. 1, pp. 5-17, 1987.

[TEN 00] P.D. Tennis, Hamlin M. Jennings, A model for two types of calcium silicate hydrate in the microstructure of Portland cement pastes, Cement and Concrete Research, Vol. 30, pp. 855-863, 2000.

[TRU 00] O. Truc, Prediction of Chloride Penetration into Saturated Concrete – Multi-species approach, Chalmers Univ. of Tech., Göteborg, Sweden, INSA, Toulouse, France, 2000.

[WAN 01] Y. Wang, L.Y. Li, C.L. Page, A two dimensional model of electrochemical chloride removal from concrete, *Computational Materials Science*, Vol. 20, pp. 196-212, 2001.

EXPERIMENTAL METHODS

CHAPTER 4

EXPERIMENTAL METHODS

4.1 Introduction

This chapter deals with the description of test methods, envisaged to acquire the input data of MsDiff. In addition, certain experimental data was needed to validate the modeling done with MsDiff. It is to recall that the package version of MsDiff requires determining five parameters i.e. porosity, density, pore solution ionic composition, chloride effective diffusion coefficient and binding isotherm at a certain material age. Among these parameters, first three are the pure material properties, which can be determined with classical methods. Here the important emphasis will be given to the methods employed for the determination of chloride effective diffusion coefficient and binding isotherm.

4.2 Material porosity and density

Material porosity and density can be determined by well-known classical methods [AFP 97]. Here only important points are given. The additional details are available in literature and can be also found in the common laboratory manuals.

In this method, the specimens are first vacuum-saturated. The mass of the vacuum-saturated specimens in water is determined. Let this mass is M_w in grams. Also the temperature of water is determined. The water density relative to its temperature ($\rho_{w,\theta}$) in g/cm^3 can be found in literature books. After that, the saturated specimens are weighed in air. Let the mass in air is M_a in grams. Further the specimens are placed in ovens to dry at 105 ± 5°C until it acquires a constant mass. The hot specimen is allowed to cool to ambient temperature. The mass of the dry specimen in grams is determined. Let this mass is M_d. The porosity (%) and density (g/cm^3) are determined as follows:

$$p = \frac{M_a - M_d}{V} = \left(\frac{M_a - M_d}{M_a - M_w} \rho_{w,\theta} \right) 100 \qquad \textbf{[4.1]}$$

$$\rho = \frac{M_d}{V} = \frac{M_d}{M_a - M_w} \rho_{w,\theta} \qquad \textbf{[4.2]}$$

4.3 Composition of pore solution ionic composition

In this method [LON 73], the concrete specimen is placed in a pore expressing apparatus. A loading pressure is applied for expressing the pore solution. For this, the specimen is subjected to cycles of loading and unloading in order to get a few cm^3 of pore solution. The evaporable water content of the specimen is also determined. The ionic composition of the pore solution is determined using chemical techniques while the pore solution volume is determined by evaporable water. From the evaporable water and ionic concentrations, the pore solution ionic composition can be calculated.

4.4 Effective chloride diffusion coefficient

The chloride penetration in concrete is a slow process. It cannot be determined directly in a time frame that would be useful as a quality control measure. Therefore, in order to asses the chloride ingress, a test method that accelerates the diffusion process is required so as to obtain the diffusion parameter in a reasonable time period. The test [TRU 00] developed in our laboratory (LMDC) is a non-steady diffusion test under an electrical field of 400 V/m. The LMDC-test set up is shown in **Figure 4.1**. In the cathodic compartment, an alkaline solution containing 4.65 g/l of KOH and 1 g/l of NaOH along with 20 g/l of NaCl is used. The anodic solution contains the same quantities of NaOH and KOH, but without NaCl. The concrete sample is saturated with 4.65 g/l of KOH and 1g/l of NaOH before being placed in the cell. A voltage of 12 V is applied across the sample. The specimen is a three cm thick cylinder with a diameter of 11 cm. The solution sampling is performed in the cathodic chamber of the test cell rather than in the anodic compartment. This is done in order to avoid the effects of the chemical reactions, which cause a loss of chlorides at the anode [TRU 00]. The flux of chloride for the case of a solution with unit activity by the Nernst-Planck equation is given as follows:

$$J_{e,i} = -D_{e,i}\left(\frac{\partial c_i}{\partial x} + z_i \frac{F}{RT} c_i \frac{\partial \psi}{\partial x}\right) \qquad \textbf{[4.3]}$$

Here in LMDC test, the flux of chloride is presented by a simplified version of equation **[4.3]**, in which several hypotheses are made. First, it is assumed that the effect of the concentration gradient is negligible in comparison with the electrical term (first term on the right-hand side of equation **[4.3]**). The electrical potential is due to the contribution of two terms, namely the membrane potential (electrical interactions between the ionic species) and the external current.

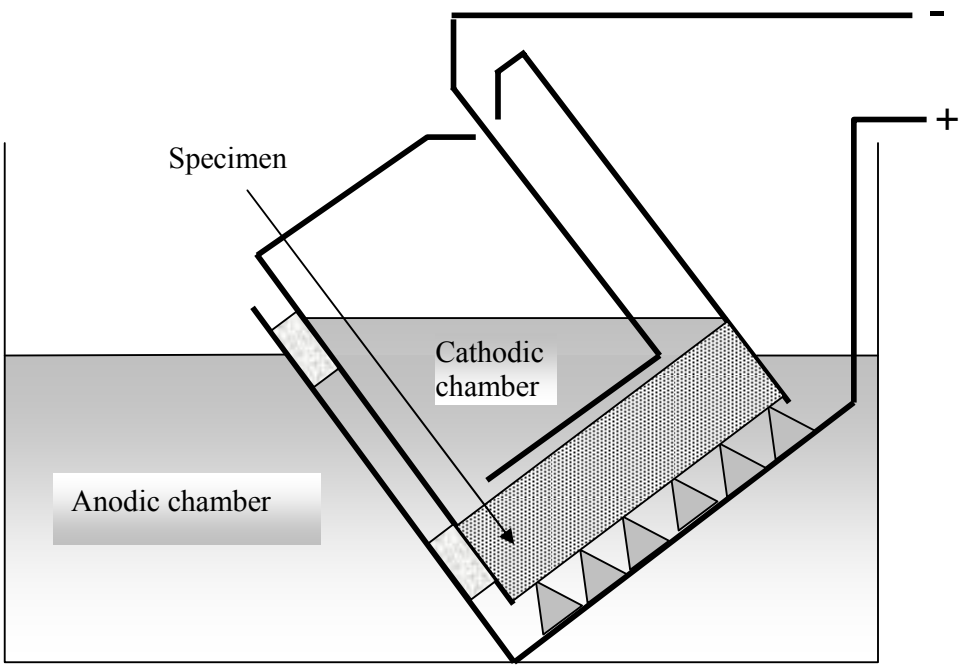

Figure 4.1 LMDC Test-setup

The latter is assumed to be preponderant and this justifies the assumption that the electrical potential is constant. As a consequence, the method proposed allows measuring the chloride diffusion coefficient through materials already contaminated with chloride. The chloride flux by the simplified version is quoted as equation **[4.4]**.

$$J_{up} = D_{NPS} \frac{F}{RT} c_0 E \qquad \textbf{[4.4]}$$

where c_0 is the chloride concentration in the cathodic compartment, E is the external electrical field and D_{NPS} represent the diffusion coefficient determined by the Simplified Nernst-Planck equation. While the parameters F, R, T, c_0 and E are known, the effective chloride diffusion coefficient can be determined if the flux of chlorides J_{up}, entering the material is known. In the following paragraph, the determination of J_{up} is presented.

It is recommended to measure the specimen diameter at two different directions, perpendicular to each other and the specimen thickness at four different points. The initial chloride content in cathodic chamber is determined prior to the start of the test. During the

test, solution samples are taken from cathodic chamber at specified intervals from the beginning to the end of the test. The chloride content in these samples is determined. The chloride content in moles, entering the concrete material at an instant t, is the difference of initial chloride content of cathodic chamber and its chloride content at instant t plus the chloride content of the solution samples taken up to instant t. A curve is drawn with chloride content entered the material at each instant t as the ordinate and the instant t as the abscissa. One such curve is shown in the **Figure 4.2**. The slope of the linear part of this curve divided by the material area exposed to chloride environment is the chloride flux, entered into the material or in other words, this is the value of parameter J_{up} encountered in relation **[4.4]**. Having known all the parameters of equation **[4.4]**, the corresponding chloride effective diffusion coefficient can be determined.

One must keep in mind that the chloride diffusivity is linked to the hypothesis of a constant boundary condition, c_0. Therefore, particular attention has to be attached to the volume of electrolyte in the cathodic chamber. If n_m is the number of chloride moles leaving the cathodic chamber and diffusing though the concrete sample during a certain time t, then n and t are related by:

$$n_m = J_{up} A t \qquad \textbf{[4.5]}$$

where A is the cross-sectional area of the concrete specimen, exposed to cathodic chamber solution. Let the initial number of moles in cathodic chamber is represented by n_0. If we suppose that a certain percentage X (or tolerance) of n_0 enters the material up to instant t, the number of moles entering the material up to this time period, n can be written as:

$$n_m = X n_0 \qquad \textbf{[4.6]}$$

with the insertion of n_m from equation **[4.5]** into **[4.6]**, we have the following relation for chloride flux J_{up}:

$$J_{up} = \frac{X n_0}{A t} \qquad \textbf{[4.7]}$$

If we put the value of J_{up} from relation **[4.7]** in **[4.4]** with $c_0 = V n_0$, we have:

$$V = \frac{FE}{RT}\frac{DAt}{X} \qquad \textbf{[4.8]}$$

where V is the volume of cathodic chamber solution. Equation **[4.8]** demonstrates that a zero tolerance X would lead to an infinite volume of solution in the cathodic chamber. Note that the needed volume is totally independent of the chloride content. The volume of the electrolyte must be the result of a trade off between the duration of the test and the tolerance X. For example, if a 5% decrease in chloride concentration is accepted for a 2.5-day test at 400 V/m (12V across a 3cm thick concrete specimen), a volume of at least 650 ml is needed for a chloride coefficient of the order of 10^{-12} m²/s.

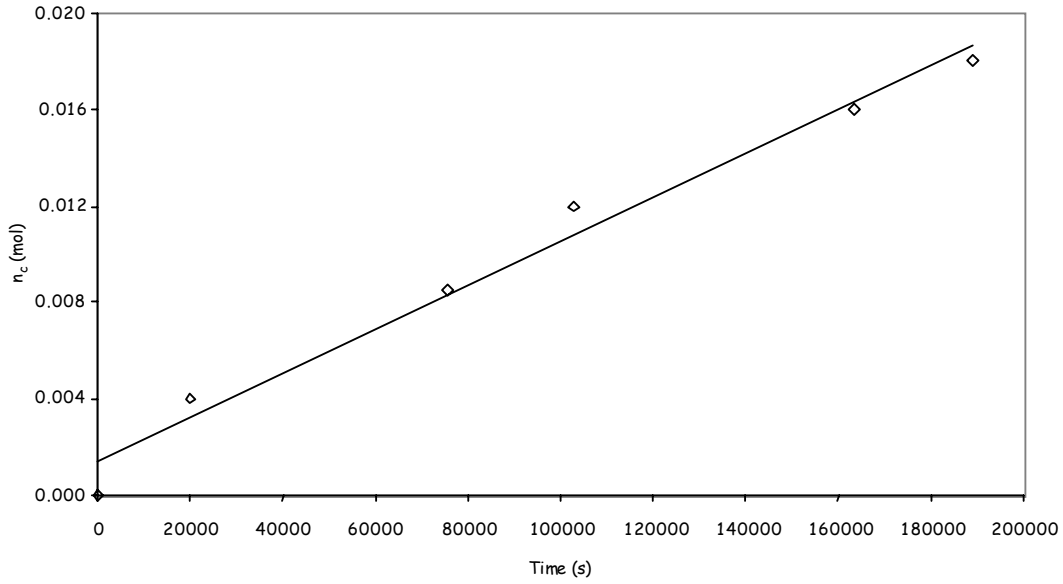

Figure 4.2 Evolution of chloride moles entering the material during LMDC test

The advantage with this method is that a concrete specimen, already polluted with chlorides can be re-employed in this method without subjecting to electrochemical extraction (to remove the chlorides from the specimen) and also the same specimen can be used again and again at different times if a time dependency of the diffusion coefficient is envisaged.

4.5 Binding isotherm

A binding isotherm is necessary as an input to the model. It is of highly importance because among the total chlorides in a concrete specimen, these are only the free contents, which participate in the corrosion of steel in reinforced concrete structures. Several techniques exist in order to determine the bound amount of chloride ions. Here we discuss two techniques, which were used during this work i.e. equilibrium method developed by Tang [TAN 96] and

the immersion tests [NOR 95]. Note that the immersion tests are not meant to produce binding isotherms. Rather they are used to obtain chloride concentration profiles, yet these profiles can be used to acquire binding isotherms, which will be discussed in the coming pages.

4.5.1 Equilibrium method

In this method, the material is reduced to powder. The crushed powder is exposed to a chloride containing solution of known initial concentration. The exposure is continued until equilibrium is reached. The chloride concentration of the solution at equilibrium is treated as the free concentration. The difference between the initial concentration and the concentration at equilibrium is attributed to bound chloride concentration.

According to the methodology of this experiment, the central regions of the 6-weeks cured specimens are wet crushed and water-sieved into 0.25-2 mm particulates. The particulate samples are vacuum dried in a desiccator filled with silica gel at room temperature for about 3 days at room temperature. Next, the samples are stored in a desiccator with de-carbonized air at 11%RH kept by saturated LiCl solution for at least 7 days. About 25 g of this sample are exposed to a known volume of a chloride containing solution, whose initial chloride concentration has already been determined. Approximately two weeks time is considered to be enough for the sample to reach equilibrium [TAN 96]. However, we used a three weeks period in order to confirm that the equilibrium has been achieved. The chloride concentration of the solution at equilibrium is determined, which corresponds to free chloride concentration. The bound chloride content in % mass of the material is determined by equation **[4.9]**:

$$c_{m,b} = \left(\frac{35.453V\left(c_0 - c_e\right)}{M_m} \right) 100 \qquad \textbf{[4.9]}$$

where $c_{m,b}$ is the bound chloride concentration in %mass of the material, V is the volume of exposure solution in cubic meter, c_0 is the initial and c_e is the equilibrium chloride concentration of the exposure solution in moles per cubic meter and M_m is the mass of the crushed powder in grams.

4.5.2 Immersion test

Usually these test methods are used to acquire water and acid-soluble chloride profiles. The idea of obtaining a binding isotherm from immersion tests came from the fact that in literature, the water-soluble chlorides are termed as the free while the acid-soluble chlorides are designated as total chlorides [BYU 04]. It is based on the view that during an immersion test a local equilibrium is reached between the chloride in the pore solution, the bound chloride on the solid phase at any distance from the exposure solution regardless of immersion time. The experimental data published by Mohammed and Hamada [MOH 03] show indeed no time effect on the chloride binding on concrete samples exposed to a marine environment for 10 to 30 years. **Figure 4.3** illustrates our view.

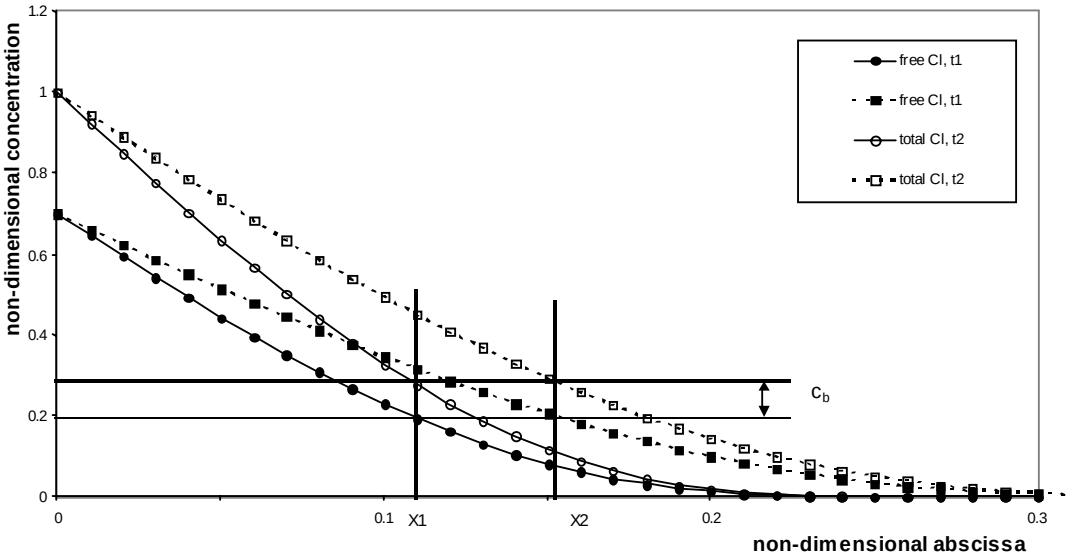

Figure 4.3 Illustration of chloride binding in concrete pores

For the sake of simplicity, non-dimensional variables are chosen. Plotted in **Figure 4.3** are the free chloride concentration profiles in the pore solution after two different exposure periods, t_1 and t_2 with $t_1 < t_2$. Also total chloride concentration profiles are shown in this figure. After an immersion time t_1, the difference between the total and the free concentration c at x_1 yields the bound amount of chloride c_b, which corresponds to the concentration c. At t_2, the free chloride

at x_1 has increased due to the diffusion of the ionic species. Yet, there exists an abscissa x_2 in **Figure 4.3** where the free chloride concentration has the same value c as before. This concentration c corresponds to the same bound amount of chlorides, c_b. This is true because chloride interactions with the solid phase are almost instantaneous. Indeed, Tang [TAN 96] noticed that equilibrium is reached after approximately two weeks, which is negligible relative to the scale of a diffusion process.

Once the acid and water-soluble chlorides at various depths from the exposed surface have been determined, the amount of bound chloride is calculated as the difference between the acid and water-soluble chlorides at each depth. In order to obtain the binding isotherm, the amount of bound chlorides is plotted on the ordinate against their water-soluble concentrations on the abscissa.

For this, only one sample of material is required. The main objective is to obtain the acid and water-soluble chloride profiles. This objective has two consequences: the direct is to generate experimental data with which numerical results could be compared, while the indirect is to determine the binding isotherm. In this sense, the proposed method of obtaining the binding isotherm belongs to the category of inverse methods.

In order to achieve these objectives, the standard bulk diffusion NT BUILD 443 method [NOR 95] was selected as the immersion test. In this method, the core concrete specimens are saturated with saturated $Ca(OH)_2$ solution (the pre-saturation method can be found in [NOR 95]) in order to minimize the sorption effects. The pre-saturated specimens are sealed on all of its sides with an appropriate sealing material except the one, which is exposed to chloride solution. Once the sealing gets dried, the specimen saturation is once again checked before putting them in the immersion cells. The specimens are exposed to a 165g/l NaCl solution prepared with distilled water. One such immersion cell is shown in **Figure 4.4**. The solution volume is so selected that the ratio of concrete exposed surface in cm^2 and solution volume in liters should be between 20 and 80. The specimens are kept in immersion for 35 days according to the specifications of this test. In case, the immersion period is increased, the existing solution should be replaced periodically (in accordance with the immersion period) by a fresh 165g/l NaCl solution in order to conserve the boundary conditions. During the test, the solution should be agitated from time to time.

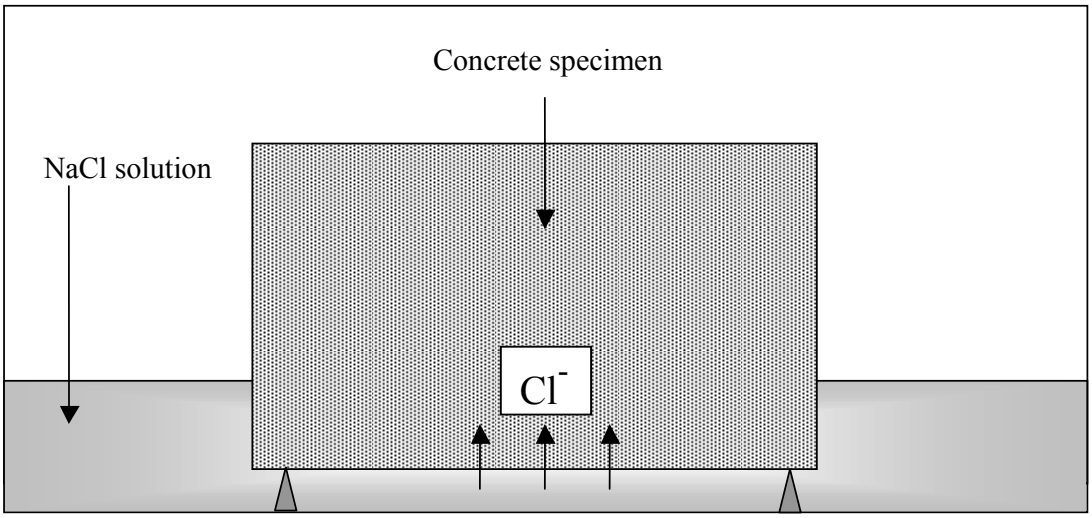

Figure 4.4 An immersion test cell

At the end of the immersion period, the concrete specimens are removed from the immersion cells. The specimens are ground with a grinding machine. One such machine used for the said purpose is shown in **Figure 4.5**. The specimens are ground in increasing depth intervals from the exposed surface and the powder corresponding to the intervals is carefully collected.

From these powder samples, the acid and water-soluble chlorides are extracted. The standard AFREM method [AFP 97] is applied to extract the acid-soluble chloride content from powdered samples. According to this method, about 5 g of homogenized dry powder are taken. Approximately 50 ml of distilled water are added and the solution is allowed to agitate for 2 minutes by means of a magnetic agitator. Then approximately 100 ml of 20% diluted nitric acid (68% concentrated) are added to this solution. The acidic solution is allowed to agitate for half an hour at 80°C. The hot solution is allowed to cool down to 20°C. The cold mix up is vacuum filtered. Approximately 250 ml of the filtrate is prepared for further analysis in potentiometric titration in order to determine the acid-chloride concentration.

The water-soluble chloride content is determined using the standard AFREM / RILEM method [RIL 02]. Approximately 5 g of homogenized dry powder are mixed with 150 ml distilled water and the solution is allowed to agitate on a magnetic agitator for 3 minutes. The mixed solution is further vacuum filtered and a 250 ml filtrate is extracted. To this solution, 2 ml of 60% concentrated nitric acid are added so as to stabilize the chlorides in the solution.

The resulted solution is then further analyzed in order to determine the water-soluble chloride concentration by potentiometric titration.

Figure 4.5 Grinding machine

The chloride concentrations in the present study were always determined experimentally with potentiometric titration. In the following, an introduction of the technique used in this study is presented.

4.6 Potentiometric titration

Titration is defined as the dissolving of an analyte and making it to react with another species in solution (titrant) of known concentration. Titrimetric analysis consists in determining the number of moles of reagent (titrant), required to react quantitatively with the substance being determined. The titrant can be added volumetrically, with a glass or automatic burette or with a low flow-rate pump.

The aim is to determine the point at which titrant amount is equivalent to the analyte amount. Once the reaction between the analyte and the titrant is perfectly characterized, the exact quantity of the analyte can be determined by simple calculations.
Potentiometric titration measures the potential of an indicator electrode as function of the titrating volume.

4.6.1 Precipitation reactions

Insoluble salts are common in nature and the most frequent use of precipitation reactions in analytical chemistry is the titration of halides in particular Cl^- by Ag^+. One of the most famous applications is the determination of chlorides in water. Precipitation reactions take place at a slightly acidic pH (~ 4.5). The precipitation of hydroxides is more delicate as their solubility can vary according to the pH of the medium.

4.6.2 Standard solution or titrant

This is a reagent of known concentration implied to make a volumetric analysis. During titration, this solution is mixed with the analyte up to a point when the reaction between the analyte and the titrant is complete.

4.6.3 Equivalence point

This is a point, which cannot be determined experimentally. We can estimate this point by observing a physical change associated with the equivalence conditions. The change during a titration is called as the "end point". The difference between the equivalence point and the end point is called the "titration error".

4.6.4 Indicator electrode

This measures an increasing or decreasing concentration of the analyte/titrant or both. This electrode is placed in the solution to observe a change (the end point) near to the equivalence point.
Reference electrode
A reference electrode contains a filling solution which does not interfere with the medium.
The two electrodes, mentioned above can either be used separately or in combined form. If a combined electrode is used, an Ag/AgCl reference element is suitable for most applications.

- Silver electrodes only require rinsing in distilled water after titration.
- The titrant addition speed is expressed in ml/min.
- When using titrant with a concentration of less than 0.1 mole/l, it is essential to work with low maximum speeds (3 to 5 ml/min). When working with a low concentration, a precipitate is formed at low rate and too fast a titration speed could lead to an "over titration".
- Precipitation reaction: $1Ag^{+} + 1X^{-} \rightarrow 1\ AgX$
- Precipitation standards:

  Silver Nitrate ($AgNO_3$): MW = 169.87 g/mole

  Sodium Chloride (NaCl): MW = 58.44 g/mole.
- The degree of the delay of the end point depends on the concentration of analyte, the composition of the solution, the concentration of titrant and the rate of the titrant adding. The larger the concentration of the analyte, the smaller the delay. The larger the amount of titrant added per unit of time, the larger the delay.

4.6.5 Instruments in the chemical laboratory (LMDC)

Electrode: METTLER TOLEDO, DM 141-SC, 0-70°C, 1mol/l KNO_3 .

Dosimat: 685 (Metrohm)

Controller: 730 SC (Metrohm)

Titrino keyboard: 736 GP

The idea behind a titration is that a reagent of precisely known concentration (the titrant) is slowly added to a known amount of an analyte until some event occurs which signals the end of the reaction. A species, which is deliberately added to produce such a signal, is called an indicator. When the signal occurs, the volume of added titrant is recorded. Knowing the stoichiometry of the reaction, and both the volume and concentration of titrant, the composition of the analyte can be found.

There are four type of equilibria used in titrimetry.

1. Acid-base,
2. Solubility,
3. Complexation,
4. Redox reactions.

In a strong acid-strong base titration for example, phenolphthalein is used as an indicator. The signal, which accompanies the end of the reaction, in this case is a change from a colorless to a pink solution. This signal known as the end point takes place at the same time that the stoichiometry of the reaction is satisfied, i.e. at the equivalence point. Similarly there are other titration techniques in which an electrode is used as an indicator.

Electrodes can be made to be sensitive to one species only

An Ag/AgCl electrode is a simple chloride ion-selective electrode, constructed by coating a silver wire with a layer of silver chloride.

Ag^+ (aq) + e^- = Ag (s); E° = 0.8 V

AgCl (s) = Ag^+ (aq) + Cl^- (aq); Ksp = $1.78 * 10^{-10}$

These two equations can be combined to yield a third half-reaction:

AgCl (s) + e^- = Ag (s) + Cl^- (aq); E° = 0.222 V

The Nernst equation for this half-reaction is as follows:

$E = 0.222V - 0.059 \log[Cl^-]$

Thus this electrode potential will be determined by the amount of chlorides in solution. This electrode can be used as an indicator electrode in a titration. The largest change in the potential and the equivalence point are determined from the data.

In case, when the chloride ion concentration is determined by potentiometric titration, a known volume of the unknown (analyte) is titrated against a solution of Ag^+ (aq). The electrode potential is plotted against the volume of the titrant added and the endpoint is determined, as demonstrated in **Figure 4.6**. In **Figure 4.7**, the titration set-up, being used in LMDC laboratory is presented.

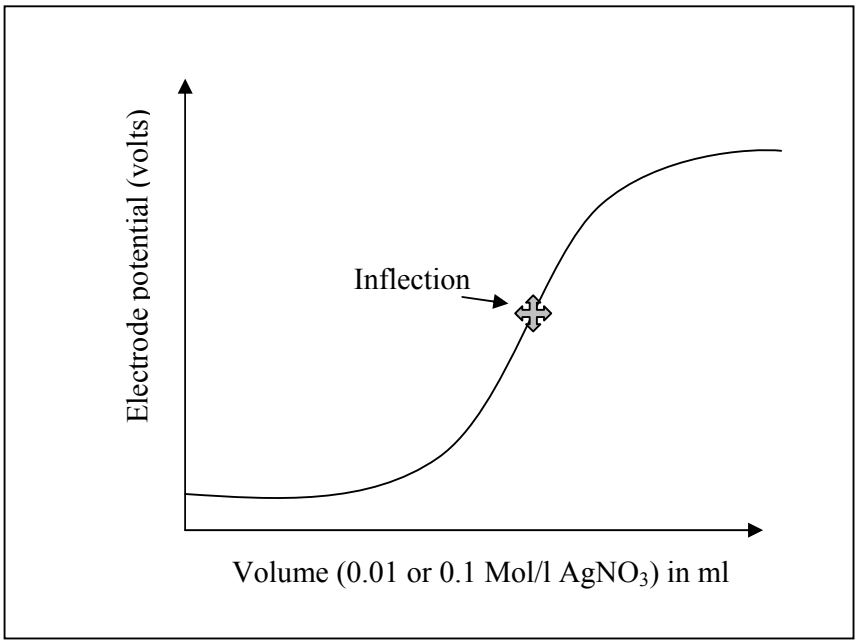

Figure 4.6 Titration curve

Figure 4.7 Titration set-up in LMDC

4.7 Conclusions

The experimental test methods have been dealt with in this chapter. These experimental methods were chosen in accordance with the input and output data of MsDiff. While the classical methods for porosity, density and composition of ionic solution have been described briefly, the importance of LMDC test and immersion tests has been highlighted. Although, immersion test reduces the number of experiments to acquire the input data, an additional test i.e. equilibrium method was also inducted to remain on safe side.

References

[AFP 97] AFPC-AFREM. Méthodes recommandées pour la mesure des grandeurs associées à la durabilité. Toulouse, France, 1997.

[LON 73] P. Longuet, L. Burglen, A. Zelwer, La phase liquide du ciment hydraté, Matériaux et Constructions, pp. 35-41, 1973.

[MOH 03] T. U. Mohammed, H. Hamada, Relationship between free chloride and total chloride contents in concrete, Cement and Concrete Research, Vol. 33, pp. 1487-1490, 2003.

[NOR 95] NORDTEST. Concrete, hardened : accelerated chloride penetration. NT BUILD 443, 1995.

[RIL 02] Rilem TC 178-TMC. Analysis of water soluble chloride content in concrete, recommendation, Materials and Structures, Vol. 35, pp. 586-588, 2002.

[TAN 96] L. Tang, Chloride transport in concrete – Measurement and predictions, Chalmers Univ. of Technology, Publication P-96:6, 1996.

[TRU 00] O. Truc, Prediction of Chloride Penetration into Saturated Concrete – Multi-species approach, Chalmers Univ. of Tech., Göteborg, Sweden, INSA, Toulouse, France, 2000.

EXPERIMENTAL PROGRAM AND CONCRETE SPECIMENS

CHAPTER 5 : EXPERIMENTAL PROGRAM AND CONCRETE SPECIMENS 90

CHAPTER 5

EXPERIMENTAL PROGRAM AND CONCRETE SPECIMENS

5.1 Introduction

In this chapter, an introduction to experimental program is presented, followed by the description of concrete material used during this work. An experimental program was unavoidable primarily to acquire input data for the model MsDiff (package of input data for MsDiff as discussed in chapter 3) and secondarily to validate modeling by MsDiff. This diverse experimental program begins with the fabrication of concrete material specimens. Next plan is to subject material specimens to standard experimental test setups described in chapter 4 in order to obtain input data to be inserted in MsDiff. At the end the modeling done with MsDiff is compared with experimental chloride profiles obtained by exposing concrete specimens to salt solutions (chapter 6).

5.2 Experimental program

Let us recall the input data package for MsDiff. It consists of five principal parameters. For the purpose of consistency these parameters are re-listed:

1. Material porosity
2. Material density
3. Material pore solution composition
4. Ionic effective diffusion coefficients
5. Chloride binding isotherm

Once this data has been achieved and inserted in MsDiff, the desired outcomes can be found out. Now the next step should be to validate these outputs experimentally. It was decided to compare free and total chloride profiles modeled with MsDiff through experimental water and acid soluble chloride profiles for the purpose of modeling validation. In order to accomplish this entire task, an experimental program was organized. The stepwise presentation of this program is given in the following few lines.

1. Fabrication of concrete specimens
2. Determination of concrete characteristics as depicted above (porosity, density and composition of pore solution)
3. Determination of chloride effective diffusion coefficient

4. Exposure of concrete specimens to immersion cells in order to obtain water and acid soluble chloride profiles
5. Determination of chloride binding isotherm

First of all concrete specimens were fabricated according to our needs keeping in view all the previewed experimentation. Its characteristics were determined with experimental methods as described in the previous chapter. The concrete porosity and density were measured at two different concrete ages following methods illustrated in chapter 4 with first measurement at 28 days and the second at 330 days in order to see a variation in these parameters with concrete age.

In the beginning when experimental program was positioned it was decided to use the composition of pore solution as determined by Nugue [NUG 02] in a concrete material similar to the one used during this work (i.e. the same cement, same aggregates and the same water to cement ratio). This composition was determined with pressure-extraction technique described in chapter 4.

The chloride effective diffusion coefficient was determined with LMDC test. Since MsDiff takes into account the variation of effective diffusion coefficient with concrete age, it was decided to execute this test more than once (at different concrete ages) so as to have a time-dependent effective diffusion coefficient. The test was carried out with the same three specimens throughout. For this purpose, in the interval between two conducted tests the specimens were conserved in a humid room (100 % humidity) under the same conditions as were kept for material curing. Additionally, the test over three specimens provides an average diffusion coefficient over all the three specimens. The accuracy of chloride diffusion coefficient was also important because the effective diffusion coefficients of other three ions (Na^+, K^+ and OH^-) are dependent upon the value of that of chloride ion. It should also be kept in mind that the least material age at exposure was 28 days. It is for this reason that the variability of D_{NPS} was watched over with effect from 28 days onward. Classically it is a normal routine to determine concrete properties at 28 days of concrete age. In addition to 28 days, the chloride diffusivity was also measured 330 and 615 days after casting.

For chloride binding isotherm, following two methods were previewed.

1. Equilibrium method
2. Immersion tests

Equilibrium method test was carried out with the material at its age of 1 year and chloride concentrations given in **Table 5.1** were chosen with keeping in view the range of chloride concentrations exercised and obtained in immersion tests. Note that up to 1 year of concrete age when equilibrium method test was carried out, we had obtained experimental results of certain immersion tests.

Table 5.1 NaCl concentrations in g/l used for equilibrium method

6	13.2	20	33	60	100	120	165	200

In the case of immersion tests, water and acid soluble chloride concentration profiles were extracted from experimental data. Bound chlorides were calculated as the difference between corresponding water and acid soluble chlorides. It should be noted that immersion tests were meant mainly to acquire chloride profiles to be compared with the modeled ones with MsDiff. Secondarily, the calculated bound chlorides from these experimental profiles also served to provide binding isotherm. Additionally some experimentation was also dedicated to certain other factors like the influence of curing period and concentration of environmental solution upon chloride ingress. At last but not least it was also previewed to determine certain parameters which were required as input data for models other than MsDiff. In brief, immersion tests were conducted in order to:

1. Acquire experimental water and acid soluble chloride profiles with different exposure periods,
2. Acquire chloride binding isotherm,
3. See the influence of curing period,
4. Observe the influence of different environmental loads,
5. Compare modeling with chloride ingress models other than MsDiff.

Firstly, immersion tests were conducted following NTBUILD 443 standard specifications [NOR 95]. The standard method takes into account 165 g/l NaCl solution as environmental load for a period of 35 days. In order to obtain chloride profiles with different exposure periods, the concrete specimens cured for 28 days were exposed to immersion durations longer than 35 days. But for that, special care was paid to the conservation of boundary conditions. The environmental solution was periodically renewed and at each renewal the concentration of old solution was checked out. Practically, the environmental solution was changed every 35 days for exposure periods longer than 35 days. Following table gives the

exposure periods exercised to carry out immersion tests with 28 days curing age and 165 g/l NaCl concentration in environmental solution. Three specimens were placed in an immersion cell per exposure period in order to obtain results averaged over 3 specimens as shown in **Figure 5.1**.

Table 5.2 Exposure periods in days for 28 days-cured concrete specimens subjected to 165g/l NaCl

35	100	200	330

In order to determine the effect of material age upon chloride penetration, certain concrete specimens were cured for prolonged durations i.e. 420 days. The exposure periods taken into account for concrete specimens cured for a longer period were 100 and 200 days.

The purpose was to compare chloride profiles with the same exposure period but with a different age at immersion. Again three concrete specimens were kept per immersion cell.

In order to observe the influence of concentration in environmental solution, certain concrete specimens with 28 days of curing were subjected to 33g/l NaCl. But for the lower concentration, the exposure periods were enhanced i.e. 180, 365 and 540 days (6, 12 and 18 months respectively). Here two concrete specimens were kept in one immersion cell keeping in view the workload.

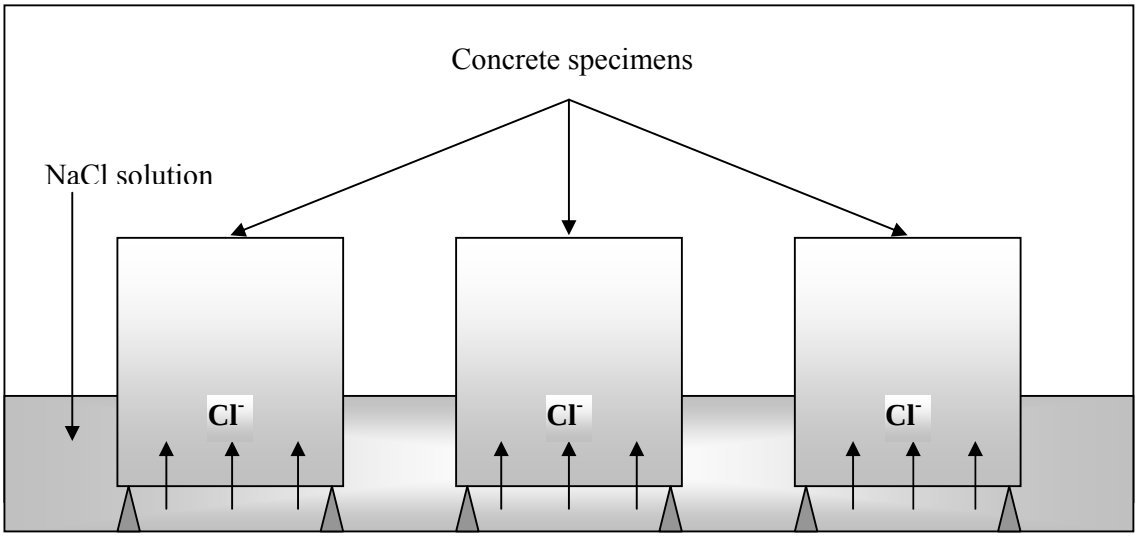

Figure 5.1 Sketch of an immersion test cell used during this work

One additional purpose of using 33g/l was to compare the experimental results with models other than MsDiff as certain chloride ingress models are based on empirical coefficients extracted from structures exposed to seawater.

A summery of the experimental program is presented in **Table 5.3**.

Table 5.3 A summery of experimental program

Exposure solution	165 g/l NaCl	33 g/l NaCl
Immersion test duration (days), 28 days of material age at exposure	35	180
	100	365
	200	540
	330	
Immersion test duration (days), 420 days of material age at exposure	100	
	200	

Once the whole experimental program has been finalized, the very next step was to have concrete specimens in hand. Following part of current chapter is dedicated to the presentation of concrete material used in this work.

5.3 Choice of material for the present work: Concrete specimens

For the concrete specimen, cement CEM I 52.5 R CP2, Garonne sand (0/4 mm) and rolled gravels (3/8 mm) were selected as the constituents.

5.3.1 Chemical composition of concrete constituents

The chemical composition of cement used in concrete specimens is given in **Table 5.4** while those of sand and coarse aggregates can be found out in **Appendix 1** of this work.

Table 5.4 Chemical composition of cement

Constituents	Percent mass
CaO	60.63 %
MgO	4.52 %
SiO_2	19.90 %
Al_2O_3	4.04 %
Fe_2O_3	2.81 %
Na_2O	0.28 %
K_2O	1.00 %
SO_3	3.81 %
Ignition loss	1.24 %

5.3.2 Bogue's phase composition

Table 5.5 gives the calculated Bogue's phase composition [BOG 50].

Table 5.5 Cement Bogue composition

Compound	Mass of each compound in Portland cement (% of cement)
C_3S	54
C_2S	22
C_3A	6
C_4AF	9

5.3.3 Concrete fabrication

Before fabrication, the following initial characteristics of concrete were envisaged [NUG 02].

Table 5.6 Concrete initial characteristics

Consistency	Slump value (cm)
Plastic	5-9

In order to obtain a concrete of plastic consistency, the following quantities of water and air were recommended in literature [BAR 96]:

Table 5.7 Water and air quantities for concrete

Water (l/m^3)	Air (l/m^3)
190	20

The maximum diameter of the gravel is 8 mm. For this gravel size, calculations allowed us to conclude the following concrete composition.

Table 5.8 Concrete composition per cubic meter of concrete

Water (l)	WC	Cement (kg)	Total aggregate volume (l)
224	0.4	560	574

A high percentage of cement content resulted due to the use of small size coarse aggregates (D_{max} = 8 mm.). In order to calculate the percentage share of sand and coarse aggregates in concrete specimens, a manual sieve analysis according to French specifications NF P 18-304 was conducted.

5.3.4 Sieve analysis for fine and coarse aggregates

The Granolumetry curve is shown in **Figure 5.2**. As shown the fine and coarse aggregates were found to be 46 and 54 % by volume of the total amount of aggregates to be used in the formulation of concrete.

5.3.5 Mass density of aggregates

The mass density of fine aggregates was determined experimentally following the French specifications NF P 18-555, while that of coarse aggregates was obtained with NF P 18-554. Their values are found to be 2630 and 2660 kg/m^3 respectively.

5.3.6 Concrete composition

Once the volume percentages and densities of sand and gravel have been determined, their dry masses in kg per cubic meter of concrete were calculated and the final concrete composition is summarized in **Table 5.9**.

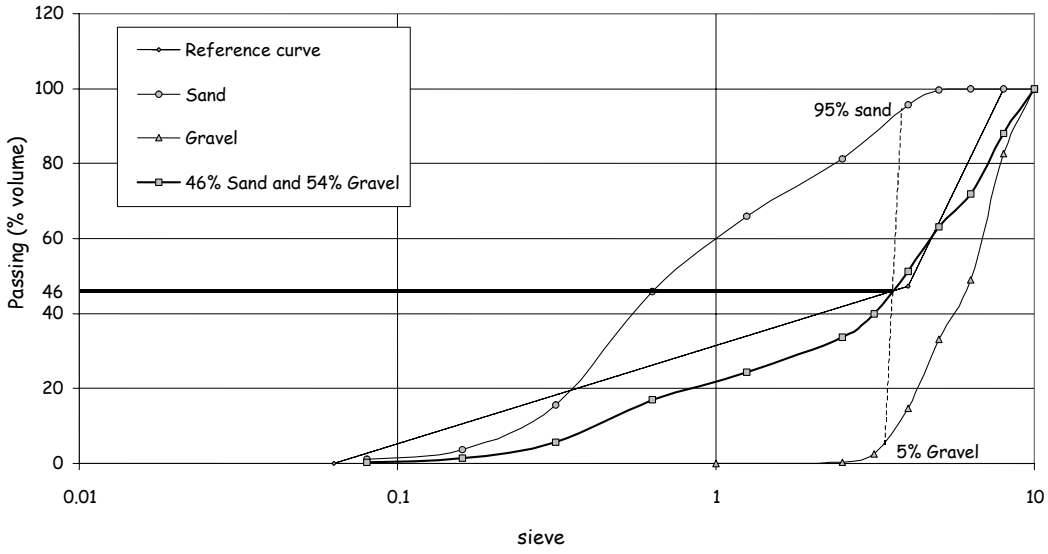

Figure 5.2 Granolumetry curve

Table 5.9 Final concrete composition per cubic meter of concrete

Cement (kg)	Sand (kg)	Gravel (kg)	Water (liters)
560	695	825	224

5.3.7 Concrete preparation and curing

The slump value of fresh concrete was measured according to French specifications NF P 18-451 and its value was found out to be 9 cm. The air content of fresh concrete was found out to be 2% according to NF EN 12350-7 standard specifications. The concrete specimens were molded following French specifications NF P18-421. The fresh concrete was poured in moulds 11 cm in diameter and 22 cm high. The cylindrical cardboard moulds were half filled with freshly prepared concrete and well shuddered with a vibrator so as to spread it uniformly within the mould. The vibration time was taken according to French specifications NF P 18-422. Next the remaining half was filled and the same vibrations were applied so as the whole mould is well packed with fresh concrete. The spilling-over concrete was removed with spatula. The moulds were covered with plastic caps. Afterwards the moulds were moved to a humid room for curing. After 24 hours the specimen were de-molded and allowed to cure for

27 days in the same wet room. After 28 days water porosity, apparent mass density and compressive strength of concrete were determined experimentally.

5.3.8 Concrete compressive strength at 28 days

For the sake of controlling the homogeneity of material, the compressive strength of three specimens after a curing period of 28 days was determined according to the French specifications NF P 18-406. The cylindrical specimens 11 cm in diameter and 22 cm in length were used for testing. The experimental values are quoted in **Table 5.10**.

Table 5.10 Experimental compressive strength at 28 days of material age

	Specimen 1	Specimen 2	Specimen 3	Average
Compressive strength (Mpa)	50.7	49.1	48.7	49.5

5.3.9 Concrete sawing to required dimensions

Prior to be used in different experimental set-ups, the concrete specimens were sawn to dimensions as per requirement for each test. The dimensions of these specimens will be discussed in the coming pages.

5.4 Conclusions

In this chapter, firstly experimental program envisaged to accomplish the task carried out during this work is illustrated. In addition, the concrete formulation, its composition and method of preparation are also demonstrated. Moreover, its properties at an age of 28 days in accordance with the version package of MsDiff have also been presented. In order to determine the variation of certain parameters with time, certain experiments were repeated at higher concrete ages.

References

[BAR 96] J. BARON and J. P. OLLIVIER, Les béton, bases et données pour la formulation, ed. Eyrolles, sous la direction de J. BARON et J. P. OLLIVIER, 1996.

[BOG 50] R. H. BOGUE, The chemistry of Portland cement, Edwards Brothers, Inc., Ann Arbor, MI, second printing, pp. 184-203, 1950.

NF P 18-304 Béton et constituents du béton, AFNOR, 1990, pp. 254-260.

NF P 18-406 Béton et constituents du béton, AFNOR, 1990, pp. 396-398.

NF P 18-421 Béton et constituents du béton, AFNOR, 1990, pp. 451-456.

NF P 18-422 Béton et constituents du béton, AFNOR, 1990, pp. 456-457.

NF P 18-554 Graulats, AFNOR, 1999, pp. 5-9.

NF P 18-555 Graulats, AFNOR, 1999, pp. 11-15.

NF EN 12350-7 Teneur en air-Méthode de la compressibilité, AFNOR, 2001.

[NOR 95] NORDTEST. Concrete, hardened : accelerated chloride penetration. NT BUILD 443, 1995.

[NUG 02] F. NUGUE, Recherche d'une méthode rapide de détermination du coefficient de diffusion en millieu cimentaire saturé, Laboratoire Matériaux et Durabilité des Constructions, Thèse de l'Institut National des Sciences Appliquées, Toulouse, 2002.

EXPERIMENTAL AND NUMERICAL OUTCOMES

CHAPTER 6

EXPERIMENTAL AND NUMERICAL OUTCOMES

6.1 Introduction

This chapter is intended to present experimental results along with their analysis and numerical outcomes of MsDiff. Experimental results were obtained following the program described in chapter 5. These results will be presented in a sequential order in which primarily the input data obtained will be described followed by the chloride profiles obtained in immersion tests and at the end, the comparison of experimental chloride profiles with MsDiff modeling will be stated. In addition, the results of the tests carried out to determine the influence of chloride concentration in environmental solution and material age at immersion on chloride ingress will also be presented and discussed. This chapter will also cover some additional data extracted from immersion tests, needed as input data for chloride ingress models other than MsDiff.

6.2 Part 1: Experimental results

6.2.1 Material specification

Although the material has been already discussed in detail in chapter 5, for the purpose of consistency the important points are re-collected. The concrete composition, its porosity, density and composition of interstitial solution are given in **Table 6.1**, **Table 6.2** and **Table 6.3** respectively.

Table 6.1 Concrete composition. All quantities are expressed as per m^3 of concrete

Constituents	Cement (kg)	Water (l)	Sand (kg)	Gravel (l)
Composition	560	224	695	825

Table 6.2 Material porosity and density at 28 and 330 days of concrete age

Water porosity (%)		Density (kg/m^3)	
Age (28 days)	Age (330 days)	Age (28 days)	Age (330 days)
15.9	15.5	2281	2252

Table 6.3 Composition of concrete pore solution in moles/m^3

Ionic entity	Na^+	K^+	Cl^-	OH^-
Composition	23	156	1	178

Recall that the pore solution composition as described in **Table 6.3** was acquired from the work of NUGUE [NUG 02] in which pore pressing technique was applied on a similar material in order to determine the ionic composition of the concrete pore solution. The obtained values were 23 and 156 mol/m^3 respectively for Na^+ and K^+. Calcium was also detected but its concentration was lower than 0.1 mol/m^3. The average measured pH value was 12.8. Therefore the hydroxyl ion concentration was adjusted in order to conserve the electroneutrality condition. For modelisation a value of [OH^-] equal to 179 mol/m^3 was decided which corresponds to a pH of 13.25.

6.2.2 Ionic diffusion coefficients

The first step towards the determination of ionic diffusion coefficients begins with that of chloride ions, which was obtained through LMDC test. This method has been described in chapter 4. The material diameter and thickness were measured as already described prior to testing. The average diameter of all the three cylindrical specimens was same i.e. 11.17 cm (as they were sawn off from the same concrete sample (11x22 cm)) while the average thicknesses of the three specimens are quoted in **Table 6.4**.

Table 6.4 Average thickness of three specimens used for LMDC test

Specimen	1	2	3
Thickness (cm)	3.04	3.05	3.05

Recall that LMDC method involves the extraction of solution from the upstream compartment at various intervals during the test. At each interval, three 1 ml samples are collected from the cell.

In order to calculate the D_{NPS}, primarily the average chloride content in moles of all the three samples taken at instant t was calculated. From this average value and all those, calculated at time $t_s<t$, the chloride content entered the material up to instant t was determined. A curve was drawn with cumulated chloride content in moles as ordinate and time t in seconds as abscissa. The curves obtained are shown in **Figures 6.1**, **6.2** and **6.3** respectively for the three conducted LMDC tests.

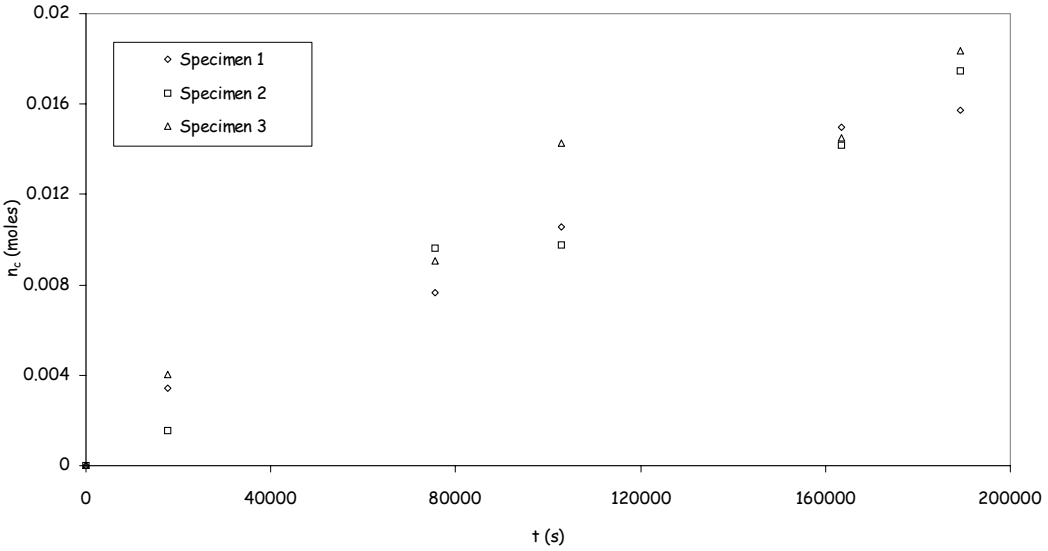

Figure 6.1 Cummulative chloride content n_c as a function of time obtained in LMDC test carried out at 28 days of material age

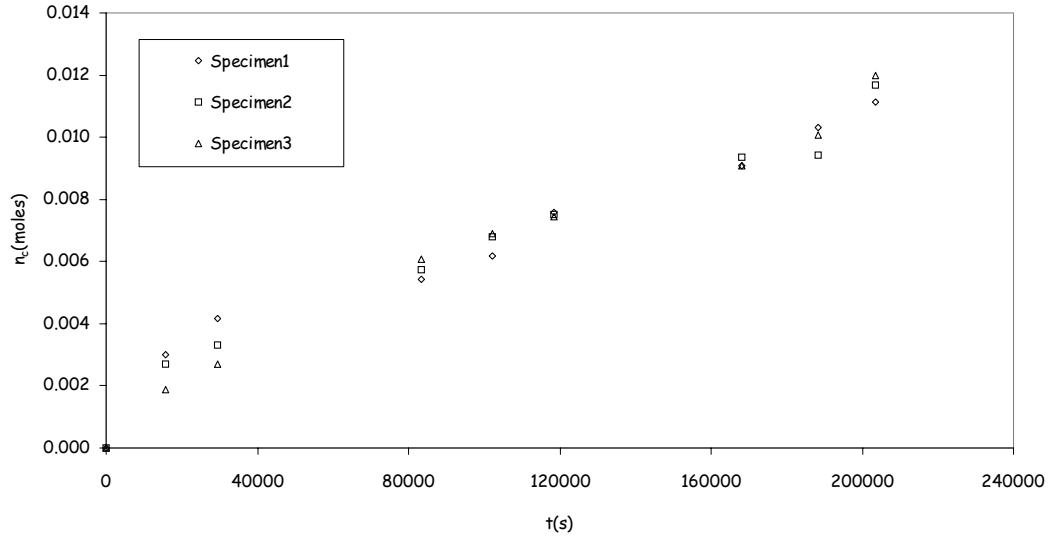

Figure 6.2 Cummulative chloride content n_c as a function of time obtained in LMDC test carried out at 330 days of material age

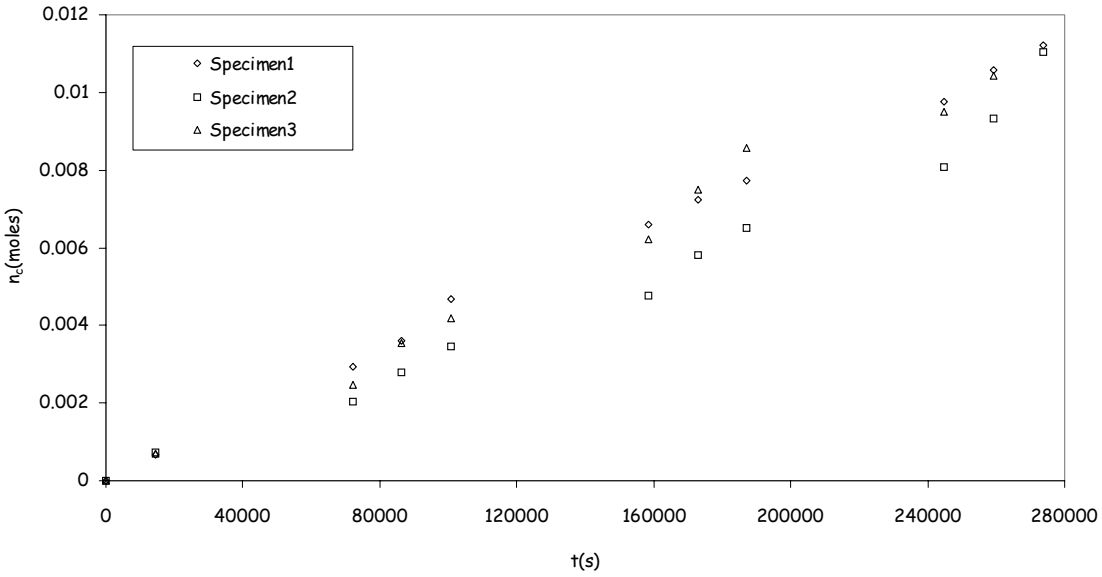

Figure 6.3 Cummulative chloride content n_c as a function of time obtained in LMDC test carried out at 615 days of material age

The fluxes as calculated from the slopes of the curves, shown in **Figures 6.1**, **6.2** and **6.3** and the corresponding cross-sectional areas of the specimens are provided in **Table 6.5**.

Table 6.5 Chloride fluxes J_{up} (moles/m^2.s) obtained from linear trend lines and concrete x-sectional areas

Material age (days)	28	330	615
Specimen 1	8.34E-06	4.76E-06	4.6E-06
Specimen 2	9.07E-06	4.93E-06	3.77E-06
Specimen 3	9.02E-06	5.34E-06	4.38E-06
Average	8.42E-06	4.76E-06	4.10E-06

The flux values were inserted in equation **[6.1]** in order to calculate D_{NPS}.

$$D_{NPS} = \frac{RT}{c_0}\frac{J_{up}}{FE} \qquad \textbf{[6.1]}$$

Recall that in relation **[6.1]** c_0 is the initial chloride concentration in moles/m^3 determined experimentally. The values of D_{NPS} so calculated are given in **Table 6.6**.

Table 6.6 D_{NPS} values in m²/s

Material age (days)	28	330	615
Specimen 1	1.58E-12	0.89E-12	0.77E-12
Specimen 2	1.72E-12	0.93E-12	0.71E-12
Specimen 3	1.71E-12	1E-12	0.8E-12
Average	1.6E-12	0.89E-12	0.77E-12

The next step after determining D_{NPS} was to develop a time dependent diffusion coefficient relation as described by relations **[3.10]** and **[3.11]** (page 62) in chapter 3. In order to achieve that, D_{NPS} so obtained were drawn against the concrete age in days at which the corresponding coefficients were determined as shown in **Figure 6.4**.

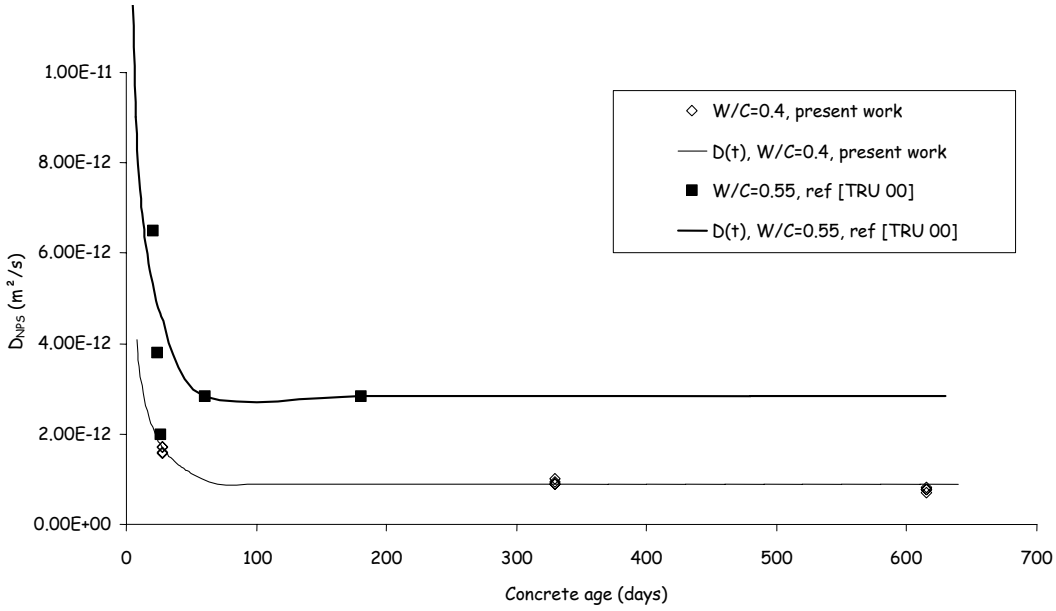

Figure 6.4 Variation of D_{NPS} with concrete age

The modeled curve (D(t), *W/C* =0.4), shown in **Figure 6.4** represents the following time dependent relationship for effective diffusion coefficient of chlorides.

$$D_e(t) = 8.10^{-13}\left(\frac{70}{t}\right)^{0.5} \qquad \textbf{[6.2]}$$

In equation **[6.2]**, D_e quoted is actually the D_{NPS} previously described. The value of D_{NPS} so calculated was used as effective diffusion coefficient. This equation was used as modeling input for MsDiff.

Equation **[6.2]** suggests that the diffusion coefficient becomes constant beyond a certain material age. The age at which the effective diffusivity is no more time-dependent varies with the type of binder [TAN 96]. For CEM I type cement, this age has been found out to be 70 days [TRU 00 KHI 05].

Up to this point, all the input data except binding isotherm has been determined. In order to acquire binding isotherm, two techniques were used i.e. equilibrium method and immersion tests and in the latter case that was achieved from experimental water and acid-soluble chloride profiles, hence its illustration will be given after the description of experimental chloride profiles obtained in immersion tests.

6.2.3 Experimental chloride profiles

In order to validate MsDiff modeling with experimental results, immersion test method NT BUILD 443 was selected. Additionally from this test, binding isotherms were acquired as discussed earlier. Recall that MsDiff calculates free and total chloride profiles, while through immersion tests we can get acid and water-soluble chloride profiles. In literature, acid-chlorides are termed as total chlorides while the extraction of chlorides through water is one of the methods used to determine the free chloride content. Thus the experimental water and acid-soluble chloride profiles can be used to validate the free and total chloride profiles calculated with MsDiff.

Immersion tests were conducted in accordance with the experimental program illustrated in chapter 5. We will discuss the experimental results in the following chronological order.

1. NaCl concentration of 165 g/l with concrete age of 28 days at exposure
2. NaCl concentration of 165 g/l with concrete age of 420 days at exposure
3. NaCl concentration of 33 g/l with concrete age of 28 days at exposure

It should be noted that the chloride profiles in the next pages are presented with chloride concentrations in units of % mass of concrete whereas the captions of the figures and tables demonstrate the concentrations in g/l. The table and figure captions are given in g/l because the conducted experiments are the standard tests in which concentrations are usually given either in g/l or moles/m^3 of NaCl. The experimental chloride concentrations are given in %

mass of concrete for the sake of consistency with the data published in literature and also because the chloride threshold values for the initiation of corrosion of steel bars are given in % mass of the material. However for convenience to the readers, the equivalent surface free concentrations in different units are presented in **Table 6.7**.

Table 6.7 Environmental concentrations in equivalent values

NaCl concentration (g/l)	Cl^- (moles/m^3)	Cl^- (g/l)	Cl^- (% mass of concrete)
165	2824	100	0.7
33	564	20	0.14

6.2.3.1 NaCl concentration of 165 g/l with concrete age of 28 days at exposure

The chloride penetration in concrete has been presented in the form of chloride penetration profiles, where the ordinate represents acid and water-soluble chloride concentrations and the abscissa demonstrates the depth from exposed surface. Except for 35 days (where two specimens were analyzed) three specimens were put in an immersion cell for one exposure period. Moreover, we were unable to determine the penetration depth for specimen 3 in the case of 100 days of immersion due to loss of material. In **Table 6.8**, the penetration depths achieved during each immersion test are given. Note that these penetration depths correspond to the distance of the center of the concrete slice, whose average chloride concentration reached a background value (Appendix 4). This background value or concrete initial chloride concentration (as is termed in literature) may be determined from a virgin concrete specimen powder. The precision in each penetration depth corresponds to half of the thickness of slice, as the chloride concentrations correspond to an average value over whole of the slice. The penetration depth slightly varies from one to the other experimental profile, as is obvious from **Table 6.8**.

Table 6.8 Achieved penetration depths (x_p) in mm for 165 g/l NaCl and 28 days of concrete age at exposure

Exposure period (days)	35	100	200	330
Specimen 1	14.4 ± 1	18.4 ± 1.5	21.9 ± 1.5	24.8 ± 2
Specimen 2	14.6 ± 1	18.3 ± 1.5	21.9 ± 1.5	26 ± 2
Specimen 3	---------	---------	21.1± 1.5	25.9± 2

If the penetration depths, x_p are plotted against the square root of exposure time, **Figure 6.5** results. In this figure, the Y-error bars correspond to the precision described in **Table 6.8**. The obtained curve shows that the penetration depth follows a non-linear path with increase of exposure period. If a linear-trend line is drawn, the following equation results:

$$x_p = 1.01\sqrt{(t - t_{ex})} + 8 \qquad \textbf{[6.3]}$$

where x_p is the penetration depth in mm, t is the materials age and t_{ex} is materials age at exposure in days. Equation **[6.3]** is quoted here just to make a comparison with the penetration depths, achieved in the case of 33 g/l NaCl. This comparison will be discussed in the coming pages. If the reinforcement bars are located at a distance of 40 mm from the concrete surface facing salt solution, the first chlorides should reach it in approximately 1003 days. **Figure 6.5** also suggests that the rate of penetration should be higher during the earlier period of exposure than in the later stage.

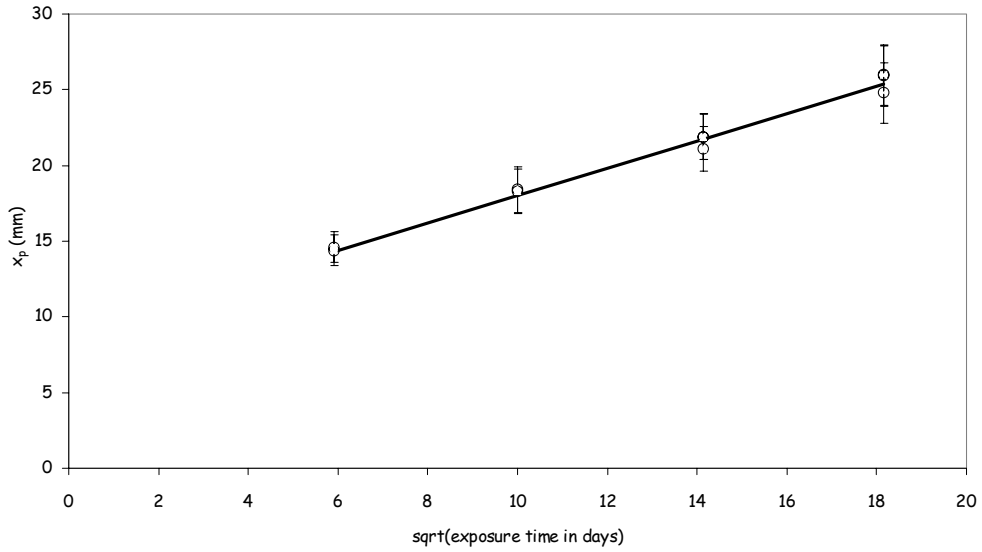

Figure 6.5 Variation of penetration depth with exposure period corresponding to 28 days-aged concrete with 165 g/l NaCl in exposure solution

The water and acid-soluble chloride profiles from immersion tests, carried out with 165 g/lNaCl and 28 days of concrete age at exposure are shown in **Figures 6.6** to **6.9** for 35, 100, 200 and 330 days of immersion respectively. The chloride concentrations are represented by different shapes, both hollow and filled ones, as a function of distance from the exposed surface. Recall that the chloride concentrations were obtained from concrete powders,

collected from slices at increasing depth from the exposed surface. The chloride concentrations determined in this way actually represent the average chloride concentration of the concrete slice and albeit it would be more appropriate to present the abscissa values with rectangular bars representing the whole slice thickness instead of individual points, yet for the purpose of simplicity and convenience, these concentrations are plotted against the distance of the center point of these slices from exposed surface. Note that in these figures, the large hollow shapes represent the acid-soluble chloride concentrations and the small filled shapes represent the water-soluble ones. The surface free chloride concentration, represented by $C_{f,s}$, corresponds to the chloride concentration in the exposure solution. Also in these figures, the chloride profile for each specimen is specified so that the difference of a pair of water and acid-soluble chloride profile relative to one specimen with respect to the other specimen could be easily observed.

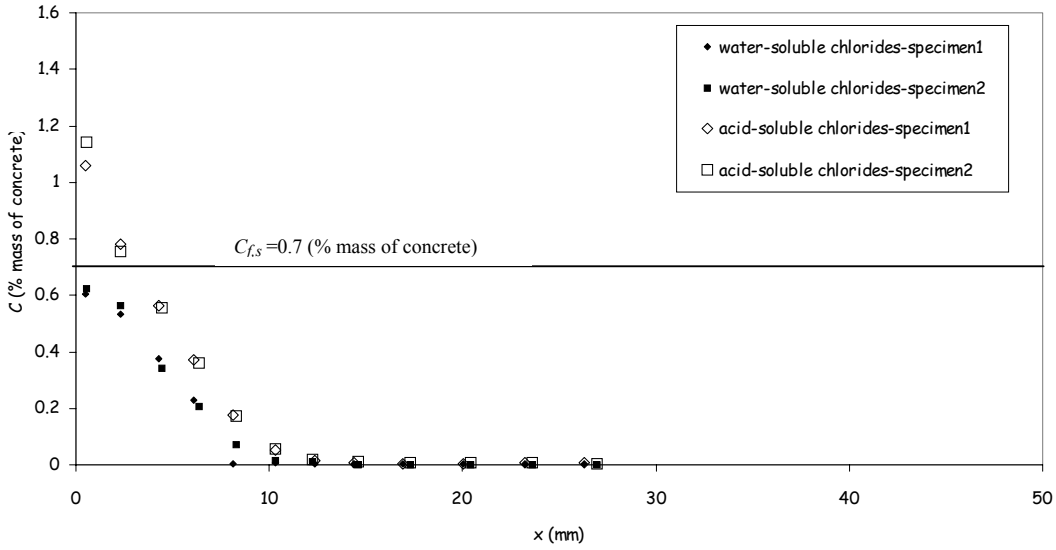

Figure 6.6 Water and acid-soluble chloride profiles obtained from immersion test with 165 g/l NaCl for an exposure period of 35 days and 28 days of concrete age at exposure

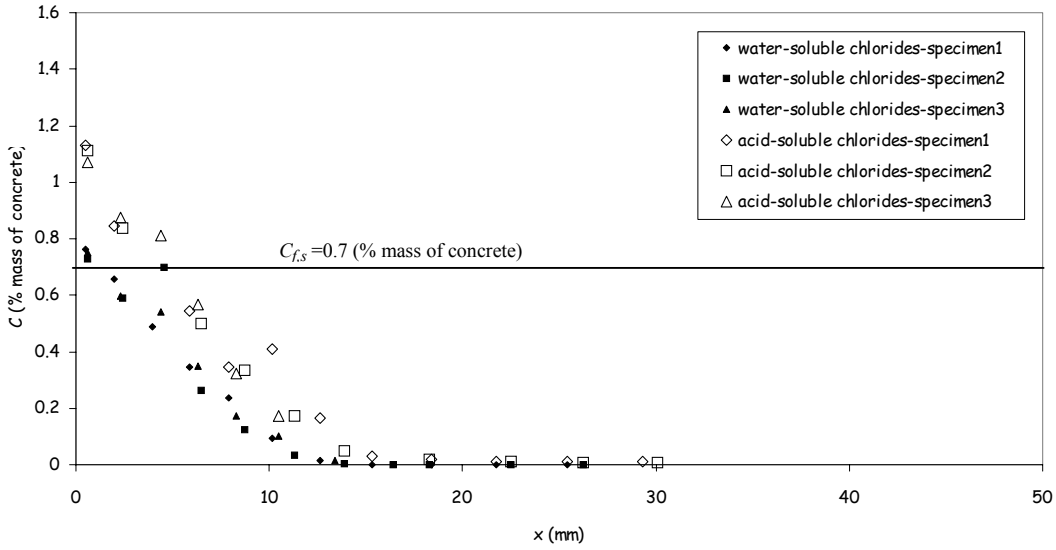

Figure 6.7 Water and acid-soluble chloride profiles obtained from immersion test with 165 g/l NaCl for an exposure period of 100 days and 28 days of concrete age at exposure

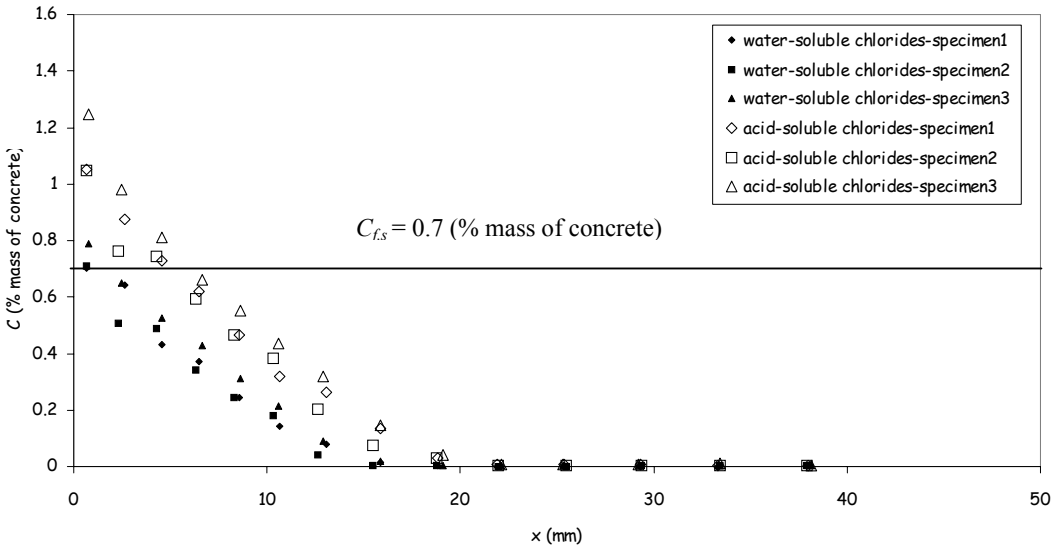

Figure 6.8 Water and acid-soluble chloride profiles obtained from immersion test with 165 g/l NaCl for an exposure period of 200 days and 28 days of concrete age at exposure

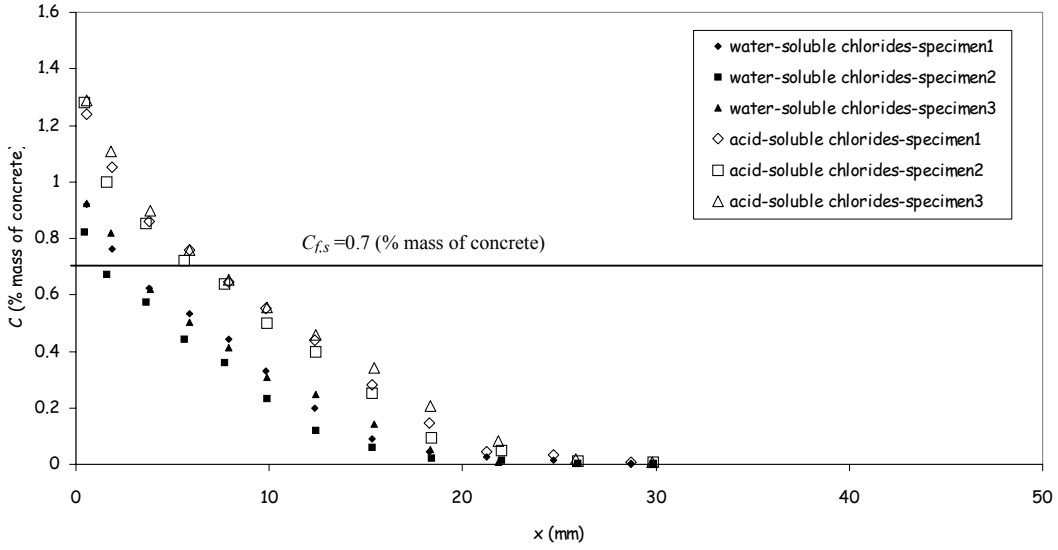

Figure 6.9 Water and acid-soluble chloride profiles obtained from immersion test with 165 g/l NaCl for an exposure period of 330 days and 28 days of concrete age at exposure

In **Figure 6.10**, the acid-soluble chloride concentrations as obtained in the four immersion tests (35, 100, 200 and 330 days), described above, are plotted on ordinate against the corresponding water-soluble chloride concentrations on absissa. This figure shows that the total chloride concentration for a given chloride concentration in pore solution does not depend on the immersion time or in other words, the acid-soluble concentration was approximately same for one value of water-soluble one whatsoever was the immersion period, this at least for the exposure times chosen in this study. Since total chlorides are the sum of free and bound contents, it can be concluded that the chloride binding was independent of the time of exposure. And if such is the case, the binding isotherm determined from one immersion test (e.g. 35 days standard NT BUILD 443 test) could be utilized to extrapolate results for higher immersion periods.

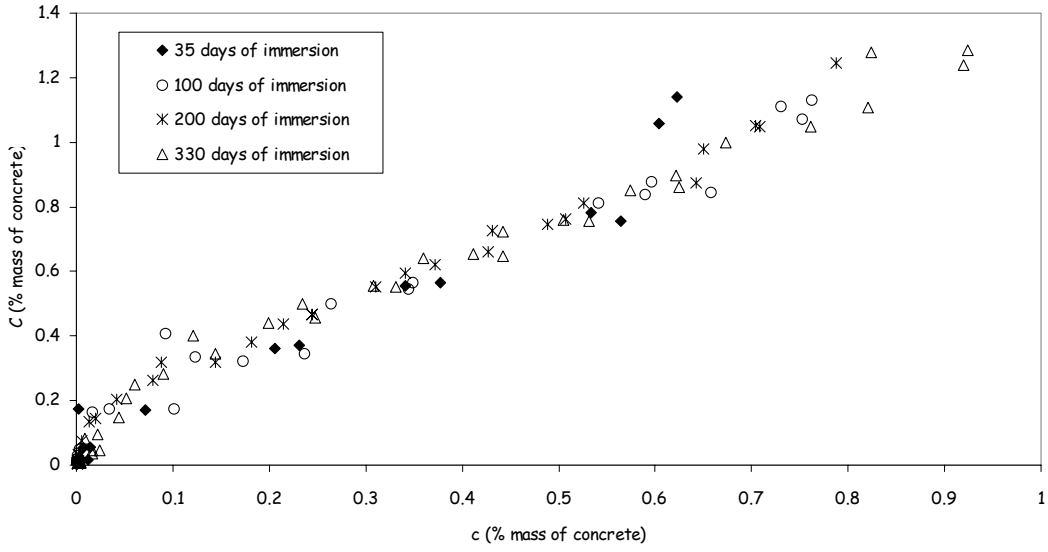

Figure 6.10 Acid-soluble chlorides versus water-soluble chloride for immersion tests of 165 g/l NaCl with 28 days of concrete age at exposure

6.2.3.2 NaCl concentration of 165 g/l with concrete age of 420 days at exposure

As described earlier, these tests were carried out in order to watch the effect of concrete age at exposure on chloride ingress. For that some specimens were cured for a much longer period of 420 days instead of 28 days. While all the other conditions were kept identical (as for 28 days-cured specimens), three specimens were exposed to 165 g/l NaCl for a period of 100 days and the other three for 200 days in order to compare with the results of 28 days-aged concrete having the same immersion period. The acid and water-soluble chloride profiles are shown in **Figures 6.11** and **6.12** respectively for 100 and 200 days of immersion.

Note that in **Figure 6.12**, the water-soluble chloride concentrations corresponding to specimen 3 have not been shown. This is because the measured values were not compatible with the values obtained with the other 2 specimens. Rather significantly dispersed values were obtained. So it was decided to discard these values [NOR 95]. In **Figures 6.13** and **6.14**, the water-soluble chloride profiles obtained with 28 and 420 days of concrete age at exposure are presented for the sake of comparison. While the acid-soluble concentrations versus water-soluble ones obtained in the two cases are demonstrated in **Figures 6.15** and **6.16**.

The penetration depths were obtained in the same way as in the case of specimens with 28 days of age at exposure. These depths are quoted in **Table 6.9**.

Table 6.9 Achieved penetration depths in mm for 165 g/l NaCl and 420 days of concrete age at exposure

Exposure period (days)	100	200
Specimen 1	16.4 ± 1	19.5 ± 1.5
Specimen 2	18.4 ± 1	22 ± 1.5
Specimen 3	16.2 ± 1	22.6± 1.5

If we compare the penetration depths in the 2 cases i.e. 28 and 420 days of concrete age at immersion, given in **Tables 6.8** and **6.9**, we come to observe that they are in quite fair agreement with each other.

The conclusions about the effect of exposure period upon chloride ingress are presented in section **6.4.2** of this chapter.

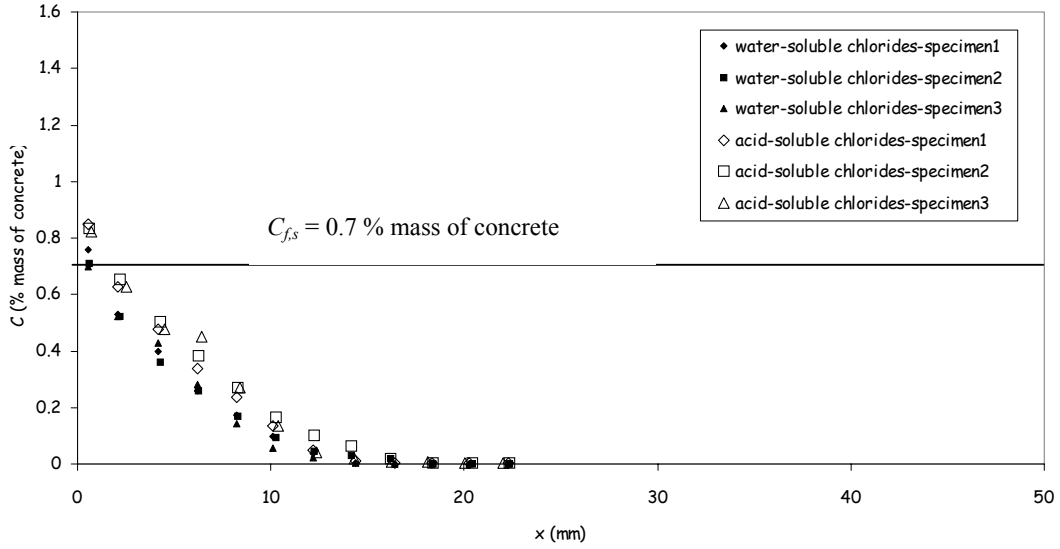

Figure 6.11 Water and acid-soluble chloride profiles obtained from immersion test with 165 g/l NaCl for an exposure period of 100 days and 420 days of concrete age at exposure

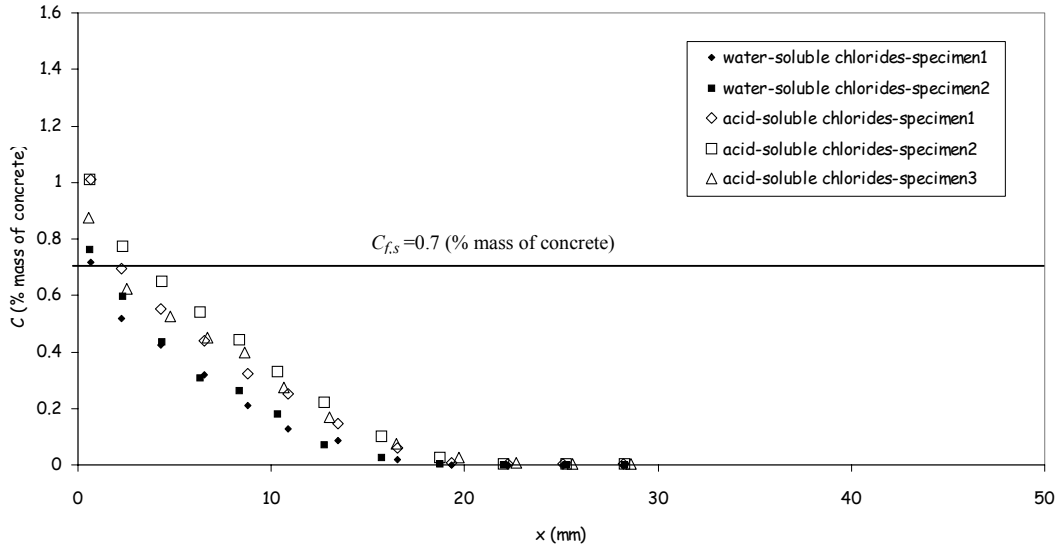

Figure 6.12 Water and acid-soluble chloride profiles obtained from immersion test with 165 g/l NaCl for an exposure period of 200 days and 420 days of concrete age at exposure

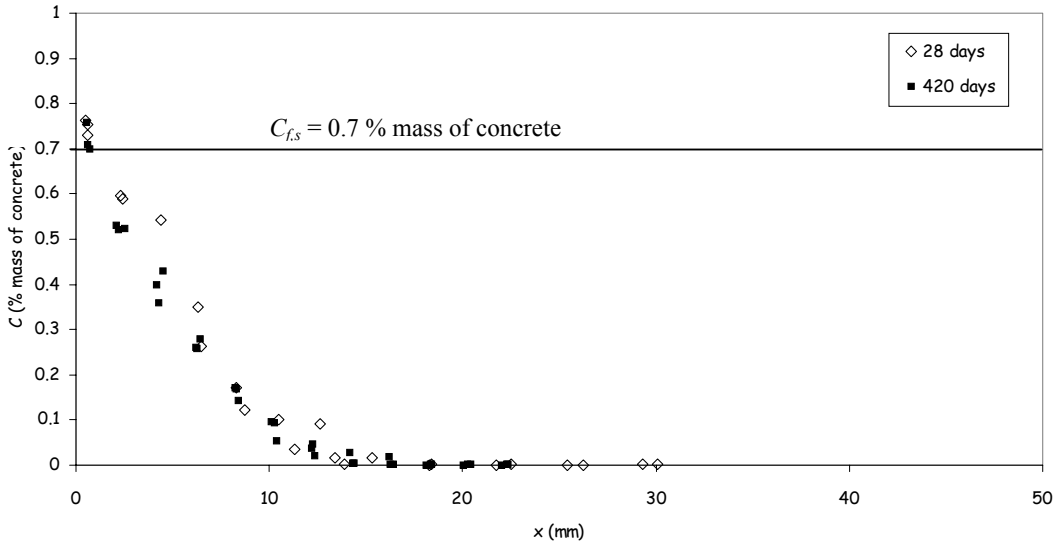

Figure 6.13 Comparison of water-soluble chloride profiles for 100 days of exposure but with different age (28 and 420 days) at exposure

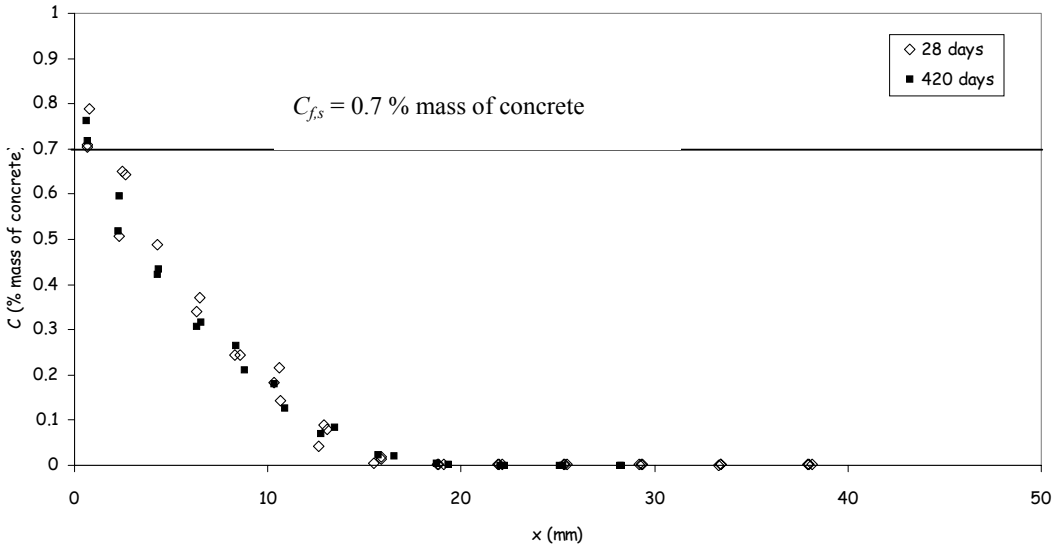

Figure 6.14 Comparison of water-soluble chloride profiles for 200 days of exposure but with different age (28 and 420 days) at exposure

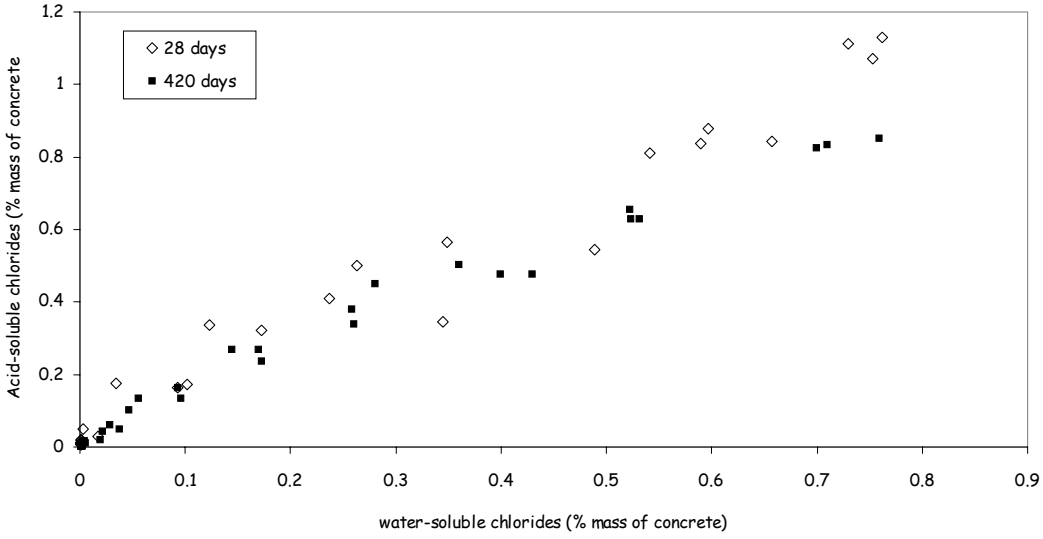

Figure 6.15 Acid versus water-soluble chloride after 100 days of immersion for concrete with 28 and 420 days of age at exposure

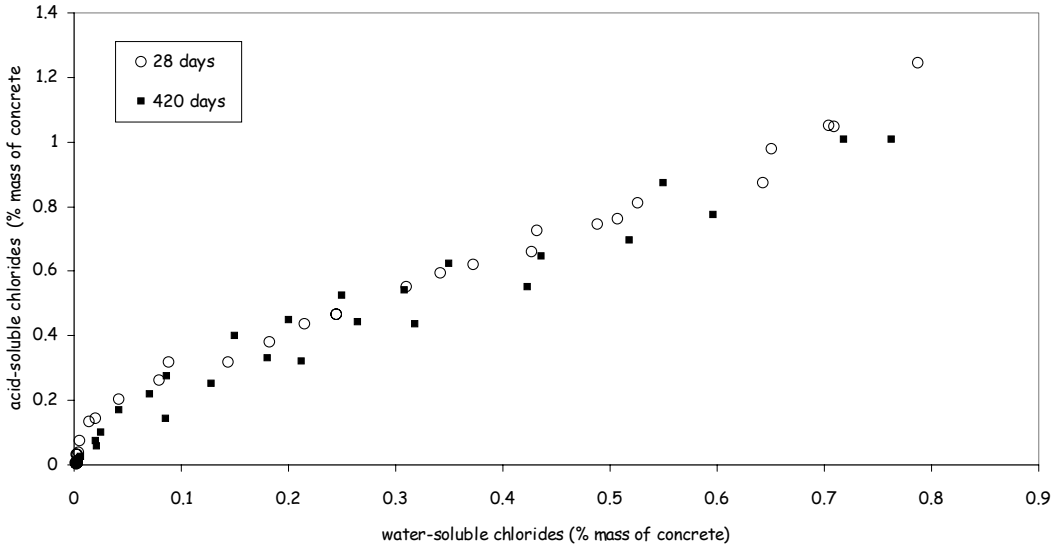

Figure 6.16 Acid versus water-soluble chloride after 200 days of immersion for concrete with 28 and 420 days of age at exposure

6.2.3.3 NaCl concentration of 33 g/l

Only 28 days-cured concrete specimens were exposed to this concentration. But where concentration of environmental solution was lowered the exposure periods were accordingly enhanced in order to obtain significant chloride penetrations after immersion. The exposure periods exercised were 180, 365 and 540 days (or 6, 12 and 18 months respectively). The observed acid and water-soluble chloride profiles are shown in **Figures 6.18**, **6.19** and **6.20** respectively.

From the plotted chloride profiles, the penetration depths for each exposure period were obtained in the similar way as described above. These penetration depths are shown in **Table 6.10**.

Table 6.10 Penetration depths in mm obtained in case of 33 g/l NaCl concentration

Exposure period (days)	180	365	540
Specimen 1	14.9 ± 1	19.9 ± 1	24.7 ± 1
Specimen 2	14.6 ± 1	19.7 ± 1	24.8 ± 1

If the penetration depths, x_p are plotted against the square root of exposure time in a similar way as above, **Figure 6.17** results. The obtained curve shows that the penetration depth follows a non-linear path with increase of exposure period. If a power-trend line is drawn, the following equation results:

$$x_p = 1.01\sqrt{(t - t_{ex})} \qquad \textbf{[6.4]}$$

where x_p is the penetration depth in mm, t is the materials age and t_{ex} is the materials age at exposure in days. Equation **[6.4]** indicates that the penetration depth is due to only diffusive process if the problem is described by the Fick's second law of diffusion, assuming a constant apparent diffusion coefficient D_a. Results are different with 165 g/l NaCl concentration as shown by equation **[6.3]**. After 35 days, the slope of the curve is the same as in equation **[6.4]**. However that is not the case during the very first days of immersion (< 35 days). If the reinforcement bars are located at a distance of 40 mm, the first chlorides should reach it in approximately 1570 days. If we compare this value of 1570 days with 1003 days, obtained in the previous case, we come to know that this is approximately 50% less than the time, obtained in the case of 165 g/l NaCl. Note that the NT BUILD 443 method implies a chloride concentration of 100 g/l of chlorides (165 g/l NaCl), which is more than 5 times the one, usually found in marine environment (14 ± 4 g/l of chlorides). The exposure solution

concentration (33 g/l NaCl) here is 5 times lesser than implied in NT BUILD 443 test (165 g/l NaCl). In that sense, NT BUILD 443 test is an accelerated immersion test, giving the same advantage as can be achieved with diffusion tests under an electrical current.

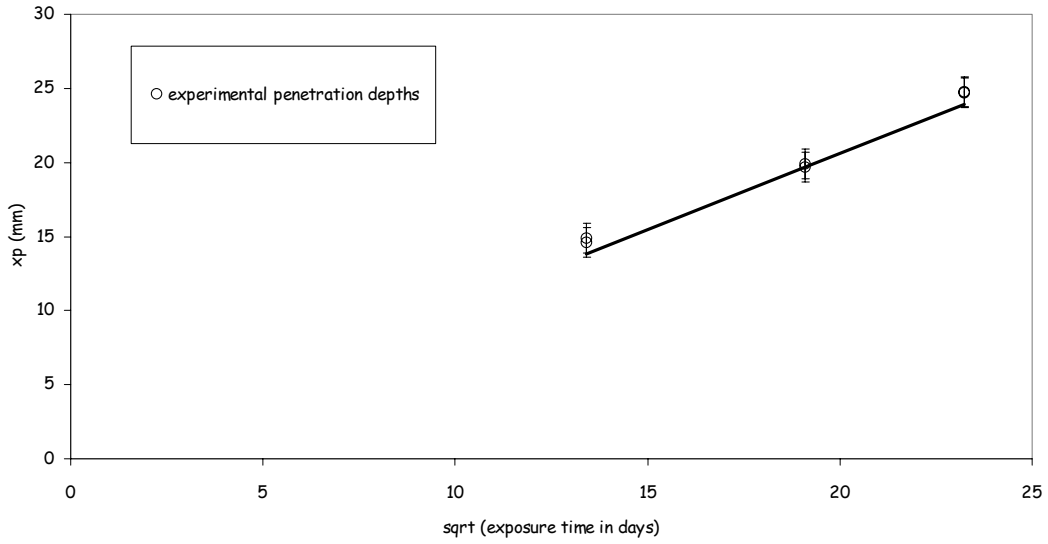

Figure 6.17 Variation of penetration depth with exposure time in 33 g/l NaCl

Look at the penetration depths, achieved in the case of 35 days of immersion with 165 g/l NaCl and 180 days of immersion with 33 g/l NaCl. Both these tests provided approximately the same chloride penetration depth. Thus a 5 times increment in exposure solution concentration led to achieve a penetration depth, which could be achieved with an exposure period 5 times more large.

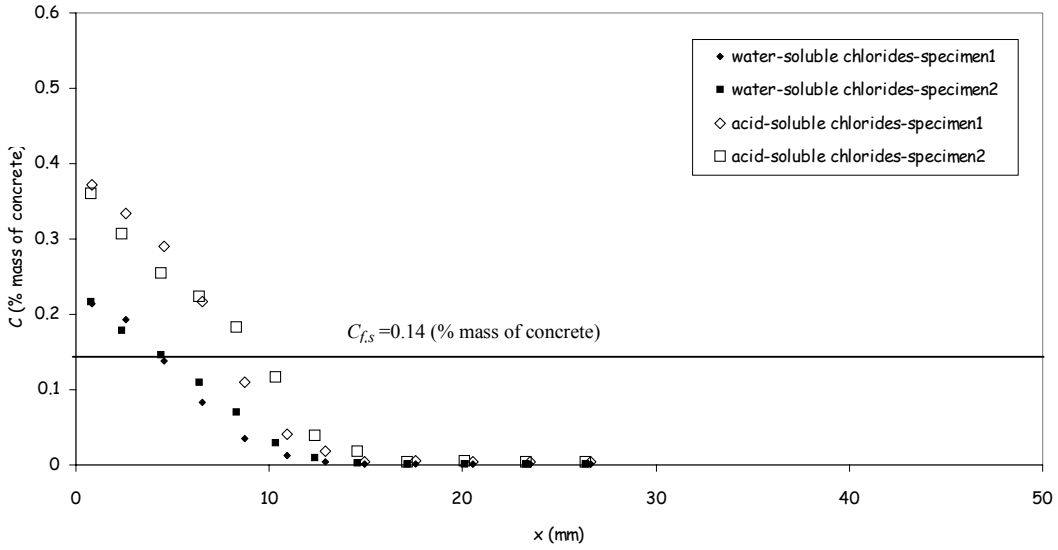

Figure 6.18 Water and acid-soluble chloride profiles obtained from immersion test with 33 g/l NaCl for an exposure period of 180 days and 28 days of concrete age at exposure

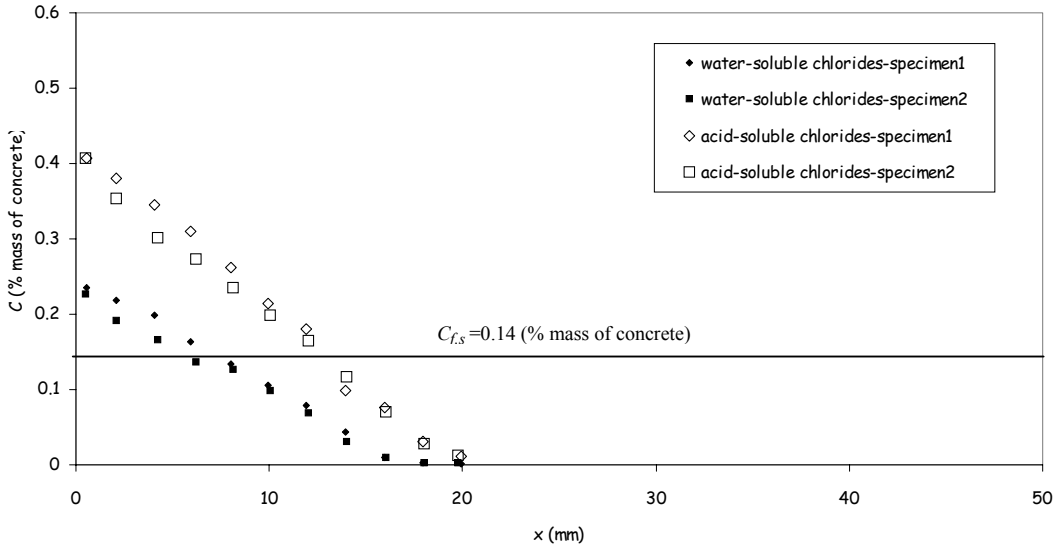

Figure 6.19 Water and acid-soluble chloride profiles obtained from immersion test with 33 g/l NaCl for an exposure period of 365 days and 28 days of concrete at exposure age

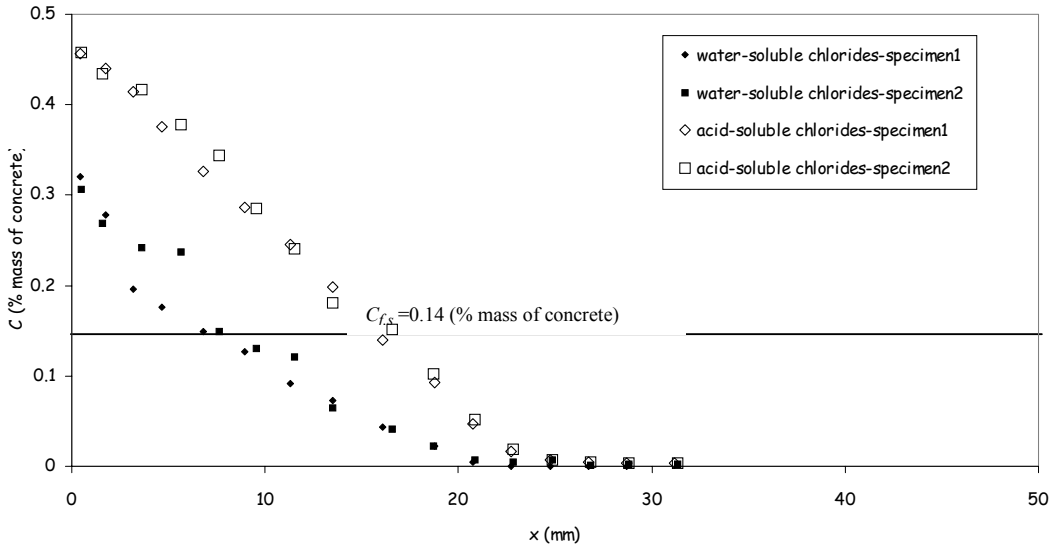

Figure 6.20 Water and acid-soluble chloride profiles obtained from immersion test with 33 g/l NaCl for an exposure period of 545 days and 28 days of concrete age at exposure

6.2.3.4 Some comments about water-soluble chloride concentrations obtained in case of 33 g/l NaCl

With reference to **Figures 6.18**, **6.19** and **6.20**, where the concentration of environmental solution is 33 g/l NaCl or 0.14 chlorides (% mass of our concrete), if we look at the water-soluble chlorides, we come to observe higher values at locations, near to the exposed surface. Logically, we should have values a little bit smaller than 0.14 (% mass of concrete) chlorides (environmental load) but we find values from 50% to more than 100% in addition to 0.14 (% mass of concrete). That is for this reason that no binding isotherm was tried with experimental data obtained in the case 33 g/l NaCl and rather the binding isotherm as obtained with 165 g/l or 0.70 (% mass of concrete) was taken as the reference-binding isotherm for 33 g/l NaCl. This binding isotherm was later on utilized while modeling chloride ingress with MsDiff. The modeled profiles are presented in second part of present chapter.

Now let us look into the possibility of having larger free chloride values than expected. The greater chloride ion solubility in water may cause loosely bound chloride ions to release into the pore solution. Therefore, the so-called free chlorides have been found more than expected.

Some researchers have argued that it is the total chloride content which should dictate the value of free content [RAM] and that the water-soluble chlorides do not represent exactly the free chlorides. Keeping that in view, other solvents with similar properties as that of water (but with lesser solubility for chlorides) were tried to extract free chlorides for example ethanol and methanol [ARY 90]. Ramachandran [RAM] washed the same powder samples with water and ethanol. As discussed above, the water-washed samples gave greater values of chlorides as compared to the ethanol-washed samples. He contributed the difference to the loosely bound chloride ions on CSH phase of the material. But while trying solvents other than water, it was also observed that the extracted chlorides are significantly less than what should actually be. So the idea was abandoned.

Another possibility was also sorted out for increased water-soluble chlorides in the case of 33 g/l NaCl. These samples were placed in ambient temperature for some time before placing in oven for drying. It was thought that the diffusion of CO_2 from ambient environment might be the cause of increased water-soluble content as carbonation leads to reduced chloride binding or increased free chlorides [LAR 03]. In order to verify whether this was due to carbonation effect, experimentation was conducted as described below.

6.2.3.5 Study for carbonation effect on chloride concentrations

A concrete specimen, 11 cm in diameter and 6 cm in height was exposed to a salt solution of 165 g/l NaCl for a period of 14 months. The specimen was reduced to powder and was dried. From the homogenized dry samples, 5 grams each were taken and analyzed to determine the water-soluble chloride content. The first two samples were placed in an oven at 50°C, immediately after grinding, then a series of two were placed after 2, 5, 8, 31 and 62 days respectively. In the period between reducing the samples to powder and introduction in oven, the samples were placed in ambient atmosphere. The samples were analyzed by potentiometric titration during the same day. An increase of 10% in the chloride content was observed between the values for non-carbonated specimens and the ones placed in ambient environment for two months as shown in **Table 6.11**.

The following table suggests that the powdered concrete should be immediately analyzed after grinding. A long time exposure to air might cause an increase of chloride content. In other words, carbonation may reduce chloride binding, leading to increased water-soluble chloride content.

Table 6.11 Effect of carbonation on water-soluble chloride content

Time after grinding (days)	Sample mass (grams)	Water-soluble chloride content (% mass of concrete)
0 (Immediately after grinding)	5.0008	0.5728
	5.0017	0.5797
2	5.0018	0.5865
	5.0015	0.5821
5	5.0018	0.5877
	5.0016	0.5883
8	5.0013	0.6048
	5.0012	0.6074
31	5.0001	0.6105
	5.0005	0.6134
62	5.001	0.6229
	5.0009	0.6269

If a curve is drawn with time after grinding during which a concrete powder specimen was placed in ambient atmosphere, on abscissa and chloride content as ordinate, the **Figure 6.21** results.

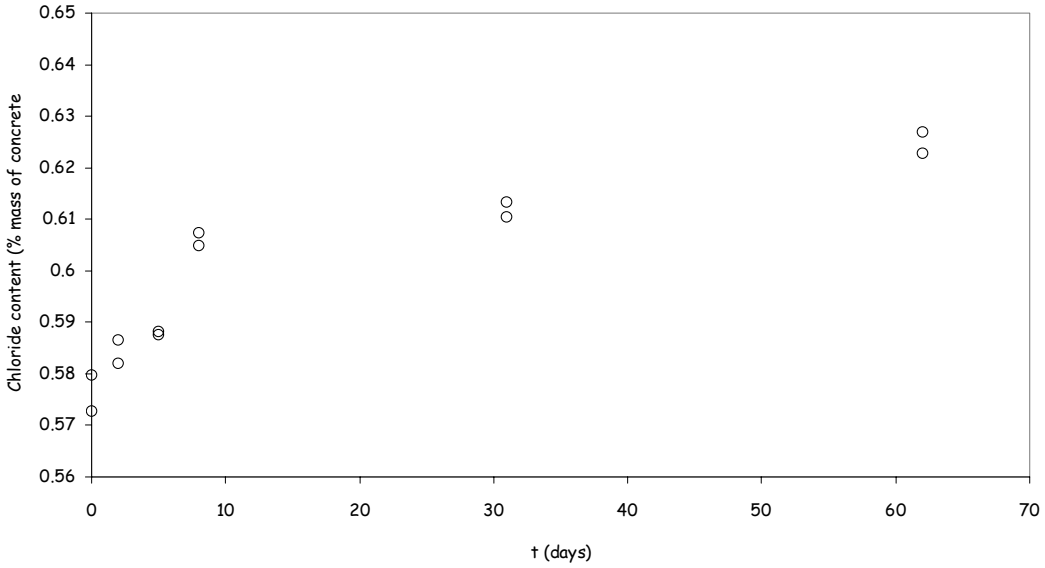

Figure 6.21 Effect of carbonation on water-soluble chloride content

Figure 6.21 suggests that the water-soluble chloride content increases with increase of time period, during which a chloride containing concrete powder is placed in contact with ambient atmosphere. However, it seems that the increasing chloride content assumes an asymptotic behavior. This might be either due to a saturation capacity of powder to absorb CO_2 from atmosphere or a saturation capacity of 150 ml distilled water to extract chlorides from powder or a combination of two. In no way, a 10 % increase in chloride content justifies the higher experimentally found water-soluble chloride concentrations (which in certain cases are more than 100 % of the expected values) in regions near the exposed surface. In other words, the increased water-soluble concentrations are not exclusively due to carbonation effect as assumed earlier.

In our case, although we have the same problem with 33 g/l NaCl as the extracted values are greater, however that was not encountered significantly while working with higher concentration of 165 g/l NaCl. It should be noted that in all the two cases, the reduced concrete powder was washed with the same quantity of distilled water i.e. 150 ml. For higher concentration, it is possible that water is not able to extract chlorides beyond a certain limit or in other words, 150 ml distilled water quantity was saturated with a chloride concentration in the vicinity of environmental solution concentration (slightly more or less than 0.7 % mass of concrete) and it was not possible to extract additional loosely bound chlorides as it did in the case of 33 g/l chloride concentration.

This might also be due the difference of scale between 165 g/l NaCl and 33 g/l NaCl, where a certain increment, which is more significant in the case of lower concentration, is no more important while dealing with higher concentrations. But there should be more loosely bound chlorides at higher concentrations as Arya et al. [ARY 90] have reported leading to more increment in water-soluble concentrations, present in regions near to the exposed surface.

6.2.4 Binding isotherm

As stated before, in order to acquire binding isotherm, two methods were implied i.e. equilibrium method and immersion tests.

6.2.4.1 Equilibrium method

The method adopted has been described in chapter 4. The initial chloride concentrations used have also been illustrated in chapter 5. Here in **Table 6.12**, these initial concentrations are reminded along with the equilibrium concentrations found out at the end of the test, which lasted for three weeks.

Table 6.12 Initial and equilibrium concentrations in Equilibrium test

Initial NaCl (g/l)	Initial Cl^- (g/l)	Equilibrium Cl^- (g/l)
186.49	113.11	112.45
156.3	94.8	94.36
113.79	69.02	68.47
97.4	59.08	58.76
59.9	36.32	36.07
33.06	20.05	19.79
20.86	12.65	12.47
14.06	8.53	8.4
6.58	4	3.85

Bound chloride concentrations in g/l were calculated as the difference of initial and equilibrium concentrations, which were later converted to mol/kg of dry concrete by using measured water porosity and concrete density.

The binding isotherm was drawn with free chloride concentrations at equilibrium as abscissa and calculated bound concentrations as ordinate. The experimental points are shown as filled squares in **Figure 6.22**.

6.2.4.2 Immersion tests

Once the total and water soluble chloride concentrations at various points for one exposure period have been determined, their corresponding difference at each point was calculated. This difference was attributed to bound chloride concentration as described in relation **[1.9]** (page 7) which narrates that the total chloride content is the sum of free and bound contents. Recall that this method presents the advantage to limit the number of different experimental procedure for obtaining input data for modeling, by giving on one hand the chloride profiles for modeling validation and on the other hand the binding isotherm. A binding isotherm was obtained when the calculated bound chloride concentrations were drawn on ordinate with water-soluble chloride concentrations on abscissa. This binding isotherm is shown in **Figure 6.22** (hollow shapes). Note that in this binding isotherm, the water-soluble chloride concentration is expressed in moles per cubic meter of porous solution and the bound chloride concentration is expressed in moles per kilogram of dry concrete. For this purpose, the water porosity and concrete mass density were utilized. Note that this binding isotherm was drawn

with all points obtained corresponding to 4 exposure periods i.e. 35, 100, 200 and 330 days with 28 days of concrete age at exposure.

The binding isotherm was modeled with Langmuir equation corrected by power law as described before. The representative equation is given as relation **[6.5]**.

$$c_{m,b} = \frac{\alpha_1 \beta_1 c}{(1+\beta_1 c)} + \alpha_2 c^{\beta_2} \qquad \textbf{[6.5]}$$

In relation **[6.5]**, $c_{m,b}$ is the bound chloride concentration in moles per kg of dry concrete and c is the free one in moles per m^3 of solution. The modeled values of coefficients of α_1, β_1, α_2 and β_2 are 0.03, 0.003, 0.00106 and 0.526 respectively.

6.2.4.3 Comparison between Equilibrium and immersion methods

With reference to **Figure 6.22**, the experimental points obtained from 2 methods seem to be in good agreement with each other except for the three last higher bound chloride concentrations

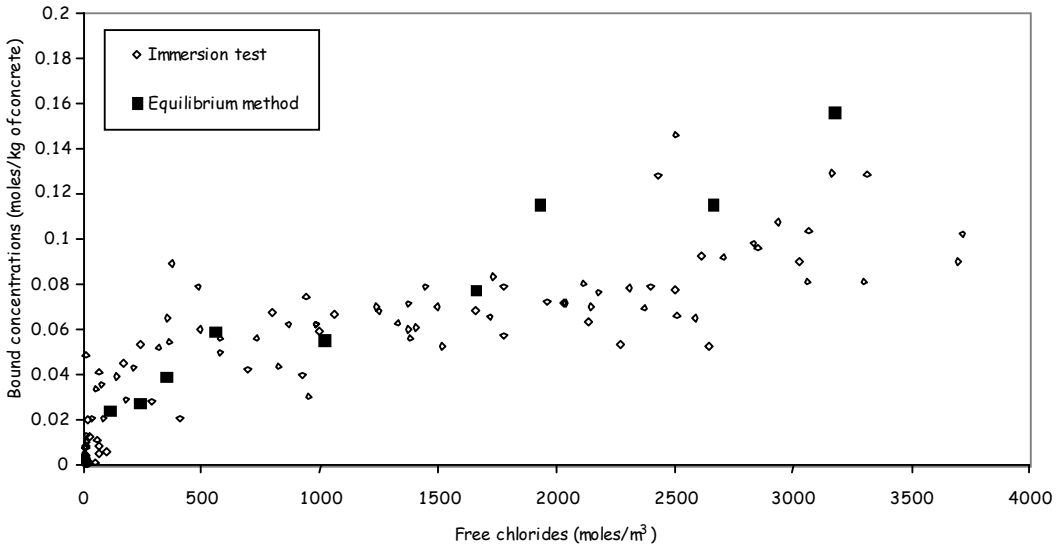

Figure 6.22 Free and bound chloride concentrations obtained from immersion and equilibrium methods

obtained in equilibrium method. Additionally the last three lower concentrations obtained from equilibrium method seem to exist at the lower exterior boundary of the cluster made by

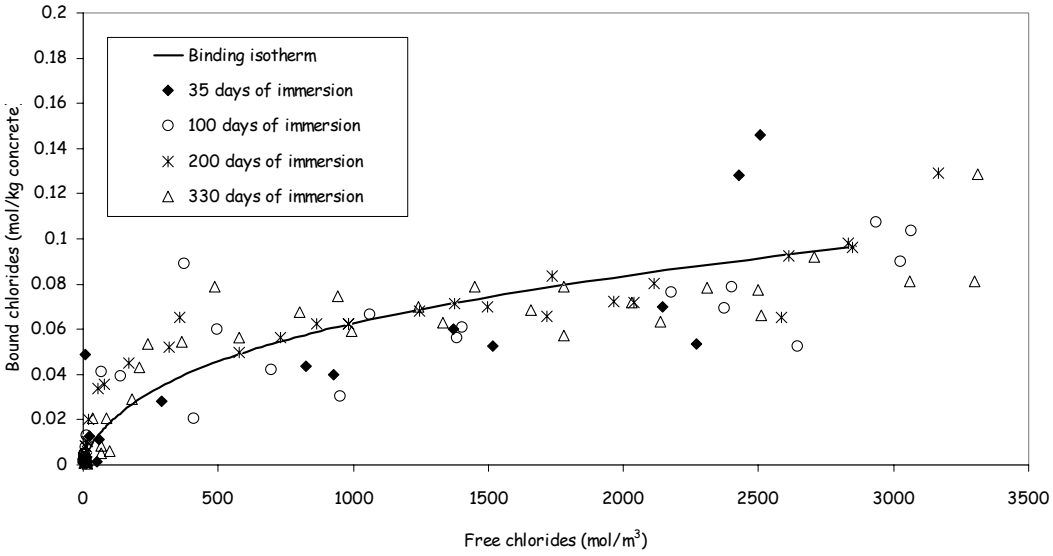

Figure 6.23 Experimental and simulated binding isotherms obtained with experimental chloride profiles of 165 g/l NaCl and 28 days of age at exposure

immersion test. Although we are unable to comment on this difference, the binding isotherm as obtained from immersion test was preferred to insert as input data for MsDiff because it was considered to be relatively true representative of reality.

Up to this points if we look back at the experimental data obtained, we come to conclusion that all the necessary data set as input for MsDiff has been achieved. Before going further, let us conclude all the data in a tabular form (**Table 6.13**) for the sake of convenience.

Table 6.13 Input data for MsDiff

Concrete composition (per m^3 of concrete)				
Cement (kg)	Water (l)	Sand (kg)	Gravel (kg)	Air (% volume of concrete)
560	224	695	825	2
Cement Bogue's composition (% mass of cement)				
C_3S	C_2S	C_3A	C_4AF	
54	22	6	9	
Porosity (% age)	16	Mass density (kg/m^3)	2281	
Composition of pore solution ($moles/m^3$)				
Na^+	K^+	Cl^-	OH^-	
23	156	1	178	
Chloride effective diffusion coefficient				
Reference age (days)	Reference D_e (m^2/s)	Reference age (days)	Reference D_e (m^2/s)	
28	18E-13	70	8E-13	
Ratio k ($D_{e,i}/D_{e,Cl^-}$) ; note that it represents the corresponding ratio in infinitely diluted solution.				
k_{Na^+}	k_{K^+}	k_{Cl^-}	k_{OH^-}	
0.65	0.96	1	2.6	
Coefficients of binding isotherm				
α_1	β_1	α_2	β_2	
0.03	0.003	0.00106	0.526	

It should be noted that in model MsDiff, porosity could also be put in as user data else wise model itself calculates the porosity varying over material age. Therefore the inclusion of a porosity value as input data should not be confused with. It is presented here just for reference purposes.

In **Figure 6.24**, the evolution of porosity with concrete age using Avrami-Powers model and the experimentally measured values are shown.

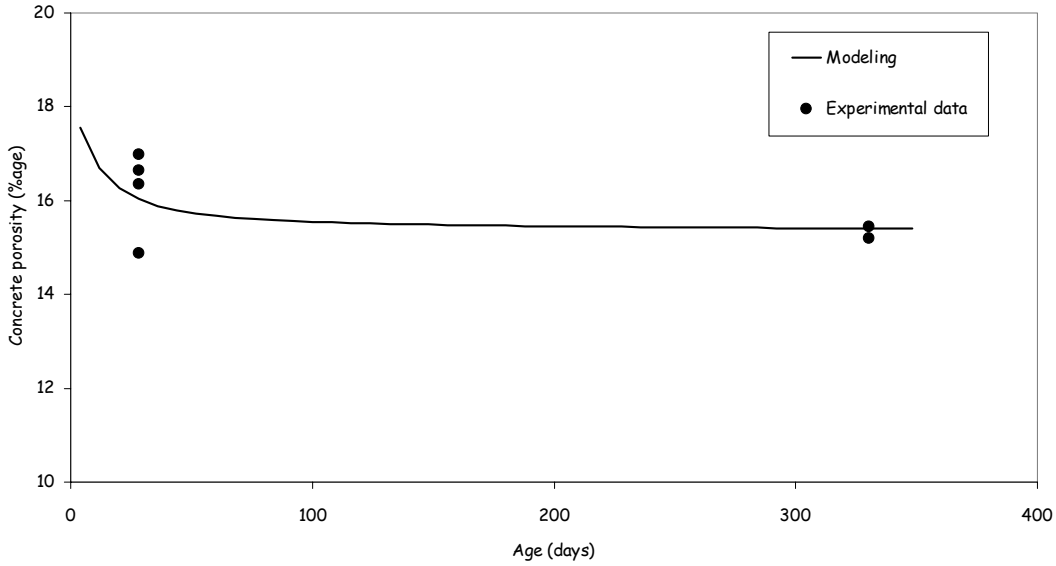

Figure 6.24 Comparison between the experimental and modeled porosity values

6.3 Part 2: Numerical modeling with MsDiff

Once we started getting experimental feedback, modeling with MsDiff was on track. The input data was used as described in **Table 6.13**, while the numerical scheme as described in section 3.4 (page 52) was followed. Currently MsDiff does not take into account the effect of temperature on chloride ingress however a temperature of 20°C was used wherever needed (can be seen in the governing equations given in chapter 3), as all the experimentation was performed at local laboratory temperature (20 ± 2°C). Additionally the parameters, presented in **Table 6.14** were used while running MsDiff for different exposure periods and environmental concentrations.

Table 6.14 Additional parameters for MsDiff

Mat. thickness L (mm)	Time step Δt (s)	Number of nodes (N)	Inter-nodal distance Δx
50	2000	50	L/(N+1)

Grid independence tests were performed. We also checked the dependence of the results on the time step. Both the grid spacing and the time step were made small enough to ensure a solution that is independent of the grid size and time step. Specifically, if the time step is Δt,

then from one test to the next the Δt value was divided by two until the criterion $\left|\frac{c_{i,\Delta t} - c_{i,\Delta t/2}}{c_{i,\Delta t/2}}\right| \leq 0.1\%$ was satisfied.

As discussed before, for modeling with MsDiff, we need a package of input data at a certain materials age. While all the other four parameters could be satisfactorily used in modeling if measured at a classical age of 28 days, the chloride effective diffusion coefficient is a parameter that needs special attention.

The chloride diffusivity of the material can be calculated from the chloride diffusion coefficient measured at 28 days after casting. But is it really necessary to account for the diffusion coefficient variation with time during the early age of the material? In other words, why not keep constant the diffusion coefficient of chloride (measured at 28 days) for predicting the chloride penetration as can be done with the other four parameters? The data available on the material may not be for a 28-day old concrete but rather for an older material: from an in-situ sample of material, a slice may be used to measure the chloride diffusivity. So, is it necessary to account for the diffusion coefficient decrease during the first 2 months after casting?

In order to answer to these questions three kinds of simulations were made. First the chloride diffusion coefficient was the one measured 28 days after casting. Second, its value was chosen to be the 'mature' value and third the chloride diffusivity followed equation **[6.2]** (page 85). The concentration profiles were calculated for 35, 100 and 200 days of immersion for demonstration purposes in order to compare with our experimental data. The input data has been illustrated in **Table 6.13**.

Figures 6.25, **6.26** and **6.27** show the numerical results obtained with the 3 different chloride diffusion coefficients (i.e. a constant D_e (measured at an age of 28 days), a varying *De (t)* and a constant D_e (concrete age = 330 days i.e. a mature concrete)) after 35, 100 and 200 days of immersion respectively. When the chloride diffusion coefficient is the one measured with the mature concrete, the chloride concentration is very close to the concentration profile computed with a time-dependent diffusion coefficient. After 35 days of immersion, a difference exists between the results obtained with age-dependent chloride diffusivity and a diffusion coefficient measured on a mature concrete. After 35 days of immersion, the concrete is still not mature. To compute the chloride profiles with a diffusion coefficient corresponding to a mature material tends to underestimate the chloride content in the sample (**Figure 6.25**),

because of the actual higher diffusivity during the early age. The difference between the two profiles decreases when increasing the immersion time (**Figure 6.26**) and becomes zero after 200 days when the chloride profiles become identical (**Figure 6.27**).

Results are different with the chloride diffusivity measured at 28 days. The chloride penetration depth is 1.7 cm after 35 days, 2.8 cm after 100 days and 3.9 cm after 200 days. This means an over-estimation of 16%, 53% and 77% respectively for 35, 100 and 200 days. Furthermore, the over-estimation increases with the time of exposure, leading to dramatically wrong chloride contents predictions.

Because the chloride diffusion coefficient is higher at 28 days, the chloride ingress is higher, keeping the diffusivity constant. Recall that the diffusion coefficients of other species are linked to the chloride diffusion coefficient as has been described earlier in chapter 3 and also depicted in **Table 6.13**. Therefore the choice of chloride diffusion coefficient has impact not only on the chloride concentration profile itself but also on the other species concentrations. This is illustrated in **Figure 6.28**, where the concentration profiles of sodium, potassium and hydroxide are plotted with constant chloride diffusivity (i.e. measured at 28 days) or depending on time. The results presented in **Figure 6.28** correspond to 200 days of exposure,

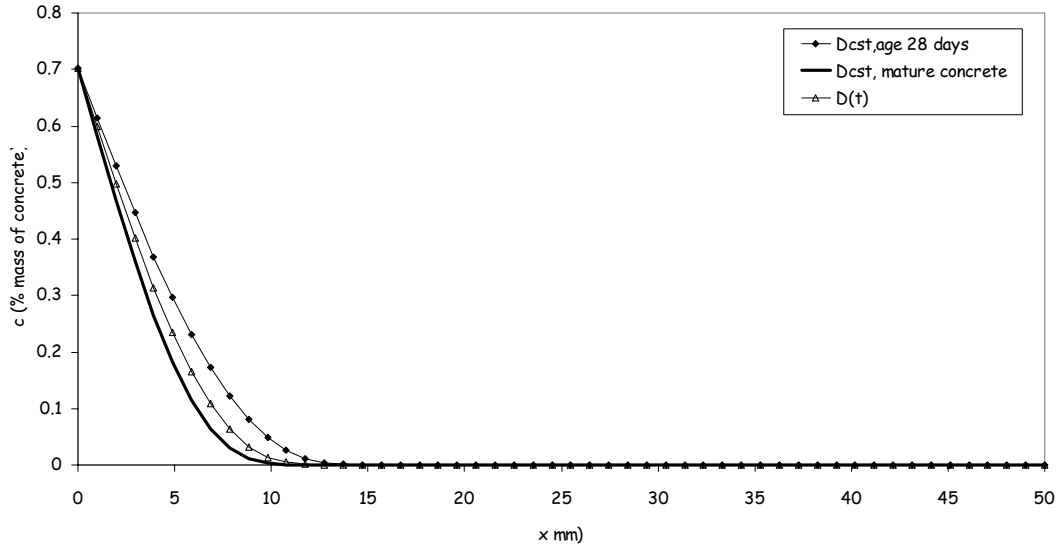

Figure 6.25 Effect of time dependency of D_e on chloride penetration, 35 days of immersion

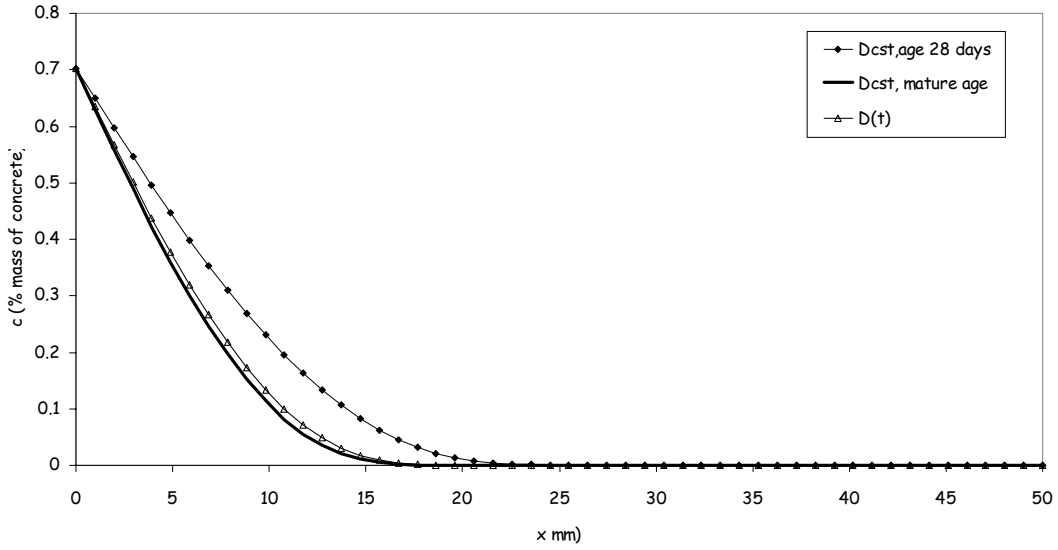

Figure 6.26 Effect of time dependency of D_e on chloride penetration, 100 days of immersion

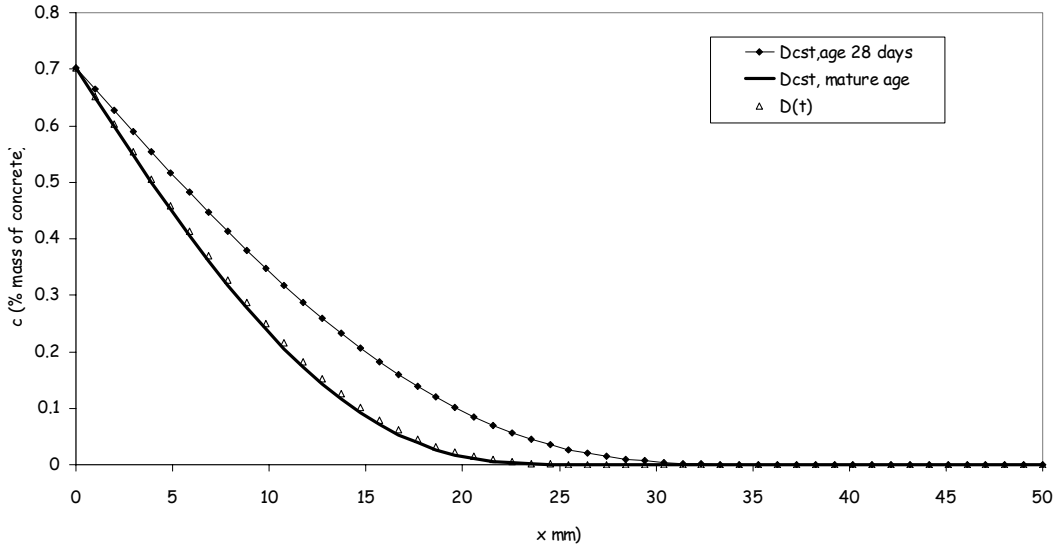

Figure 6.27 Effect of time dependency of D_e on chloride penetration, 200 days of immersion

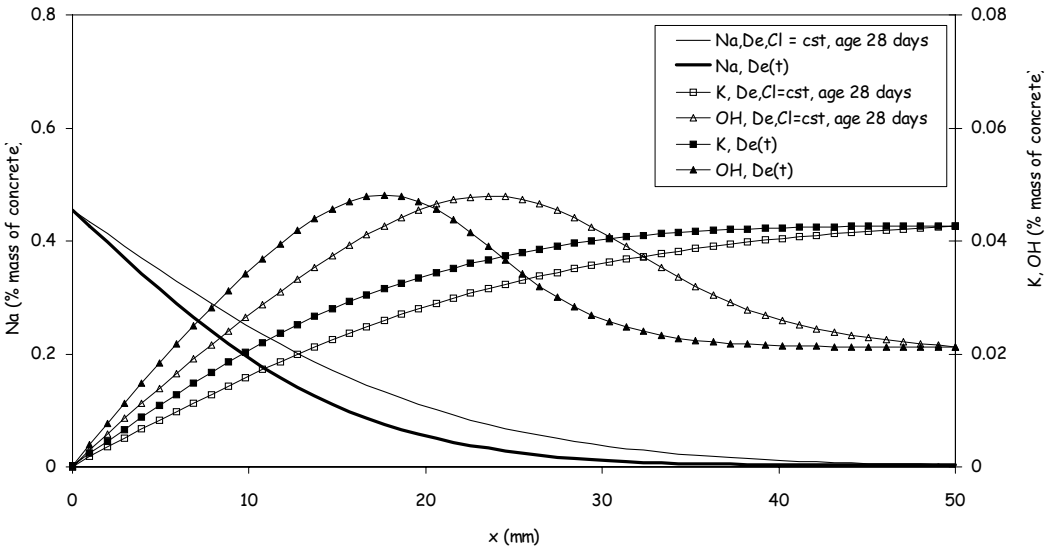

Figure 6.28 Effect of time dependency of De on ionic penetration, 200 days of immersion

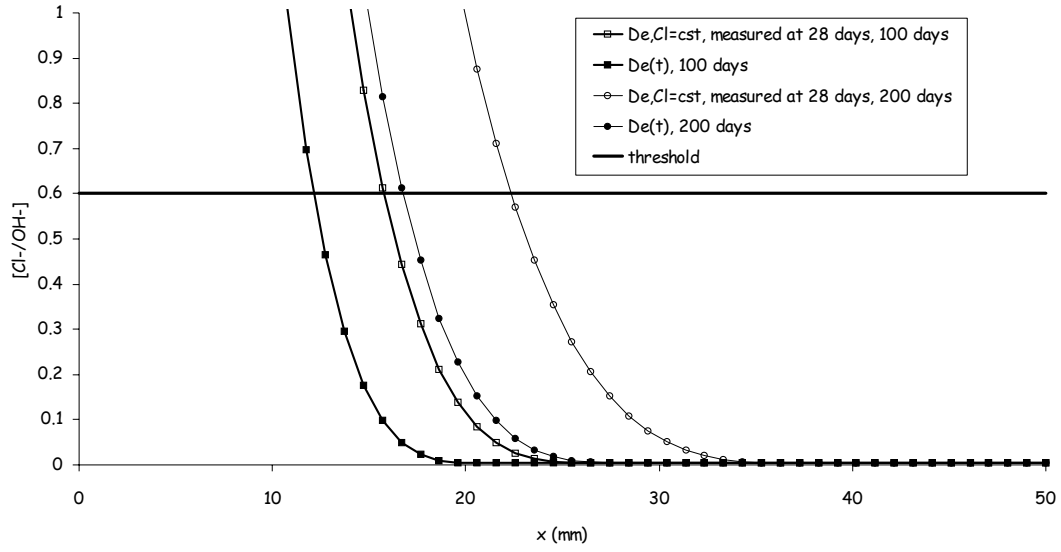

Figure 6.29 Effect of time dependency of D_e on corrosion initiation criterion [Cl^-

yet the trend remains the same for other exposure period. (Please note that the ordinate graduation on left hand side corresponds to only Na^+ ions). When the effective diffusion coefficients are linked to the constant value of the chloride diffusivity measured at the age of 28 days, the numerical results show higher sodium content in the material. At the same time, the leaching of potassium and hydroxide is lower because their concentration gradients are lower in comparison with the chloride and sodium. Note the peak on the hydrxyl ions profiles due to the desorption of hydroxides.

Assuming that the initiation of corrosion occurs when the ratio $[Cl^-/OH^-]$ is 0.6, **Figure 6.29** shows that the results computed with the chloride diffusivity at 28 days tend to over-estimate the abscissa where the limit is 0.6 is reached, this in the vicinity of 31% after 100 days of immersion and 33% after 200 days. Note that the ordinate scale has been intentionally enlarged.

The experimental results obtained after 35, 100 and 200 days of immersion have already been presented in **Figures 6.6**, **6.7** and **6.8**. Recall that in all these cases, the concrete was placed in contact with the NaCl solution after a 28-days cure. Thus in the case when the immersion time is 35 days the material is still not mature, which means that the time-dependence of the diffusion coefficients has to be accounted for. The simulations were made with a time-dependent diffusion coefficient following equation **[6.2]**. The shape of the numerical concentrations profiles follows with a good accuracy the experimental data. The penetration depths, which increase with the time of exposure, are also in good agreement with the experimental results. Therefore, if the objective is to study the chloride penetration before the material reaches maturity, the effective diffusion coefficients of the species of interest have to be time-dependent. If not, the time-dependence of the diffusivities is not necessary and the diffusivities can be the ones that correspond to the mature material.

6.3.1 NaCl concentration of 165 g/l with concrete age of 28 days at exposure

From **Figures 6.30** to **7.33**, the comparison of experimental water and acid-soluble chloride profiles with respective modeled free and total chloride profiles from MsDiff is presented.

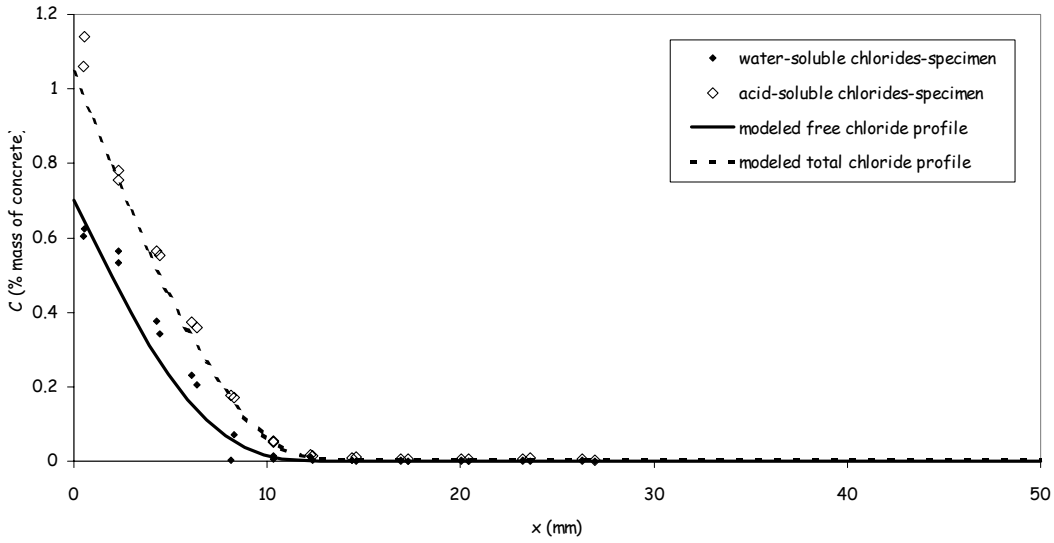

Figure 6.30 Comparison between experimental and modeled chloride profiles for immersion test of 35 days duration with 165 g/l NaCl environmental load and 28 days-cured concrete specimens

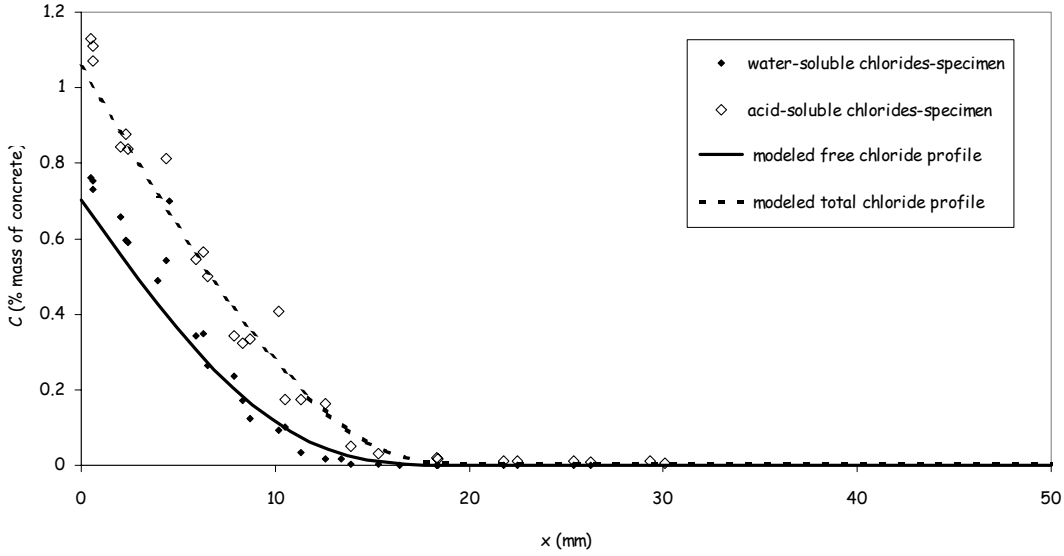

Figure 6.31 Comparison between experimental and modeled chloride profiles for immersion test of 100 days duration with 165 g/l NaCl environmental load and 28 days-cured concrete specimens

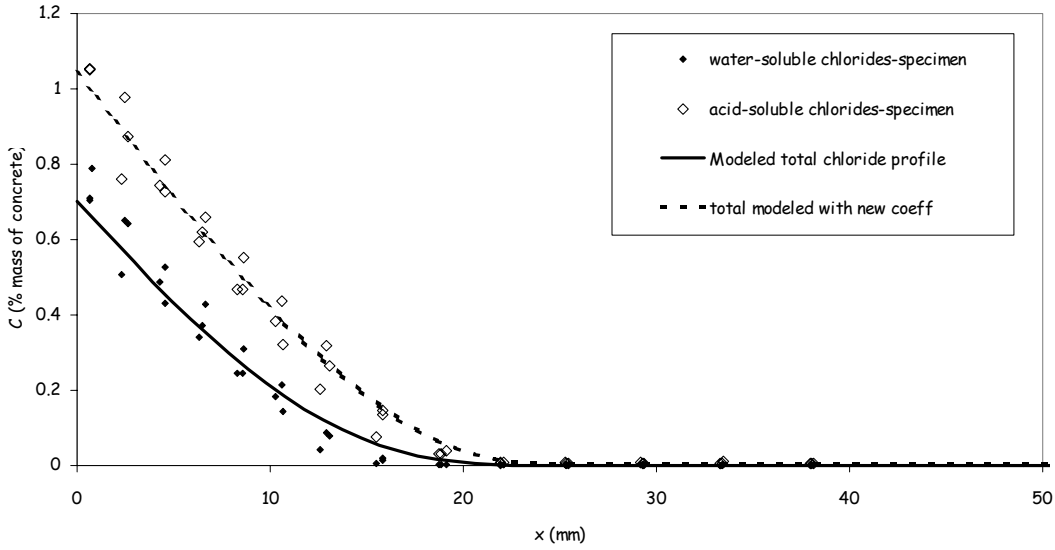

Figure 6.32 Comparison between experimental and modeled chloride profiles for immersion test of 200 days duration with 165 g/l NaCl environmental load and 28 days-cured concrete specimens

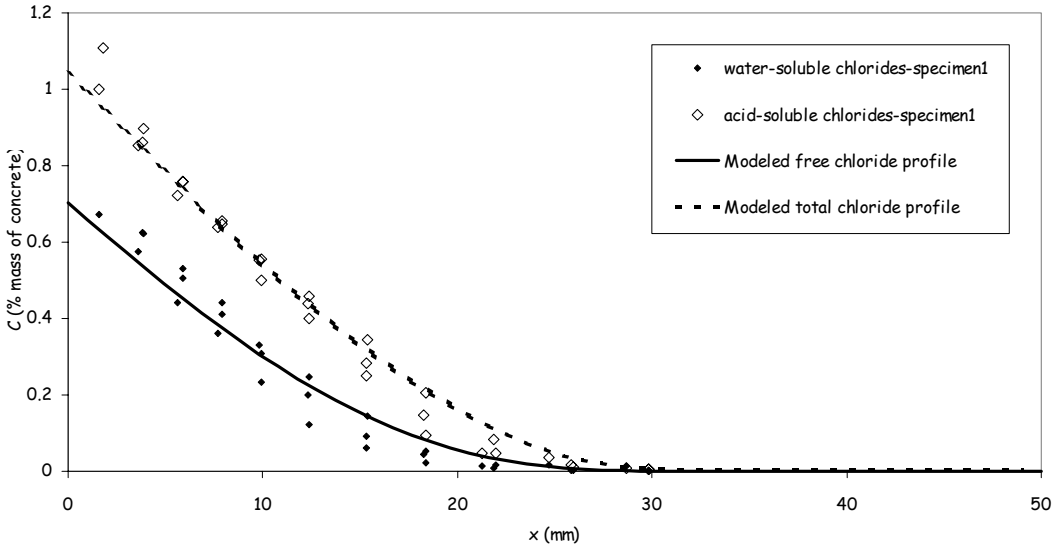

Figure 6.33 Comparison between experimental and modeled chloride profiles for immersion test of 330 days duration with 165 g/l NaCl environmental load and 28 days-cured concrete specimens

It would be well to notify that the chloride profiles presented here are in different units than the input data presented in **Table 6.13**. The experimental chlorides are described in mass percentage of concrete. These are the concentrations obtained directly from potentiometric titration.

6.3.2 NaCl concentration of 33 g/l with concrete age of 28 days at exposure

In **Figures 6.34** to **6.36**, the comparison between experimental water and acid-soluble chloride profiles and numerical modeling with MsDiff is presented. Again recall that the effective diffusion coefficient was allowed to vary from 28 days to 70 days of concrete age. Additionally the boundary conditions were changed from 165 g/l NaCl to 33 g/l NaCl.

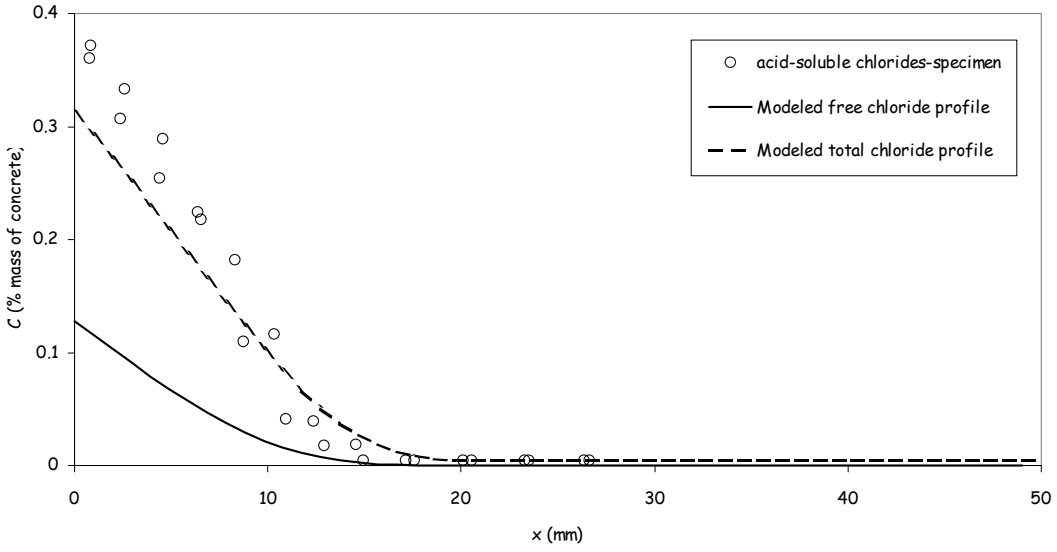

Figure 6.34 Comparison between experimental and modeled chloride profiles for immersion test of 180 days duration with 33 g/l NaCl environmental load and 28 days-cured concrete specimens

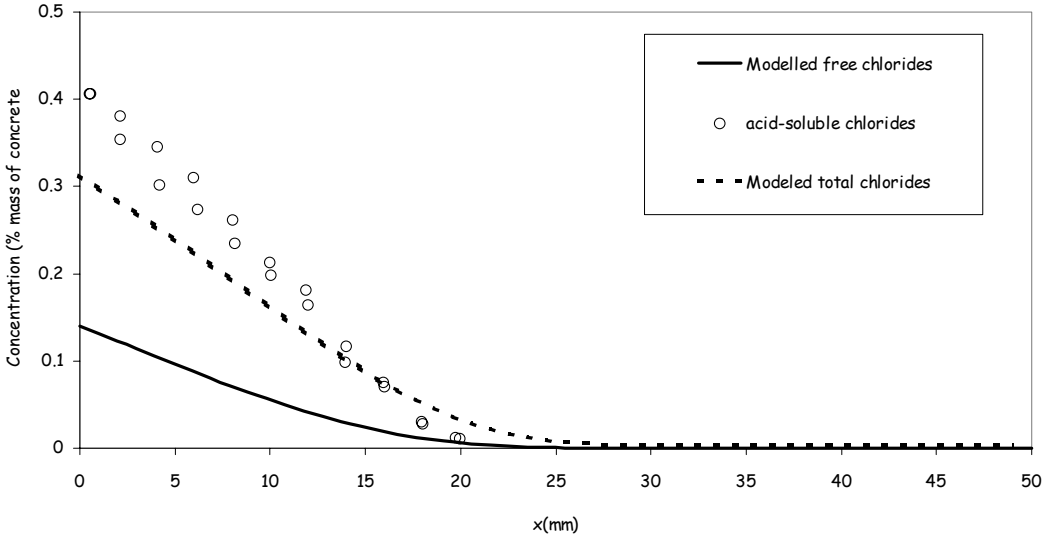

Figure 6.35 Comparison between experimental and modeled chloride profiles for immersion test of 365 days duration with 33 g/l NaCl environmental load and 28 days-cured concrete specimens

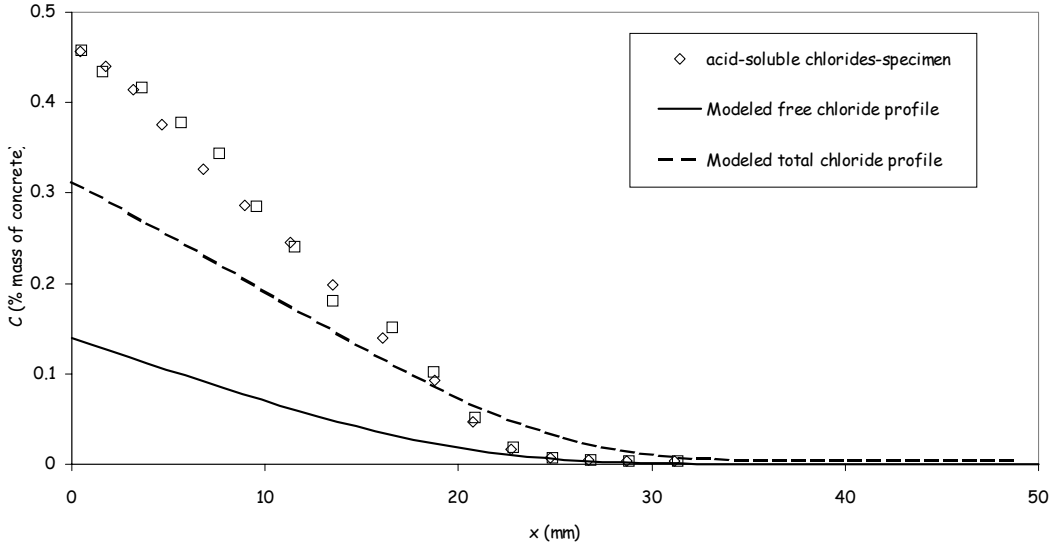

Figure 6.36 Comparison between experimental and modeled chloride profiles for immersion test of 545 days duration with 33 g/l NaCl environmental load and 28 days-cured concrete specimens

From Figures **6.34** to **6.36**, it seems that the modeled chloride profiles do not catch well the experimental profiles, as was observed for higher concentrations of 165 g/l NaCl. So far the acid-soluble chlorides are concerned, the comparison between the modeling and experience is acceptable for 6 months immersion period (**Figure 6.34**). However, due to increase in surface chloride concentration with exposure time, the discrepancy between the experience and modeling also increased specially at regions near the exposed surface. This point will be clarified in section **6.4.2.2**. At least the penetration depths from modeling match well with the experience.

The binding isotherm was obtained from experiments with 165 g/l NaCl [KHI 05]. It was chosen so as to fit the range of concentrations 0-2800 moles/m^3. The objective was to represent the average interactions at best. Note that the resulting binding isotherm (equation **[6.5]**) does not account binding in the range 0-570 moles/m^3 with high accuracy. A slight difference in the bound amount of chlorides leads to a large discrepancy in total chlorides. Thus the difference of modeling with experimental results for 33 g/l NaCl must not be surprising. In order to ameliorate the modeling for this range, another alternative was thought over. The idea was to employ a new binding isotherm for the region 0-570 moles/m^3 which should better match the experimental data in this range in comparison with the present isotherm. As earlier discussed, the difference of modeling with the experimental data of 33 g/l NaCl is due to the divergence of modeled binding isotherm with respect to experimental data in the range of lower concentrations. While this difference was acceptable for larger concentrations, this led to significant deviation of modeling with respect to experience.

Further it was decided that in the range of 0-570 moles/m^3 a Langmuir type binding isotherm should be fitted. The experimental binding isotherm of **Figure 6.22** in the region 0-570 moles/m^3 is shown in **Figure 6.37**. In addition to the experimental data shown in **Figure 6.37**, we have also a set of some other bound chloride values obtained from the experimental acid-soluble chloride profiles (**Figures 6.18** to **6.20**) and the surface free chloride concentrations i.e. 570 moles/m^3 Cl^-. More clearly, corresponding to each acid-soluble chloride profile we have a set of two points i.e. the surface acid-soluble chlorides (**Figures 6.18** to **6.20**) and the surface free chloride concentration which is off course the environmental chloride load or 570 moles/m^3 and thus the bound chlorides at the surface can be determined while deducting the environmental load from surface acid-soluble content. These data points are presented in addition to experimental points of **Figure 6.37** in **Figure 6.38**. Now the surface points reveal (shown by the symbol + in **Figure 6.38**) that the surface bound concentration increased from a value of approximately 0.06 to 0.09 mol/kg of concrete from 180 to 545 days of immersion

respectively. Keeping that in view, three binding isotherms were thought to fit the experimental data. The first isotherm covering the highest bound chlorides observed in this domain, the second the lowest bound chlorides and the third one a weighted average of the two former isotherms. These three modeled binding isotherms in addition to experimental data are shown in **Figure 6.39**.

The coefficients of these three binding isotherm are given in **Table 6.14**. As discussed earlier a Langmuir type binding isotherm was chosen for the modeled binding isotherm for this region as given by the following equation.

$$C_{m,b} = \frac{\alpha\beta c}{(1+\beta c)} \qquad \textbf{[6.6]}$$

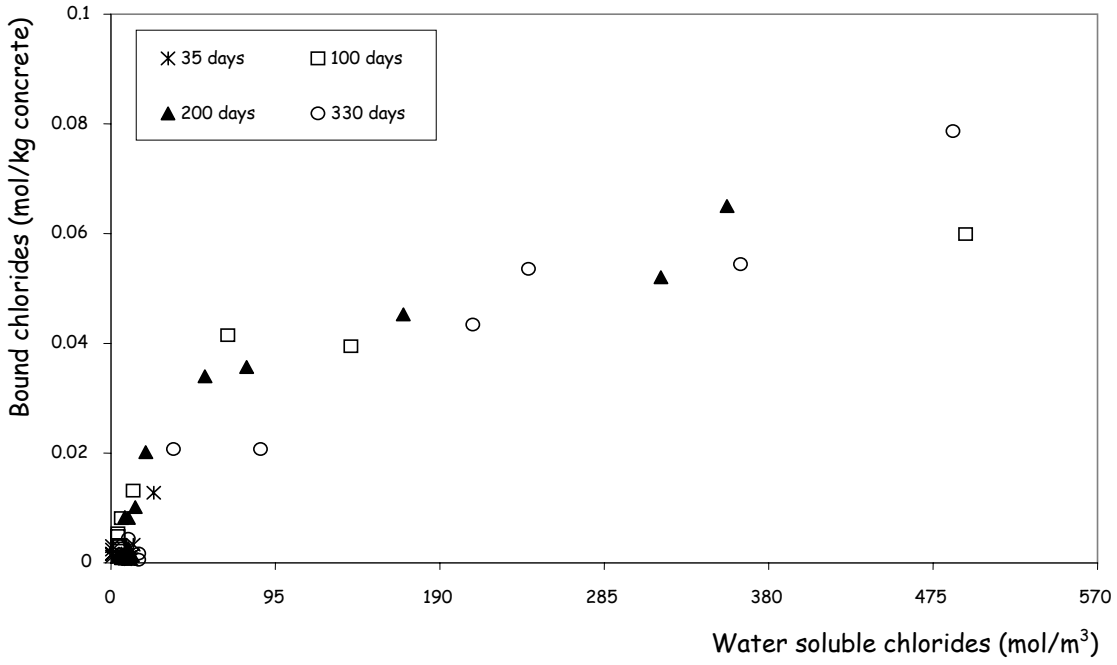

Figure 6.37 Experimental binding isotherm (165 g/l NaCl) in the range of 0-570 moles/m^3 Chlorides

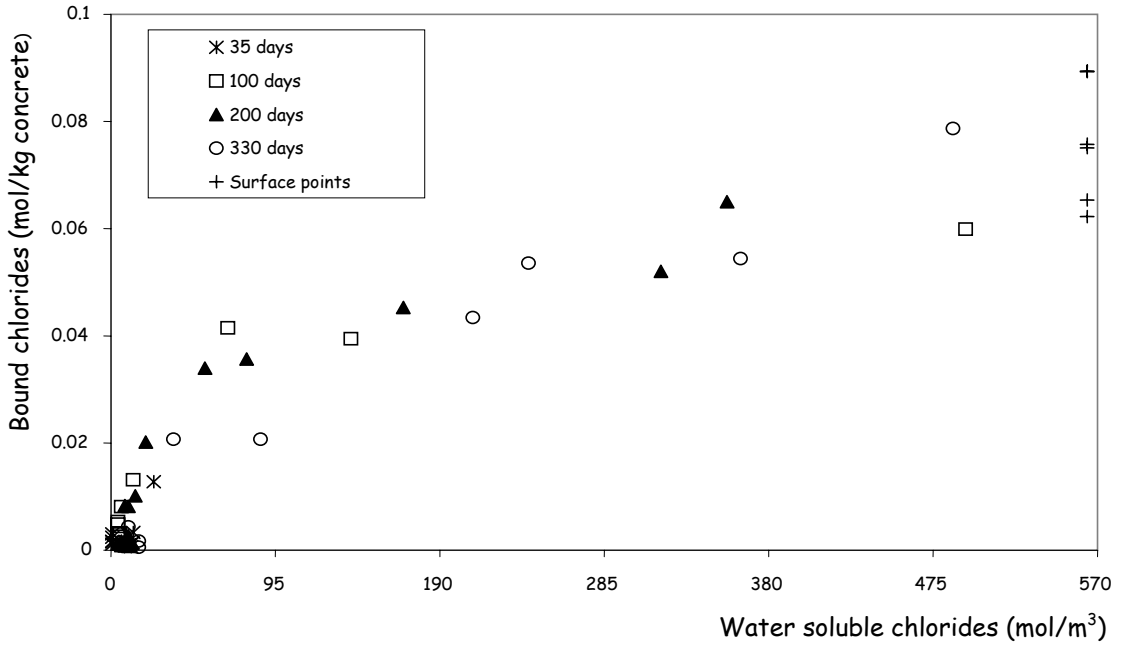

Figure 6.38 Experimental binding isotherm (165 g/l NaCl) in the range of 0-570 moles/m^3 Chlorides plus surface points

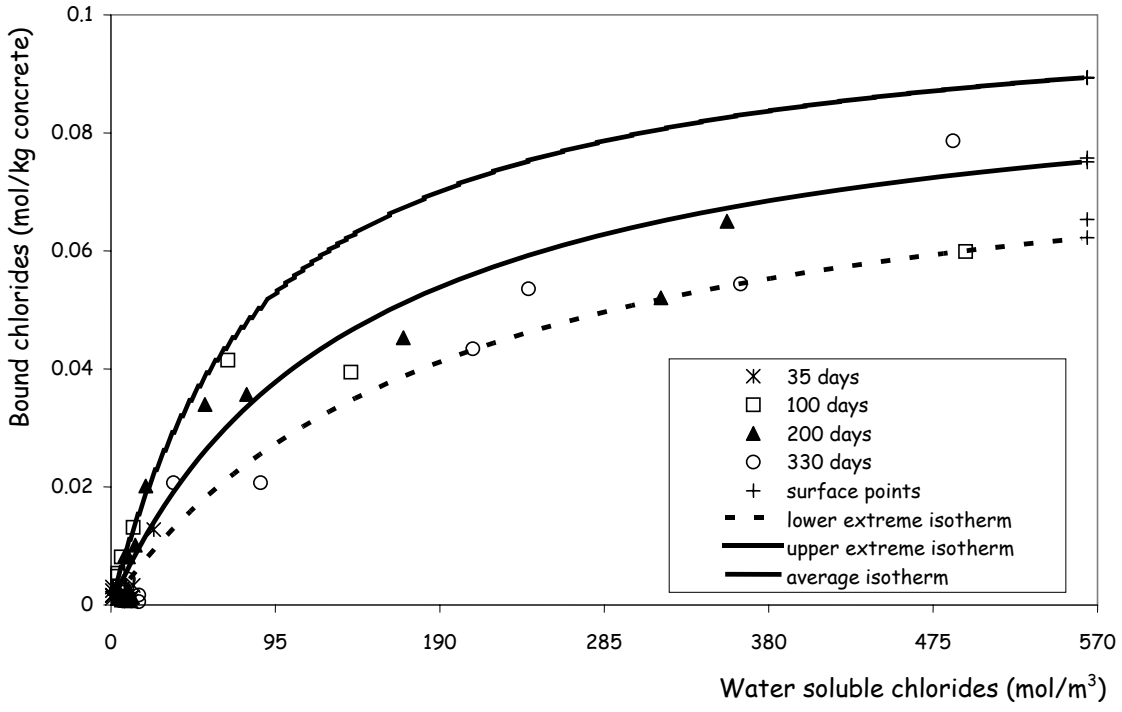

Figure 6.39 Experimental data and simulated binding isotherms for the region 0-570 mol/m^3 free chlorides

Table 6.14 Coefficients of modeled isotherm for the region 0-570 mol/m^3 Cl$^-$

	α	β
Upper isotherm	0.104	0.01
Lower isotherm	0.084	0.005
Average isotherm	0.094	0.007

Out of these three isotherms, the average one was chosen to further modelise the total chloride profiles obtained while using the 33 g/l NaCl. The results are shown in **Figures 6.40**, **6.41** and **6.42** for 180, 365 and 545 days of immersion respectively.

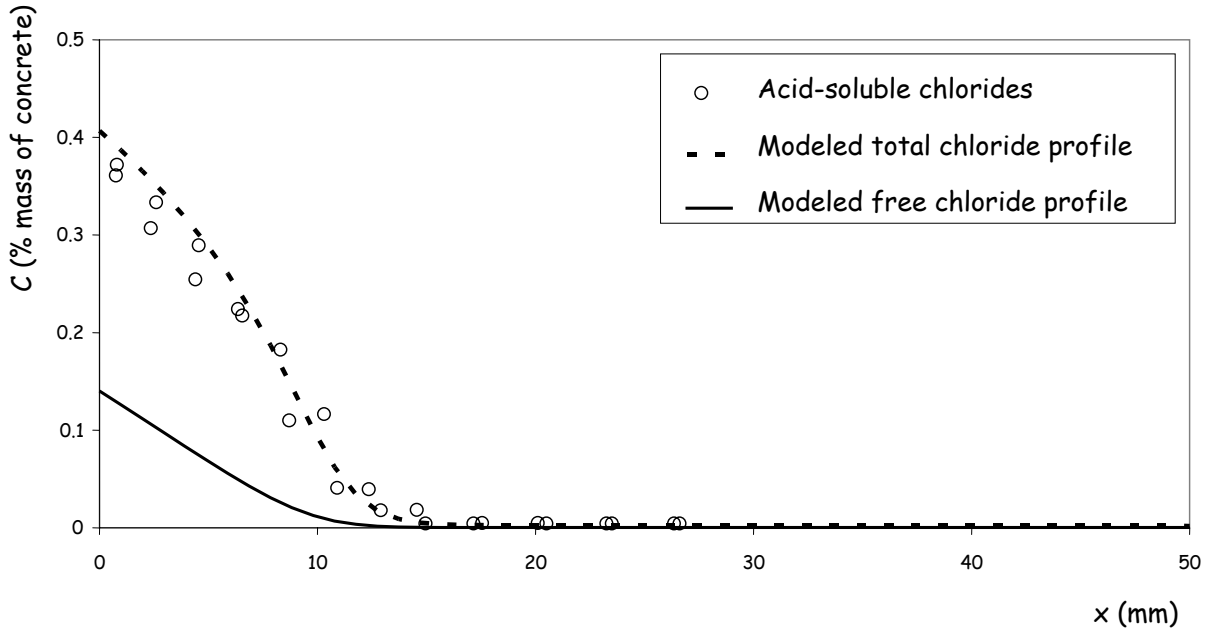

Figure 6.40 Comparison between the experimental data and modeling with MsDiff for immersion test employing 33 g/l NaCl for a period of 180 days using a binding isotherm by exploiting the 0-570 mol/m^3 region

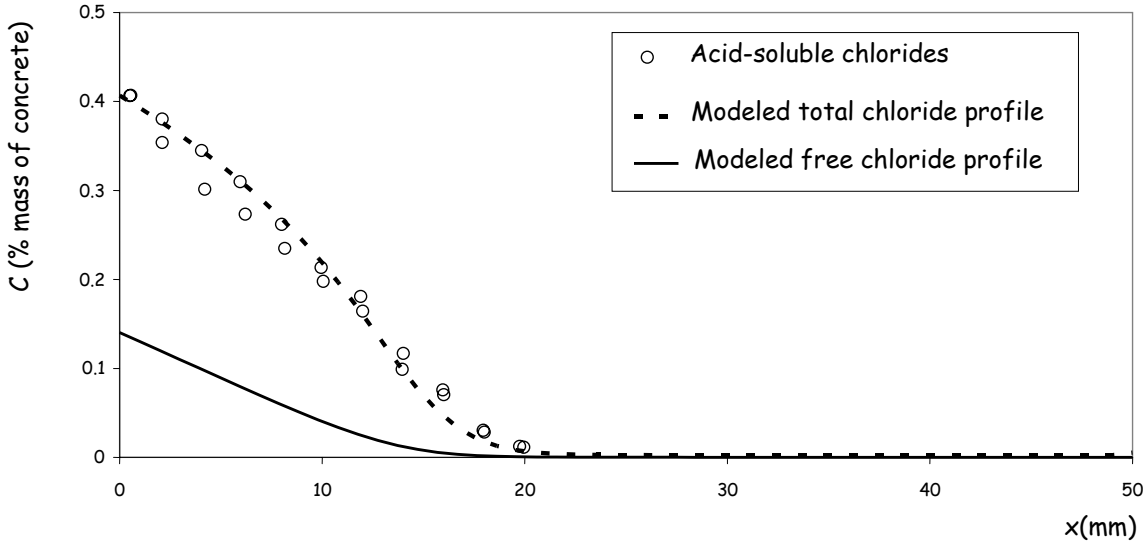

Figure 6.41 Comparison between the experimental data and modeling with MsDiff for immersion test employing 33 g/l NaCl for a period of 365 days using a binding isotherm by exploiting the 0-570 mol/m^3 region

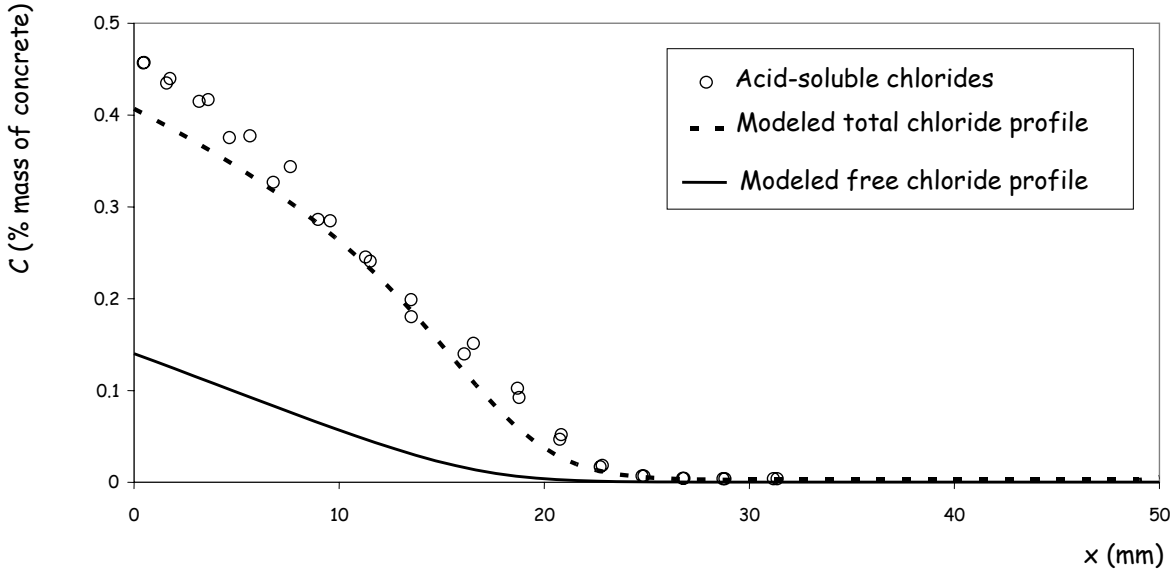

Figure 6.42 Comparison between the experimental data and modeling with MsDiff for immersion test employing 33 g/l NaCl for a period of 545 days using a binding isotherm by exploiting the 0-570 mol/m^3 region

The above three figures (**6.40** to **6.42**) reveal that while modeling, the range of the concentrations also plays an important role. While a certain divergence from the experience is acceptable at higher values, the same might not be acceptable at lower values or in other words, the role of scale is equally important.

6.3.3 Conclusions-MsDiff modeling

MsDiff modeling including for a variable effective diffusion coefficient and a non linear binding based on Langmuir modified with a power law isotherm showed good agreement with experimental acid and water soluble chloride concentrations for the case of 165 g/l NaCl in environmental solution and to some extent with only acid soluble chloride concentrations in the case of 33 g/l NaCl. Its validation for free chloride profiles in the case of 33g/l NaCl could not be verified experimentally due to the reasons stated before.

Recall that MsDiff requires a package of five input data; out of these five, porosity, mass density and composition of pore solution are pure material properties whereas coefficients of binding isotherm and chloride effective diffusion represent materials properties vis-à-vis chloride ingress. Porosity can either be entered as user data or the model itself can calculate it whereas all the other four are user data. Anyway a correct estimation of these data is necessary to acquire good results from the model. In this work, all these properties were known in one or the other way.

The first three input data i.e. porosity, density and composition of pore solution can be determined by well known classical methods as discussed in chapter 4. The chloride diffusivity is supposed to vary up to 70 days of material age after which this parameter is no more treated as a variable (refer to **Figures 3.1** and **6.4**). Simulations with constant effective diffusion coefficient (measured at 28 days of concrete age by LMDC test) led to over-estimated chloride concentrations. So while simulating results for materials having higher curing periods with 165g/l NaCl in environmental solution, a constant D_e was introduced for example in the case of 420 days (>70 days) old material at exposure. Due to similarity of results with 28 days-aged concrete and 165 g/l NaCl, these simulations have not been presented here.

For 33 g/l NaCl, total chloride profile for 6 months is somewhat in good agreement with all the experimental points, while for 1 year and 18 months the predicted total chloride profiles deviate not only from the experimental data at points near the exposed surface but also penetration depths are different which if not the worst is also not acceptable enough. Perhaps, it is due to the accumulation of chlorides: this accumulation increases with exposure time.

Currently MsDiff model does not take into account the increase of surface chloride content with increase in exposure period as observed and shown in the current chapter. Moreover the binding isotherm deviates from the bound concentrations at small water-soluble chlorides (in the pore solution). This deviation while satisfactory for the case of 165 g/l NaCl seems not to be suitable for the smaller water-soluble chloride concentrations.

Therefore the idea of using the same isotherm for smaller concentrations was abandoned and the modeling was executed with a new binding isotherm for the range of chlorides from 0-570 moles/m^3. The simulations with this new binding isotherm led to acceptable modeled total chloride profiles. The modeling is at best with an average binding isotherm. For lower immersion time of 180 days, the total chloride concentrations in the region near to the surface are somewhat lower than the modeled values. Similarly for higher immersion time of 545 days, the modeled values are lower than the experience. This is due to increased surface concentration values of total chlorides with immersion time. Yet the better matching of total chloride concentrations in the interior of the material (at increasing depths from exposed surface) and more importantly the penetration depth are very satisfactory.

6.4 Extraction of some additional parameters of interest from experimental chloride profiles

From experimental chloride profiles, some other parameters were also calculated. These parameters were needed as input data for models based on Fick's second law of diffusion.

6.4.1 Apparent diffusion coefficient and surface concentration

The purpose to determine apparent diffusion coefficient and surface concentration was to deduce total chloride profiles from models based on the error function solution of Fick's second law of diffusion. With the obtained total chloride profiles, a curve was fitted with analytical solution of the Fick's second law as described in chapters 1 and 2. It should be noted that the curve fitting with only total chloride profiles was exercised in accordance with the standard models, which take into account only the total chloride profiles. Recall relation **[1.33]** in chapter 1. For the sake of consistency this relation is re-quoted here as equation **[6.7]**. While using this relation, due attention was paid to the units of parameters comprising this relation. Look at the **Table 6.15**. For demonstration purposes, one such curve fitting is shown in **Figure 6.43**. The recommendations, which were followed while curve fitting are described in Appendix 4 of this work.

$$C = C_i + (C_s - C_i)erfc\left(\frac{x}{2\sqrt{D_a t}}\right) \quad \textbf{[6.7]}$$

In the above relation, the parameter D_a is known as the apparent diffusion coefficient and C_s is called as the chloride surface concentration.

Table 6.15 Units of parameters used in curve fitting with error function solution of Fick's second law

Parameters	$C(x,t)$, C_i, C_s	x	D_a	t
Units	% mass of concrete	m	m²/s	s

6.4.1.1 NaCl concentration of 165 g/l with concrete age of 28 days at exposure

The values of apparent diffusion coefficient and surface concentrations are quoted in **Tables 6.16**, **6.17**, **6.18** and **6.19**.

Table 6.16 Curve fitting data obtained from total chloride profiles of 35 days exposure period

	Specimen 1	Specimen 2
D_a (1E12- m²/s)	5.56	6.11
C_s (% mass of concrete)	1.13	1.2

Table 6.17 Curve fitting data obtained from total chloride profiles of 100 days exposure period

	Specimen 1	Specimen 2	Specimen 3
D_a (1E12- m²/s)	3.98	4.31	3.63
C_s (% mass of concrete)	1.17	1.12	1.16

Table 6.18 Curve fitting data obtained from total chloride profiles of 200 days exposure period

	Specimen 1	Specimen 2	Specimen 3
D_a (1E12- m²/s)	3.09	2.95	3.17
C_s (% mass of concrete)	1.11	1.06	1.26

Table 6.19 Curve fitting data obtained from total chloride profiles of 330 days exposure period

	Specimen 1	Specimen 2	Specimen 3
D_a (1E12- m²/s)	2.63	2.36	2.9
C_s (% mass of concrete)	1.21	1.21	1.26

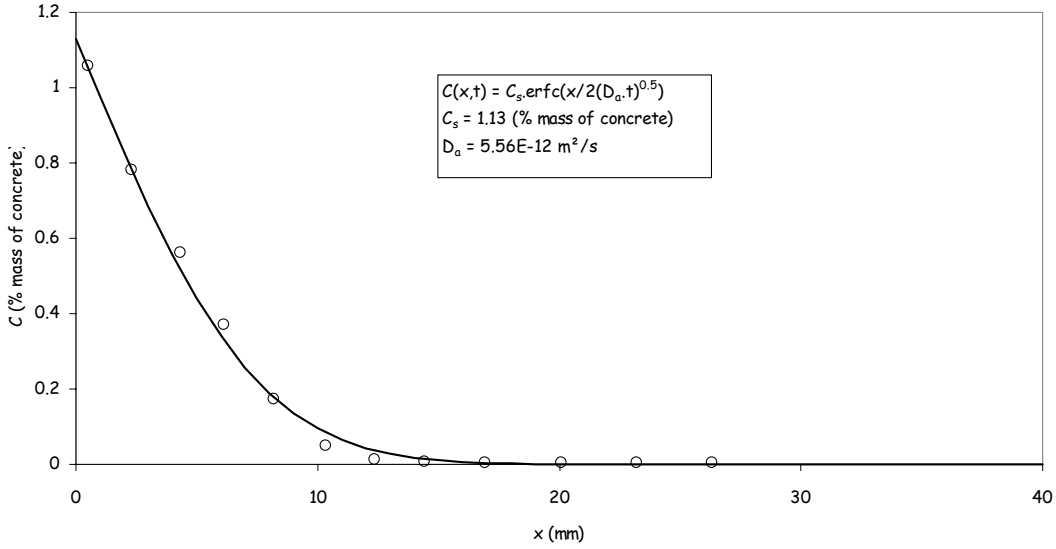

Figure 6.43 Curve fitting with error function solution of Fick's second law of diffusion over total chloride profile (specimen 1) obtained with 165 g/l NaCl and 35 days of exposure period

Figures 6.44 and **6.45** demonstrate the variation of apparent diffusion coefficient and surface chloride concentration as a function of concrete age and exposure period for the same concrete age (28 days) at exposure respectively.

The time dependent apparent diffusion coefficient was deduced in the form of power law as follows:

$$D_a(t) = 2.53E-12t^{-0.46} \quad \textbf{[6.8]}$$

In equation **[6.8]** t represents the material age in years.

The following logarithmic relation was observed with the experimental surface chloride concentration.

$$C_s(t - t_{ex}) = 0.053\ln(t - t_{ex}) + 1.24 \quad \textbf{[6.9]}$$

Where t_{ex} is the age of material at exposure in years and C_s is the chloride surface concentration in % mass of concrete.

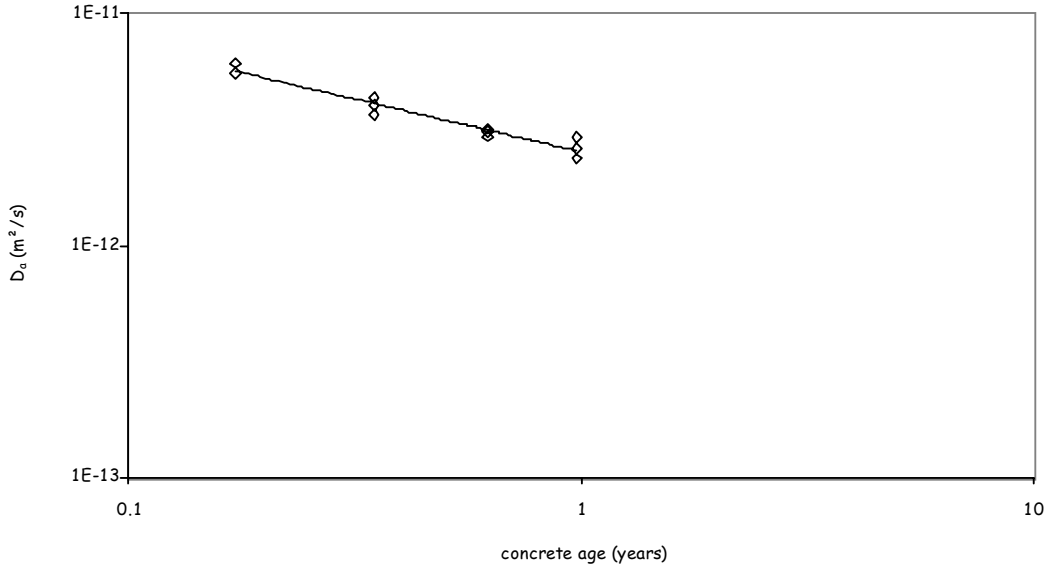

Figure 6.44 Variation of apparent diffusion coefficient with concrete age for 165 g/l NaCl and 28 days of age at exposure

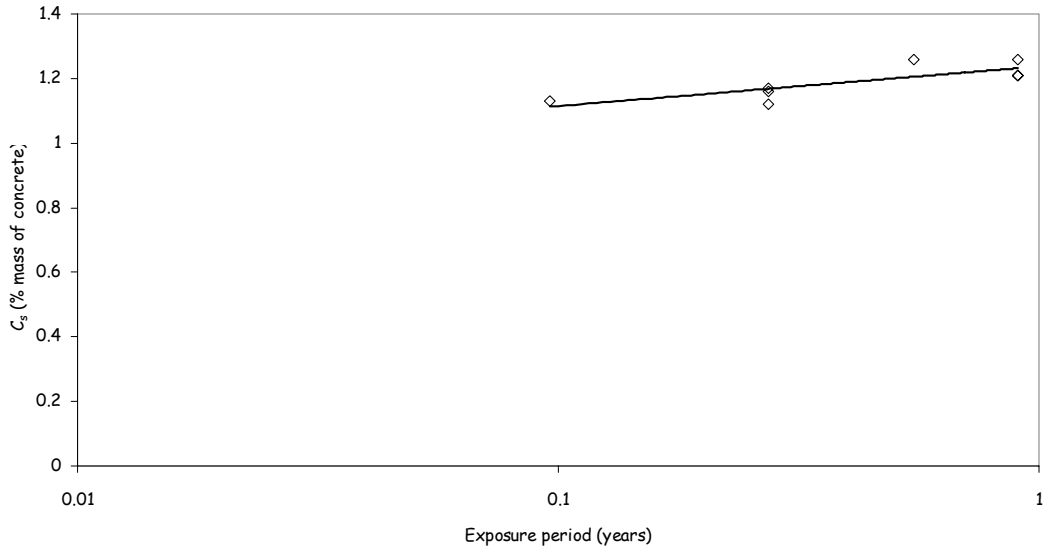

Figure 6.45 Variation of chloride surface concentration with concrete age for 165 g/l NaCl and 28 days of age at exposure

Equation **[6.8]** demonstrates that the apparent diffusion coefficient decreases with an increase in materials age. Similarly chloride surface concentration increases with increase in exposure period.

Equations **[6.7]** and **[6.8]** are useful relations for certain chloride ingress models based on error function solution of Fick's second law of diffusion. Availability of several total chloride profiles also makes possible to run error function solution of Fick's second law of diffusion with a variable apparent diffusion coefficient instead of a constant one: recall relation **[2.56]**. Additionally an average diffusion coefficient from the beginning to the end of immersion period can also be calculated for use in error function solution: recall relation **[2.57]**. All the two parameters are varying continuously still at the end of one year of concrete age, which is in agreement with literature.

Note that here years has been selected as the time unit against days approximately everywhere else. This is for the purpose of coherence with the models based on error function solution of Fick's second law of diffusion where these units are generally used so as to do predictions over very long periods, which are of the order of tens of years. Additionally the variation of D_a is presented with concrete age whereas that of C_s is shown with exposure period in accordance with these models.

6.4.1.2 NaCl concentration of 165 g/l with concrete age of 420 days at exposure

The two parameters D_a and C_s determined in the same way as above are demonstrated in **Tables 6.20** and **6.21** respectively for 100 and 200 days of exposure.

Table 6.20 Curve fitting data obtained from total chloride profiles of 100 days exposure period

	Specimen 1	Specimen 2	Specimen 3
D_a (1E12- m²/s)	2.8	3.43	3.13
C_s (% mass of concrete)	0.9	0.9	0.97

Table 6.21 Curve fitting data obtained from total chloride profiles of 200 days exposure period

	Specimen 1	Specimen 2	Specimen 3
D_a (1E12- m²/s)	2.78	2.21	3
C_s (% mass of concrete)	1.06	1	0.85

The evolution of D_a with concrete age and C_s with exposure period, both in years is shown in **Figures 6.46** and **6.47**.

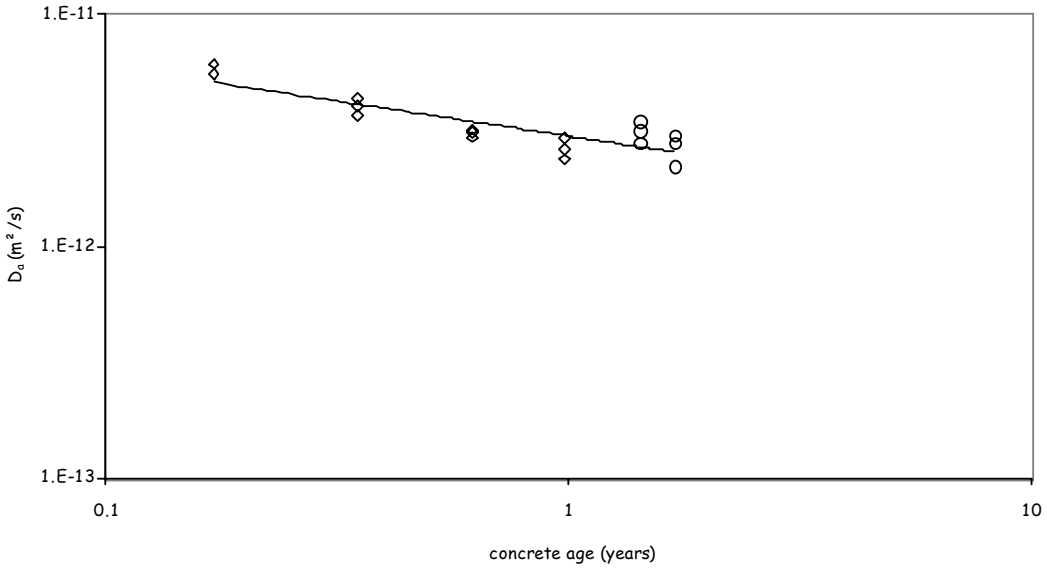

Figure 6.46 Variation of apparent diffusion coefficient with concrete age for 165 g/l NaCl for 28 and 420 days of age at exposure

Note that **Figure 6.46** is based upon values of D_a with 165 g/l of NaCl regardless of concrete age at exposure.

In **Figure 6.46**, the last 6 hollow circles correspond to 100 and 200 days of exposure with 420 days of curing. The time dependent apparent diffusion coefficient relation was changed as follows.

$$D_a(t) = 2.98E-12t^{-0.3} \quad \textbf{[6.10]}$$

While the following logarithmic relation for C_s was observed with the experimental data for 420 days of curing as shown in **Figure 6.47**.

$$C_s(t - t_{ex}) = 0.0673\ln(t - t_{ex}) + 1.01 \quad \textbf{[6.11]}$$

The logarithmic trend line shows that the surface chloride concentration has slightly increased but visually a horizontal line is also possible in between the points (even a decreasing trend is

can also be found). Anyway there is no harm in assuming that the surface chloride concentration is constant between the two series of points.

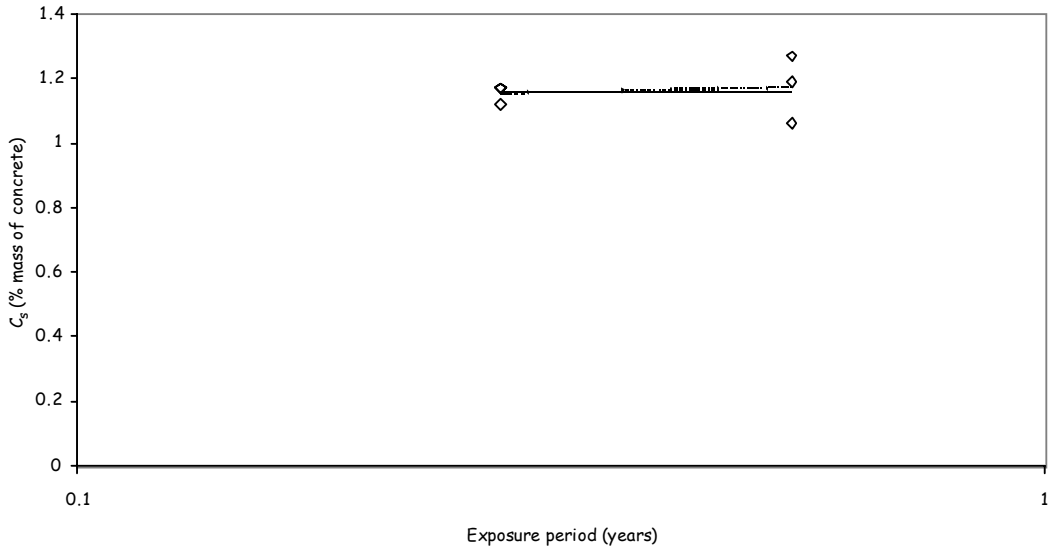

Figure 6.47 Variation of chloride surface concentration with concrete age for 165 g/l NaCl and 420 days of age at exposure

6.4.1.3 NaCl concentration of 33 g/l with concrete age of 28 days at exposure

With the obtained total chloride profiles, the values of apparent diffusion coefficient and surface concentrations, determined in the same way, are quoted in **Tables 6.22**, **6.23** and **6.24**.

Table 6.22 Curve fitting data for 180 days exposure period

	Specimen 1	Specimen 2	Average
D_a (1E12- m²/s)	1.97	2.73	2.32
C_s (% mass of concrete)	0.44	0.4	0.42

Table 6.23 Curve fitting data for 365 days exposure period

	Specimen 1	Specimen 2	Average
D_a (1E12- m²/s)	2.44	2.43	2.44
C_s (% mass of concrete)	0.45	0.42	0.44

Table 6.24 Curve fitting data for 540 days exposure period

	Specimen 1	Specimen 2	Average
D_a (1E12- m²/s)	2.11	2.21	2.17
C_s (% mass of concrete)	0.5	0.51	0.51

The following time dependency relation was obtained with the experimental data obtained while working with 33 g/l NaCl.

$$D_a(t) = 2.43E-12t^{-0.24} \quad \textbf{[6.12]}$$

Where t is the concrete age in years and D_a is the apparent diffusion coefficient in m²/s.

The following logarithmic relation was observed with the experimental data.

$$C_s(t - t_{ex}) = 0.097\ln(t - t_{ex}) + 0.45 \quad \textbf{[6.13]}$$

Where t_{ex} is the age at exposur in years and C_s is the chloride surface concentration in % mass of dry concrete.

The evolutions of D_a and C_s are shown in **Figures 6.48** and **6.49** respectively. Although two specimens per exposure period, the first point at 180 days (0.5 years) of exposure period was discarded due to its large divergence with the rest of the data. Note that in **Figure 6.48**, the two points at 1 year exposure period superpose each other.

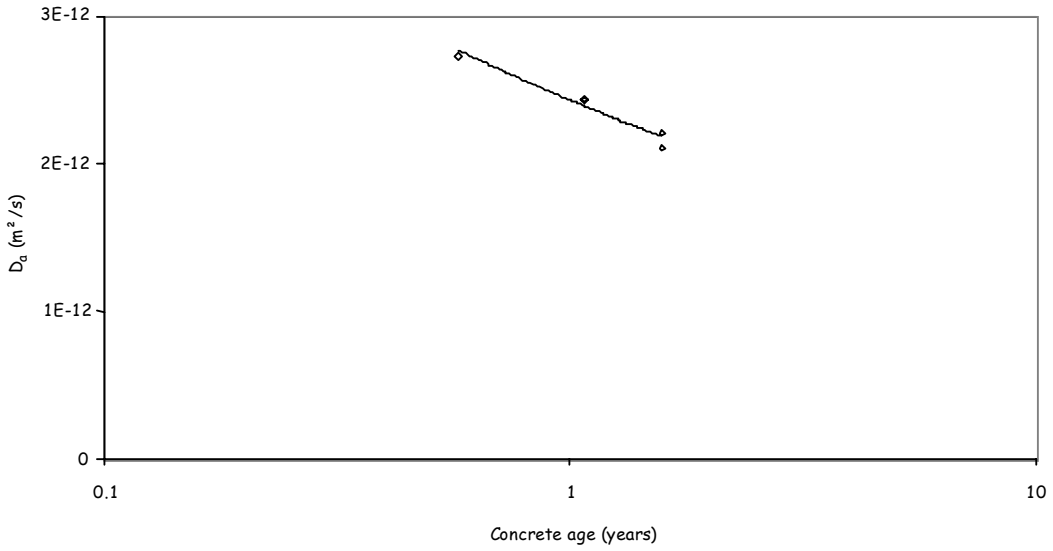

Figure 6.48 Variation of apparent diffusion coefficient with concrete age for 33 g/l NaCl and 28 days of age at exposure

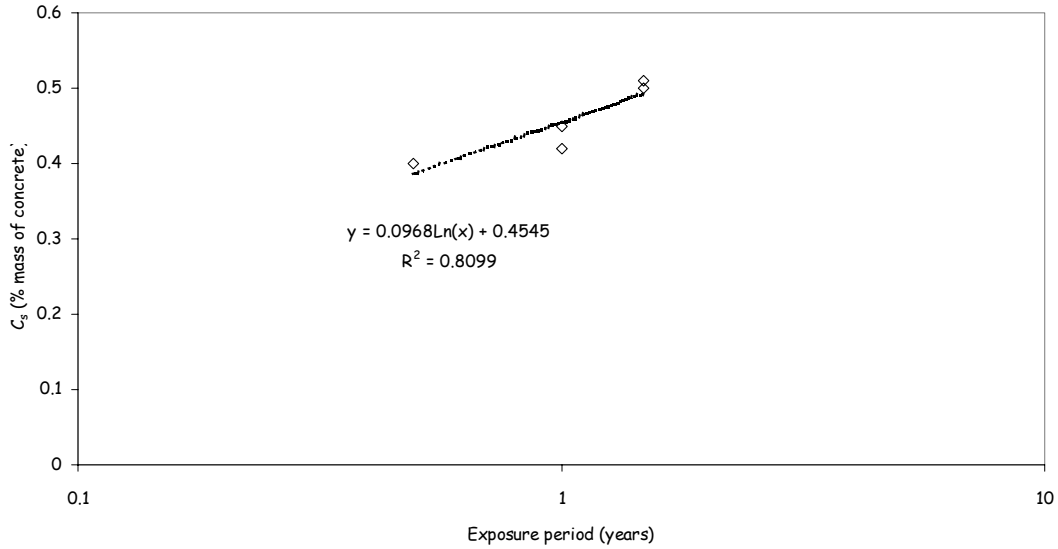

Figure 6.49 Variation of surface concentration with concrete age for 33 g/l NaCl and 28 days of age at exposure

6.4.2 Conclusions-effect of exposure period on chloride penetration

6.4.2.1 Experimental chloride profiles

From experimental chloride profiles, whether water or acid-soluble, it is clear that:

1. The penetration depth increases with an increase in exposure period for the same age of concrete at exposure. However the penetration rate is non linear with respect to exposure period. The experimental data has shown that the penetration depth curve follows the same slope in square root of immersion time regardless of the exposure solution concentration.
2. The immersion test NT BUILD 443 is a good tool, where significant chloride penetrations are required in a minimum possible time frame by employing a larger concentration of 165g/l NaCl.
3. The average water-soluble chloride concentrations are mostly 40-70% of the average acid-soluble chloride concentration in a concrete slice. This result highlights the importance of chloride interactions with the solid phase of cement-based materials. Binding deserves a lot of interest because bound chlorides are not available for diffusion and therefore reduce the risk of corrosion of the reinforcement bars.

4. **Figure 6.10** demonstrates that chloride binding is independent of immersion time, thus only one binding isotherm is needed if simulation is needed for a higher immersion period. However to remain on safe side, it is recommended that this binding isotherm should correspond to a mature concrete for the reasons similar to those, described in the case of chloride diffusion coefficient in section 6.3.

6.4.2.2 Surface chloride content

Surface chloride content herein is defined as the total chloride load accumulated at the materials surface. In all the cases, it is evident that this parameter increases with increase in exposure period for the same environmental solution and same material age at exposure. If the extracted trend lines are given significance, its evolution could be seen in **Figure 6.50**. From this figure, it seems that C_s should assume an asymptotic value after a certain time of exposure. Hence on the basis of this, it would not be inappropriate to think of a constant C_s for older structures. But for very younger concrete specimens as the one used during this work, this parameter has some significance.

With increase in acid-soluble surface content, it was also observed that the corresponding water-soluble surface content also increases. This could be easily observed in **Figures 6.6** to **6.9** (pages 110 and 111). The near surface water-soluble chloride concentration in **Figure 6.6** is below $C_{f,s}$ but with increase in exposure period, its value exceeds $C_{f,s}$. One reason could be the carbonation effect described in section **6.2.3.5**. The other possible reason could be that described in section **6.2.3.4** i.e. while more total chloride content was present in a concrete powder, more chlorides were extracted while filtering powder with distilled water or in other words, some loosely bound chlorides were also snatched by water leading to higher water-soluble chlorides.

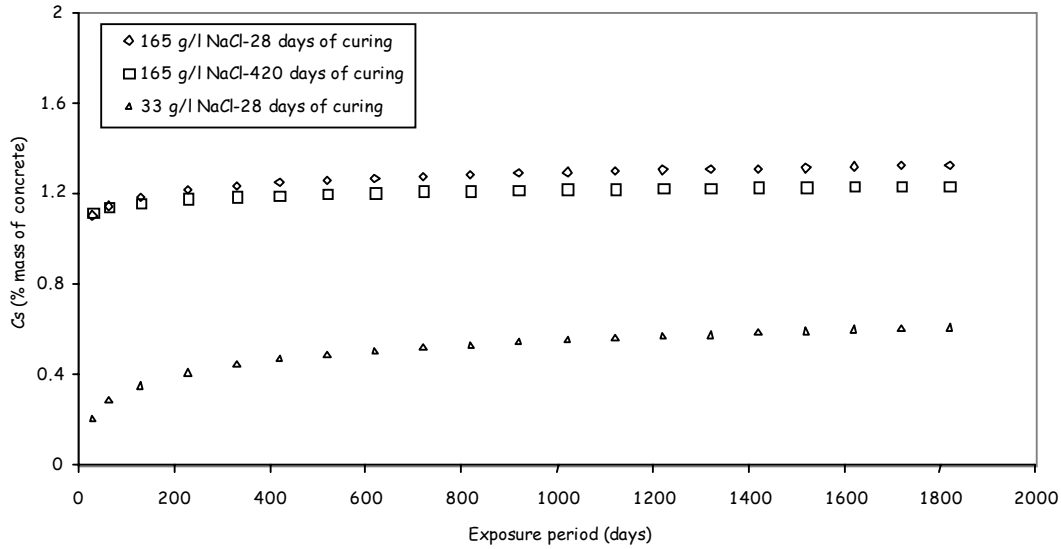

Figure 6.50 Evolution of C_s with exposure period

6.4.2.3 Apparent diffusion coefficient

The general trend shows that apparent diffusion coefficient reduces with increase in exposure period for the same concrete age at exposure and for the same environmental concentration.

Similar to **Figure 6.50**, if a similar figure is drawn to watch the evolution of D_a with concrete age, an asymptotic value for D_a is achieved at longer periods. Which means that similarly a constant D_a for old structures would not be a bad option while using models based on error function solution of Fick's second law of diffusion.

6.4.3 Conclusions-effect of age at exposure on chloride penetration

6.4.3.1 Comparison of experimental chloride profiles

From **Figures 6.13** to **6.16** (pages 115 and 116), it seems that an approximately one year difference in the age of concrete has no impact on the chloride penetration both for chloride in the pore solution and total chloride. The penetration depths, which increase with the time of exposure, are also in good agreement with the experimental results.

6.4.3.2 Surface chloride content

The parameter C_s decreases with increase in curing period before exposure to chlorides if we compare relations **[6.9]** (page 146) and **[6.11]** (page 149) in the case of 165g/l NaCl. This parameter is significant in the sense that concrete structures with smaller curing period at exposure to sea water will be subjected to a higher accumulated surface content as compared to the structures with larger curing periods before exposure and according to error function solution of Fick's second law of diffusion should lead to higher concentrations and probably to shorter structures life [EUR 99]. From **Figure 6.47**, it is also obvious that a constant C_s with effect from 420 days of concrete age is possible noting that the curing conditions itself acted as a continuous exposure but without chlorides [EUR 99].

6.4.3.3 Apparent diffusion coefficient

As evident from **Figure 6.46**, D_a appears to follow the same trend line regardless of materials age at the time of exposure. In the same manner as C_s, at higher curing period before exposure D_a should be smaller as it follows the age dependency and thus should lead to smaller penetrations compared to lower curing periods before exposure. If we compare the profiles with 28 days of curing with those with 420 days of curing with respect to models based on Fick's second law of diffusion, a lower D_a at higher curing period should lead to smaller chloride penetrations at respective depths. This might lead to smaller total surface concentration and vice versa.

6.4.3.4 Parameter σ

This is a parameter that denotes the time dependency of apparent diffusion coefficient with concrete age i.e. how fast the diffusion coefficient decreases when exposed to saline environment. The time-dependent apparent diffusion coefficient relationship has been discussed in chapter 2 and is here given for reminder as relation **[6.14]**. The values obtained for higher concentration with two concrete ages at exposure and lower concentration can be summarized in the **Table 6.25**.

$$D_a(t) = D_{a,ref}\left(\frac{t_{ref}}{t}\right)^{\sigma} \qquad \textbf{[6.14]}$$

Table 6.25 Time dependency parameter for D_a

Concentration NaCl (g/l)	165	33
Curing time (days)	28 and 420	28
σ	0.30	0.24

The above table demonstrates that σ value is insignificantly affected by curing period before exposure.

6.4.4 Conclusions-effect of exposure NaCl concentration on chloride penetration

6.4.4.1 Apparent diffusion coefficient

If we compare D_a values for 165 g/l NaCl and 33 g/l NaCl, no significant difference for difference of concentrations was observed i.e. D_a seems to be independent of environmental concentration. For example if we look at the D_a values for higher concentration with 330 days of exposure period, it varies between 2.36E-12 to 2.9E-12 m²/s, while for lower concentration with 365 days of exposure period, its value is around 2.44E-12 m²/s.

6.4.4.2 Parameter σ

Table 6.25 suggests that σ values are higher for higher concentrations. The possible reason could be that the interactions between the chloride ions are enhanced due to higher concentrations or in other word the chloride ions are more tightened which leads to higher σ at higher concentrations as compared to lower concentrations.

6.5 General conclusions

This chapter consists of two main parts: Part 1 deals with experimental data while part 2 comprises numerical modeling conducted with MsDiff. Experimental part is mainly dedicated to water and acid-soluble chloride profiles along with input data, determined experimentally. The experimental profiles were meant to validate modeled free and total chloride profiles with MsDiff. These experimental profiles also served to provide binding isotherm needed as input data for MsDiff. In addition, some other data was also deduced from chloride profiles, which was either necessary to run certain chloride ingress models other than MsDiff or to explain certain experimental results with respect to error function solution of Fick's second law of diffusion. The induction of this data to run the error-function models will be discussed in the

next chapter. Comparison between the experimental and data simulated with MsDiff is also discussed. Here in this chapter a new idea has been given to determine the chloride binding isotherm. Where the binding isotherm used for modeling 165 g/l NaCl test results was obtained from experimental chloride profiles (NT BUILD 443 method with prolonged immersion times) in the range 0-2800 moles-m^{-3}, the binding isotherm for simulating 33 g/l NaCl conditions was obtained with the same profiles but in the range of 0-570 moles-m^{-3} along with the assistance of surface bound amounts obtained from 33 g/l NaCl tests profiles. The simulated results seem to be satisfactory for all the two environmental concentrations tested i.e. 165 g/l and 33 g/l NaCl both in terms of concentrations at different levels and the penetration depth. The experimental results have revealed a large amount of total chlorides as compared to the free quantities. This is perhaps due to a higher cement content, which should result in a larger amount of bound chlorides and consequently more total chlorides. More cement content will lead to more hydrated CSH phase so more space will be available for chloride ion adsorption than in case of lower cement content.

References

[ARY 90] Arya, C., Buenfled, N.R., Newman, J.B., Factors influencing chloride-binding in concrete, Cement and Concrete Research, Vol. 20, pp. 291-300, USA, 1990.

[EUR 99] EuroLightCon document BE96-3942/R3, 1999.

[KHI 05] A. Khitab, S. Lorente, J.P. Ollivier, Predictive model for chloride penetration through concrete, Magazine of Concrete Research, accepted.

[LAR 98] C.K. Larsen, Chloride binding in concrete, effect of surrounding environment and concrete composition, PhD thesis, Norwegian University of Science and Technology, Trondheim, Norway, 1998.

[NOR 95] NORDTEST. Concrete, hardened : accelerated chloride penetration. NT BUILD 443, 1995.

[NUG 02] F. NUGUE, Recherche d'une méthode rapide de détermination du coefficient de diffusion en millieu cimentaire saturé, Laboratoire Matériaux et Durabilité des Constructions, Thèse de l'Institut National des Sciences Appliquées, Toulouse, 2002.

[RAM] Ramachandran, V.S., Seeley, R.C., Polomark, G.M., Free and combined chloride in hydrating cement and cement components, Division of Building Research, National Research Council Canada, Ottawa, Ontario, Canada KIA OR6.

[TAN 96] L. Tang, Chloride transport in concrete – Measurement and predictions, Chalmers Univ. of Technology, Publication P-96:6, 1996.

[TRU 00] O. Truc, Prediction of Chloride Penetration into Saturated Concrete – Multi-species approach, Chalmers Univ. of Tech., Göteborg, Sweden, INSA, Toulouse, France, 2000.

CHLORIDE INGRESS MODELING WITH MODELS OTHER THAN MSDIFF

CHAPTER 7 : CHLORIDE INGRESS MODELING WITH MODELS OTHER THAN MSDIFF..... 160

CHAPTER 7

CHLORIDE INGRESS MODELING WITH MODELS OTHER THAN MSDIFF

7.1 Introduction

This chapter deals with modeling through chloride ingress models other than MsDiff for the sake of comparison. All these models have already been described in chapter 2 of present work. Here only governing equations are recollected along with description of input parameters. The simulated profiles are compared with experimental data concerning 33 g/l NaCl in the exposure solution.

7.2 Error function model

Recall equation **[2.1]**. The equation is quoted again here as relation **[7.1]**.

$$C(x,t) = C_i + (C_s - C_i)\,erfc\left(\frac{x}{\sqrt{4D_a t}}\right) \qquad \textbf{[7.1]}$$

The input data for the model is quoted in **Table 7.1**.

Table 7.1 Input data for Erf model, constant D_a and constant C_s

Parameters	C_i	C_s	D_a
Units	% concrete mass	% concrete mass	m²/s
Values	0	0.1123	2.73E-12

Note that these values were obtained from curve fitting of total chloride profile with 33g/l NaCl solution and 6 months of exposure period using error function solution of Fick's second law of diffusion. The results from 6 month long immersion test were used as input data to simulate chloride profiles for 12 and 18 months immersion periods as this model treats D_a and C_s as invariable parameters over time. The total chloride profiles obtained are compared with experimental profiles in **Figures 7.1** and **7.2**.

7.3 False error function model

Remind that this model takes into consideration a variable D_a and a variable C_s. The model is described by the following equations while the input data is arranged in **Table 7.2**.

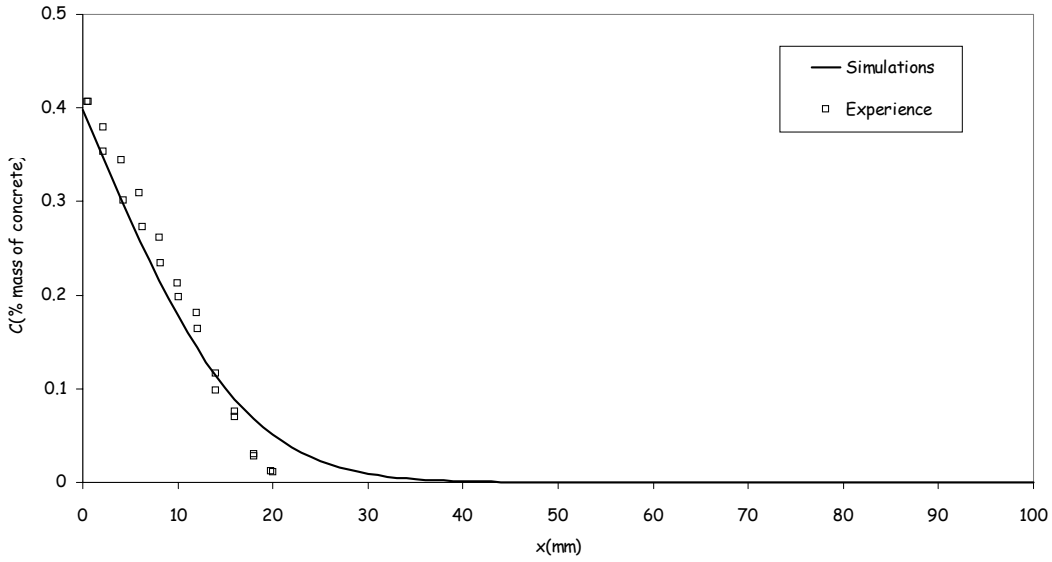

Figure 7.1 Comparison of total chloride profile simulated with Erfc model and experimental data for one year of immersion and 33 g/l NaCl

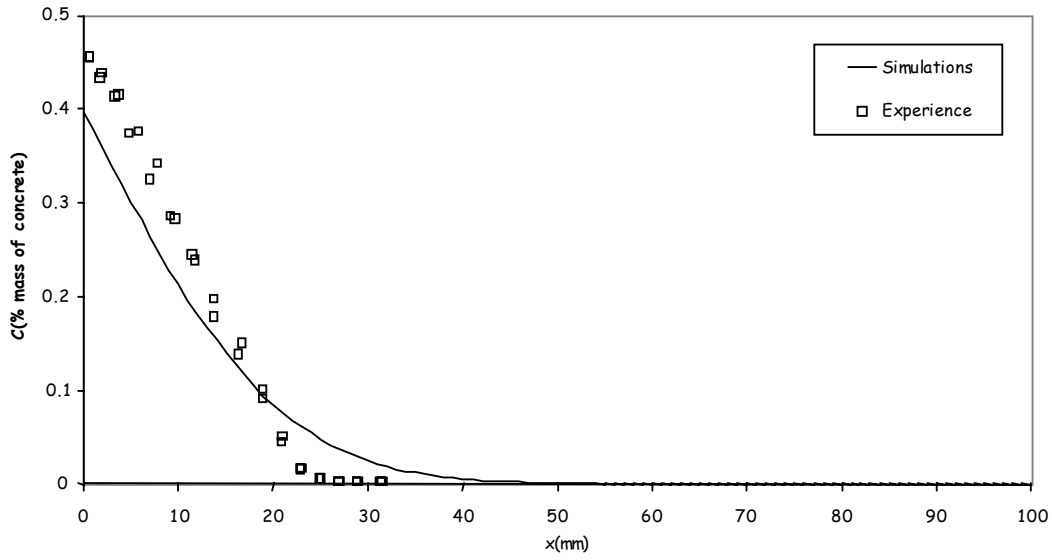

Figure 7.2 Comparison of total chloride profile simulated with Erfc model and experimental data for 18 months of immersion and 33 g/l NaCl

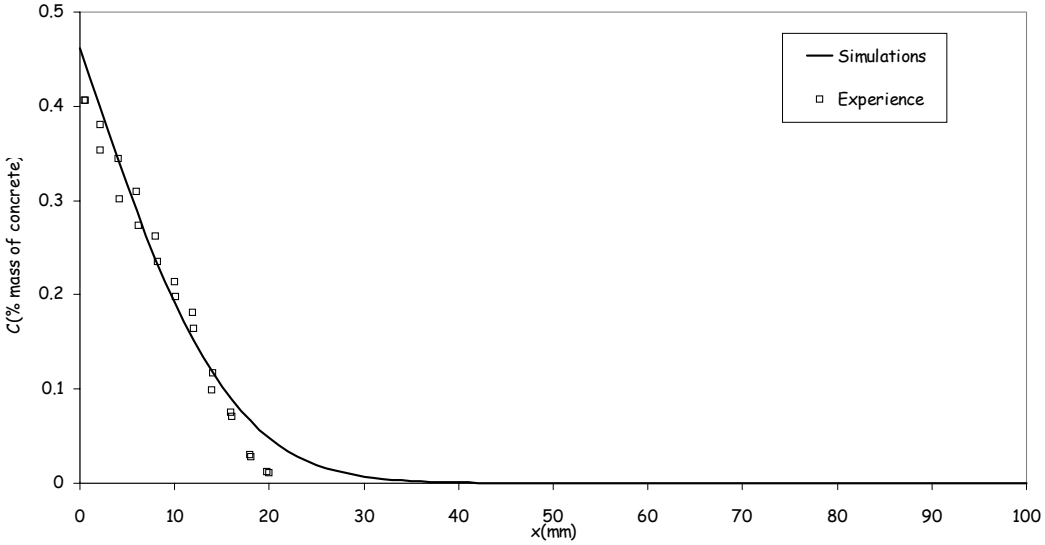

Figure 7.3 Comparison of total chloride profile simulated with False-Erfc model and experimental data for one year of immersion and 33g/l NaCl

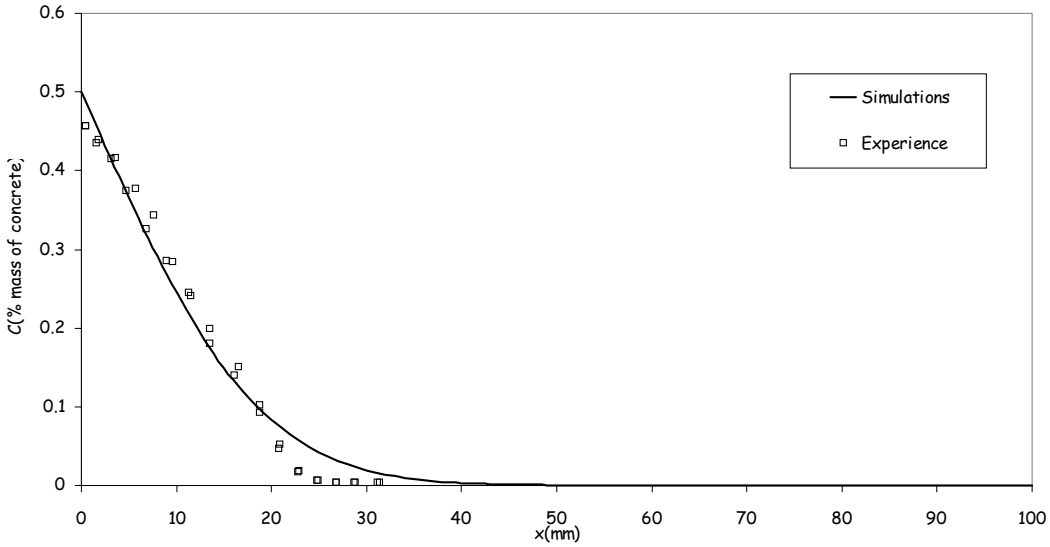

Figure 7.4 Comparison of total chloride profile simulated with False-Erfc model and experimental data for 18 months of immersion and 33g/l NaCl

$$C(x,t) = C_s(t)erfc\left[\frac{x}{2\sqrt{D_a(t)t}}\right] \quad \textbf{[7.2]}$$

$$D_a(t) = D_{a,r}\left[\frac{t_r}{t}\right]^{\sigma} \quad \textbf{[7.3]}$$

$$C_s(t) = A\,ln(t - t_{ex}) + B \quad \textbf{[7.4]}$$

Table 7.2 Input data used for False Erfc model

Parameters	$D_{a,r}$	t_r	σ	A	B
Units	m²/s	years	------	------	------
Values	2.43E-12	0.5	0.24	0.097	0.45

7.4 Duracrete model

The constitutive equation for Duracrete model is quoted as follows:

$$C(x,t) = C_s\left[1 - erf\left(\frac{x}{\sqrt{4k_c k_e k_t D_{RCM,r}\left(\frac{t_r}{t}\right)^{\sigma} t}}\right)\right] \quad \textbf{[7.5]}$$

While all the other parameters were used as quoted in literature, the value for $D_{RCM,r}$ was used as obtained by means of LMDC test for concrete age of 28 days with σ as obtained from a series of 3 LMDC tests conducted during the present work. All the input data is illustrated in **Table 7.3**.

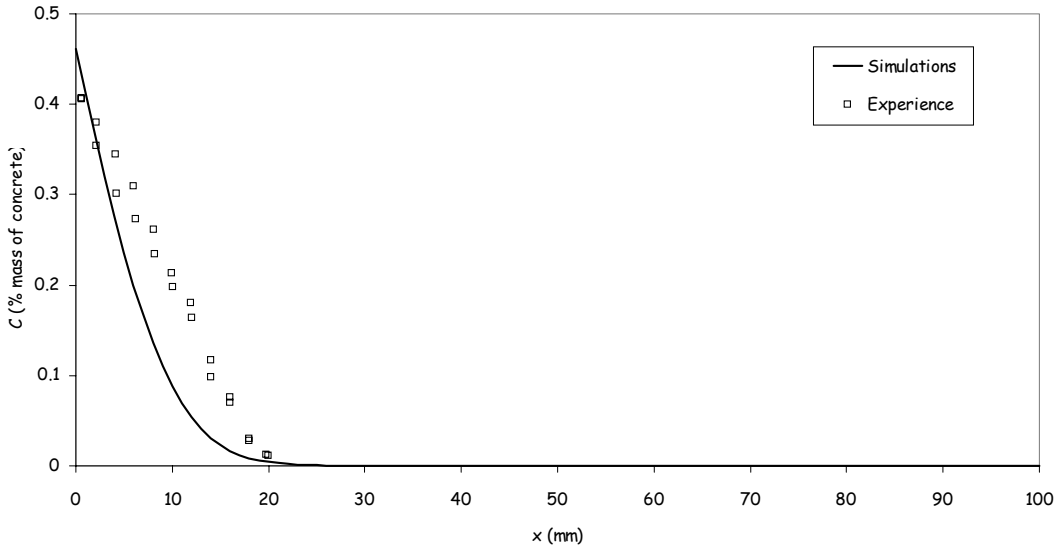

Figure 7.5 Comparison of total chloride profile simulated with Duracrete model and experimental data for one year of immersion and 33g/l NaCl

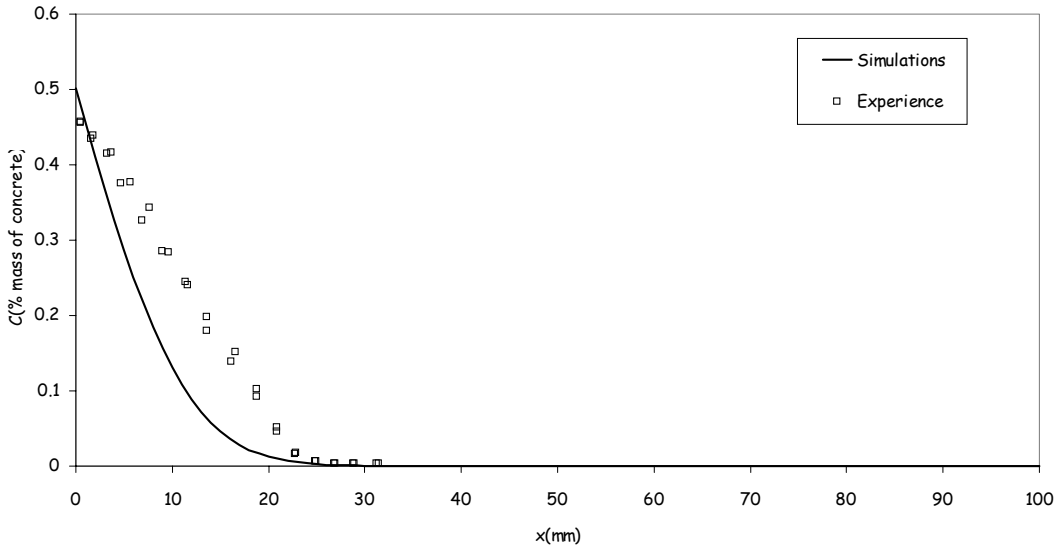

Figure 7.6 Comparison of total chloride profile simulated with Duracrete model and experimental data for 18 months of immersion and 33g/l NaCl

Table 7.3 Input data for Duracrete model [BE 00]

Parameters	C_s	k_c	k_e	k_t	$D_{RCM,r}$	t_r	σ
Units	% mass of concrete	------	------	------	m²/s	days	------
Values	0.1123	1	1	1	18E-13	28	0.89

Note that in the above table k_c is unity as the material with which $D_{LMDC,r}$ was measured and the one subjected to immersion test were from the same lot of materials undergone curing for 28 days under exactly the same conditions. The parameter k_e is also unity as the material was fully saturated. Also it was decided to take a unity value for k_t in conjunction with modeling through MsDiff, where $D_{LMDC,r}$ was taken as the effective diffusion coefficient. The results of modeling with Duracrete model are shown in **Figures 7.5** and **7.6**.

7.5 Modified Duracrete model

This version of Duracrete consists of modifications proposed by Gehlen. The governing equations are again presented as **[7.6]** and **[7.7]**.

$$C(x,t) = (C_{s,\Delta x} - C_i)\left[1 - erf\left(\frac{x - \Delta x}{\sqrt{4k_{RH}k_t k_T D_{RCM,r}\left(\frac{t_r}{t}\right)^{\sigma} t}}\right)\right] + C_i \qquad \textbf{[7.6]}$$

$$k_T = \exp\left[b_T\left(\frac{1}{T_r} - \frac{1}{T}\right)\right] \qquad \textbf{[7.7]}$$

Since T_r and T are same, the value of k_T turns out to be unity. The values for other parameters are specified in **Table 7.4**.

Table 7.4 Input data for modified Duracrete model

Parameters	C_i	Δx	K_{RH}	k_T
Units	% concrete mass	m	------	------
Values	0	0.04	1	1

Although all the data to run this model is available, the thickness of Δx, i.e. the convection zone depth is incompatible with our experimental results. During this work, the maximum penetration depth achieved is approximately 3 cm, while a test value of 4 cm has been given as the thickness of this zone, due to which it is not possible to compare the simulations made with model with our experimental data.

7.6 JSCE model

The governing equations are given below:

$$C(x,t) = \gamma_{Cl} Cs\left[1 - erf\left[\frac{x}{2\sqrt{D_d t}}\right]\right] + C_i \quad \textbf{[7.8]}$$

$$D_d = \gamma_c D_k \quad \textbf{[7.9]}$$

$$D_k = \gamma_P D_P \quad \textbf{[7.10]}$$

$$\log_{10} D_P = 4.5(W/C)^2 + 0.145(W/C) - 8.47 \quad \textbf{[7.11]}$$

While C_s and C_i values have already been summarized, the other 4 unit less parameters are described in **Table 7.5**.

Table 7.5 Input parameters for JSCE model

Parameters	γ_{Cl}	γ_c	γ_p	W/C
Values	1.3	1.0	1.0	0.4

In **Table 7.5**, γ_p is the safety factor taking into account the errors for predicted coefficient. Recall that during this work, no experimental value has been adjusted for MsDiff modeling. All the values are outcome of experiments. Therefore, it was decided to take the value of γ_p as unity because never the effective diffusion coefficient as determined from LMDC test was multiplied with a safety factor at the time of modeling. The value of C_s was taken as tabulated in **Table 7.1** i.e. 0.1123 (% mass of concrete) as the model takes no C_s evolution in exposure time, rather C_s has been considered a function of distance from coastline.

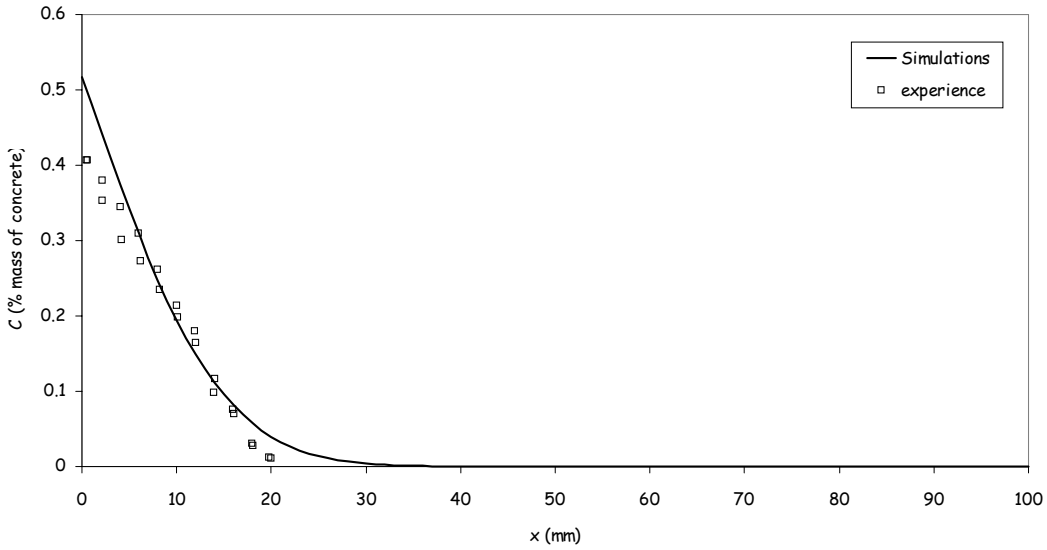

Figure 7.7 Comparison of total chloride profile simulated with JSCE model and experimental data for one year of immersion and 33g/l NaCl

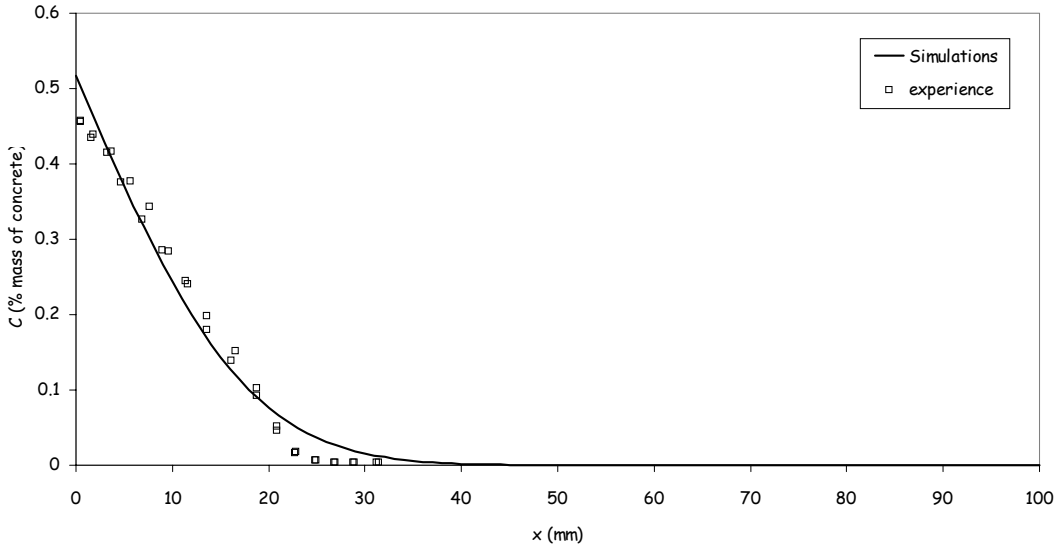

Figure 7.8 Comparison of total chloride profile simulated with JSCE model and experimental data for 18 months of immersion and 33g/l NaCl

7.7 Life-365 model-Base

The governing equations are quoted as follows:

$$\frac{dC}{dt} = D_a \frac{d^2C}{dx^2} \quad \textbf{[7.12]}$$

$$D_a(T) = D_r \, exp\left[\frac{U}{R}\left(\frac{1}{T_r} - \frac{1}{T}\right)\right] \quad \textbf{[7.13]}$$

$$D_a(t) = D_a(T)\left(\frac{t_r}{t}\right)^{\sigma} \quad \textbf{[7.14]}$$

$$D_{28} = D_r = 10^{\,-12.06+2.40(WC)} \quad \textbf{[7.15]}$$

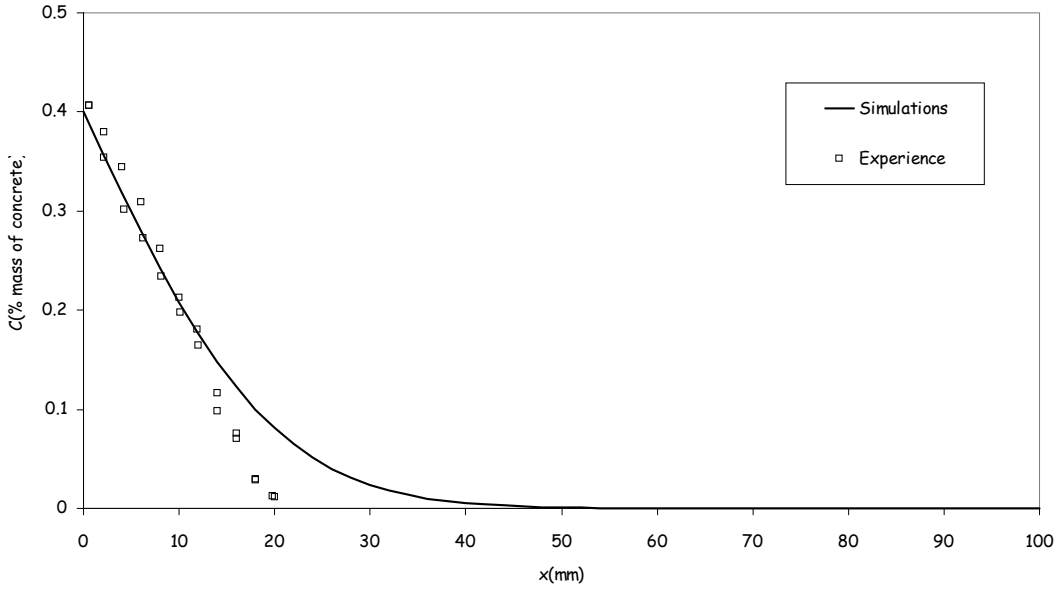

Figure 7.9 Comparison of total chloride profile simulated with Life-365 model with experimental data for one year of immersion and 33g/l NaCl

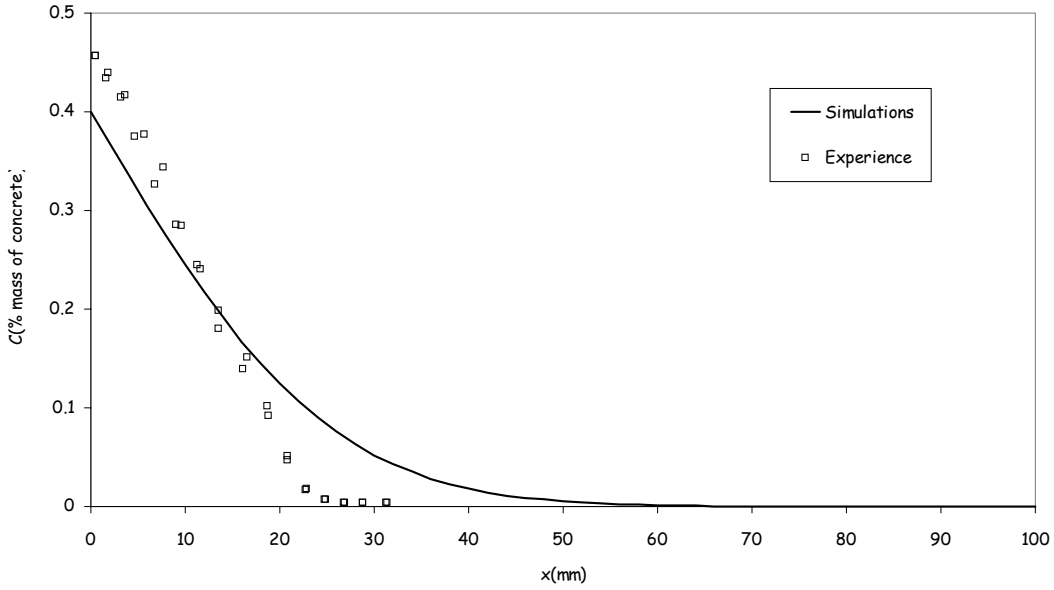

Figure 7.10 Comparison of total chloride profile simulated with Life-365 model with experimental data for 18 months of immersion and 33g/l NaCl

7.8 LEO model

Following are the equations structuring LEO model.

$$C(x,t) = C_i + (C_s - C_i)\left(1 - erf\left(\frac{x}{2\sqrt{k\eta D_a(T)t}}\right)\right) \quad \textbf{[7.16]}$$

$$k = 1 + \frac{1}{4[Cl^-]} \quad \textbf{[7.17]}$$

$$\eta = \frac{1}{1 + 0.5\frac{W_{gel}}{w}} \quad \textbf{[7.18]}$$

$$D_a(T) = D_{a,20°C}\, e^{E_a\left(\frac{1}{293} - \frac{1}{T}\right)} \quad \textbf{[7.19]}$$

Since all the tests were performed at local laboratory temperature (20±2°C), the equation **[7.19]** can be re-written as follows:

$$D_a(T) = D_{a,20°C} \quad \textbf{[7.20]}$$

Table 7.6 Input data for LEO model for 12 and 18 months of immersion

Parameters	W_{gel}	w	Cl^-	k	η
Units	kg/m^{3}concrete	kg/m^{3}concrete	moles/l	----	----
Values	149	160	0.564	1.44	0.68

With the induction of input parameters in relation [**7.16]** we have the following equation. Note that no significant difference was observed for equation **[7.21]** between the calculated values for 12 and 18 months of exposure periods.

$$C(x,t) = C_i + (C_s - C_i)\left(1 - erf\left(\frac{x}{2\sqrt{0.98 D_a t}}\right)\right) \quad \textbf{[7.21]}$$

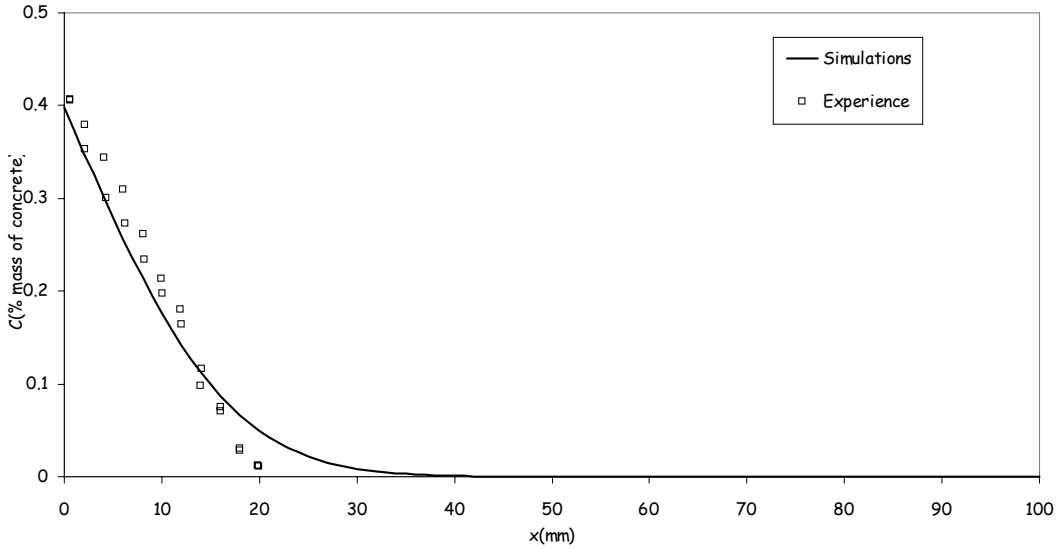

Figure 7.11 Comparison of total chloride profile simulated with LEO model with experimental data for one year of immersion and 33g/l NaCl

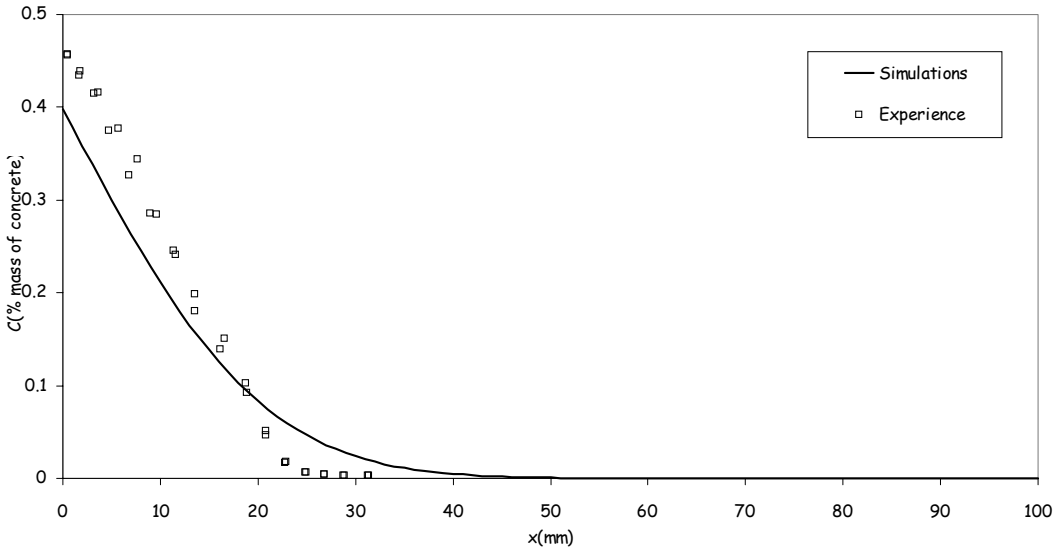

Figure 7.12 Comparison of total chloride profile simulated with LEO model with experimental data for 18 months of immersion and 33g/l NaCl

7.9 HETEK model

The empirical model in the form of sequence of equations is written as follows. Keeping in view these equations, it was decided to carry out simulations using experimental data of 12 and 18 months of immersion period with concrete age at exposure of t_{ex} = 28 days or 0.0767 years in the following equations.

$$C(x,t) = C_s - (C_s - C_i)erfc\left(\frac{0.5x}{\sqrt{(t-t_{ex})D_a(t)}}\right) \quad \textbf{[7.22]}$$

$$C_s = C_i + S_p \tau^q \quad \textbf{[7.23]}$$

$$S_p = C_1\left(\left(\frac{D_1}{D_{100}}\right)^{\lambda}\frac{t_{ex}}{(1-t_{ex})}\right)^q \quad \textbf{[7.24]}$$

$$\tau = \left(\frac{t}{t_{ex}}\right)^{1-\sigma} - \left(\frac{t_{ex}}{t}\right)^{\sigma} \quad \textbf{[7.25]}$$

$$q = \frac{\log_{10}\left(\frac{C_{100}}{C_1}\right)}{\log_{10}\left(\frac{(100-t_{ex})D_{100}}{(1-t_{ex})D_1}\right)} \quad \textbf{[7.26]}$$

$$\sigma = (U(WC)+V)k_{\sigma,env} \quad \textbf{[7.27]}$$

$$\lambda = 0.5\log_{10}\left(\frac{1}{t_{ex}}\right) \quad \textbf{[7.28]}$$

$$C_1 = A_H(WC)k_{C1,env}(\%mass - binder) \quad \textbf{[7.29]}$$

$$C_{100} = C_1 k_{C100,env}(\%mass - binder) \quad \textbf{[7.30]}$$

$$D_1 = B_H \exp\left(-\sqrt{\frac{10}{(WC)}}\right) k_{D_1,env}(mm^2/year) \quad \textbf{[7.31]}$$

$$D_{100} = D_1\left(\frac{1}{100}\right)^{\sigma} \quad \textbf{[7.32]}$$

The input data for 18 months of exposure period is described in the following tables just for the sake of demonstration. It should be kept in mind that these empirical values correspond to the case of structures submerged in seawater.

Table 7.7 Input parameters for diffusion coefficient in HETEK model [FRE 97]

Parameters	A	B	$k_{c1,env}$	$k_{c100,env}$	$k_{\sigma,env}$	$k_{D1,env}$	U	V
Values	3.7	25000	1.4	1.8	0.3	1	1.5	1

With the above coefficients, one year and 100 years diffusion coefficients were calculated, the corresponding values are quoted in **Table 7.8**.

Table 7.8 Diffusion coefficients and surface concentrations

σ	D_1 (m²/s)	D_{100} (m²/s)	C_1 (% mass of concrete)	C_{100} (% mass of concrete)
0.48	5.34e-12	5.86e-13	0.5	0.92

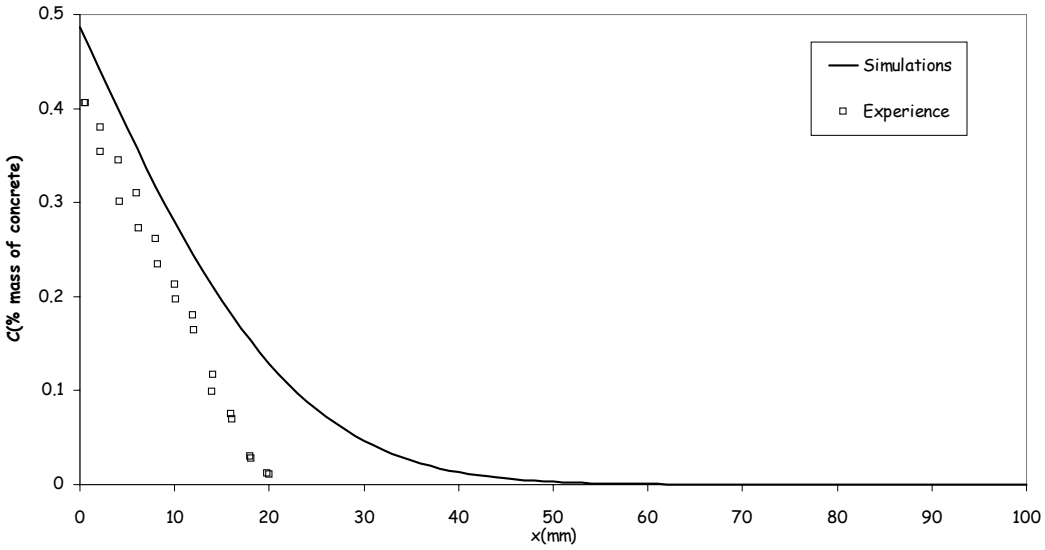

Figure 7.13 Comparison of total chloride profile simulated with HETEK model with experimental data for one year of immersion and 33g/l NaCl

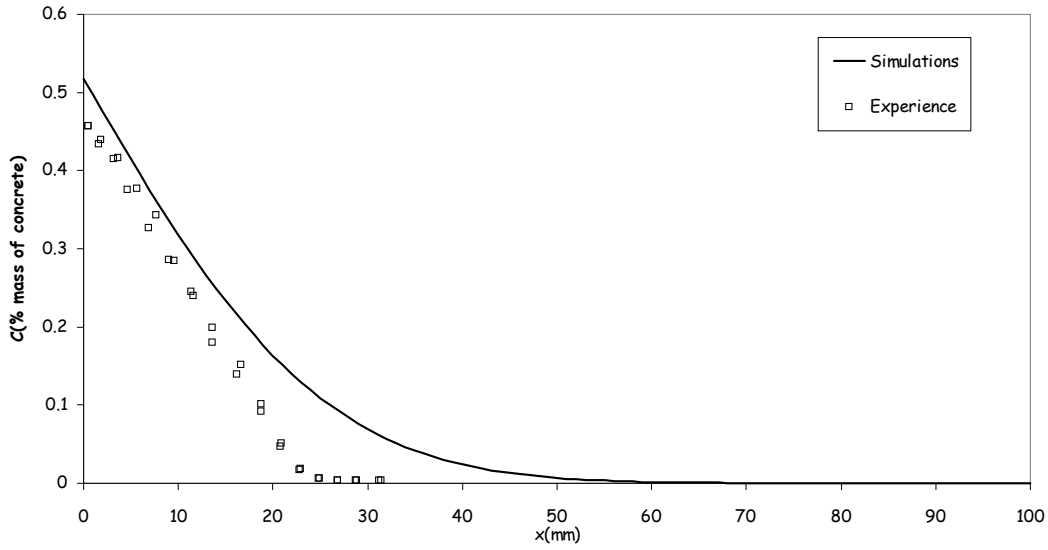

Figure 7.14 Comparison of total chloride profile simulated with HETEK model with experimental data for 18 months of immersion and 33g/l NaCl

Table 7.9 Other model parameters

λ	q	S_P	τ	C_s (%mass of concrete)
-0.0881	1.33	6.92	0.05	0.54

The last parameter to resolve is the time dependent diffusion coefficient $D_a(t)$ which is determined in the following manner.

$$D_a(t) = D_{aex}\left(\frac{t_{ex}}{t}\right)^{\sigma} \quad \textbf{[7.33]}$$

$$D_{aex} = D_1\left(\frac{D_1}{D_{100}}\right)^{\lambda} \quad \textbf{[7.34]}$$

Solving equation **[7.34]** we have D_{aex}= 1.83E-11 m²/s. Putting this value of D_{aex} in relation **[7.33]** we have.

$$D_a(t) = 1.83E-11\left(\frac{0.0767}{t}\right)^{0.557} \quad \textbf{[7.35]}$$

Where t is the materials age at the end of immersion period in years. Now the equation **[7.22]** can be used in order to have simulations with HETEK model. It may be worthy to note that the empirical coefficients were determined from structures exposed to marine environment of 14 ± 4 g/l Cl^- whereas specimens in the present work were exposed to 19.8 g/l Cl^-.

7.10 False-Erfc with modification proposed by Visser

The governing equation is re-written as follows:

$$C(x,t) = C_i + (C_s - C_i)erfc\left(\frac{x}{\sqrt{4\frac{D_r}{1-\sigma}\left(\frac{t_r}{t}\right)^{\sigma} t}}\right) \quad \textbf{[7.36]}$$

The input parameters have already been defined in **Table 7.2** and the comparison of this model with experimental data is shown in **Figures 7.15** and **7.16**.

7.11 False-Erfc with modification proposed by Stanish

The principle equation is re-quoted here as **[7.37]**.

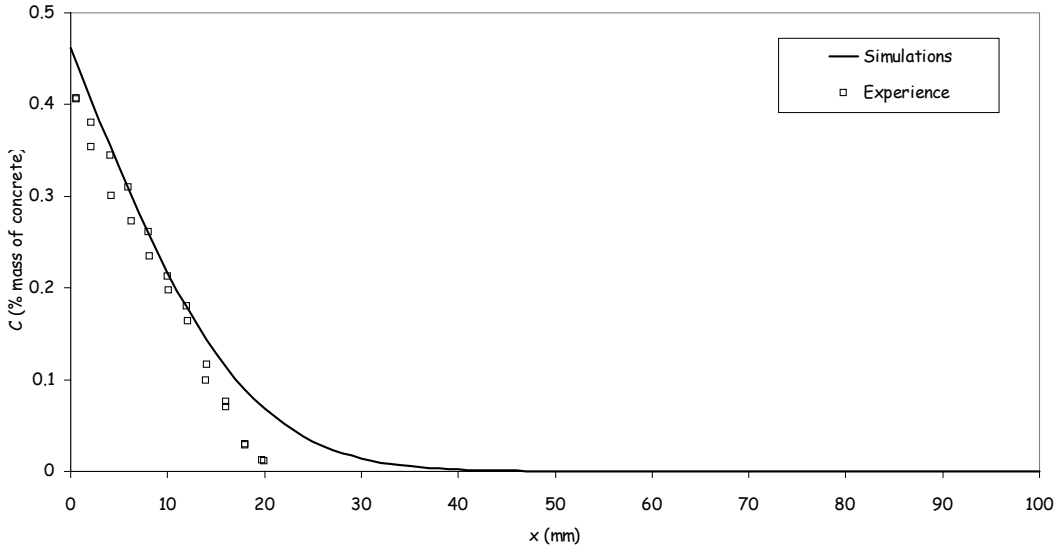

Figure 7.15 Comparison of total chloride profile simulated with False-Erfc model with Visser modifications and experimental data for one year of exposure

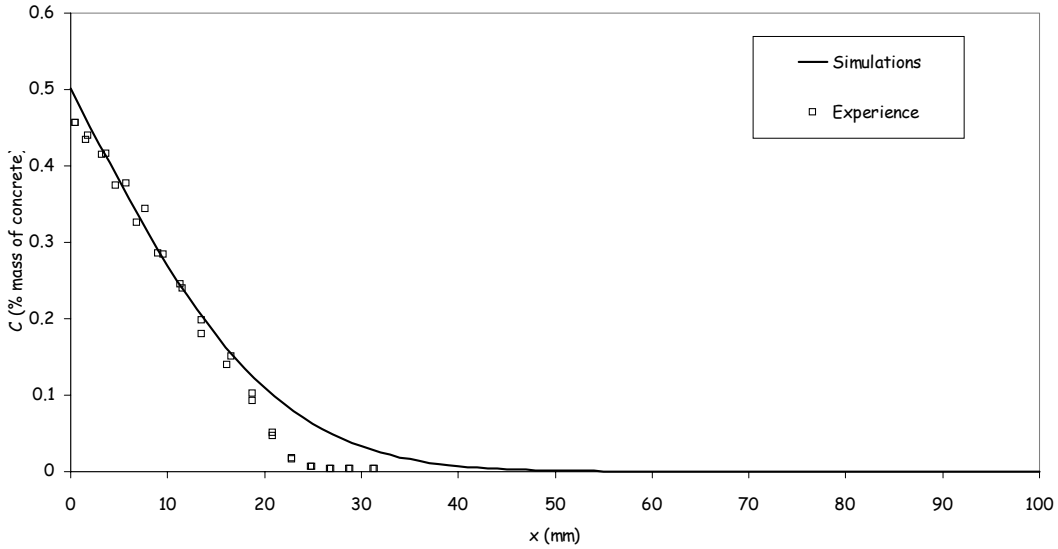

Figure 7.16 Comparison of total chloride profile simulated with False-Erfc model with Visser modifications and experimental data for 18 months of exposure

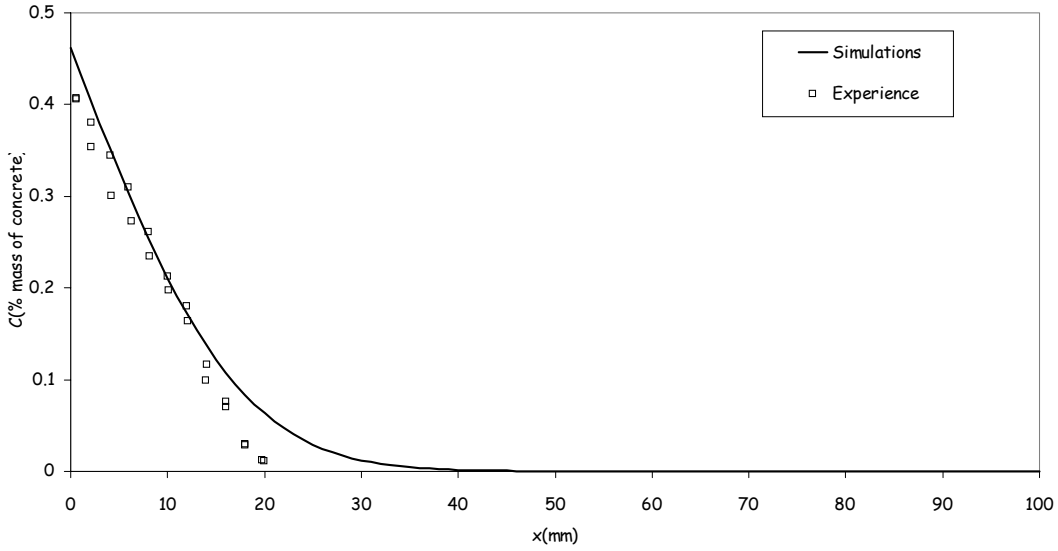

Figure 7.17 Comparison of total chloride profile simulated with False-Erfc model with Stanish modifications and experimental data for 12 months of exposure

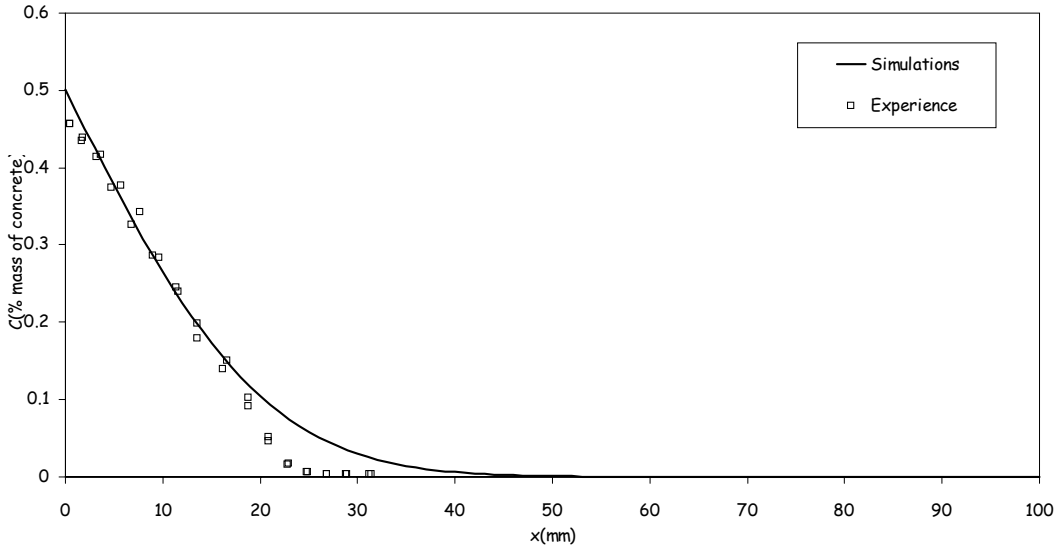

Figure 7.18 Comparison of total chloride profile simulated with False-Erfc model with Stanish modifications and experimental data for 18 months of exposure

$$C(x,t) = C_i + (C_s - C_i)\,erfc\left(\frac{x}{\sqrt{4D_{average}(t_{average})t}}\right) \quad \textbf{[7.37]}$$

$$D_{average} = D_r t_r^{\sigma}\left(\frac{t_2^{1-\sigma} - t_1^{1-\sigma}}{(1-\sigma)(t_2 - t_1)}\right) \quad \textbf{[7.38]}$$

$$t_{average} = \left(\frac{(1-\sigma)(t_2 - t_1)}{t_2^{1-\sigma} - t_1^{1-\sigma}}\right)^{\frac{1}{\sigma}} \quad \textbf{[7.39]}$$

In the above equations t_2 is the concrete age at the end of immersion period while t_1 is the concrete age at the start of immersion period. While simulating for 1 year of immersion, the $t_{average}$ comes out to be 0.46 years with $D_{average}$ of 2.86E-12 m²/s. While 1.5 years of immersion period gives a $D_{average}$ of 2.67E-12 m²/s at $t_{average}$ of 0.64 years. The chloride profiles are shown in **Figures 7.17** and **7.18**.

7.12 Comparison of experimental data with the simulations from all models

In this section, all the simulations presented previously in this chapter along with those made with the MsDiff in chapter 6 are presented for the sake of comparison in a single graphical area. Previously these simulations have been shown separately for each model so that they can be easily compared one by one with the experimental data for the sake of clarity. In **Figures 7.19** and **7.20**, the experimental data obtained from one year and 18 months of immersion with 33 g/l NaCl are compared with the calculated profiles using different models. These two figures demonstrate that the HETEK model provides the largest while the Duracrete model offers the smallest total chloride concentrations at approximately all the depths from the exposed surface with respect to the experimentally observed values. We are unable to reproduce experimental depth with all the models except MsDiff. With the exception of Duracrete, we obtain higher penetration depths than experimentally observed. The determination a reasonable penetration depth is key to the calculation of the just life span of a reinforced concrete structure.

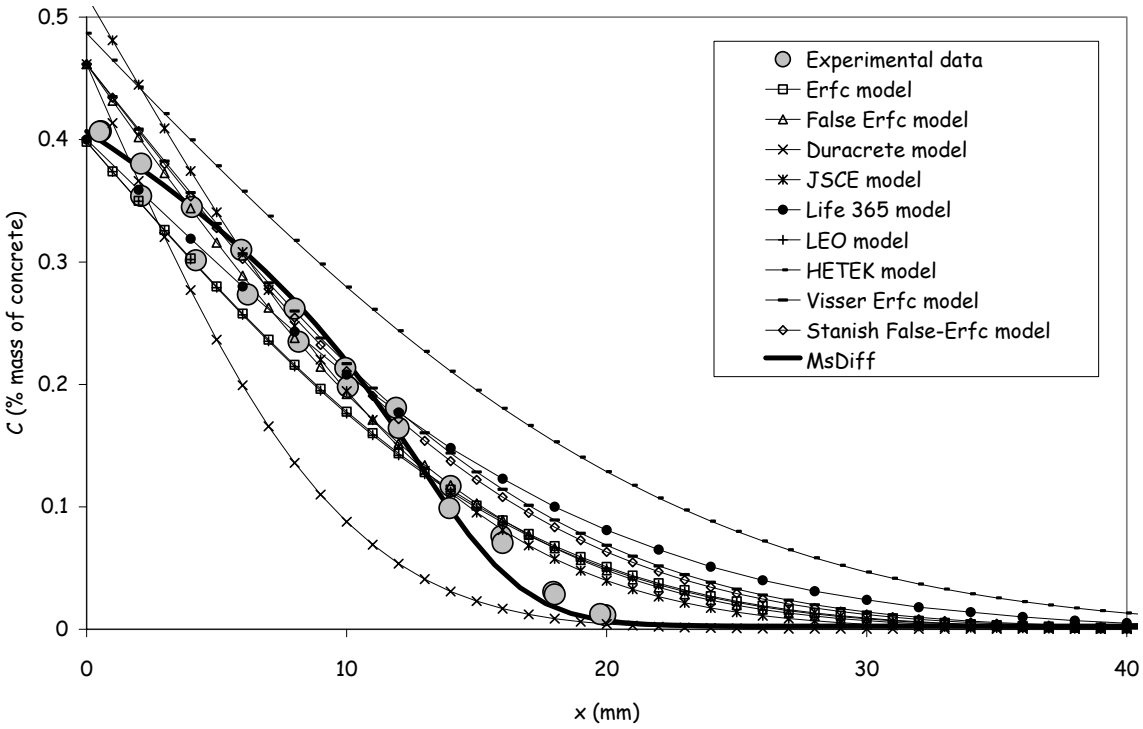

Figure 7.19 Comparison of modeling conducted with different models with experimental data for 1 year of immersion with 33 g/l NaCl

It should be also noted that these comparisons are focused on a very small time span of up to 18 months of immersion. While the greater penetration depths than the experimentally observed values obtained with all the models except two should lead also to shorter life span of a reinforced structure, one has also to keep in mind that in most of these models, the apparent diffusion coefficient previously discussed is assumed to decrease with the material age and the results calculated over larger time spans of the order of tens of years might present an inverse situation i.e. a longer life period of a structure. Therefore, it will be too irrational to predict on this stage that these models give an under estimated life period a reinforced structure. One such case where apparent diffusion coefficient is assumed to decrease with material age will be discussed in the next chapter.

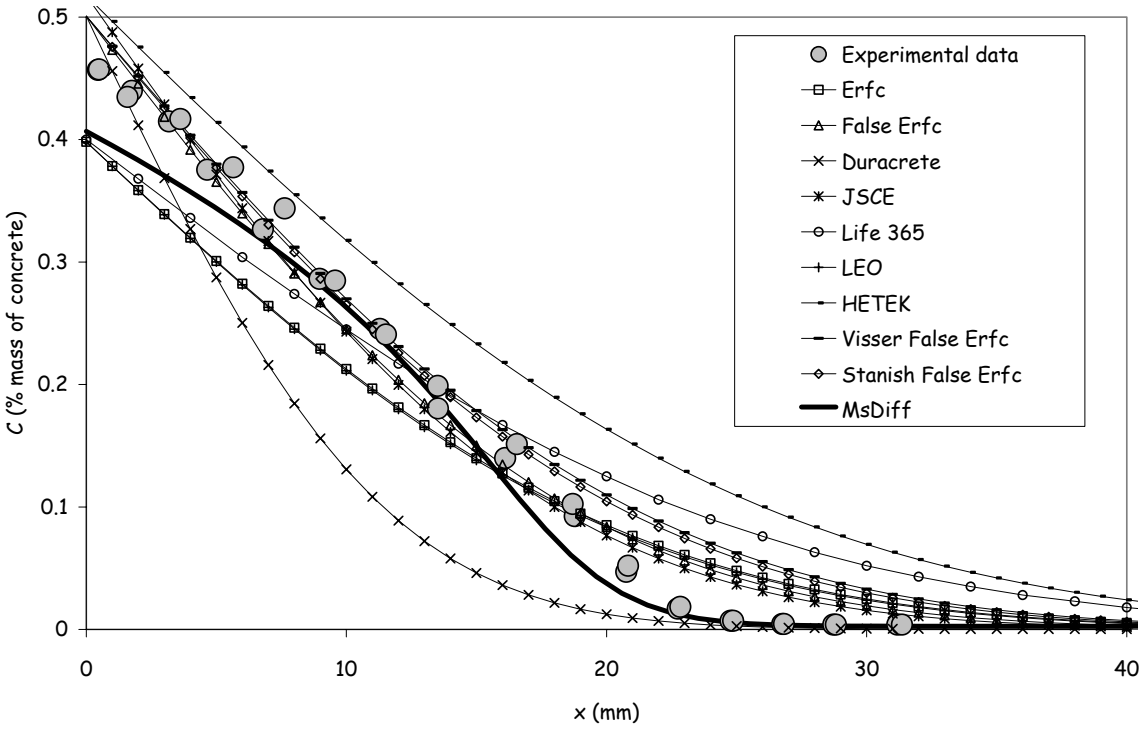

Figure 7.20 Comparison of modeling conducted with different models with experimental data for 18 months of immersion with 33 g/l NaCl

7.13 Conclusions

In this chapter, the experimental data obtained during present work was compared with simulations performed using certain chloride ingress models. The input parameters were either extracted from experimental data obtained with our own experiments or from literature. If neither of the two was available, some existing model was utilized. Modifications proposed by Visser and Stanish et al. are new advances in Erfc-model. While Visser proposes a time dependent D_a in expression **[7.1]**, Stanish proposes an average D_a for the whole immersion period. The simulations show little difference with respect to each other as can be observed from **Figures 7.15** to **7.18**. If we compare all the simulations, it appears that they are more or less similar. The experimental data obtained during this study corresponds to a time of less than two years of concrete age, where the things might not change much, resulting in similar simulations. Also the similarity of models might lead to similar simulations.

Furthermore the modeling done with MsDiff is more satisfying in the sense that not only the modeled profile meets well with most of the experimentally determined values at different depths from exposed surface, it also matches well with the penetration depth.

MSDIFF AND CORROSION INITIATION TIME

CHAPTER 8

MSDIFF AND CORROSION INITIATION TIME

8.1 Introduction

This chapter envisages different possibilities of using MsDiff as a tool to determine the corrosion initiation time. Recall that at the moment MsDiff determines free concentration profiles of Na^+, K^+, Cl^- and OH^- ions. Additionally total chloride concentrations, ionic fluxes and electrical potential are also calculated. Keeping that in view, 3 different prospects were worked out. A threshold value for steel corrosion initiation was chosen in each case. Corrosion is supposed to initiate with effect from the moment when the so-called threshold value is crossed over.

8.2 Threshold values for corrosion initiation

As previously discussed, all the chloride ingress models dealing with the chloride-induced corrosion assume a threshold value that when exceeded by the chloride content or in some cases the hydroxyl content, leads to the initiation of corrosion. When it was decided to utilize MsDiff for chloride-induced corrosion studies, the ideas as adopted by the existing models were previewed. Different existing chloride-ingress models have been described in chapter 2 of present work. In the following paragraphs, the criteria adopted by the different models are quoted.

8.2.1 Life-365 model

For a base case with no special corrosion protection applied the model Life-365 proposes a value of critical chloride content, C_{cr} of 0.05% mass of concrete. The critical chloride content increases with increase in CNI (Calcium Nitrate Inhibitor) in concrete. In the **Table 8.1**, the critical chloride contents as a function of CNI content in concrete are quoted. Since this model calculates the total chloride concentrations, the threshold is also a total one.

Furthermore, it is assumed that grade 316 stainless steel has a corrosion threshold of C_{cr} of 0.50% of concrete i.e. ten times that of black steel.

Table 8.1 The critical chloride values as a function of CNI dose in concrete, adopted by Life-365 model

CNI Dose (liters /m^3 concrete)	Threshold C_{cr} (% concrete)
0	0.05
10	0.15
15	0.24
20	0.32
25	0.37
30	0.40

8.2.2 JSCE specifications

Threshold chloride content for corrosion initiation is 1.2 kg/m^3 of concrete in **atmospheric zone**. For **splash** and **submerged zones**, higher values must be expected but they are not quoted in the JSCE specifications.

8.2.3 HETEK

Threshold values for submerged, splash and atmospheric zones are 1.45, 0.54 and 0.54 % mass of binder respectively.

8.2.4 BRIME

While HETEK model covers the marine environment, BRIME model was developed for road environment. For the case of road environment, the threshold values are 0.43, 0.35 and 0.35 % mass of binder for wet splash zone (WRS), dry splash (DRS) and distant road atmosphere (DRA) respectively.

8.2.5 EuroLightCon

EuroLightCon report addresses the SELMER model discussed in chapter 2. This report proposes nomogrammes where critical value can be determined if apparent diffusion coefficient D_a, time-dependency factor σ of D_a, concrete cover depth and concrete age are known.

Table 8.2 Threshold chloride contents as adopted by different organizations and personals [BYU 04]

	Threshold chloride content, % mass of cement	
	Free (water-soluble)	Total (acid-soluble)
ACI 201	0.10-0.15	
ACI 222		0.20
ACI 318	0.15-0.30	0.20
BS 8110		0.40
Australian codes		0.60
RILEM		0.40
Norweigian codes		0.60
Hope and Ip		0.10-0.20
Evertte and Treadaway		0.40
Thomas		0.50
Hussain et al.		0.8-1.2
Page and Havdahl	0.54	1.00
Strafull		0.15

8.3 Corrosion initiation time with MsDiff

For free and total chlorides, the threshold values at steel were set to be 0.15 % and 0.4 % by mass of cement were employed. These test values were set in accordance with the European and American standards [THO 96]. Thirdly a threshold value for $[Cl^-/OH^-]$ ratio was set to be 0.6 [HAU 67]. These threshold values are summed up in **Table 8.3**.

Table 8.3 Threshold values intended for corrosion initiation in MsDiff

Free chloride (% mass of cement)	Total chloride (% mass of cement)	$[Cl^-/OH^-]$
0.15	0.4	0.6

During all these simulations, a cover depth of 4 cm from exposed surface was supposed. Free and total chloride contents along with hydroxyl ion concentrations at this level were determined. From free chloride and hydroxyl ion contents, the ratio $[Cl^-/OH^-]$ was calculated. All the three thresholds were compared with these parameters at steel level. The moment, at

which the threshold values become equal or smaller than the three parameters values, was set to be equal to the time for initiation of corrosion.

A maximum exposure period of 20 years was chosen for trial purposes in order to determine the time of exposure when the threshold value for corrosion (free chloride) at 4 cm from the exposure surface is reached. It is to be noted that all the other input data for MsDiff has already been narrated in previous chapter in **Table 6.13**. The simulations conducted in this chapter concern to 33 g/l NaCl solution.

The free chloride content at steel bar as a function of exposure time is shown in **Figure 8.1**. In this figure, it is demonstrated that after an exposure period of 8.8 years, the free chloride content at steel rebar will exceed the threshold value set at 0.15 % mass of cement. Hence 8.8 years is the corrosion initiation time in the present case. As discussed before, the current version of MsDiff considers 4 ionic species i.e. Na^+, K^+, Cl^- and OH^- ions. In **Figure 8.2**, the free ionic (Na^+, K^+, Cl^- and OH^-) and total chloride profiles corresponding to an exposure period of 8.8 years, previously determined are presented. Note that in this figure, 0.57 free chlorides (% mass of cement) at surface are equivalent to 0.14 chlorides (% mass of concrete) or 33 g/l NaCl. At steel rebar, the total chloride content along with the free hydroxyl content and pH value was determined. These values are summarized in **Table 8.4**.

Table 8.4 Other parameters obtained after 8.8 years of exposure

Cl^-_{free} (mol/m^3)	Cl^-_{free} (% mass of cement)	C_{total} (% mass of cement)	OH^- (mol/m^3)	$[Cl^-/OH^-]$	pH
144.7	0.15	0.5	156.6	0.9	13.2

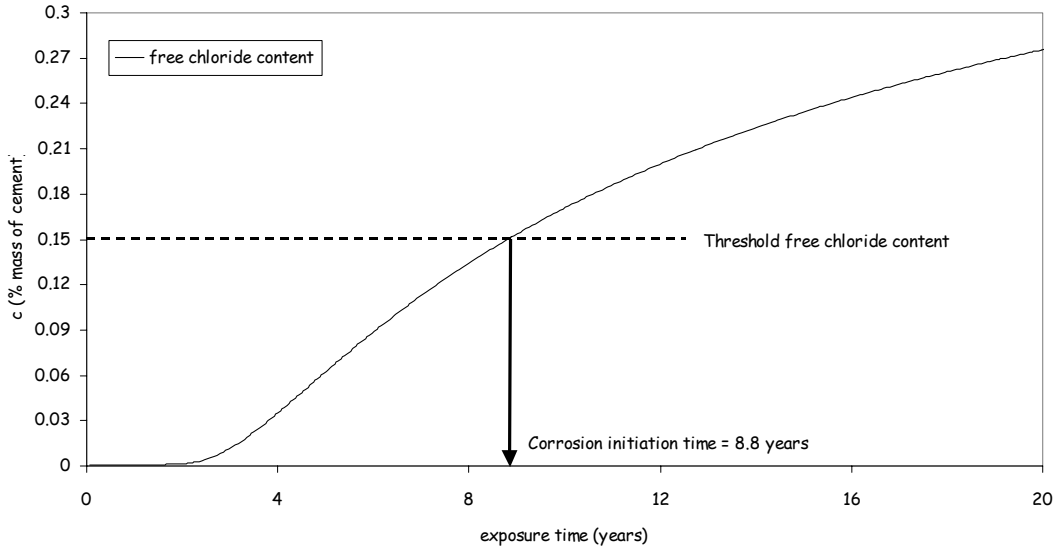

Figure 8.1 Free chloride content at steel level after 20 years of exposure

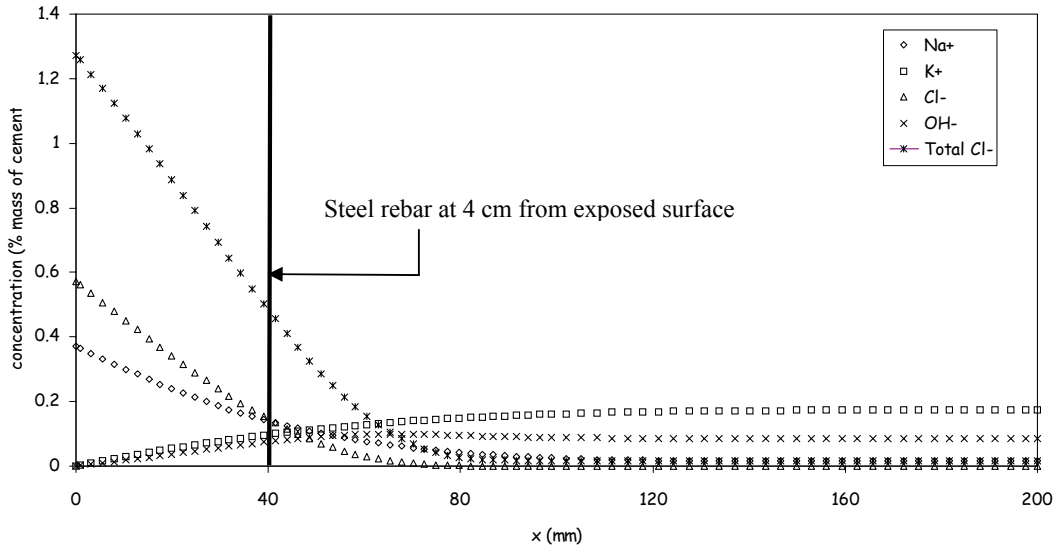

Figure 8.2 Concentration profiles after an exposure period of 8.8 years calculated with MsDiff

Note that the initial pH value of the pore solution is 13.25 (178 mol/m^3). The ratio [Cl^-/OH^-] has been calculated with Cl^- and OH^- concentrations in mol/m^3 of pore solution, as the corresponding ratio in the units of % mass of cement leads to a ratio of 2 due to different molar masses of chlorides and hydroxides. **Table 8.4** suggests that if free chloride content is used as a criterion to determine the corrosion initiation time, it is not necessary that the other criteria be also met. Or in other words, different criteria, adopted for corrosion initiation would lead to different corrosion initiation times.

Now let us move towards the determination of corrosion initiation period based upon a threshold total chloride content at steel rebar. As discussed above, the threshold value is set to be 0.4 % mass of cement. In the same way, a maximum exposure period of 20 years was chosen for trial purposes in order to calculate the time of exposure when the threshold value for corrosion (total chloride) at 4 cm from the exposure surface is reached. The total chloride content at steel bar as a function of exposure time is shown in **Figure 8.3**. In this figure, it is demonstrated that after an exposure period of 7 years, the total chloride content at steel rebar will exceed the threshold value set at 0.4 % mass of cement. Hence 7 years is the corrosion initiation time in the present case. In **Figure 8.4**, the free ionic (Na^+, K^+, Cl^- and OH^-) and total chloride profiles corresponding to an exposure period of 7 years are presented. At steel rebar, the free chloride content along with the free hydroxyl content and pH value was determined. These values are summarized in **Table 8.5**.

Table 8.5 Other parameters obtained after 7 years of exposure

Cl^-_{free} (mol/m^3)	Cl^-_{free} (% mass of cement)	C_{total} (% mass of cement)	OH^- (mol/m^3)	[Cl^-/OH^-]	pH
108.6	0.11	0.4	173	0.63	13.23

Again if we compare the corrosion initiation time with that, previously determined with a free chloride threshold value, we obtain a difference of about 2 years. One interesting point is that the corrosion initiation time of 7 years has produced a value of [Cl^-/OH^-] of 0.63, which is very close to the threshold value set for the criterion, based upon this ratio i.e. 0.6. Next, the calculations performed with this ratio are presented.

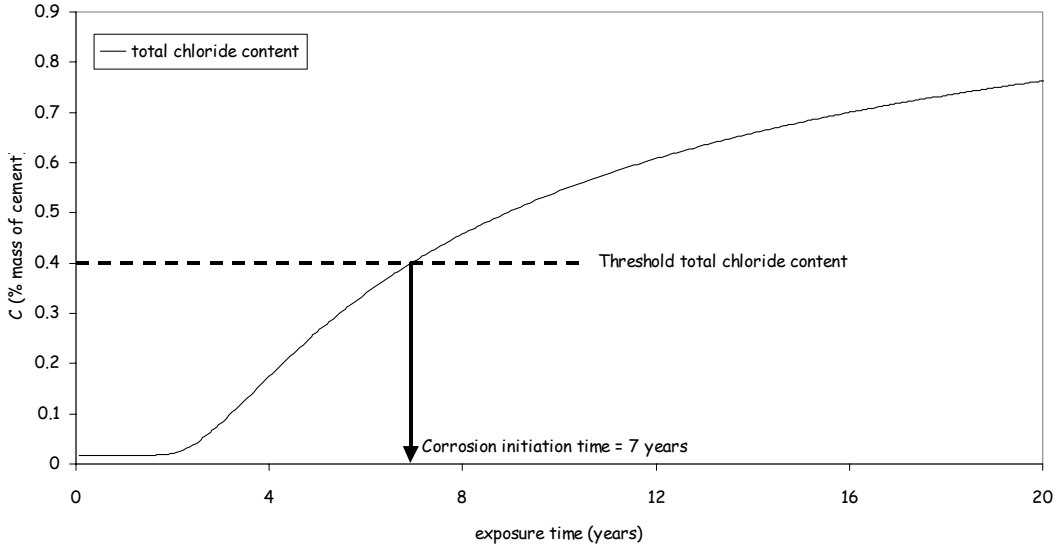

Figure 8.3 Total chloride content at steel level after 20 years of exposure

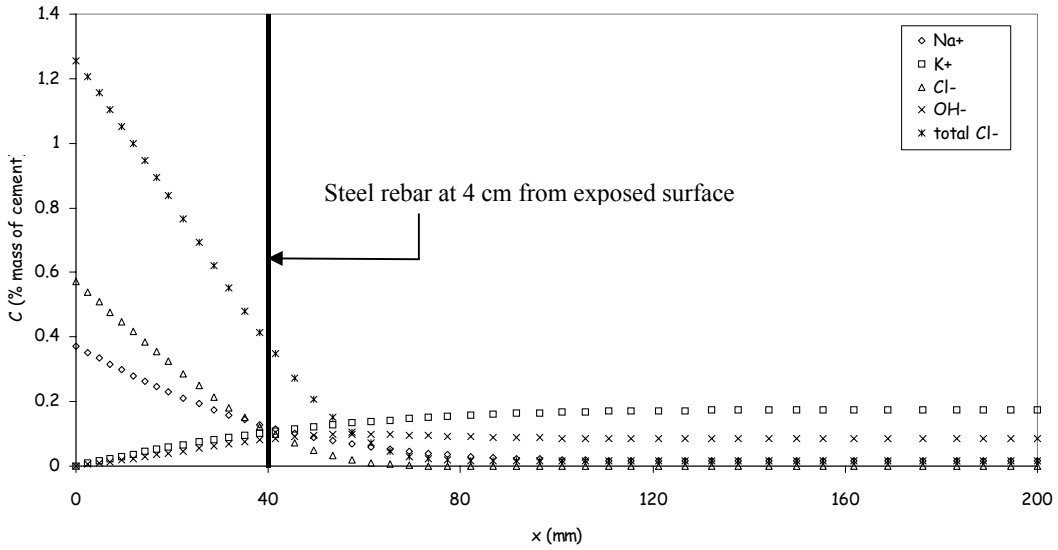

Figure 8.4 Concentration profiles after an exposure period of 7 years calculated with MsDiff

In the third case, the determination of corrosion initiation period is based upon a threshold value of [Cl^-/OH^-] at steel rebar. As discussed above, the threshold value is set to be 0.6. Here a maximum exposure period of 10 years was chosen for trial based on the value as determined from total chloride content. The [Cl^-/OH^-] ratio at steel bar as a function of exposure time is shown in **Figure 8.5**. In this figure, it is demonstrated that after an exposure period of 6.75 years, the ratio at steel rebar will exceed the threshold value set at 0.6. Hence 6.75 years is the corrosion initiation time in the present case. Since this much time is very close to the one, as obtained in the previous case, no need was realized to present the tabulated values for other parameters. Anyway a [Cl^-/OH^-] ratio profile is presented in **Figure 8.5**.

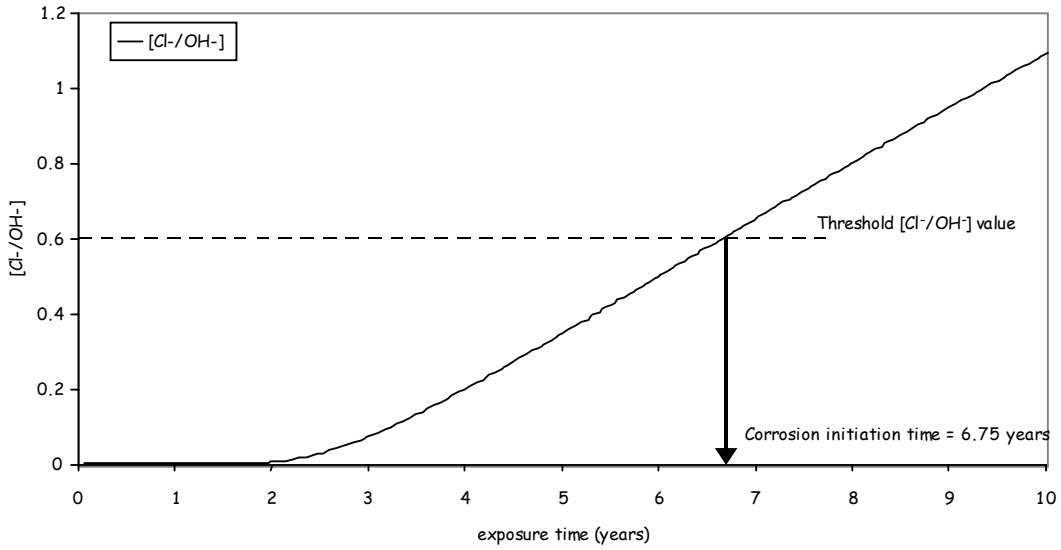

Figure 8.5 [Cl^-/OH^-] profile at steel level after 10 years of exposure

Model MsDiff concerns the evolution of [OH^-] content in the pore solution of cementitious materials. If it is supposed that this content has a constant value of 178 mol/m^3 (initial pore composition in the concrete under study during this work), the situation will be a little bit different. The result based on [Cl^-/OH^-] criterion is presented in **Figures 8.6** and **8.7**.

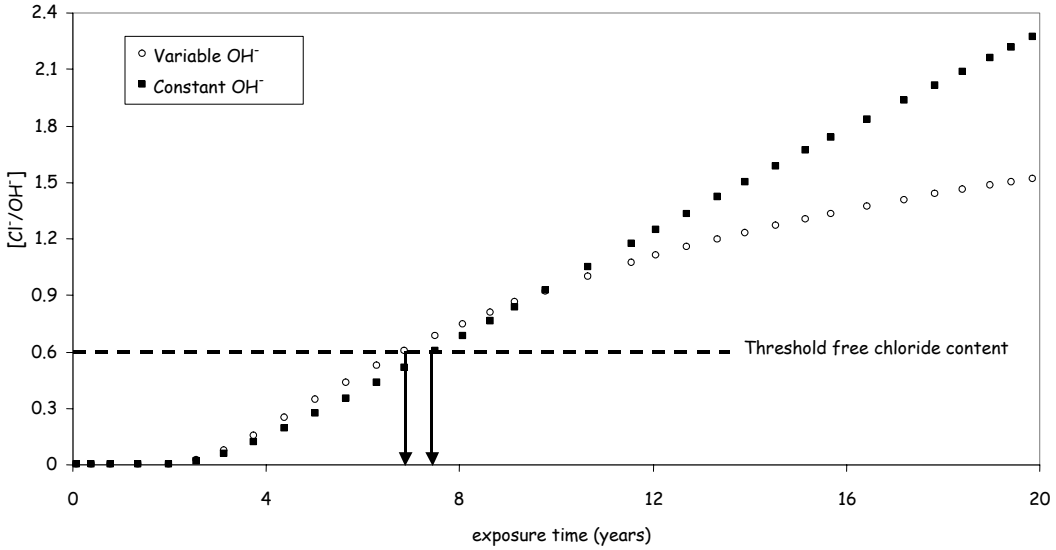

Figure 8.6 Effect of variability of OH^- (4 cm) on initiation period

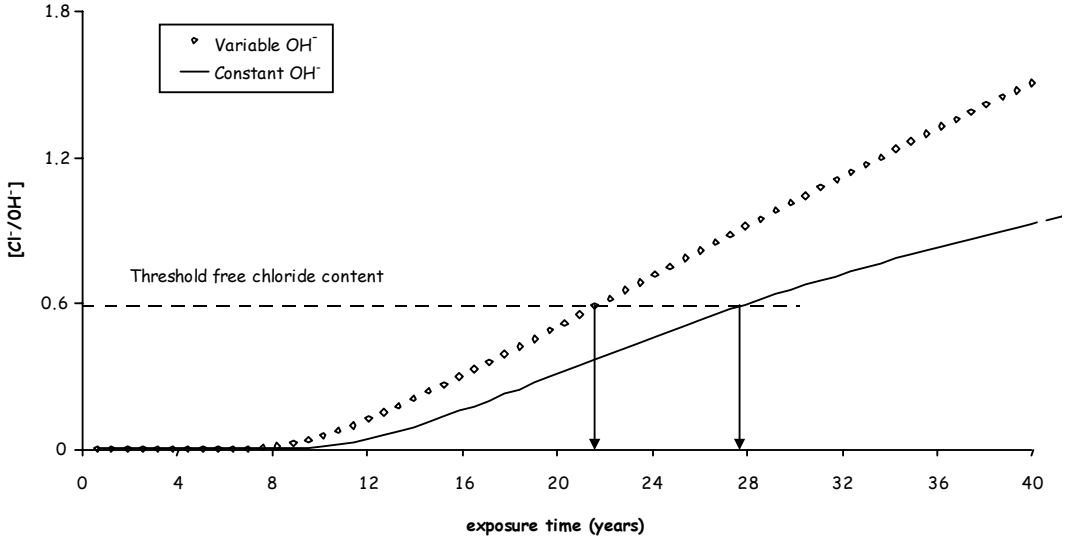

Figure 8.7 Effect of variability of OH^- (8 cm) on initiation period

In **Figure 8.6**, the simulations are made over a concrete cover depth of 4 cm. In this case, the value of [OH^-] seems to put a very little influence on the corrosion initiation time. The corrosion initiation time is around 7 years. But in practice, in marine environment very huge structures might exist with very large cover depths. In **Figure 8.7**, 8 cm has been taken as the concrete cover depth. Now if it is supposed that the hydroxyl ion concentration remains constant in pore solution; the results might lead to over-estimated corrosion initiation times or in other words, over-estimated life spans. In **Figure 8.7**, the corrosion initiation time comes out to be 21.5 years if [OH^-] content is allowed to vary, while in the opposite case, this has been calculated as approximately 28 years.

Now if we compare the corrosion initiation times, meant for 4 cm cover depth both in the total chloride case and the [Cl^-/OH^-] one, we come to conclude that they are approximately same i.e. in the vicinity of 7 years.

8.4 Corrosion initiation by Erfc model

A similar corrosion initiation time was also calculated using Erfc model for the sake of comparison. Since Erfc models are used to provide total chloride profiles, the calculations here are based on total chloride threshold content.

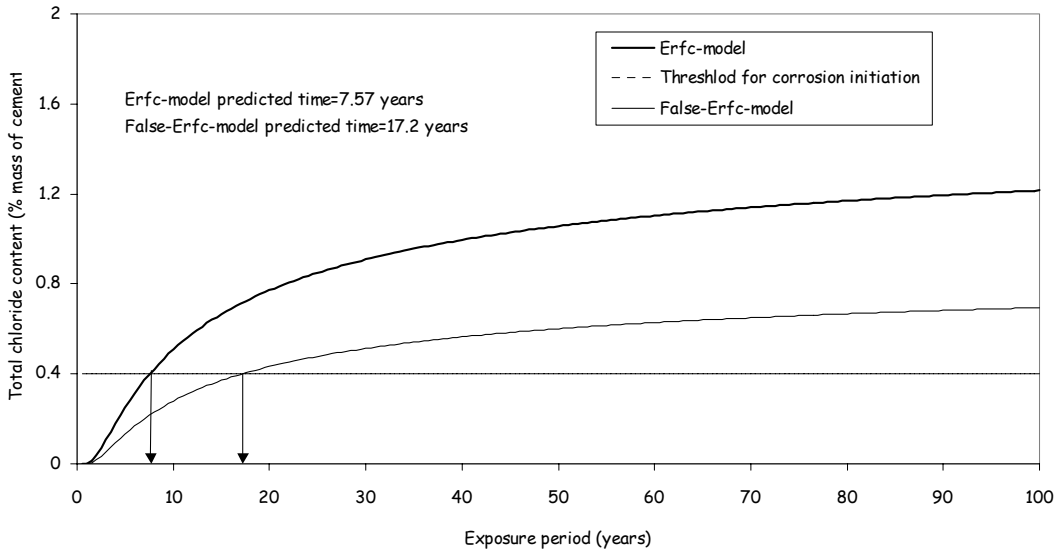

Figure 8.10 Total chloride content at steel level (4 cm from exposed surface), as calculated by Erfc and False-Erfc models

Table 8.6 Summery of corrosion initiation times (years) in MsDiff and Erfc models

MsDiff-free Cl^-	MsDiff-total Cl^-	MsDiff-[Cl^-/OH^-]	Erfc	False-Erfc
8.8	7	6.75	7.57	17.2

The False-Erfc mode gives much delayed corrosion initiation time as compared to Erfc model. This is logical as apparent diffusion coefficient of chloride is continuously allowed to decrease. It also seems from the above table, that although the corrosion initiation time is different in each case, the values lie in the same order of magnitude for the primary three cases i.e. not too much different from each other.

The corrosion initiation time, calculated from Erfc-model is based upon a total chloride content of 0.4 % mass of cement. A similar study is made with Erfc-model for a corrosion initiation criterion, based upon [Cl^-/OH^-] ratio. Since this model does not allow a variable OH^- value, the study consists of a constant OH^- value in the pore solution.

The corrosion studies, carried above correspond to a cover depth of 4 cm. This cover depth in actual marine structures might be many times the value, tested in the above case. One such case with an 8 cm cover depth is shown in **Figure 8.7**.

8.5 Conclusions

In this chapter, the description of MsDiff as a means to determine the corrosion initiation time is given. The physical and numerical structure allows calculating the chloride-induced corrosion initiation time by all the three means available to date, which could not be performed with the classical models (with the exception of ClinConc model which takes into account the leaching of hydroxyl ions) based on Fick's laws of diffusion. The simulations give corrosion initiation times, which otherwise could be over-estimated if classical models are worked with. All the test simulations, presented in this chapter correspond to the concrete, which was in use during this work. Similar calculations could be performed for any concrete structures, provided their properties as mentioned in this work are known.

References

[BYU 04] O.H. Byung, S.J. Bong, C.L. Seong, Chloride diffusion and corrosion initiation time of reinforced concrete structures, Proceedings of the International Workshop on Microstructure and Durability to Predict Service Life of Concrete Structures, Sapporo, Japan, 2004.

[HAU 67] D.A. Haussmann, Materials Protection, pp. 19-23, 1967.

[THO 96] M. Thomas, Chloride thresholds in marine concrete, Cement and Concrete Research, Vol. 26, pp. 513-519, 1996.

CONCLUDING REMARKS

CHAPTER 9

CONCLUDING REMARKS

In this work the ionic transport in concrete has been presented. In this regard, two techniques have been discussed, one is the classical one or Fick's laws of diffusion and the other is the Nernst-Planck technique. The drawback of classical technique to tackle ionic species as uncharged entities led towards the utilization of Nernst-Planck equation in which these species are considered to be charge-carrying bodies. Our own work consists of studying the ionic transport in concrete through Nernst-Planck equation.

A numerical model MsDiff was developed by Truc et al in 2000. This model is based on the multi-species description of diffusion, meant for saturated porous media (both reactive and inert). This description explains that the ionic species are not the isolated bodies in the concrete medium. These ions influence the movement of one another. During this study, MsDiff was chosen as the target model. In this work, the modeling was performed with a modified version of MsDiff. The modified model consists of the same governing equations, but a more stable and accurate numerical scheme. A new model for porosity calculation has been included. Also with the newer version, the reinforcement-corrosion initiation time can be calculated based on a threshold value of corrosion initiation.

MsDiff requires a package of five input data at any age of concrete. These input data are summarized in the following chronological order.

1. The porosity of the material,
2. The density of the material,
3. The ionic composition of pore solution,
4. The effective diffusion coefficient of chloride,
5. The chloride-binding isotherm.

Among these five input data, the material porosity (for cements CEM I only) is a parameter that the model itself can also calculate provided the material composition and the cement Bogue's composition are known. The porosity calculations are based on the Avrami-Powers work, in which the degree of hydration of the material is calculated using the Avrami's equation while the porosity is calculated on the basis of Powers model. It is further specified that the parameters, described above, as the input data should be preferably for a mature material if the simulations are meant for longer durations or older structures. Very often the

concrete properties are measured at its age of 28 days. Yet it is possible that the properties measured at this age are not just sufficient to account for predictions at later stages or in other words, the material at 28 days of the age is not mature enough and the corresponding parameter is still changing. For example, while using the model MsDiff for various immersion periods, materials age at exposure or different environmental chloride concentrations, the parameters 1 and 2 were those that were measured at 28 days of concrete age. The ionic composition of the pore solution was taken from the work of Nugue, which was also deduced from a mature material of the same characteristics as was used in this work. During this work, it was emphasized that if the chloride diffusion coefficient is measured at 28 days of the age and is then used for simulations for older age or longer durations, the results can lead to totally wrong predictions. Our work was carried out with CEM I cement for that it was observed that the diffusion coefficients generally vary up to an age of 70 days after which they are considered to be constant. This was what Truc et al. [TRU 00] quoted while working with this cement and which was also observed during this work.

The effective diffusion coefficients of chloride was determined with LMDC test, developed in our laboratory while those of other ions (Na^+, K^+ and OH^-) were determined by using the effective diffusion coefficient of chloride determined by LMDC test and the ratio of diffusion coefficients of chloride and the corresponding ion in water.

The binding isotherm was obtained with immersion tests. While using this method, it was observed that with effect from 28 days of concrete age (165 g/l NaCl), the chloride binding phenomenon is independent of time at least for the durations exercised during this work. Yet it should be avoided to obtain a binding isotherm with a material that is not mature enough (less than 28 days of age) to be used in simulations meant for longer durations or older structures as is evident from the results of Sumranwanich et al. [SUM 04], where a time dependent chloride binding has been proposed with experiments on materials having different ages (much less than 28 days to more than 28 days). The experimental results reveal that since a binding isotherm independent of time was observed for a material that had a least age of 28 days, an immersion test (NT BUILD 443) can be carried out to achieve this purpose for any duration like 35 days. It is recommended that if this method is chosen to obtain a binding isotherm, the duration of immersion should be higher than 35 days or at least the age at exposure should be more than 28 days. The reasonable results can be achieved with more points, which can be achieved if the duration of immersion is significant. Alternatively, more than one specimen should be used per test so as to achieve an average assessment.

Once the five input data as described above have been determined and inserted in MsDiff, the following parameters can be calculated.

1. The free ionic concentrations of Na^+, K^+, Cl^- and OH^- ions,
2. The total chloride concentrations,
3. The ionic fluxes of all the four ions,
4. The potential profiles.

The modeling done with MsDiff was validated through experimental chloride profiles. This goal was achieved via immersion tests. It is of interest that all input data inserted while modeling with MsDiff was achieved through experiments and not a single value was adjusted in order to improve the comparison between experiments and modeling. The modeling was tested using two environmental solutions, one containing 165 g/l NaCl and the other containing 33 g/l NaCl. All the other four input data of MsDiff were kept the same along with a single binding isotherm for all the two cases. This isotherm was acquired from the results of immersion tests with 165 g/l NaCl and thus this isotherm covers a range of 0-165 g/l NaCl. Although that gives satisfactory results while comparing modeling with 165 g/l immersion test outcomes, the same was not achieved for 33 g/l NaCl test results. The differences between the experiments and modeling go on increasing with immersion time. Later on it was thought that the situation needs to be re-evaluated because there exists a difference of scale between 165 g/l NaCl and 33 g/l NaCl (of the order of five times) i.e. while a certain variation (between simulated and experimental bound contents) is smaller for larger concentrations that might be significant for the lesser concentrations giving wrong predictions. In order to remove this discrepancy, the region 0-33 g/ NaCl of the previous isotherm was re-evaluated. A new binding isotherm was developed which runs much closer to experimental data in comparison to the primary isotherm. Further this isotherm was also provided a feedback of addition experimental points. These points were the bound chloride amount at the surface of the concrete which were exposed to 33 g/l NaCl. The acid soluble chlorides at the concrete surface for each 33 g/l NaCl test were known also the free chloride content at these surfaces was known which is obviously the environmental load. The difference of two results in bound chloride content at the surface. With that the 33 g/l NaCl total chlorides were re-modeled. The obtained results are satisfactory both in term of concentration profiles and penetration depth.

Here in this work a new method to determine the binding isotherm is proposed which consists of exploiting the water and acid soluble chloride contents at different depths from exposed surface using an NT BUILD 443 method of standard 35 days duration as we found no change

in bound chlorides at different water soluble chloride content in pore solution with increasing immersion time (at least up to one year time). This isotherm was satisfactorily used for a different concentration of 33 g/l NaCl while exploiting only the region 0-33 g/l NaCl. This binding isotherm was also given a feedback of some additional points.

In addition to the modeling by MsDiff, certain other areas of interest were also envisaged in this work. In order to watch the effect of concrete age while subjected to exposure solution, the concrete specimens with different ages were used in immersion tests. The results revealed that no effect was observed at least for the range of ages considered during this work. In addition, it was also thought to study the chloride ingress using models other than MsDiff. In this regard, certain models were chosen, which are based on Fick's laws of diffusion. The input data for these models was either obtained from experiments or from literature. For that certain concrete specimens were subjected to seawater chloride concentration-containing solutions, because certain models are based on empirical coefficients which were derived by exposing the material to seawater e.g. HETEK, JSCE etc.. The simulated curves with these models are more or less identical.

In the end, the corrosion initiation time was calculated with MsDiff. In this regard three possibilities were sorted out. These possibilities correspond to three criteria being used by different research organizations for the initiation of reinforcement corrosion.

Although satisfactory modeling was performed during this work, yet there are some areas of interest that need to be taken into account by MsDiff.

Recall that all the experimentation conducted throughout this work was done at the local laboratory temperature (20 ± 2°C). There are situations or circumstances where the temperatures are different; might be low (e.g. freezing temperatures) or high as in marine environments in Gulf countries in summer. It has been emphasized by different researchers that the temperature has a significant influence on ionic transport e.g. the chloride diffusion coefficient is large at higher temperatures and vice versa. Currently the work is going on in our group to watch the effects of temperature on ionic transport. Mr. Tanh Son Ngueyen, a PhD student is doing the job since 2003.

It is a well known fact that the surface total chloride content increases with the exposure period, which was significant in the case of 33 g/l NaCl during the present study. This change is rapid during the early ages than in the later ones. It has also been shown that this parameter assumes an asymptotic value in the end. While the surface free chloride content being always the same (if the boundary conditions do not vary), a binding isotherm independent of time, should give a constant surface chloride content, which is not the case with33 g/l NaCl. Indeed

with the current version of MsDiff, a chloride-binding isotherm that varies over time can compensate for the discrepancies that might occur in the case of increasing surface chloride content with exposure period. Again the binding isotherm should consist of parameters that while varying with exposure time acquire stable values after certain time.

The ionic composition of pore solution is an important parameter, which is usually determined by pore solution extraction technique, a cumbersome and costly method. Other ways (easy to conduct) should be searched so as to determine this parameter e.g. from the chemical compositions of the constituents (cement, sand, gravel, water etc.) comprising concrete. The ions in the concrete pore solution are charged particles, therefore the conductivity experiments can also be useful as the ions move towards the electrodes of opposite signs in case the concrete is applied with an electrical field via electrodes. If a significant quantity of these ions is forced to accumulate at the electrodes sites, the ionic composition can be determined to a fair extent.

The work presented in this report is limited to experiments conducted in a laboratory controlled environment. It is further proposed to carry out experiments using *in situ* specimens. In uncontrolled *in situ* environments, the conditions are variable. The concentrations in the marine environment usually change throughout the year. There are different temperatures in different seasons. Furthermore the conducted tests were meant for submerged conditions. While in practice there are three well defined marine zones namely submerged, splash and tidal. The degree of saturation is different in each case. It is proposed to work for these practical cases in future.

A uni-dimensional diffusion was studied during this work. Practically we may have multi-dimensional diffusion for example in bridge pillars in marine environment. Marine water itself does not consist of NaCl only. There are also other species present. Some species like Mg ions in marine water are also found to create pore blocking at the concrete exposed surface. It will be worthwhile if a future work consists of an exposure to actual marine environment like *in situ* specimens as discussed earlier. At the same time the concrete specimens could be exposed to artificial sea water prepared in laboratory.

REFERENCES

REFERENCES

[ARY 90] Arya, C., Buenfled, N.R., Newman, J.B., Factors influencing chloride-binding in concrete, Cement and Concrete Research, Vol. 20, pp. 291-300, USA, 1990.

[AFP 97] AFPC-AFREM. Méthodes recommandées pour la mesure des grandeurs associées à la durabilité. Toulouse, France, 1997.

[BAR 96] J. BARON and J. P. OLLIVIER, Les béton, bases et données pour la formulation, ed. Eyrolles, sous la direction de J. BARON et J. P. OLLIVIER, 1996.

[BEN 00] http://www.silicafume.org/specifiers-lifecycle.html.

[BER 88] N. S. Berke, D. W. Peifer, Y. G. Weil, Protection against chloride induced corrosion, Concrete International, Vol. 10, pp. 45-55, 1988.

[BE 00] BE95-1347, Statistical Quantification of the variables in Limit State Functions, Report 9, 2000.

[BIF 90] K. Bifors, Chloride-initiated reinforcement corrosion, chloride binding, CBI report 1:90, 1990.

[BOG 50] R. H. Bogue, Calculation of phase composition: The chemistry of Portland cement, Edwards Brothers, Inc., Ed., Ann Arbor, MI, second printing, pp. 184-203, 1950.

[BRI 98] Brite-Euram project BE95-1347 'DuraCrete', 1998.

[BYU 04] O.H. Byung, S.J. Bong, C.L. Seong, Chloride diffusion and corrosion initiation time of reinforced concrete structures, Proceedings of the International Workshop on Microstructure and Durability to Predict Service Life of Concrete Structures, Sapporo, Japan, 2004.

[COL 70] M. Collepardi, A. Marcialis, R. Turriziani, The kinetics of chloride ions penetration in concrete, *Il Cemento*, Vol. 67, pp. 157-164, 1970.

[EUR 99] EuroLightCon document BE96-3942/R3, 1999.

[FRE 97] J. M. Frederiksen, H. E. Sørensen, A. Andersen, O. Klinghoffer, HETEK, The effect of w/c ratio on chloride transport into concrete, The Danish Road Directorate, Report 54, 1997.

[FRE 97] J. M. Frederiksen, L. O. Nilsson, E. Poulsen, P. Sandberg, L. Tang, A. Andersen, HETEK, A system for estimation of chloride ingress into concrete, Theoretical background. The Danish Road Directorate, Report 83, 1997.

[FRE 97] J. M. Frederiksen, E. Poulsen, HETEK, Chloride penetration into concrete-Manual. The Danish Road Directorate, Report 123, 1997.

[GEH 00] C. Gehlen, Probabilistische Lebensdauerbemessung von Stahlbetonbauwerken-Zuverla¨ssigkeitsbetrachtungen zur wirksamen Vermeidung von Bewehrungskorrosion, Deutscher Ausschuss fur Stahlbeton, Heft 510, Beuth Verlag, Berlin, 2000.

[HAU 67] D.A. Haussmann, Materials Protection, pp. 19-23, 1967.

[HET 96] HETEK Chloride penetration into concrete, State of the Art, Report No. 53, 1996.

[HOP 85] B. B. Hope, J. A. Page, J. S. Poland, The determination of the chloride content of concrete, Cement Concrete Research, Vol. 15(5), pp. 863-870, 1985.

[HOU 00] O. Houdusse, H. Hornain, G. Martinet, Prediction of long-term durability of Vasco de Gama Bridge in Lisbon, proceedings of the 5th CANMET/ACI International conference, Vol. 11, pp. 192-200, Barcelona, Spain, 2000.

[JEN 94] H.M. Jennings, P.D. Tennis, Model for Developing Microstructures in Portland Cement Pastes, Journal of American Ceramic Society, Vol. 77 (12), pp. 3161-3172, 1994.

[JUS 98] H. Justnes, A review of chloride binding in cementitious systems, SINTEF Civil and environmental Engineering, Cement and Concrete, N-7034 Trondheim, Norway.

[KHI 05] A. Khitab, S. Lorente, J.P. Ollivier, Predictive model for chloride penetration through concrete, Magazine of Concrete Research, accepted.

[LAR 98] C.K. Larsen, Chloride binding in concrete, effect of surrounding environment and concrete composition, PhD thesis, Norwegian University of Science and Technology, Trondheim, Norway, 1998.

[LI 00] L.Y. Li, C.L. Page, Finite element modeling of chloride removal from concrete by an electrochemical method, Corrosion Science, Vol. 42, pp. 2145-2165, 2000.

[LIT 82] G.G. Litvan, Deterioration of Indoor Parking Garages, Canadian Building Digest, CBD-224, 1982.

[LON 73] P. Longuet, L. Burglen, A. Zelwer, La phase liquide du ciment hydraté, Matériaux et Constructions, pp. 35-41, 1973.

[MAR 01] J. Marchand, Modeling the behavior of unsaturated cement systems exposed to aggressive chemical environments, Materials and Structures, Vol. 34, pp. 195-200, 2001.

[MAR 02] J. Marchand, E. Samson, Y. Maltais, R.J. Lee, S. Sahu, Predicting the performance of concrete structures exposed to chemically aggressive environment-field validation, Materials and Structures, Vol. 35, pp. 623-631, 2002.

[MEJ 96] L. Mejlbro, The complete solution of Fick‘s second law of diffusion with time-dependent diffusion coefficient and surface concentration, Durability of concrete in saline environment, Cementa AB, Dandcryd Sweden, pp. 127-158, 1996.

[MOH 03] T. U. Mohammed, H. Hamada, Relationship between free chloride and total chloride contents in concrete, Cement and Concrete Research, Vol. 33, pp. 1487-1490, 2003.

[NAD 03] B. Nadler, Z. Schuss, A. Singer, R.S. Eisenberg, Ionic Diffusion Through Protein Channels: From molecular description to continuum equations, Technical Proceedings of the 2003, Nanotechnology Conference and Trade Show, Vol. 3, 2003.

NF EN 12350-7 Teneur en air-Méthode de la compressibilité, AFNOR, 2001.

[NIL 01] Nilsson, L., Prediction models for chloride ingress and corrosion initiation in concrete structures, Nordic Mini Seminar & fib TG 5.5 meeting, Göteborg, 2001.

[NIA 89] Q. Niang, T. J. Sejnowiski, An electro-diffusion model for computing membrane potentials and ionic concentrations in branching dendrites, spines and axons, Biol. Cybern, Vol. 62, pp. 1-15, 1989.

[NIL 01] Nilsson, L., Prediction models for chloride ingress and corrosion initiation in concrete structures, Nordic Mini Seminar & fib TG 5.5 meeting, Göteborg, 2001.

[NT 99] NT Build 492, Chloride diffusivity in hardened concrete, NORDTEST, 1999.

NF P 18-304 Béton et constituents du béton, AFNOR, 1990, pp. 254-260.

NF P 18-406 Béton et constituents du béton, AFNOR, 1990, pp. 396-398.

NF P 18-421 Béton et constituents du béton, AFNOR, 1990, pp. 451-456.

NF P 18-422 Béton et constituents du béton, AFNOR, 1990, pp. 456-457.

NF P 18-554 Granulats, AFNOR, 1999, pp. 5-9.

NF P 18-555 Granulats, AFNOR, 1999, pp. 11-15.

[NOR 95] NORDTEST. Concrete, hardened : accelerated chloride penetration. NT BUILD 443, 1995.

[NUG 02] F. NUGUE, Recherche d'une méthode rapide de détermination du coefficient de diffusion en millieu cimentaire saturé, Laboratoire Matériaux et Durabilité des Constructions, Thèse de l'Institut National des Sciences Appliquées, Toulouse, 2002.

[OLL 02] J.P. Ollivier, M. Carcassès, J. P. Bigas, O. Truc, Diffusion des ions dans le béton saturés, Revue française de Génie Civil, Vol. 5, pp. 227-250, 2002.

[PET 00] I. Petre-Lazar, Evaluation du comportement en service des ouvrages en béton armé soumis à la corrosion des aciers, EDF, PHD thesis, France, 2000.

[PIT 79] K.S. Pitzer, Activity coefficients in electrolyte solutions, in R.M. Pytkowitz ed., Theory: on interaction approach. CRC Press, Boca Raton, Florida, pp. 157-208, 1979.

[POW 47] T.C. Powers, T.L. Brownyard, Studies of the physical properties of hardened Portland cement paste, Vol. 18, pp. 669-712, Michigan, USA, 1947.

[RAM] Ramachandran, V.S., Seeley, R.C., Polomark, G.M., Free and combined chloride in hydrating cement and cement components, Division of Building Research, National Research Council Canada, Ottawa, Ontario, Canada KIA OR6.

[REV 99] A. Revil, Ionic diffusivity, Electrical conductivity, membrane and thermoelectric potentials in colloids and granular porous media: a unified model, Journal of colloid and interface science, Vol. 12, pp. 503-522, 1999.

[RIL 02] Rilem TC 178-TMC. Analysis of water soluble chloride content in concrete, recommendation, Materials and Structures, Vol. 35, pp. 586-588, 2002.

[ROO 03] M.R. de Rooij, and R.B. Polder, Accuracy of chloride penetration predictions based on chloride profile analysis, Advances in Cement and Concrete, Proceedings of Engineering Conferences International, Colorado, pp. 339-348, 2003.

[SAM 99] E. Samson, G. Marchand, J. Beaudoin, Modeling chemical activity effects in strong ionic solutions, Computational Material Sciences, Vol. 15, pp. 285-294, 1999.

[SNY 01] K. A. Snyder, J. Marchand, Effect of speciation on the apparant diffusion coefficient in non reactive porous systems, Cement and Concrete Research, Vol. 31, pp. 1837-1845, 2001.

[STA 03] K. Stanish, M. Thomas, The use of bulk diffusion tests to establish time-dependent concrete chloride diffusion coefficients, Cement and Concrete Research, Vol. 33, pp. 55-62, 2003.

[STA 04] K. Stanish, R.D. Hooten, M. Thomas, A novel method for describing chloride ion transport due to an electrical gradient in concrete, Cement and Concrete Research, Vol. 34, pp. 43-49, 2004.

[SUM 04] T. Sumranwanich and S. Tantermsirikul, A model for predicting time-dependent chloride binding capacity of cement-fly ash cementitious system, Materials and Structures, Vol. 37, pp. 387-396, 2004.

[TAN 96] L. Tang, Chloride transport in concrete – Measurement and predictions, Chalmers Univ. of Technology, Publication P-96:6, 1996.

[TAY 87] H. F. W. Taylor, A method for predicting alkali ion concentration in cement pore solution, Adv Cem Res, Vol. 1, pp. 5-17, 1987.

[TEN 00] P.D. Tennis, Hamlin M. Jennings, A model for two types of calcium silicate hydrate in the microstructure of Portland cement pastes, Cement and Concrete Research, Vol. 30, pp. 855-863, 2000.

[THO 96] M. Thomas, Chloride thresholds in marine concrete, Cement and Concrete Research, Vol. 26, pp. 513-519, 1996.

[TRU 00] O. Truc, Prediction of Chloride Penetration into Saturated Concrete – Multi-species approach, Chalmers Univ. of Tech., Göteborg, Sweden, INSA, Toulouse, France, 2000.

[VIS 02] J.H.M. Visser, G.C.M. Gaal, and M.R. de Rooij, Time dependency of chloride diffusion coefficients in concrete, RILEM TMC Workshop, Madrid, 2002.

[WAN 01] Y. Wang, L.Y. Li, C.L. Page, A two dimensional model of electrochemical chloride removal from concrete, Computational Materials Science, Vol. 20, pp. 196-212, 2001.

APPENDIXES

APPENDIX 1 CHEMICAL COMPOSITION OF SAND AND COARSE AGGREGATES

Table A.1 Chemical composition of sand

Constituents	Percent mass
CaO	1.38 %
MgO	1.35 %
SiO_2	70.13 %
Al_2O_3	11.45 %
Fe_2O_3	4.22 %
Na_2O	1.49 %
K_2O	2.20 %
SO_3	0.05 %
Ignition loss	3.08 %

Table A.2 Chemical composition of coarse aggregates

Constituents	Percent mass
CaO	36.12 %
MgO	0.86 %
SiO_2	26.28 %
Al_2O_3	2.47 %
Fe_2O_3	1.09 %
Na_2O	0.57 %
K_2O	0.46 %
SO_3	0.05 %
Ignition loss	30.25 %

APPENDIX 2 JENNINGS AND TENNIS MODEL FOR CALCULATING GEL CONTENT

CHS gel content (γ_{CSH}) = CSH gel weight/ concrete weight = $m_{CHS\text{-}gel}/m_{concrete}$

$$\gamma_{CSH} = \frac{m_{CSH-gel}}{m_{concrete}} = V_{CSH-solid}\,\rho_{CSH}\,\frac{m_{cement-paste}}{m_{concrete}} \quad \textbf{[1]}$$

$$V_{CSH-solid} = c\left(0.347\theta_1 p_1 + 0.461\theta_2 p_2\right) \quad \textbf{[2]}$$

Where θ_1 and θ_2 are the degree of hydrations of C_3S and C_2S respectively, p_1 and p_2 are the proportions of C_3S and C_2S compounds in cement respectively. θ_1 and θ_2 can be calculated using Avrami equation while p_1 and p_2 can be determined from Bogue phase composition model.

In equation **[2]**, c is the cement content used in cement paste, which can be determined by relation **[3]** as follows:

$$c = \frac{1}{\left(1 + \frac{W}{C}\right)} \quad \textbf{[3]}$$

Let us now determine the gel content of concrete used in present work. The calculated parameters are quoted in **Table 2.1**. Note that the calculation correspond to 28 days of curing period plus 1 year (365 days) of immersion time or a total of 393 days of concrete age.

Table A.3 Calculated parameters to determine gel content for 393 days of concrete age

Parameters	θ_1	θ_2	p_1	p_2	ρ_{CSH}
					$Kg\text{-}m^{-3}$
Values	1	0.61	54	22	2340

The output can be quoted in **Table 2.2**.

Table A.4 Calculated gel content for 393 days of concrete age

Parameters	c	$V_{CSH\text{-}solid}$	γ_{CSH}
			$Kg\text{-}m^{-3}$ concrete
Values	0.714	0.18	149

In the following tables, the values corresponding to 18 months of exposure period are quoted.

Table A.5 Calculated parameters to determine gel content for 573 days of concrete age

Parameters	θ_1	θ_2	p_1	p_2	ρ_{CSH}
Values	1	0.63	54	22	2340

Table A.6 Calculated gel content for 573 days of concrete age

Parameters	c	$V_{CSH\text{-}solid}$	γ_{CSH}
			$Kg\text{-}m^{-3}$ concrete
Values	0.714	0.18	149

APPENDIX 3 LINEAR BINDING ISOTHERM

A non linear binding isotherm between free chlorides and bound ones for the case of 165 g/l NaCl has already been presented. Here the same experimental data is used to extract a linear isotherm using water and acid soluble chloride concentrations. This binding isotherm is given just for demonstration purposes as there are chloride ingress models which propose a linear binding isotherm.

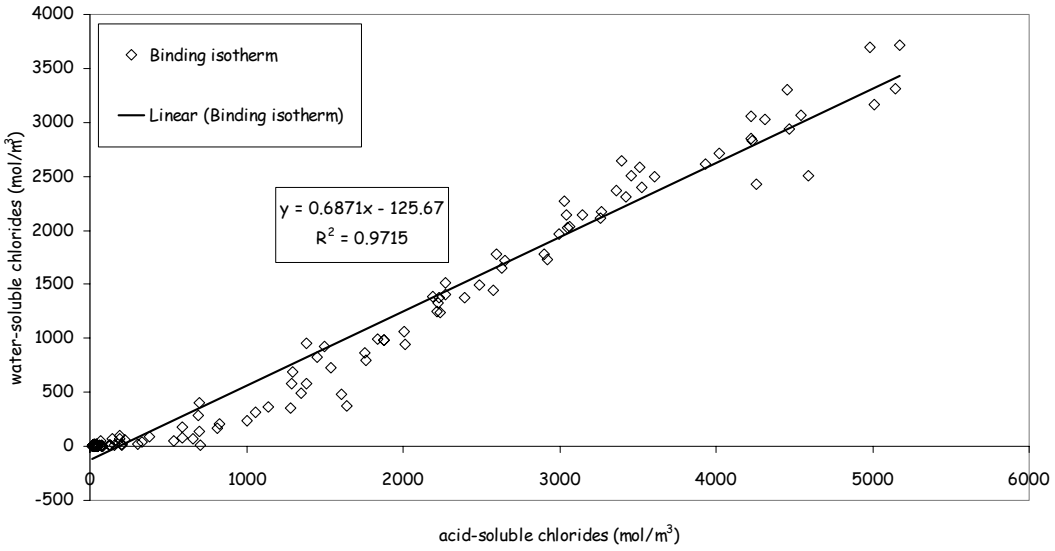

Figure 1 Linear binding isotherm

While making simulations with the above isotherm, all negative free chloride values should be set to zero.

APPENDIX 4 CURVE FITTING WITH ERFC MODEL OF CHLORIDE INGRESS IN CONCRETE

Look at the Fick's second law of diffusion.

$$C(x,t) = C_i + (C_s - C_i).erfc(\frac{x}{\sqrt{4tD}}) \quad \textbf{[1]}$$

1. The above equation cannot handle a decrease in chloride content near the material surface, therefore all such points should be omitted while applying equation **[1]** to a chloride profile. Only those points should be selected which favor a natural fit with the above equation. A data point should not be considered, when it is located in the decreasing zone of chloride content near the surface as equation (1) cannot deal with this phenomenon (for example point 1 and 2 in the **Figure 2**).
2. A chloride profile is obtained by determining chloride content over depth. Although such a profile is usually presented as a line graph, it should be kept in mind that the determined chloride content is the content of a slice (1 or 2 mm in depth) and therefore represents the mean chloride content over the width of the slice. Hence, a chloride profile presented as a bar diagram instead of a line graph would represent more closely the actual determination.
3. For a chloride profile in bar diagram, it is understandable that the measured profile represents reality more closely when smaller slices are taken for the determination of the chloride content.
4. For each point on a chloride profile, a minimum quantity of concrete powder is needed to carry out further analysis. In case smaller slices are selected, it should be assured that enough powder is obtained from each slice. Otherwise, the diameter of the sampling should be increased so as to obtain more powder from a smaller slice.
5. Again look at **Figure 3**. Points 1, 2 and 3 do not coincide with the natural fit of experimental chloride profile and if such points are included, the results might lead to wrong conclusions. Such calculations were made for demonstration purposes. For example, if we include the points 1, 2 and 3 in curve fitting with equation **[1]**, the results are as followed.

   C_s = 1.08 % mass of concrete,

   D_a = 2.51E-12 m²/s.

   If these points are exempted, the following results are met with.

   C_s = 0.95 % mass of concrete,

   D_a = 2.31E-12 m²/s.

It might seem to be little difference at this level but an under or over-estimation of these values might lead to severe mis-calculations, which are based on early age results.

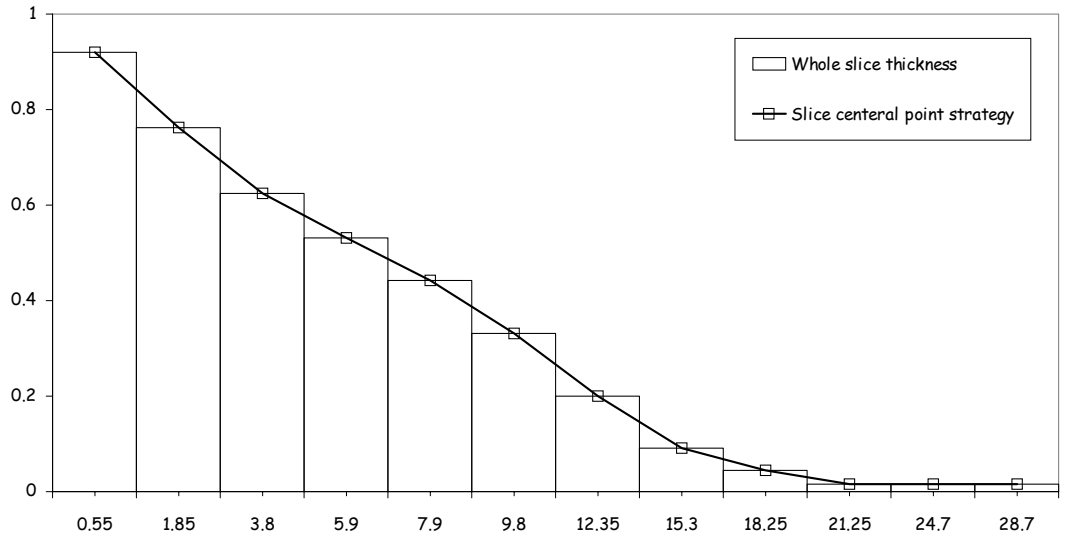

Figure 2 Chloride profile

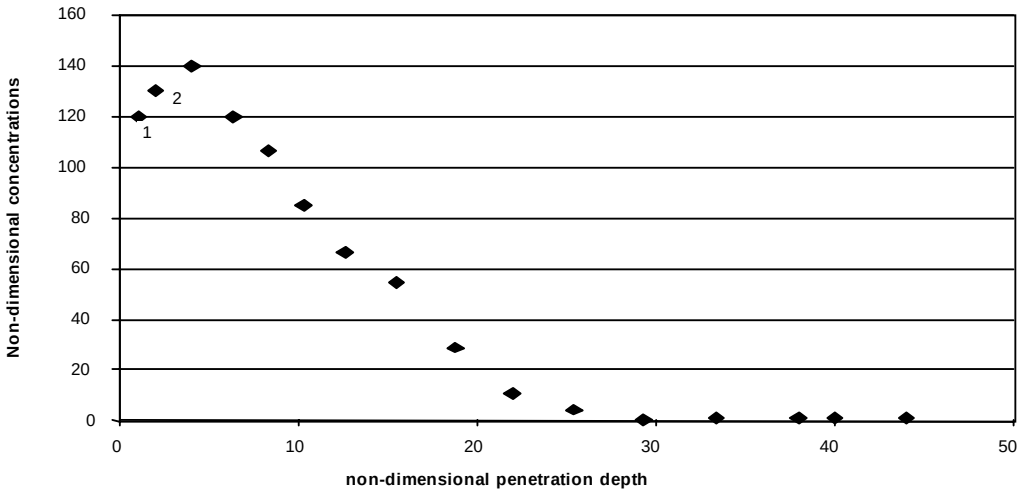

Figure 3 A Chloride profile

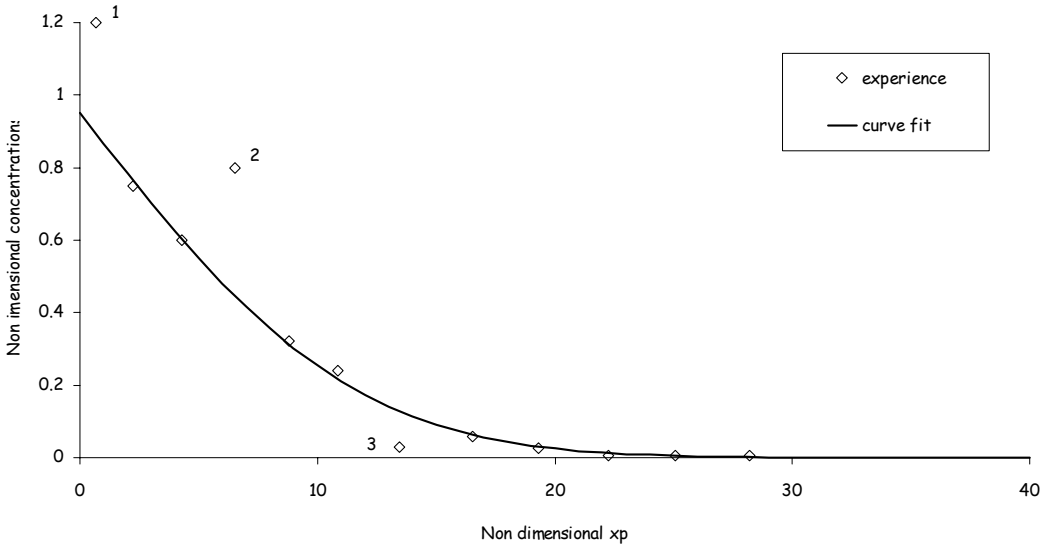

Figure 4 Curve fitting with experimental data

Ecole Doctorale Matériaux-Structure-Mécanique

Thèse préparée aux

Laboratoire Matériaux et Durabilité des Constructions